Trinity College Dublin
Coláiste na Tríonóide, Baile Átha Cliath
The University of Dublin

Identification and Measurement of Variables Affecting Component Lifetime: A Case Study of Polymer Degradation in the Biopharmaceutical Industry

Darren McDonnell

Department of Mechanical and Manufacturing Engineering
Trinity College Dublin

A thesis submitted to the University of Dublin in partial fulfilment of the requirements for the degree of

Doctor of Philosophy

April 2018

Supervisors:

Dr. Garret E. O'Donnell

Dr. Nora Balfe

Declaration

I declare that this thesis has not been submitted as an exercise for a degree at this or any other university and it is entirely my own work.

I agree to deposit this thesis in the University's open access institutional repository or allow the Library to do so on my behalf, subject to Irish Copyright Legislation and Trinity College Library conditions of use and acknowledgement.

Darren McDonnell

April 2018

This work was funded under the Innovation through Human Factors in risk analysis and management (INNHF) project, financed under EU FP7 Marie Curie Actions Initial Training Networks - FP7-PEOPLE-2011-ITN: Project ID 289837. See http://www.innhf.eu

Summary

Modern maintenance methods are dependent upon understanding and monitoring component degradation; however, many industrial situations exist where monitoring is impossible, and component degradation mechanisms are not well understood. This research explored the hypothesis that data to support maintenance operations may be extracted within industrial situations where pre-existing data on component degradation is scarce and understanding of the physics of the degradation process is low. In order to investigate this hypothesis, a case-study in the biopharmaceutical industry was followed which attempted to discover the significant variables leading to component degradation. In such industrial scenarios, data fusion techniques, where multiple data sources are pooled together, are necessary to adequately model complex manufacturing systems. In addition, the interaction between humans and the system is an important consideration that should be taken into account. In order to develop models that will predict component lifetime, a beneficial modelling framework is: 1) data inspection, 2) selection of appropriate historical data, and 3) data pre-processing. However a knowledge gap remains to guide the elicitation of the appropriate data required for such models in many real world industrial scenarios. To help bridge this gap a methodology is proposed here to aid in significant data identification and measurement in complex industrial environments where data is both scarce and siloed.

The case study followed in this work was that of valve diaphragms used in the biopharmaceutical industry, manufactured from the polymer Ethylene Propylene Diene Monomer (EPDM). The central question in this work was therefore, what data, both machine and human related, are useful to predict the lifetime of EPDM diaphragms? In order to answer this question, data from the process level, the system level, the equipment level, and the component level were required. These disparate data sources, including data from both diaphragm supplier and end-user, each contain valuable information which needs to be extracted. The significance of that data can then be determined, and if significant, this information can be then used within appropriate models.

The first step in this work was the modelling of the degradation of the component as a stepwise process, known as a Markov chain. The stepwise nature of the Markov-chain approach allowed the use of bespoke statistical techniques to determine the significant degradation data, a significant step given the scarcity of data. To enable the multi-state approach, a qualitative assessment method was created which categorised the components into different health states for the first time.

Once the initial list of significant data had been filtered using the developed method, four key chemical interactions were investigated further using multiple material characterisation techniques. This acted as an additional aid to the selection of the set of significant process variables contributing to component degradation. It was necessary to perform these analyses as the statistical techniques employed could not identify, with a sufficient level of confidence, which data should be taken into account when developing models of component lifetime. The material characterisation afforded, for the first time, an understanding of the chemical and physical mechanisms responsible for EPDM degradation that occur during exposure to the chemicals commonly used in biopharmaceutical production. An understanding of the physics of failure of the components also acts as a first step in potentially developing condition based monitoring solutions for this application.

To fully encapsulate all possible root causes of component degradation, it was critical to assess if human interaction during maintenance activities played a role in the sudden failure of the components in-situ. To accomplish this, a methodology was developed enabling the integration of human factors as quantitative data within component degradation models, utilising human knowledge of the maintenance process. The case study investigation suggested that incorrect installation has a significant impact on component lifetime, and that correct procedures were not always being following in the valve installation process. Modelling the factors which influence technician performance in this way allows individual

components to have their own local hazard rates, a first for human-system interaction effects due to maintenance intervention.

In conclusion, the central hypothesis of this work was substantiated, as useable quantitative data was extracted from scarce and siloed data sources via a multi-disciplinary approach which unified several sources of information. The gathered data would enable the development of predictive lifetime models. It is important to note that the approach of this work is not intended to provide an exact data elicitation solution for all industrial scenarios, as this will change depending on a multitude of factors related to the case study in question, such as data availability, required resources, time constraints etc. Rather, this work should be interpreted as a template to guide the identification and quantification of appropriate data for inclusion in reliability models which can be adapted as required for different systems.

Acknowledgments

In July 2013, just after I first began my PhD, I met Dr. Kjell Hausken, Professor of Economics at the University of Stavanger, in a gym during a conference we were both attending. I was wearing a t-shirt at the time which had the words 'Hell&Back' on the front. Reading this, Professor Hausken immediately quipped "I presume 'Hell&Back' is in reference to doing a PhD thesis?". I had no immediate response, however I would have liked to quote to him the words of the late American Senator Benjamin Wade, who remarked "heaven has the better climate, but hell has the better company". With this in mind, I would like to thank the following people for sharing this journey with me over the last four years.

Firstly, I owe a huge debt of gratitude to both of my supervisors, Dr. Garret E. O'Donnell and Dr. Nora Balfe, who not only gave me the opportunity to pursue this work, but offered constant guidance, invaluable advice, and excellent mentorship throughout.

A special thank you to all of those I worked with in both Pfizer and ITT over the last 4 years. While there are far too many to name, a special thank you to those in the Equipment Technology group, and to Gerard Clarke for his guidance throughout my time there. Thank you to Gerard Coey, Raymond McGuirk, and Guy McDonnell, for helping facilitate and streamline the research. Thank you to Peter Nelson for his willingness to share his valuable knowledge whenever I needed it. Finally a very special recognition and thank you to Thorsten Fischer, who was ever present when I needed advice, which tended to be more often than I'm sure he would have liked, and to whom I am indebted. His knowledge, foresight, commitment, and work ethic made this project realisable.

To my fellow postgrads in TCD, who have all now graduated, thank you for all the advice, guidance, proof-reading, and laughs. You all blazed the trail before me and showed me the way. In no particular order I would like to thank Jeff Morgan, Barry Aldwell, Kevin Kerrigan, Daniel Trimble, Robin Mooney, Rory Stoney, Paul Ervine, Emma Brazel, Paul Harris, Stuart Murphy, and Eoin O'Driscoll. Thank you also to all the TCD technical staff, in particular to Michael Reilly and Peter O'Reilly for all their help.

Thank you to all the wonderful people I was fortunate to be able to meet and work with through the INNHF program, in particular to Dr. Piero Baraldi and all his team at Politecnico di Milano. Your professionalism, knowledge, and friendship will live long in the memory.

To my friends, thank you for the most welcome distractions, and for helping me remember that life still exists outside of the PhD bubble.

To my family and extended family, who if I named would take up an entire page. You have been my bedrock since day one. You continue to motivate and support me every day. Thank you all.

To my parents, Eamonn and Fiona McDonnell. You gave up a holiday home and a converted attic to seeing this through, not to mention the crates of food! Thank you for all you've done for me. You've always been, and always will be, my greatest inspiration. This is for you.

Lisa. My beautiful wife. A thank you would not be enough. I owe you a debt I cannot repay. Thank you for being by my side me all these years. I could not have achieved this without you.

Finally, I would like to dedicate this work to the memory of my late family: my grandparents, Josie, Ita, Willy, and Kevin, my uncle Noel, and my aunt Ger.

For all Compositions are dissoluble, and whatever has a Beginning has an End.

Though 'tis produc'd but one way, it may be destroy'd many Ways

- Epicurean Philosophy –

Contents

List of Figures

List of Tables

Nomenclature

A&E	Alarms and emergency events
ADM	Accessibility difficulty metric
AESOP	ArchitecturE for Service-Oriented Process-Monitoring and-Control
AIC	Aikake Information Criterion
ASME	American Society of Mechanical Engineers
CAS	Chemical Abstracts Service
CBM	Condition based maintenance
CIP	Clean-in-place
DMTA	Dynamic mechanical thermal analysis
DN	Nominal diameter
DNA	Deoxyribonucleic acid
EAMS	Enterprise asset management software system
ECO	Elastomer change out
ENB	Ethylidene Norborene
EPDM	Ethylene propylene diene monomer
Exp	Exponent
FDA	Federal Drug Administration
FDS	Functional design specification
FTIR-ATR	Fourier transform infrared spectroscopy attenuated total reflection
GCMS	Gas chromatography mass spectroscopy
GMP	Good manufacturing practice
H_2O	Dihydrogen Monoxide
H_3PO_4	Phosphoric acid
HEART	Human Error Assessment and Reduction Technique
HOF	Human and Organisational Factors
HR	Human related
HRA	Human Reliability Analysis
Hrs	Hours
I/O	Input/Output
ID	Identification
IRHD	International Rubber Hardness Degrees
ISO	International Organization for Standardization
IT	Information technology
MCS	Management control system
MR	Machine related
NaClO	Sodium hypochlorite
NaOH	Sodium hydroxide
OEM	Original equipment manufacturer
P&ID	Piping and instrumentation diagram
pH	Power of Hydrogen
PHM	Prognostics and Health Management
PI	Process Intelligence
PLC	Programmable logic controller
PSF	Performance shaping factor
PTA	Procedural task analysis
PTFE	Polytetrafluoroethylene
QBMS	Qualified building management system
QMS	Quality management system
R&D	Research and development
RM	Rubbermaker
RO	Return osmosis
RUL	Remaining useful life

SIP	Steam-in-place
SIRENA	Service Infrastructure for Real-time Embedded Networked Applications
SOCRADES	Service-Oriented Cross-layer Infrastructure for Distributed smart Embedded devices
SODA	Service Oriented Devices Architecture
SOP	Standard operating procedure
SPAR-H	Standardised Plant Analysis Risk-Human Reliability Analysis
TAC	Triallylcyanurate
TES	Through-life engineering services
TGA	Thermogravimetric analysis
THERP	Technique for Human Error Rate Prediction
TRACEr	Technique for the Retrospective and Predictive Analysis of Cognitive Errors
USP	United States Pharmacopeia
UV	Ultraviolet
VIF	Variance Inflation Factor
WFI	Water for injection

Chapter 1

Introduction

1.1 The role of maintenance in system reliability

Maintenance is the major engineering service required within organisations where there exists the need to maximise component or system availability based on continued expected component or system performance [1,2]. The entire maintenance effort involves a combination of technical, administrative and managerial actions during the life cycle of a component or system with the aim of either retaining it in, or restoring it to, a state in which the required industrial function can be executed [3]. Maintenance can thus be described as any activity carried out on an asset in order to ensure that the asset continues to perform its intended functions by restoring it to a favourable operational condition [4]. Manufacturers continuously aim to increase the useable life of components, reduce maintenance costs and subsequently help maximise net profit. Through-life engineering services (TES) are the myriad of technical services and decision making processes that are necessary to guarantee this required and predictable performance of complex engineering systems throughout their operational life [5]. TES are therefore essential to the support of complex manufactured products. Within TES, maintenance decision making ability is the combination of managerial, supervisory, technical and corresponding administrative activities facilitated by the ability to predict the Remaining Useful Life (RUL) of components or systems [1].

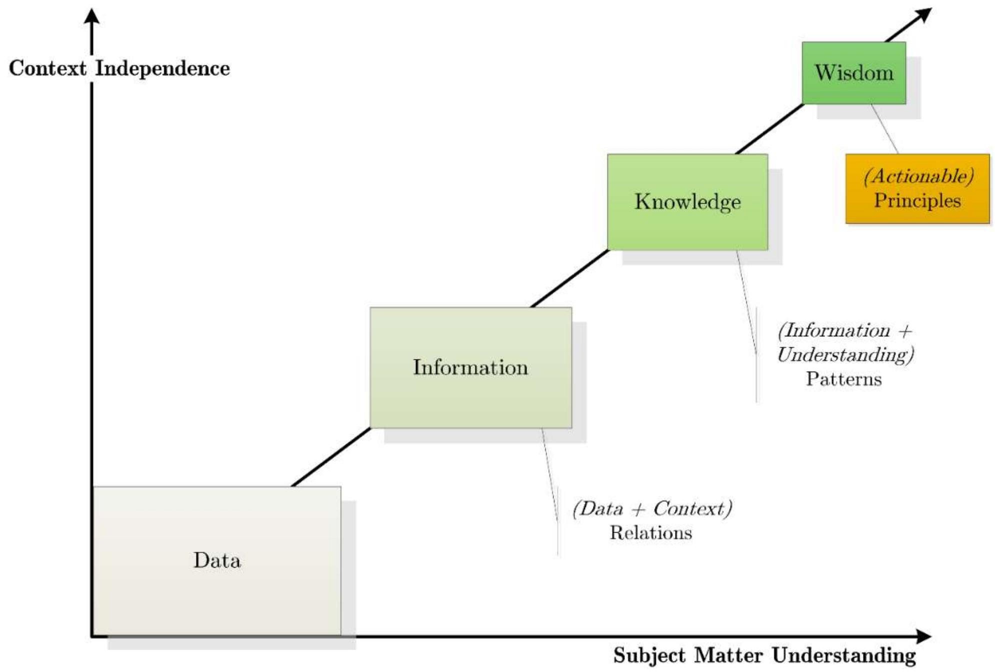

Figure 1.1: Data, Information, Knowledge, Wisdom. Adapted from [6]

The ultimate aim of TES in industry is to achieve a state of ‘wisdom’, where there exists an equal or greater actionable benefit returned for the reliability activity undertaken to achieve production sustainability. The process of converting data to actionable wisdom is shown in figure 1.1. When data is collected, the data together with the industrial context creates relations, turning it into information. When this information is combined with an understanding of the underlying principles, it becomes knowledge. Patterns are formed at this level, and when these patterns are further enriched, they become actionable wisdom [6].

The mission of the maintenance department in a world-class organisation is to achieve and sustain optimum equipment life and system operating conditions, to react quickly, and to maximise maintenance resource utilisation while minimising spares inventory [4]. Different sub-divisions within TES tie into these mission in numerous ways, as depicted in figure 1.2.

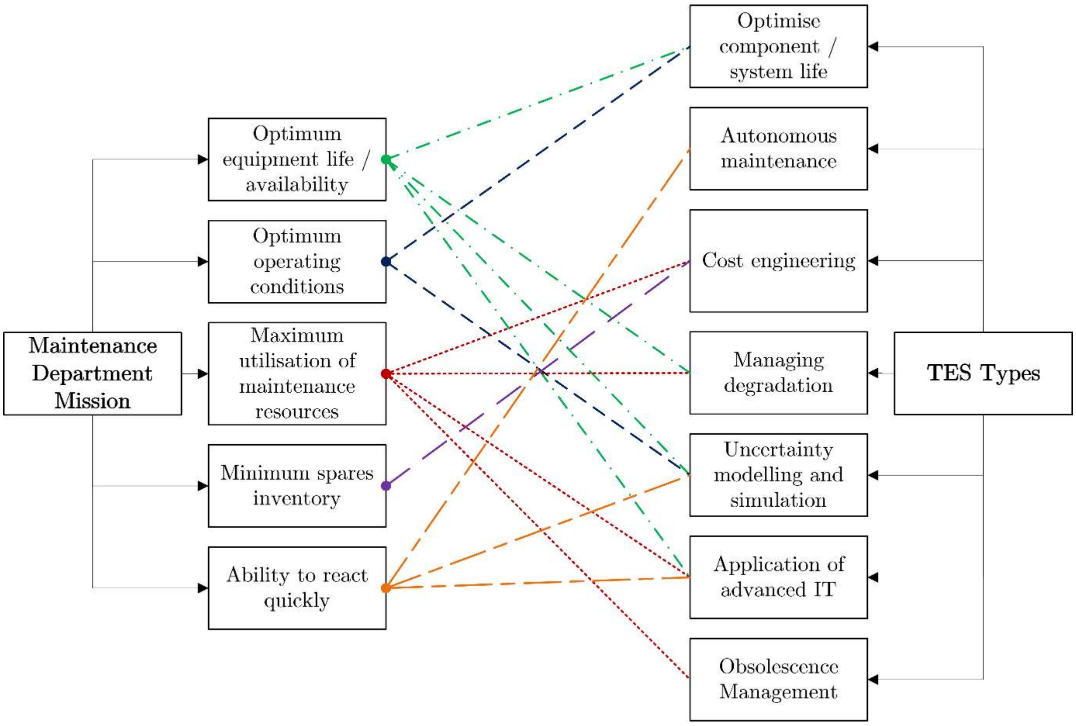

Figure 1.2: Relationship between TES and maintenance department mission goals. Adapted from [4,5]

Reliability is critical in the assessment of industrial products and systems. While good product design is essential to enable high reliability, all products inevitably deteriorate over time whilst operating under environmental stresses and loads, which can often be random. To combat this deterioration, different types of maintenance approaches have been introduced and refined over generations in order to efficiently achieve reliability during the useful life of a physical asset [7]. Given its criticality to mission success, between 15-40% of production costs and up to 30% of the total manpower of an organisation can be attributed to maintenance, the largest part of any operational budget next to energy [4,8,9]. Without well maintained equipment, a plant will be at a disadvantage in a market that requires low cost products of high quality to be delivered quickly [10–12]. These maintenance costs can be divided into direct costs, indirect costs, and non-realised revenue. Direct costs consist of labour costs, spare parts, and other costs directly linked to maintenance activities. Indirect costs include the cost of lost production due to equipment failure and the cost of insufficient product quality. Non-realised revenue refers to the income loss due to reduced sales volumes, missed delivery dates etc., attributed to poor production system maintenance [13]. As maintenance plays such a critical role in the availability of industrial equipment, optimising maintenance strategies and equipment intervention schedules has a significant impact on the ability of a system or asset to contribute to revenue generation. The role of maintenance within industry therefore can be described as preventing all losses that are caused by component or system related problems, rather than simply repairing breakdowns as quickly as possible.

The relationship between maintenance and the availability of industrial equipment is demonstrated in figure 1.3. The quantity of units produced, the total potential profits from those units, and the impact that an efficient and effective maintenance strategy can have on those is shown. Assuming product quality and unit selling cost as constants, it is shown how the total cost of manufacturing a single unit decreases with the number of units produced / sold. It can be seen how increasing system capacity via more efficient and effective maintenance strategies by increasing system availability can then increase potential profit margins.

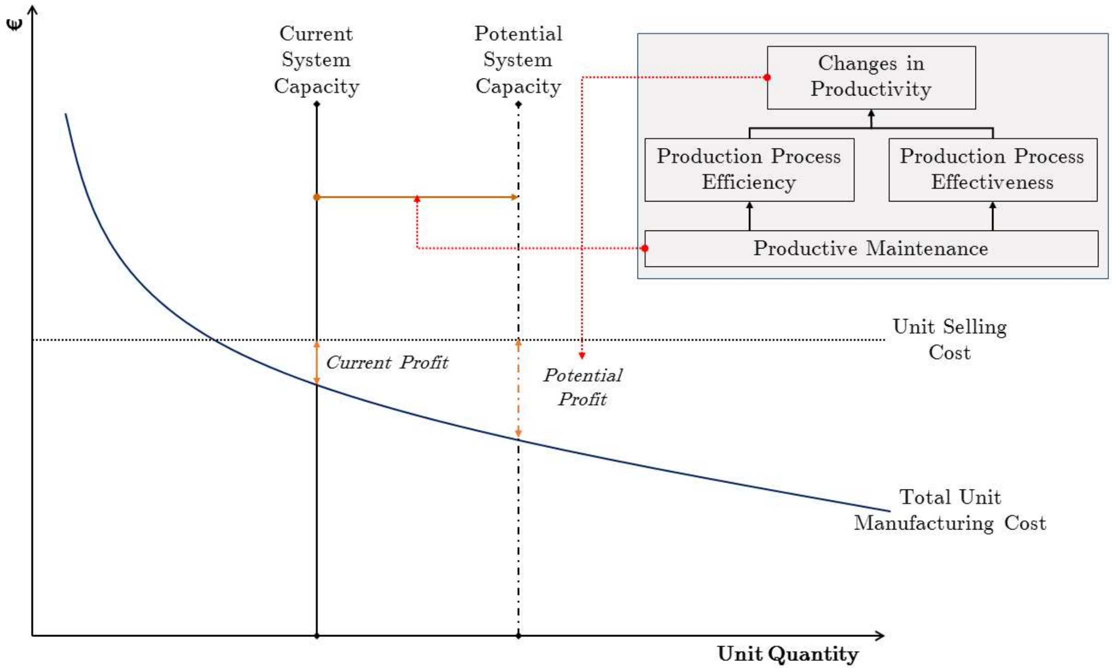

Figure 1.3: Quantity of units manufactured and total unit profits. Adapted from [14]

To achieve optimum system availability, three types of maintenance programs are typically adopted in industrial applications; corrective maintenance, preventive maintenance, and condition based maintenance [15]. The advantage of preventive maintenance over corrective maintenance is that preventive maintenance reduces maintenance costs by minimising unscheduled downtime, however preventive maintenance is conducted without considering the condition of the equipment or component [16]. Therefore, equipment useful life is not fully exploited and the possibility of human errors occurring during maintenance interventions is increased due to increased human system interactions. Condition based maintenance differs from preventive maintenance in that maintenance decisions are made based on observations of the system degradation condition rather than a priori planning of the intervention times [16]. This requires that the equipment is monitored and that there is the possibility of determining the component degradation state.

Along with TES, Prognostics and Health Management (PHM) is an approach to system life-cycle support that seeks to reduce/eliminate inspections and time-based maintenance through accurate monitoring, incipient fault detection, and prediction of impending faults [17]. Both PHM and TES represent paradigm shifts from legacy condition based maintenance frameworks by expanding the potentials to accurately and robustly detect and diagnose incipient system faults. The goal of PHM and TES within reliability analysis is to accurately predict the RUL of systems and components to allow for efficient maintenance scheduling either autonomously or by human decision makers. To do so, different information and data sets relating to the past, present and future behaviour of the equipment in question are required. Traditionally, accurate reliability models required the availability of sufficient and relevant equipment failure data. Typical industrial case studies however often involve failure events where little failure data is available and where the component degradation process is not well characterised or understood. The problem for maintenance decision makers in establishing maintenance plans in these circumstances is exacerbated for components which cannot be assessed by condition based maintenance methods, meaning the actual degradation state of the system at any time t is not known [18].

One sector where the role of maintenance plays a crucial role is the biopharmaceutical industry. This is due to the high value creation of biological medicinal products, which equates to significant financial losses as a result of unexpected equipment failures. Classically, the term pharmaceutical concerns medicinal products, technologies, related R&D, and companies, with two major subsets: biopharmaceutical and active pharmaceutical ingredient. The basic distinction is that biopharmaceuticals pertain to biological products containing active agents intrinsically biological in nature and manufactured using biotechnology and biological sources and processes, whereas active pharmaceutical ingredient production involves chemical, non-biological, manufacturing sources and processes [19].

1.2 Maintenance in the biopharmaceutical industry

Biopharmaceutical products are clinical reagents, vaccines, and drugs produced using modern biotechnology methods for in vivo diagnostic, preventive, and therapeutic uses. Essentially, biologics are medicines in which the clinically active ingredient is made in or isolated from a living system [20,21]. Ireland is the largest net exporter of pharmaceuticals in the world. Ireland is also the number one European location for international pharmaceutical investment, with over one hundred and twenty pharmaceutical companies operating within Ireland, thirty-three of which are approved by the U.S. Federal Drug Administration (FDA). Nine of the top ten global pharmaceutical and biopharmaceutical companies have integrated manufacturing operations in Ireland, and six out of ten of the world's top selling drugs are produced in Ireland. In 2014, exports of pharmaceutical and medicinal products exceeded €58bn, accounting for over 50% of total Irish exports [22]. Within biopharmaceutical production operations, seal maintenance is the most cost intensive part of all maintenance activities next to calibrations. Unexpected failure of just one seal, static or dynamic, can result in a serious good manufacturing practice (GMP) issue and high financial losses due to production batch loss.

Corrective maintenance typically cannot be applied to safety critical equipment often found in biopharmaceutical operations, with preventive maintenance schemes the most commonly used. Condition based maintenance is feasible only when the components are fully accessible to inspections or when sensors or other suitable monitoring devices are available for the particular application. The maintenance intervention is then performed when some indicators of the degradation state of the component overtake a fixed threshold or exit from a predetermined range [23]. With respect to preventive maintenance, condition based maintenance allows the exploitation of a longer duration of the equipment useful life, increasing availability and reducing the risk of failures. Despite these additional benefits, in several industrial applications either the technology or the ability to continuously or periodically monitor component degradation is not available. For example, condition based maintenance is rarely used for static mission critical equipment in the biopharmaceutical industry due to regulatory concerns around embedded sensors within product streams. In these cases the equipment degradation process remains unobserved during its working life and inspections are possible only when corrective or preventive maintenance interventions are applied. For these reasons convenient periodic maintenance frequencies must be decided.

Given the lack of available and/or suitable sensor hardware for particular industrial applications within CBM, soft/virtual sensors have become an active area of research as proxy measurement systems which have a functional relationship with target process variables that can be measured online [24]. A virtual sensor or soft sensor is an algorithm that estimates the value of a variable based on related measurements and a model of the process where the variable participates [25]. Soft sensors are essentially inferential estimators which draw conclusions from process observations regarding the non-linear behaviour exhibited by many industrial processes [26]. The range of tasks fulfilled by soft sensors is broad, however the original and still most dominant application area of soft sensors is the prediction of critical processes which can be determined either at low sampling rates or through off-line analysis only [27].

Despite their industrial applicability there exists an underutilisation of soft sensor approaches for the characterisation and prediction of component and system lifetimes. There is scope for the novel exploitation and fusion of multiple sources of data to develop and adapt virtual sensors using hybrid modelling frameworks. However, in order to develop such models, appropriate and requisite data pertaining to component or system degradation must first be elucidated, before it can be transformed into actionable wisdom. However, despite the importance of identifying the critical variables and parameters required for model developemnt, research in this area is scant and has been overlooked in the published literature [28]. As such, this work explores how such information can be elucidated in order to enable modern, novel, 'Industry 4.0' type modelling solutions. This work is based on an industrial case study and encompases the typical difficulties encountered in such real world scenarios.

1.3 Research aims and objectives

Following from this, the goal of this research is the elicitation of the significant variables leading to component degradation, which would enable the development of degradation models for components which cannot be assessed by traditional CBM methods, where little failure data is available and where the component degradation process is not well characterised or understood. The hypothesis of this research is that pertinent data which could be transformed into actionable wisdom may be extracted within industrial situations where available data is scarce, and context independence and subject matter understanding is low. In these scenarios, data from the process level, the system level, the equipment level, and the component level become valuable sources of information. In spite of the fact that these situations are quite common in industrial practice, for example with innovative and/or very highly reliable components, recently introduced technologies, bespoke manufacturing environments etc., a knowledge gap exists to guide the elicitation of the significant variables responsible for component degradation under these conditions. To help bridge this gap a holistic methodology is proposed which addresses several issues:

1. Component degradation is effected by the operational environment, but appears to have no affect on the environment itself. Therefore there is a lack of known monitorable phenomenon with which to make direct inferences on the health state of the components. This necessitates, in the first instance, a soft sensor prognostics approach. To develop soft sensor driven degradation models however, it is necessary to include therein the environmental process conditions experienced by the components which have an impact on their degradation. It is also necessary to effectively correlate the effect of those conditions to the progression of the component degradation. However, these significant conditions and their effects are not known.
2. The physics of the degradation processes of the components, initiated by certain process variables, are not well characterised or understood. This lack of knowledge adds to the uncertainty pertaining to the significant process variables which contribute to component degradation, and makes physics based model development impossible. A data-driven prognostics approach would therefore be required. To elucidate potential monitorable phenomenon for CBM solutions, characterisation of the component degradation mechanisms from a first-principles perspective is necessary.
3. It is suspected that installation issues are also a contributory factor in the early failure of the components. However this has never been empirically investigated or confirmed. If significant, to

develop accurate component level data-driven degradation models it is necessary to capture this information in order to reduce prognostic lifetime variability.

The research objectives of this work are therefore:

1. Identification of significant process variables contributing to component degradation utilising disparate data sources.
2. Characterisation of the industrial components via material analysis techniques in order to understand the physics of the degradation process, i.e. the mechanisms by which degradation occurs and the chemical and physical changes that occur in the material.
3. Definition of a methodological framework to integrate human and organisational factors (HOFs) as quantitative metrics within parametric degradation models.

This methodology is demonstrated using a case study of an elastomer component, an ethylene propylene diene monomer (EPDM), used as the sealing diaphragm element in flow control valves in the biopharmaceutical sector. EDPM diaphragms are a product contact material, and maintain the integrity of the hermetically sealed production environment, defining the sterile boundary of the process preventing environmental contamination. Critically, elastomers can be described as the weakest link in the integrity chain, as failures are exceedingly rare at all other potential points of failure in the system, for e.g. welded pipe joints [29]. As such there is a significant production risk associated with the failure of the diaphragms in situ. This risk is mitigated via frequent elastomer change outs (ECOs) implemented as part of a planned maintenance strategy. To date, there exists little EPDM diaphragm reliability data available from OEMs, forcing industrial end-users to make best guess lifetime estimates based on data made available through direct industrial usage of the components over time. The frequency of the ECOs, the time-based planned valve maintenance strategy involving replacing the elastomer diaphragm, are therefore based on scarce industrial data and rough OEM recommendations, resulting in reduced system availability. This has significant financial implications due to lost production revenue, spare-parts costs, and labour costs. Traditionally in the biopharmaceutical industry, it has proven impossible to a-priori accurately predict the usable life of a diaphragm. A-posteriori lifetime assessments can only be made when a diaphragm has been fully utilised in the user's full-size commercial system, an expensive and risky process. This has also meant that suppliers are often distanced from the end user's real-world application and reliability experiences. Meanwhile, replacement parts are often supplied through distributors, further distancing suppliers from end-user's performance issues [30].

1.4 Thesis layout

The developed approach in this work utilises a combination of quantitative and qualitative information in the form of industrial process data, material characterisation data, human knowledge, and human factors analysis, the combination of which is unique in the literature. Ease of industrial applicability is important in this context due to the low interest in structured maintenance improvement work cited in manufacturing industries, as these industries find many available maintenance tools too complicated to use [13].

For clarity, this scope of this work did not factor in flaws that may be inherent in the manufacturing process of the EPDM diaphragm components, as this work provides a framework for component end-users only. End-users are presumed to have little or no impact over the component production process, and so including these factors was not deemed pertinent. Likewise, residual stresses and crack propagation mechanisms were out of scope, as the goal was to develop an approach on how to elicit data in such a way that it can be utilised in maintenance prognostic models, and neither of these data sources are measureable in real time. Finally, this work is not intended to provide an optimal or definitive mathematical treatise for the determination of the statistical significance of the derived variables or their parameters, machine or human related. Nor is it intended to provide a comprehensive mathematical treatment of component lifetime prognostics. The literature on covariate significance determination and RUL prediction is vast, and the method of choice for both depends on a number of factors related to the context of the case study being investigated, in particular data type, format, and abundance. This work aims to overcome the stated challenges by adopting the methodology outlined in figure 1.4.

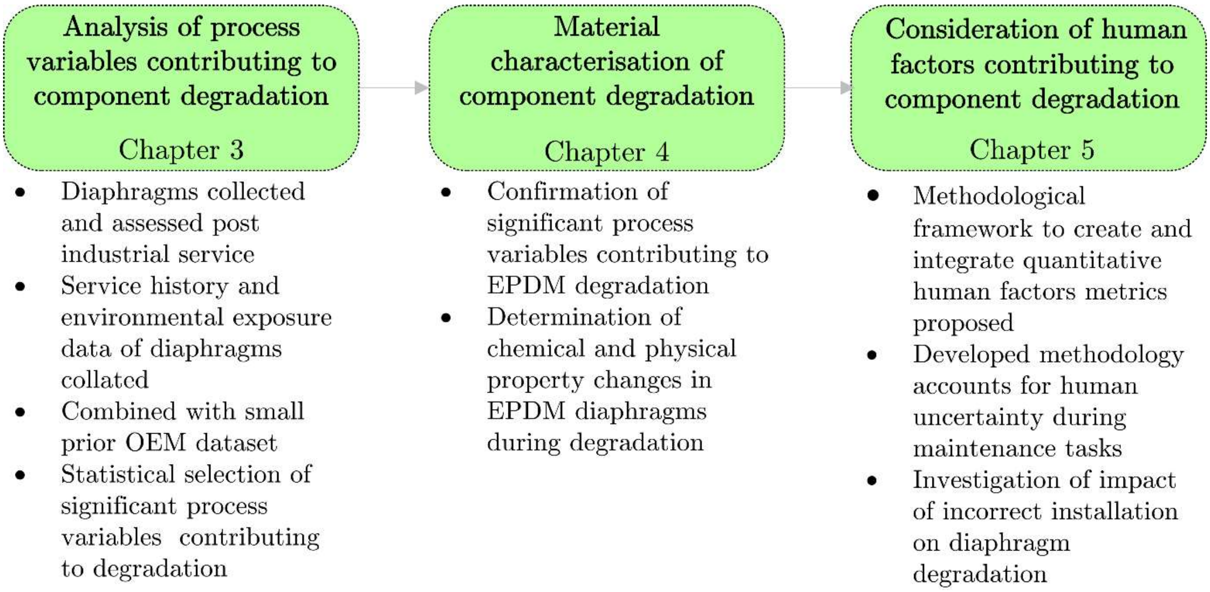

Figure 1.4: Thesis chapter layout and methodology

Chapter 2

Literature review

Given the multidisciplinary nature of this work, the following chapter contains several distinct areas of knowledge, each of which is critical in the solution of the overall problem. Both the fundamentals and the current state of the art in each of these areas is reviewed. Where appropriate, overlap between the disciplines is called out. The connections of each of the disciplines and the layout of the rest of this chapter will follow that described in figure 2.1.

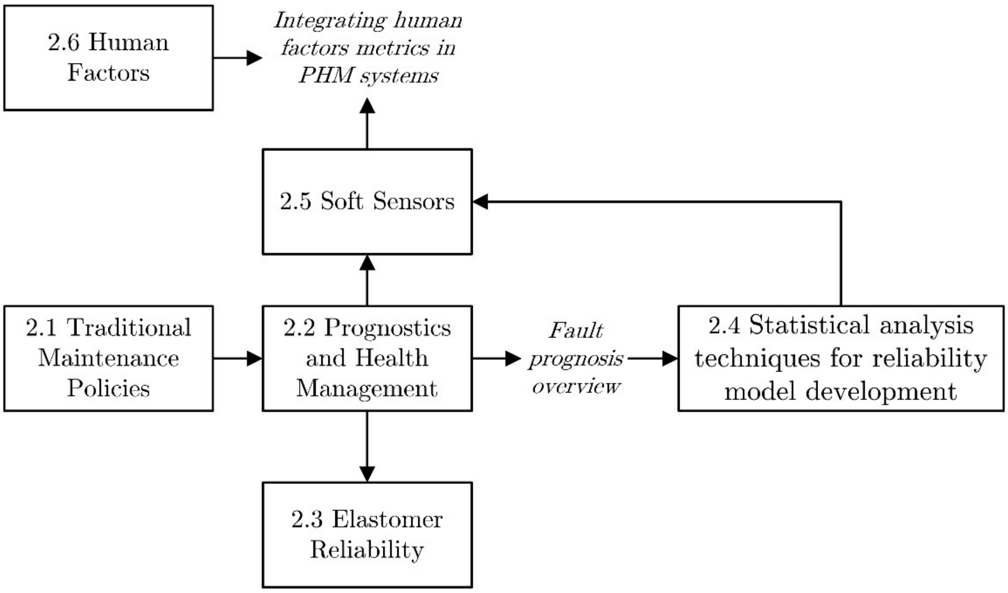

Figure 2.1: Literature review overview

Firstly, a general overview of maintenance is given, followed by a review of the state of the art in maintenance methodologies, known as prognostics and health management (PHM). The knowledge from PHM then feeds into a section on elastomer reliability, which focuses in part on EPDM and its degradation mechanisms. The PHM section also contains an overview of fault prognosis, which feeds directly into the statistical techniques used in reliability model development. The knowledge of both the PHM and statistical technique sections feeds into the review of soft sensor technology. This in turn feeds into the knowledge of integrating human factors metrics in PHM systems, which is supplemented by a review of the state of the art in the human factors discipline.

2.1 Traditional maintenance policies

Maintenance is an essential element in ensuring the performance and profitability of world class manufacturing organisations. Accordingly maintenance costs represent between 10 to 40 percent of total production costs and up to 30 percent of the total manpower of an organisation [8,9]. Next to energy, these maintenance costs can be the largest part of any operational budget [9]. As an example of this, estimates suggest that U.S. industry, per annum, spends more than $200 billion on maintenance of plant equipment and facilities, with the result of ineffective maintenance management contributing to losses of more than $60 billion [4]. Maintenance costs can be divided into direct costs, indirect costs, and non-realised revenue. Direct costs consist of labour costs, spare parts, and other costs directly linked to maintenance activities. Indirect costs include the cost of lost production due to equipment failure and the cost of insufficient product quality. Non-realised revenue refers to the income loss due to reduced sales volumes, missed delivery dates etc., attributed to low equipment availability due to poor production system maintenance [13]. As maintenance plays such a critical role in the availability of industrial equipment, one of the most important questions faced by maintenance management is whether the maintenance output contributes effectively to company profits [9]. The importance of optimising maintenance strategies and equipment intervention schedules, in order to have a significant impact on the ability of a system or asset to contribute to revenue generation, is illustrated in figure 2.2.

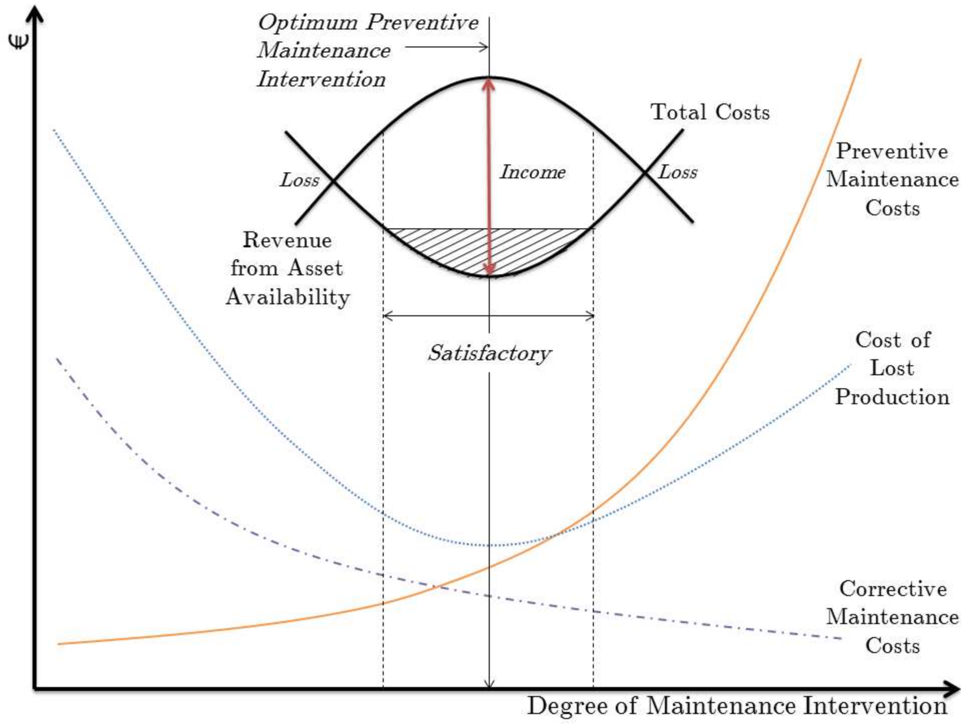

Figure 2.2: Maintenance strategy optimisation effects on industrial revenue. Adapted from [4,31]

Figure 2.2 outlines the cost-benefit balance that must be achieved in order to have an effective maintenance strategy within an organisation. The main balance to be achieved is that between corrective maintenance and preventive maintenance costs, the two most prevalently applied maintenance schemes. Corrective maintenance is carried out on an unscheduled basis when components fail or if faults are detected during routine inspection [32]. It is an expensive strategy due to the high risk of prolonged machine downtime, potentially exacerbated by unavailable spare parts or conditions that inhibit maintenance activities, all contributing to potential revenue loss. By contrast preventive maintenance aims to repair or replace components before they fail, most commonly by scheduled maintenance activities at regular time intervals regardless of component condition. Time based maintenance minimises downtime when the maintenance intervention times are appropriately set. If not appropriately set however, then unnecessarily frequent maintenance tasks increase the maintenance cost, because component lifespan is not entirely utilised [33]. In this scenario, costs associated with lost production rise again contributing to losses in revenue.

While the implementation of an efficient maintenance strategy within a manufacturing organisation can help improve the productivity, competitiveness and profitability of an organisation, a considerable number of manufacturing organisations still fail to develop, maintain or improve their current maintenance strategy to improve their overall performance. For example, Alsyouf [34] produced an empirical study on the maintenance strategies of over 300 Swedish manufacturing organisations and reported that more than half of the organisations did not have any written maintenance strategy. Similar results were reported previously by Jonsson [35]. Cholasuke and Bhardwa [10] carried out a pilot survey on the maintenance management strategies of 18 UK manufacturing organisations and reported that 40% still do not realise the importance of effective maintenance management. A report of the maintenance strategies implemented by 300 multinational companies in various manufacturing sectors found that although 87% of organisations report that maintenance is very or extremely important to their organisations overall financial performance, only 7% of companies were satisfied with their maintenance performance [36]. Mobley [4] suggests that the dominant reason for this ineffective maintenance management is the lack of factual data to quantify the need for repair or maintenance of plant equipment and systems.

An example of a maintenance management performance improvement strategy is the implementation of condition monitoring. Until recently, the concept of CBM has been primarily fault diagnosis, involving fault detection, identification, and isolation [37]. The basic philosophy behind CBM is to compare data from a monitored source with baseline data with the purpose of observing significant operating differences indicating the presence of a developing failure. The inherent disadvantage of this approach is its typically limited coverage to preselected known failure modes only [37]. In recent years, the relative affordability of online monitoring technology has led to a growing interest in CBM, and its successor predictive maintenance. Predictive maintenance is founded on the possibility of monitoring a system to obtain information on its conditions, and then using that information to both identify problems at an early stage and predict their evolution in the future. On this basis, a decision is taken on the next maintenance action. This allows a dynamic approach to maintenance based on failure anticipation, aimed at optimising the equipment lifetime usage, also known as remaining useful life (RUL) [32]. A synopsis of the effect of corrective, preventive, and predictive maintenance strategies on system availability is shown in figure 2.3. As shown, with a corrective maintenance approach, equipment is allowed to run to failure before being repaired. This results in large downtime of equipment due partly to the inability to pre-plan maintenance activities. Preventive maintenance instead attempts to periodically intervene before the system fails, resulting in decreased downtime during maintenance and increased uptime overall. The system is still not immune to unexpected failure events however. Predictive maintenance builds upon scheduled maintenance and attempts to detect faults in real time and intervene before the system fails. This results in further increased system uptime in comparison to scheduled maintenance. Again however, the system is not immune to undetected failures, although these events are considered rare. Predictive maintenance allows for a more dynamic systems intervention approach.

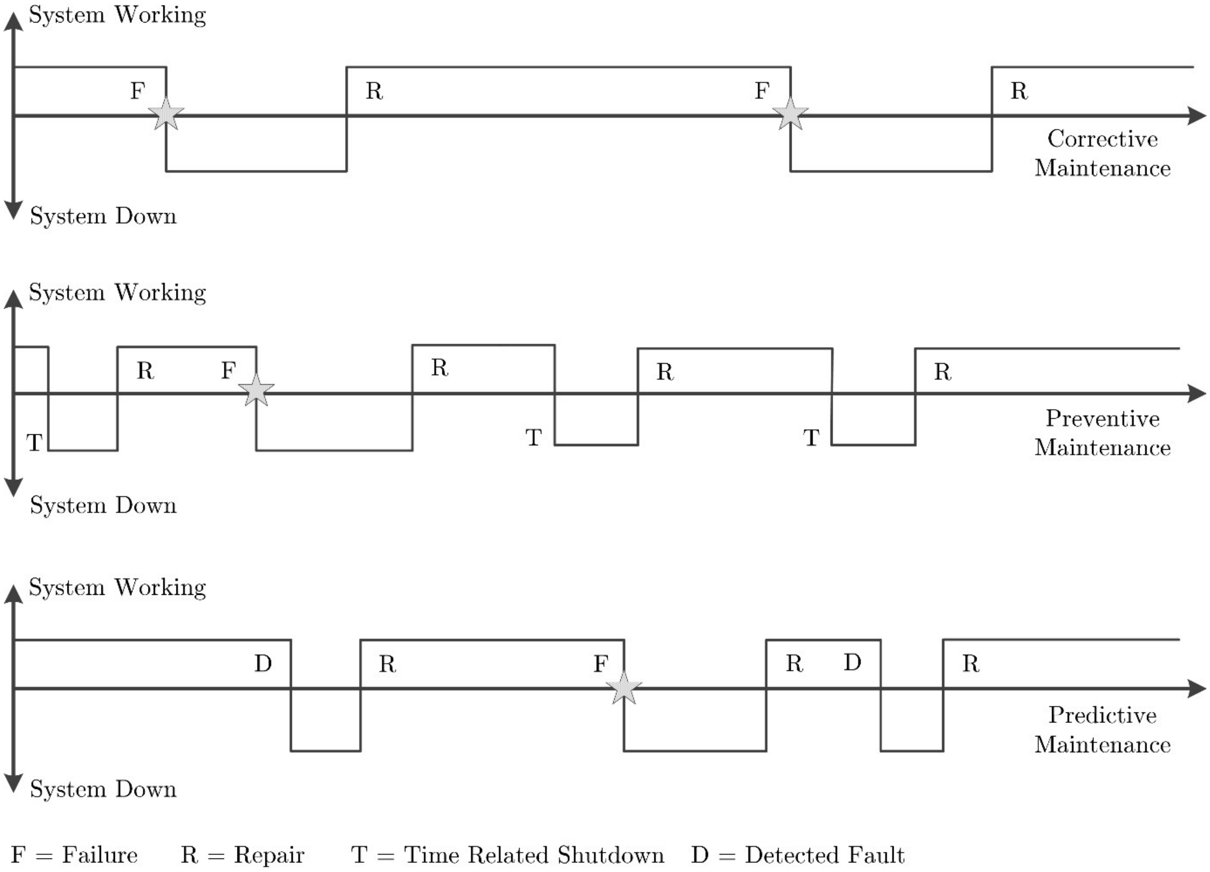

Figure 2.3: Maintenance policy synopsis. Adapted from [32]

There are numerous maintenance optimisation techniques which exist, which can be classified as qualitative or quantitative in nature [9]. One common qualitative approach is reliability centred maintenance, developed within the aircraft industry and later adapted by several other industries [9,38]. Reliability centred maintenance is a systematic approach for establishing priority based preventive maintenance programs considering personnel safety and organisational economics with a focus on system function rather than on system hardware. Its primary objective is to determine the combination of maintenance tasks which will significantly reduce the major contributors to unreliability and maintenance cost in light of the consequences of failures [38]. Developing a reliability centred maintenance methodology involves a structured approach, outlined comprehensively by Rausand [38]. Two of the critical steps in this approach include the determination of maintenance intervals and the in-service collection of data and updating of same. While traditionally within reliability centred maintenance schemes static preventive maintenance intervention times have been used, there have been calls to integrate modern quantitative approaches such as CBM alongside traditional qualitative ones [9]. Reliability centred maintenance also emphasises identification of the root cause of failures [38].

Garg and Deshmukh [9] have extensively reviewed the literature on maintenance management research and suggest possible research gaps within traditional maintenance schemes from the point of view of both researchers and practitioners. Among their conclusions, they opine that while many researchers are pursuing the development of various mathematical maintenance models to estimate system reliability measures, these models may only be useful to maintenance engineers if they are also capable of incorporating numerous other sources of information. These include information about an organisations repair and maintenance strategies, the methods of failure detection, equipment failure mechanisms, etc. that justify the applicability of a particular model in a given system environment, thereby giving greater confidence in reliability estimates based on small amounts of data. Other relevant gaps identified between maintenance theory and practice can be summarised as follows [9]:

- Complex quantitative maintenance models have flourished in recent years, but only as a mathematical discipline. Few attempts have been made to integrate these quantitative approaches with qualitative ones, like reliability centred maintenance
- The industrial application of quantitative models has been very limited as very few case studies have been published
- The impact of quantitative maintenance modelling research on decision making within maintenance organisations has been limited
- More industrial application will be seen if models are developed in conjunction with the problem owners

Rausand [38] agrees with these conclusions, citing the earlier work of Malik [39] in stating "…there is more isolation between practitioners of maintenance and the researchers than in any other professional activity". Rausand [38] goes on to conclude that many of the articles on maintenance optimisation are written by statisticians and scientists in operations research with limited knowledge about the practical context in which the quantitative models are supposed to be used, and in a language that is more or less inaccessible to maintenance practitioners. Maintenance models need to be both tractable and accessible to practitioners which is often not the case as modelling work has predominantly been undertaken by mathematicians rather than problem solvers. Unfortunately, it seems that little has changed in the last decade [40]. As well, a general problem with most quantitative models is that the necessary input data is seldom available in real industrial applications, or at least not in the format required by the models. Many practitioners have found these problems so overwhelming that they do not attempt to use quantitative models to optimise maintenance intervals, relying solely instead on qualitative assessments such as manufacturers' recommendations and past experience, resulting in maintenance intervals that are too frequent and consequentially in asset lifetime that is not fully exploited [38]. Smith [41] remarks "...it is the author's experience that any introduction of quantitative reliability data or models into the reliability centred maintenance process only clouds the preventive maintenance issue and raises credibility questions that are of no constructive value". There is a clear need to better integrate modern quantitative knowledge within the needs, abilities and context of industrial maintenance organisations, and to root reliability recommendations not only on the outputs of complex models, but also by taking in to consideration the physics of failure mechanisms and utilising human knowledge, i.e. expert judgment, about both the relevant failure mechanisms of equipment and the industrial context in which maintenance models are to be applied [38].

2.2 Prognostics and Health Management

2.2.1 PHM overview

With time based preventive maintenance schemes, maintenance actions are performed at pre-determined time intervals to restore a system to an 'as good as new' state. When the system condition can be monitored however, a condition based maintenance (CBM) strategy can be implemented where maintenance actions are dependent on the dynamic state of the system, determined typically from sensors embedded within the production process, through which health inferences are made about the system [42,43]. Within condition monitoring, sensors and sensing strategies constitute the foundational basis for fault detection [44]. Although sometimes described as an indirect measurement methodology, measured auxiliary quantities such as dynamic and static forces, vibrations, noise, temperatures etc. are in fact directly influenced by the phenomena under investigation. For example, in the machining operations domain, several such process variables can be measured online simultaneously and directly correlated to known conditions of a cutting tool [45]. This is because these process variables are affected as the cutting tool degrades. In this regard sensor suites can be described as being specific to the application domain, and are designed to measure quantities directly related to the equipment fault modes identified [44]. However, there exist many industrial situations where effective measurement methodologies do not exist for specific applications. One area where this is particularly true is in the condition monitoring of elastomers. This is discussed further in section 2.3. For further information on condition based maintenance see appendix A.

Prognostics and Health Management (PHM) expands the potentials of CBM by facilitating the prediction of equipment RUL. PHM has been defined as *an approach to system life-cycle support that seeks to reduce/eliminate inspections and time-based maintenance through accurate monitoring, incipient fault detection, and prediction of impending faults* [17]. The ultimate goal of PHM is reliably predicting system failure times to allow for efficient maintenance scheduling either autonomously or by human decision makers. To do so, different information and data sets relating to the past, present and future behaviour of the equipment in question are required. An accurate PHM system requires the availability of sufficient and relevant equipment failure data. However, the common scarcity of such data has led to the development of numerous approaches based on different sources of information and data, modelling and computational schemes, and data processing algorithms [18]. A typical PHM scheme consists of three main facets, fault detection, fault diagnosis, and fault prediction. Fault detection normally includes fault isolation, which is a task to locate the specific component that is faulty. Fault detection in a broader sense indicates whether standard operating conditions are changing/deteriorating in the monitored system, and fault diagnosis determines the nature of the fault after it has been detected. Fault detection and diagnosis fall under the CBM archetype. Building on this, prognostics deals with fault prediction, and is a task to determine whether a fault is impending and to estimate how soon and how likely that fault is to occur. Diagnostics therefore can be defined as posterior event analysis and prognostics as prior event analysis. Prognostics is much more efficient than diagnostics in achieving zero-downtime performance. Diagnostics is still required however when fault prognostics fails and a fault occurs, and is important from a root cause analysis perspective to avoid future failures of a similar nature [7].

Fault prognosis

Fault prognosis is a fundamental task of a PHM system, aiming to reliably and accurately forecast the RUL of the equipment/system so that it may function for as long as its design intended [17,18]. RUL is typically a time, cycle, or some other specific context driven expression. The RUL is the prediction of a component or systems functional/operational usage expectancy based on measured, detected, modelled, and/or predicted health state. The RUL is dependent on the intended set of operating conditions or mission to be performed [17]. An overview of the different RUL modelling approaches is outlined in figure 2.4. More information on these modelling approaches illustrated can be seen in appendix A.

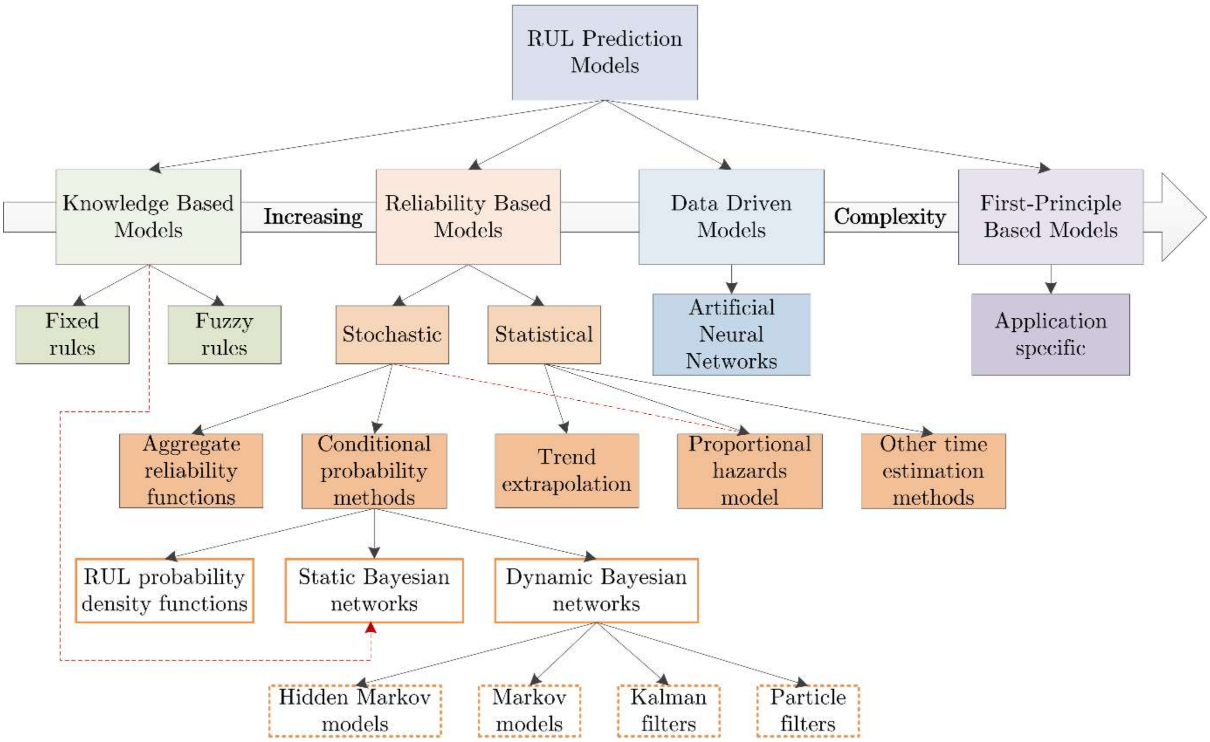

Figure 2.4: Main model categories for prediction of remaining useful life. Adapted from [40]

Engineering prognostics is used by industry to manage business risks that result from equipment failing unexpectedly. In practice, it is still predominantly intuitive and based on the experience of personnel familiar with the equipment. However, due to improved asset reliability and an ageing engineering workforce, experience is becoming increasingly hard to accumulate [40]. Sikorska et al [40] discussed a number of literature reviews covering prognostic models which have been presented by various authors. The authors opine however that although useful in appreciating the state of the art in the field, they do little to help typical industry users select an appropriate model for their specific needs, as they tend to concentrate on the technical and often theoretical merits and deficiencies of each approach, rather than practical implementation issues. In fact, Sikorska et al [40] suggest that most prognostic research work to date has been theoretical, disparate, and restricted to a small number of models and failure modes. Unfortunately, there are few published examples of prognostic models being applied in the field, on complex systems, exposed to a range of operating and business conditions. Furthermore, these reviews rarely contain a comprehensive examination of each model's practical and theoretical limitations in sufficient detail to understand exactly when and where each model should and should not be applied [40].

2.3 Elastomer Reliability

In the field of reliability engineering there is little literature on the condition monitoring of elastomers in industrial applications. However, within the polymer science domain, much work has been done on so called 'smart' elastomers, which have the potential to be used as sensors which detect their external environment and their own degradation. Such materials could be utilised readily in 'Industry 4.0' smart factory solutions. However, a concerted multidisciplinary effort is required if such devices are to be further employed and continually adapted as standard solutions in applications of high criticality.

Smart materials are defined as materials that can sense the environment and/or their own state, make a judgment and then change their functions according to a predetermined purpose. Such smart functions provided by smart materials are distinct from smart systems or facilities because they do not rely on a sense-response structure of a feedback system. Instead, they can be intrinsically sensitive to changes in their ambient environment, such as temperature, optical wavelength, absorbed gas molecules and pH values [46]. Smart materials are solid-state transducers that have piezoelectric, pyroelectric, electrostrictive, magnetostrictive, piezoresistive, electroactive, or other sensing and actuating properties. Existing smart materials such as electroactive polymers have various limitations preventing them from practical applications. These limitations centre on the requirement for high voltage or high current. Material may be too brittle, too heavy, or have a small range of strain or force actuation. Smart nanoscale materials may reduce these limitations and represent a new way to generate and measure motion in devices and structures [47].

Among the various nanoscale materials, carbon nanotubes have been described as the strongest and most flexible molecular material known due to the unique C–C covalent bonding and seamless hexagonal network. Carbon nanotubes also have electrical conductivity or semi-conductivity, and high thermal conductivity in the axial direction [48,49]. Multi-wall carbon nanotubes and single wall carbon nanotubes have opened the possibility for a new class of smart materials based on nanoscale materials [47,50,51]. Many potential applications have been proposed for carbon nanotubes, including as conductive and high-strength composites, for energy and hydrogen storage, as energy conversion devices, as sensors, field emission displays and radiation sources, and nanometre-sized semiconductor devices and probes. Nanotube sensors exhibit a fast response and a substantially higher sensitivity than that of existing solid-state sensors at room temperature [52]. Some of these applications are already utilised in products, while others are demonstrated in early to advanced devices [53]. However, Despite their promising potential, carbon nanotube production cost and limitations in processing and assembly methods are significant barriers for some applications [53].

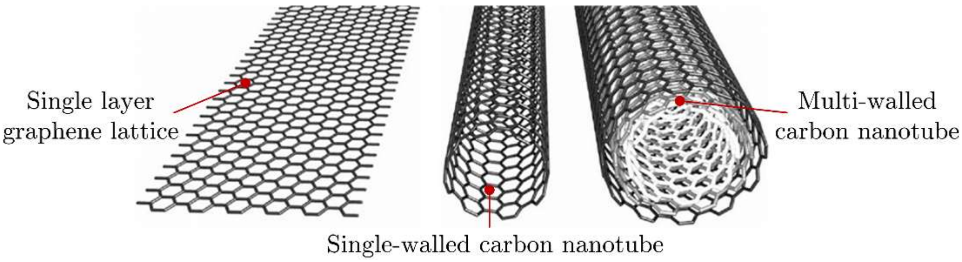

Figure 2.5: Carbon nanotube structure. Adapted from [54].

Carbon nanotubes derive their name from their long hollow structure, with the walls formed by one-atom-thick sheets of carbon, otherwise known as graphene. Graphene is the name given to a one-atom-thick two-dimensional layer of hybridised carbon [55,56]. Graphene has a range of unusual properties, for example its thermal conductivity and mechanical stiffness may rival graphite, its fracture fracture strength is comparable to that of carbon nanotubes for similar types of defects, and studies have shown that individual graphene sheets have excellent electronic transport properties. To harness these properties for applications would be to incorporate graphene sheets in a composite material [56]. However, although single-molecule detection from mechanically exfoliated graphene was an exciting proof-of-principle, the difficulty of producing thin specimens and the requirement of ultrahigh vacuum limits the practicality of these devices [55]. Despite this, Boland et al [57] recently described the production of 'G-band' strain sensors whereby liquid exfoliated graphene was infused into natural rubber to create conducting composites. The authors report that the strain sensors display a number of advantages over other nanocomposite strain sensors prepared using fillers such as carbon black, carbon nanotubes, carbon nanofibers or nanographite. Some of the cited advantages include the fact that while carbon nanotubes have large aspect ratios and have been used to produce composites with low percolation thresholds, they are expensive, making most composite applications economically unviable.

Also, due to their relatively large dimensions, carbon fibre-filled elastomers tend to have very low extensibility, making them unsuitable for high-strain applications. The authors claim that their strain sensors combine high sensitivity and high rate capability with the potential to work at high strain, and perform very well compared to the literature. They opine on the potential applications for such strain sensors, from vibration monitoring in the automotive or aerospace industry to kinaesthetic sensing in the medical devices industry. However, the instability and non-linear responses of graphene and carbon-nanotube infused polymer matrices poses a major drawback to using them as sensors in the short term. Significant bench testing is required before this technology can be used in many industries. Another drawback is that this bench testing will likely have to be adapted for each specific application.

In addition to carbon nanotubes, applications for stimulus-responsive shape memory polymers have been rapidly developed in the past few decades[46]. Such materials respond to stimulus such as, heat, chemical, and light, and change their shape at the presence of the right stimulus. Stimulus-responsive shape memory materials are able to recover their original shape after being quasi-plastically distorted, and are ideal for integrated intelligent systems, whereby the material itself can sense and then generate reactive motion [58]. As smart materials, the applications of stimulus-responsive shape memory polymers and their composites are vast. For example, current research efforts are focused on utilising them for automatic chemical sensing and water cleaning, as built-in temperature sensors for temperature monitoring, as implants for minimally invasive surgery, and as vascular stents where the shape-memory polymer is used as the drug delivery system. Future potential uses include space deployable structures, such as hinges, trusses, mirrors and reflectors, for morphing aircraft wings, smart textiles and fabrics, self-disassembling mobile phones, and shape-memory toys [59].

Included in the potentials for shape memory polymers is for self-healing purposes [59,60]. Smart materials are able to achieve healing, either intrinsically via reversible bonds present in the material itself, or extrinsically via a pre-added healing agent, in response to some external stimulus. A downside to this however is that fact that the mode of damage must be taken into consideration, as repair strategies that work well for one failure mode might be completely useless for another. For example, matrix cracking can be repaired by sealing the crack with resin, where fibre breakage would require new fibres or a fabric patch to achieve recovery of strength [61]. One of the most studied configurations for self-healing elastomers is the one proposed by White et al [62] whereby the polymer matrix incorporates a microencapsulated healing agent that is released upon crack intrusion. Polymerisation of the healing agent is then triggered by contact with an embedded catalyst, bonding the crack faces. Their fracture experiments yield as much as 75% recovery in toughness. The process is illustrated in figure 2.6.

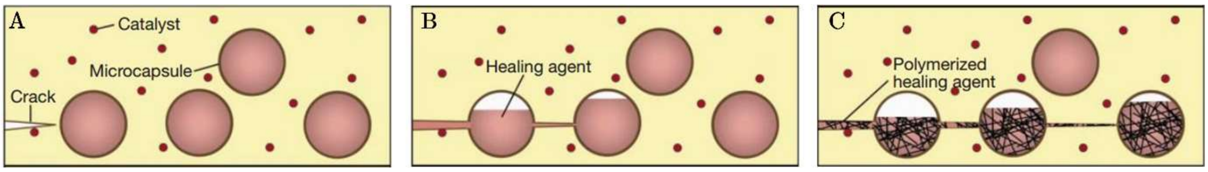

Figure 2.6: The autonomic healing concept. A: Cracks form in the polymer matrix. B: the crack ruptures the microcapsules, releasing the healing agent into the crack plane through capillary action. C: the healing agent contacts the catalyst, triggering polymerisation that bonds the crack faces closed. Adapted from [62].

Advances recently made in spectroscopy techniques, such as Raman, also have the potential to be further utilized as powerful tools to examine the degradation of mechanical properties in polymers. As composite materials are finding increasing applications in military and commercial vehicles and aircrafts, damage detection and repair becomes a crucial factor. However damage detection in polymers presents several challenges due to the anisotropy of the materials. Many existing non-destructive testing techniques are not practical for large structures and components; therefore, new reliable damage detection techniques, which are cost-effective and easily operated, need to be developed. While recent advances in autonomous repairs of polymer and composites have opened up exciting opportunities in the field of polymers, there are still several challenges of considerable interest that need to be overcome before full adoption of the self-repair technology by industry. Currently, even the best self-healing polymers can only repair damage on a small-scale and the long-term performance of autonomously healed polymers for the most part has remained unexamined. Also, there need to be more methods developed to evaluate and monitor the potential healing ability after multiple repair events. Once again, nature-inspired solutions that have evolved over millions of years can be a good starting point [63].

In this work, the component under investigation is a dynamic polymeric seal composed EPDM, consisting of ethylene, propylene, and unsaturated diene. Despite being used in many critical applications in various industries, EPDM has not been extensively studied within the smart elastomer literature. In order to advance the potential sensorisation of EPDM, it is imperative that its physical and chemical degradation processes are well characterised and understood in a multitude of applications.

2.3.1 Ethylene Propylene Diene Monomer

EPDM is an unsaturated polyolefin rubber and is one of the fastest growing rubber materials today [64,65]. The last letter "M" refers to the polymethylene, a backbone of -(CH_2)-. A rubber is composed of macromolecules, or polymers, the behaviour of which is influenced by their long-chain character. The chains are flexible such that the carbon atoms present are able to rotate around their axes. This enables the polymer chains to conform to various shapes relatively easily. The average molecular weight of EPDM is between 30,000 and 150,000, depending on the polymerisation variables and the ethylene:propylene:diene ratio. The diene is a diene as a co-monomer, which introduces unsaturation into the macromolecule [66]. The molecular structure of EPDM is shown in figure 2.7.

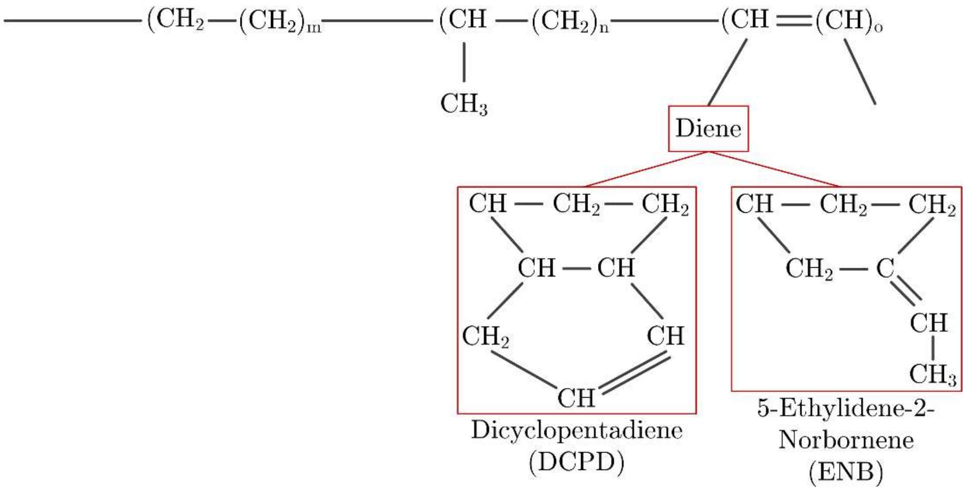

Figure 2.7: Chemical structure of EPDM with common dienes employed. Adapted from [66,67]

EPDM typically contains a mixture of the following common ingredients added during compounding [29]:

- Polymer
- Fillers, black and non-black
- Plasticisers
- Processing Aids
- Cure System(s)
- Antioxidants
- UV stabilisers
- Ozone resistance

The performance of the final compound depends not only on the selection of the specific type and grade of all ingredients, but also on the compounding and moulding process.

EPDM manufacture

Methods of EPDM manufacture include extrusion, compression moulding, and vertical and horizontal injection moulding [29]. EPDM is typically manufactured containing phenolic antioxidants ensuring good storage stability. When stored in a cool, dark environment, EPDM should have a long shelf life. However, with exposure to heat, light, or chemical agents, the shelf life of EPDM is reduced [66]. EPDM is usually produced in a hydrocarbon solvent, for example hexane, or in a suspension such as propene. The manufacturing of EPDM is based on Ziegler-Natta catalysis, a complex method of vinyl polymerisation using the Vanadium compounds VCl_4 or $VOCl_3$ as catalysts with alkyl aluminium halogens, Et_2AlCl or $Et_3Al_2Cl_3$, as co-catalysts [64]. Carbon black is the typical reinforcing material in EPDM, but more recently studies have reported that by adding a small amount of carbon nanotubes the thermal stability, flammability and mechanical properties of EPDM is strongly improved [68–70]. Recently, halloysite nanotubes have been used as a new type of filler for polymers, such as epoxy, polypropylene and polyvinyl alcohol, to improve the mechanical and thermal properties of the composites [64].

As with other elastomers, EPDM has to be crosslinked to achieve its optimum performance in terms of elasticity, tensile and tear strength, and solvent resistance. Cross-linking corresponds to the formation of a covalent link between two adjacent macro-molecules, resulting in the formation of a three dimensional network. Introduction of a peroxide cure allows the formation of thermo-stable carbon-carbon (C-C) bonds, which have the same bond strength as the C-C bonds in the polymer backbone [71–73]. Peroxide crosslinking therefore has a great effect on a number of structural and physical properties of the cured compound, such as allowing the full exploitation of the excellent heat resistance of EPDM. The peroxide curing efficiency of EPDM is determined by the structure of the diene [71]. Peroxide crosslinking occurs during curing of the EPDM compound via abstraction of the hydrogen atoms, proceeded by a rapid recombination of the residual elastomer radicals. In details, peroxide curing is initiated by the thermal decomposition of the peroxide. The resulting free radicals subsequently abstract hydrogen atoms from the EPDM polymer, yielding EPDM macro-radicals which then combine to yield direct C-C cross-links between the two polymer chains. Peroxide cross-linking occurs in about 15% of commercial EPDM applications because of the enhanced performance characteristics at high temperature [72]. The EPDM components under investigation in this work are peroxide crosslinked [74]. The amount of peroxide to be added to an EPDM rubber compound, in order to obtain an adequate state of cure usually ranges from 9 to 15 mmol per 100g of polymer.

EPDM Applications

EPDM is a distinguished synthetic elastomer with excellent properties that have made significant contributions to many fields. EPDM rubber exhibits outstanding resistance to oxidation, ozonisation, electricity and polar solvents, it has excellent thermal and chemical stability, good weathering performance, and good mechanical properties, particularly under dynamic loading conditions, [65,75]. For this reason it has been used in multiple industries in a myriad of applications, including as a high voltage polymeric insulator, roof sheeting, automotive sealing systems, building profiles, white side walls of tires, roofing sheets, and belting and sporting goods [64,75–78]. In the aerospace industry, EPDM rubber became an alternative as a thermal protection medium for rocket motors because of its low density, low processing cost, and the fact that it does not produce toxic compounds while burning. These are particularly strong advantages in relation to the copolymer nitrile butadiene rubber, which was traditionally used for this application [79]. In the biopharmaceutical industry, EPDM is one of the most common polymers employed, along with Polytetrafluoroethylene (PTFE), and polysiloxan derivatives, commonly known as silicone rubber. Within the biopharmaceutical industry, EPDM is typically used as either a static or dynamic mechanical seal; static in the form of gaskets and O-rings, and dynamic in the form of valve diaphragms, such as those considered in this work.

Unfortunately, issues with EPDM lifetime and sudden failure in service have been reported across the industry. These issues stem from the fact that polymers used in the biopharmaceutical industry are typically based on purity requirements for either the food and dairy or chemical process industries, as opposed to reliability requirements. This drives a lower demand for material performance and less rigorous sanitisation and sterilising requirements. Economics is therefore working against the true product performance need, as most seal manufacturers acquire mass produced compounds optimised for moulding throughput while meeting regulatory compliance needs. For regulatory compliance, biopharmaceutical operators must use elastomers which are USP Class VI compliant, which demands biocompatibility of materials and that the polymer must be animal derived ingredients free. This however gives no indication of how the elastomer will function as a seal, static or dynamic. This drives a commodity status of seals which demands constant lowering of price to maintain competitiveness often at the expense of performance [29].

EPDM degradation mechanisms

The degradation of EPDM rubber has been extensively studied, and the two most commonly investigated mechanisms involve two types of degradation; photo-degradation and/or thermo-degradation, both of which can be oxidative or non-oxidative [73,80–90]. It is accepted that temperature and radiation are the most crucial environmental factors affecting the aging of the polymers in general [84]. It is also commonly accepted that photo-degradation and thermo-degradation starts on the ENB moiety and eventually reaches the ethylene-propylene units [87]. Despite the extensive literature studying photo and thermo degradation, there is scant literature on the effects of acidic and basic environments on the rate of EPDM composite degradation. McGrath et al [91] studied the accelerated aging of EPDM polymer insulators subjected to acid rain with a pH of 4.6. The samples were also subjected to UV radiation. They concluded that due to the acid and UV exposures that surface roughening and the removal of low molecular weight oils will occur. They did not report on any other change in mechanical or chemical properties due to the degradation effects. Mitra et al [92–94] and Nandakumar and Philip [95] investigated the effect of 20% and 60% aqueous solution of H_2SO_4 sulphuric acid on EPDM rubbers respectively. These studies concluded that acid induced chemical degradation of EPDM results in an initial decrease in crosslink density due to hydrolytic attack of the crosslink sites. Upon further exposure however, these oxygenated species lead to new crosslinks and thus higher crosslink density. They also note that most of the degradation products are confined to the EPDM surface, but that this degradation in enough to affect the bulk mechanical properties.

Most polymeric materials are subject to oxidation, the rate of which depends on the polymer type, processing method and end use conditions. Oxidation of rubber in particular can result in loss of physical properties such as tensile strength, elongation and flexibility. Crosslinking and chain scission, which is the scissioning of the macromolecular chains, due to oxidation modifies the macromolecular chains of the material, the consequence of which is the change in the mechanical properties of the material. [73]. Although chain-scission is an issue, Zhao et al [85] demonstrate that the degradation aging process of EPDM proceeds predominantly via crosslinking. The oxygenated species generated combine with each other and cause new crosslinks, which result in an increase in the crosslink density. For example, cross-linking causes the polymer to increase in molecular weight, leading to brittleness, gellation, and decreased elongation at break [96]. Kwak and Choi [88] studied the aging behaviours in the top layer and the interior of EPDM components subjected to thermo-oxidative stresses of 125°C and 180°C for periods of 2, 4, and 7 days. They found that crosslink density increased with increasing thermo-oxidative stress corresponding to the amount of time the samples spent in the accelerated aging environment. They noted that as additional crosslink bonds were formed, the crosslink density of the inner part of the sample, at an approximate depth of 2mm, increased by approximately 7% compared to the cross link density at the surface. Little oxidation in the inner part allowed for the formation of additional crosslink bonds during the vulcanisation reactions.

Redline et al [97] recently demonstrated that EPDM shows visible signs of degradation following thermo-oxidative conditions but maintains integrity under thermo-hydrolytic and thermo-hydrolytic plus thermo-oxidative conditions. They showed that steam reduces oxidative degradation levels in EPDM.

Surprisingly, this inhibition effect seems to be amplified as temperature is increased. It was shown that the effect of steam was not limited to one specific EPDM formulation as three different formulations showed the same trend. A combination of chemical and physical property changes in the presence of steam, such as oxidation rate and O_2 permeability changes, additional sensitivity to hydrolytic damage, as well as mechanistic changes in relation to hydro-peroxides may act in parallel and result in these surprising material degradation behaviours. This is significant as it shows that EPDM still offers some limited performance at high temperatures in the presence of steam. Importantly however, Pourmand et al [98] recently revealed that EPDM oxidation occurring at higher temperatures causes more hardening of the rubber for a given degree of oxidation than lower temperatures. They propose that EPDM oxidation yields more crosslinking at higher temperatures than at lower temperatures. This would mean that despite oxidation being retarded due to steam exposure as demonstrated by Redline et al, higher temperature steam may still cause significantly more hardening of EPDM despite a reduction in oxidation present.

Both Harper [96] and Nair [83] et al note that changes in tensile strength in EPDM blends can be attributed to two causes. Firstly, chain scissoring of EPDM composites decreases molecular weight, leading to increased melt flow, increased elongation, and reduced tensile strength, while higher cross-link density increases tensile strength but reduces plastic deformation under tension and elongation. Dijkhuis et al [99] also studied the relationship between the crosslink density of EPDM composites and a number of mechanical properties. They concluded that with increasing crosslink density, tensile strength, surface hardness, and elastic modulus increased, while the elongation at break and the tear strength decreased. They reported that compression set improves with increasing crosslink density, meaning with more crosslinking the rubber is better able to return to its original shape after compression. However, Nabil et al [86] state if the crosslink density becomes too high, that the average molar mass of the rubber chain between two successive crosslink points decreases, restricting the mobility of the chain segment. This limits the orientation of the network chain, and the reduced number of effective network chains results in a decrease in the tensile strength, as the number of effective network chains influences the tensile strength. Secondly, they agree that generally a reduction in tensile strength can be attributed to chain scissions. Scission of the larger molecular chains increases the number of shorter chains of the respective polymer, which leads to fewer entanglements, and thereby decreases the tensile strength. They also note that decomposition temperatures are lower in EPDM blends which are exposed to a thermo-oxidative degradation environment of 100°C for 48 hours, indicating that thermo-oxidation degradation also lowers the future thermal stability of EPDM blends.

While tensile and impact strength are specifically governed by the short molecules, for other properties like solution viscosity and low shear melt flow, the influence of the middle class of the chains is predominant, while other properties such as melt elasticity are highly dependent on the amount of the longest chains present [100]. George et al. [101] state that less crystalline materials are degraded more rapidly by heat, and that crystallinity, crystalline size, order, degree of polymerisation and crystal structure influence thermal decomposition rates. It is reported that increasing the crystallinity of polymers increases the interaction between polymer chains. In the highly ordered state associated with crystalline materials, it is less possible for polymer chains to move relative to one another, as additional forces must be overcome in the transformation to the unordered fluid state. Crystallinity is enhanced by a symmetric regular polymer structure and highly polar side groups. Regular polar polymers, such as polyesters and polyamides, crystallize readily [102]. Peroxide curing is known to improve the chances of crystallisation in EPDM as compared to sulphur curing, as the macromolecules are aligned and brought closer because of intermolecular C-C bond formation [103]. Tear strength has been shown to be more vulnerable to different crosslink structures, while cyrstallisability has been shown not to be an important factor in tensile strength. EPDM is also capable of undergoing strain-induced crystallisation, as it contains reactive monomer units which are distributed randomly by the polymerisation process and thus a random network is obtained [104].

The role of shear force is also significant in EPDM degradation, particularly as EPDM is a high molecular weight polymer [66]. Shear force causes stretching of the EPDM matrix, and when the EPDM matrix stress limit is exceeded, network breakdown will occur. As the crosslink density decreases, the network becomes looser and the chain stability of the EPDM matrix increases [67]. The energy applied to the matrix must be sufficient to create high tension between the crosslinks, leading to bond ruptures and to the dissociation of the crosslink bonds [66]. Aside from oxidative degradation, many rubber materials contain oil extenders, also known as plasticisers, which migrate to the surrounding media during service or accelerated ageing. The loss of these substances over time also impacts the mechanical properties of the rubber. Typically, the elastic modulus is increased and the strain at break is decreased with the loss of oil extender. The kinetics for the loss of oil extender is different from that of oxidation and the diffusion of oxygen [105].

Naebe et al [63] extensively reviewed crack initiation and propagation in polymers, although they don't analyse EPDM specifically. The authors explain that crack initiation in a polymer matrix can happen as a result of several phenomena such as mechanical fatigue, surface breaking, thermo-mechanical stress, as well as environmental factors such as UV exposure and hydrothermal aging. For instance, subsurface delamination, transverse ply cracking, surface cracking, and polymer matrix cracking would be created as a result of impact loading. When the energy required for crack growth is equal or larger than required energy for the creation of a new surface the crack will propagate. Cracks will propagate through polymer once the crack geometry and applied stress varies throughout cyclic or monotonic loading, reaching a critical stress intensity. During a monotonic load, the size of crack growth is directly correlated to the experienced maximum stress. However, during cyclic loading crack growth and damage volume is a more complex mechanism, associated not only with the experienced maximum stress but also with changes in loading conditions, the undamaged polymeric structure, and the polymer geometry. In the near future, advanced theoretical modelling and simulations are required to accurately predict crack-induced changes in mechanical properties, such as shear and transverse modulus and the model predictions need to be validated by experimental data. Better knowledge of the theoretical and practical aspects of crack and micro-crack damage directly influences the design of more durable polymeric materials, which is of high safety and economic importance.

2.3.2 EPDM Degradation Testing Methods

Elastomer degradation through environmental exposures can provide additional insights into the nature of underlying relationships between network microstructure and mechanical properties [106]. Such relationships could then be formalised for use in degradation models describing component lifetime. To determine the exact mechanisms responsible for EPDM degradation, multiple testing methods be used. In elucidating the various degradation products in a rubber system, more than one analysis technique is typically employed and the results are correlated, as no single methodology can provide a complete evaluation of the complex mechanisms involved [107]. A number of the most pertinent testing methods for EPDM degradation are discussed below, including reasons for their particular use.

Shore hardness

Shore hardness is the measurement of a polymers ability to withstand indentation. In the EPDM polymer chain, oxidised substances, such as carbonyl, hydroxyl, and ester groups, raise the strength and hardness of an oxidised polymer 'skin' layer. This oxidised layer becomes thicker as aging time increases. Where oxidation is active in the polymer, hardness is sharply increased. In aged EPDM composites, an oxidised skin layer with a thickness of about 1.5-2mm develops. Deeper than 1.5 to 2mm, hardness values are largely the same as virgin samples. Therefore, as EPDM samples become thinner, the oxidised skin layer has more of an influence on the degradation behaviour of the component [88,105]. The hardness that occurs in EPDM blends after ageing is associated with the increase in crosslink density, which is strongly related to the high rate of radical termination in the polymer bulk [83,86]. A major limitation of this method is that it can only determine bulk material properties. In terms of the material properties of the rubber, the hardness is a complex response to an applied indentation which depends upon the elastic modulus of the rubber and the viscoelastic properties of the rubber [108].

Dynamic flexural testing

The tensile strength of EPDM having undergone chemical or thermal degradation is a complex function combining the nature and type of crosslinks, crosslink densities, and the chemical structure of the rubber, in particular whether the EPDM has been vulcanised with sulphur or peroxide, the former typically having higher strength [104,109]. It has been reported that while keeping strain and strain rates as a constant, observing the differences in the elastic modulus and induced stress under these conditions can identify if crosslinking or chain scission has occurred in the material [99,106]. It is reported that if crosslinking is predominant in EPDM, both the modulus and the induced stress for a given strain increase, while both the modulus and the stress for a given strain decrease if chain scissions are prominent [99,106]. Flexural compression testing, also known as a three-point bend test, is conducted keeping the flexural strain rate constant until the material yields. From this the final strain at yield, the work required to final strain, and the flexural modulus of the material are calculated.

Observing the force required to strain EPDM samples allows the indirect observation of the stress required to strain the material and the modulus of the samples. Assuming the EPDM behaves as an incompressible, isotropic, and perfectly elastic neo-Hookean solid, as strain (ε), strain rate ($\varepsilon(t)$), and the cross sectional area (A) of each sample is constant, using the relationship $F = {}^{\sigma}/_{A}$ implies that an increase in force equals an increase in stress (σ). Similarly, as Young's modulus $E = {}^{\sigma}/_{\varepsilon}$, an increase in force also relates to an increase in the material modulus. The flexural compression testing confirms this by measuring the flexural modulus of the samples from the slope of the resultant stress-strain curve.

Flexural modulus E_F is an intensive material property, considered proportional to the elastic modulus E, and is calculated via [110]:

$$E_F = {}^{\sigma_{F2} - \sigma_{F1}}/_{\varepsilon_{F2} - \varepsilon_{F1}} \tag{2.3.1}$$

where σ_F is the flexural stress, calculated as:

$$\sigma_F = {}^{3FL}/_{2bh^2} \tag{2.3.2}$$

where F is the applied force in Newtons, L is the span in millimetres, b is the specimen width in millimetres, and h is the sample height in millimetres. The flexural strain ε_F is calculated as:

$$\varepsilon_F = {}^{6sh}/_{L^2} \tag{2.3.3}$$

where s is the sample displacement in millimetres.

Compression set

Compression set, i.e. elastomeric creep, testing measures the ability of rubbers to retain their elastic properties at a specified temperature after prolonged compression at constant 25% strain. When rubber is held under compression, physical or chemical changes can occur that prevent the rubber returning to its original dimensions after release of the deforming force [111]. Compression set values of EPDM depends on the overall crosslink density, whereby compression set improves with increasing crosslink density, because more crosslinks are present to restore the rubber to its original shape after deformation. However, the length of the crosslinks also plays a role, because polysulphidic bonds rearrange at high temperatures forming new, shorter crosslinks, which eventually prevent the full recovery of the deformed material, potentially worsening the compression set [88,99]. The creep percentage C_S is expressed as a percentage of the initial compression and is given by the formula [111]:

$$C_S = {}^{h_0 - h_1}/_{h_0 - h_s} \; x \; 100 \tag{2.3.4}$$

where h_0 is the initial sample thickness, h_1 is the sample thickness after recovery, and h_s is the height of the spacer used in the compression fixture. Again, a drawback of compression set testing is that it only provides insight into bulk mechanical properties.

Dynamic mechanical thermal analysis

Polymers display properties of both elastic solids and liquids. This leads to a specific relationship between stress (σ), which changes according to a periodic law for viscoelastic bodies, and strain (ε) whereby:

$$\sigma = E^{*}.\,\varepsilon \tag{2.3.5}$$

where E^{*} is the complex modulus of elasticity, given by:

$$E^{*} = E' + iE'' \tag{2.3.6}$$

where E' is known as the dynamic modulus of elasticity, or the storage modulus, while the imaginary component iE'' is called the loss modulus. The phase shift between the sinusoidally varying stress and strain is expressed as

$$tan\;\delta = {}^{E''}/_{E'} \tag{2.3.7}$$

where $tan\;\delta$ is known as the mechanical loss factor, the loss tangent, or the damping factor [86,103]. Among the most reliable ways of determining these components is via dynamic mechanical thermal analysis (DMTA) which enables the thorough investigation of the relaxation mechanisms in viscoelastic materials. The most common use of DMTA is the determination of the glass-transition temperature (T_g), where the molecular chains of a polymer obtain sufficient energy to overcome the energy barriers for segmental motion. This energy is typically thermal. The glass-transition temperature region is where the maximum loss of applied energy is observed as a peak in the damping factor versus temperature curve [103].

It is widely accepted that both the storage modulus and the glass transition temperature are directly proportional to the degree of elasticity, and chemical or physical crosslink density [86,103,112,113]. This is because the higher the crosslink density, the harder it is for individual chains to move when the elastomers are subjected to mechanical stress. Therefore, higher energy is then needed to overcome any type of molecular interactions that affect the molecular motion [86]. Lower temperatures favour a more 'glassy', elastic response due to insufficient time or mobility for viscous or dissipative deformation mechanisms to take place. Similarly, higher temperatures lead to a more viscous or rubber-like response [113]. Therefore, DMTA is a useful method to study the influence of chemical exposure on material flexibility, degree of crosslinking, and the shifting of the glass transition temperature.

Thermogravimetric analysis

Solid polymeric materials undergo physical and chemical changes when heat is applied, which result in changes to the material and to material properties [102]. For clarity, a distinction should be made between thermal decomposition and thermal degradation. Thermal decomposition is a process of extensive chemical species change caused by heat, whereas thermal degradation is a process whereby the action of heat or elevated temperature on a material causes a loss of physical, mechanical, or electrical properties [102]. Thermogravimetric analysis (TGA), in which the weight loss of a sample is measured as a function of increasing temperature, is an accepted technique in determining the thermal and oxidative stabilities and the compositional properties of polymers and polymer blends. It remains the most commonly used thermal decomposition test in both homogenous and non-homogenous polymer blends [73,80,84,86,101–103,114,115]. Compositional analysis via TGA is used to determine the amounts of organics, such as polymer, carbon black, and ash fillers in a rubber compound [116].

Fourier transform infrared spectroscopy

Generally, polymeric materials are subjected to oxidation, the rate of which depends partly on the polymer type and end use conditions. It is important to characterise the degree of polymer oxidation in the exposed samples as oxidation leads to both chain scission and crosslinking of polymer chains which may result in embrittlement [73]. This occurs because during oxidation processes, additional saturation reactions of the residual carbon double bonds occur. The additional saturation reactions result in crosslinking reactions very similar to those occurring during the initial vulcanisation processes of elastomer manufacture [89]. Oxidation of rubber can result in the loss of physical properties such as tensile strength, elongation, and flexibility. For this reason, oxidation stability can be used as a determinate of service life [86]. With FTIR-ATR the bands that characterise EPDM rubbers are found via the wavenumbers attributed to their vibrational modes [79].

Soxhlet extraction

Crosslinking and chain scission kinetics are related to the evolution of the soluble and insoluble fractions of a material. A decrease of the soluble fraction can be due to the formation of new crosslinks, while an increase in the soluble fraction relates to chain scission having occurred in the polymer matrix [83,106,117,118]. Solid-liquid solvent extraction of solid samples serves to remove and separate compounds of interest from insoluble high-molecular-weight fractions. The Soxhlet extractor is the most widely used leaching technique for this purpose, whereby the sample is placed in a thimble-holder that is gradually filled with solvent from a distillation flask. When the solvent reaches the overflow level, a siphon aspirates the solute from the thimble-holder and unloads it back into the distillation flask, thus carrying the extracted analytes into the bulk liquid. This operation is repeated until extraction is complete. Although a simple technique, Soxhlet extraction can extract more sample mass than most of the latest alternatives including microwave-assisted and supercritical fluid extraction [119].

Once extraction is complete, the soluble and insoluble fractions of the vulcanised EPDM are separated. The gel fraction is defined as the insoluble fraction of the polymer matrix. This comprises potential filler additives such as MgO or ZnO, sulphur, and carbon black which are all fixed within the polymer network and thus contribute to the insoluble fraction. Other chemicals, in particular oil and accelerator residues, are assumed to be extractable, and are collectively known as the soluble fraction of the polymer [99].

The gel fraction G_F is determined via [118,120]:

$$G_F = {}^{M_{insoluble}}\!/_{M_{initial}}\ x\ 100\% \tag{2.3.8}$$

where $M_{insoluble}$ is the mass of the dry gel post extraction and $M_{initial}$ is the mass of the rubber sample pre extraction. The soluble fraction S_F, containing all the non-polar substances, is equal to $1 - G_F$ [106].

In many studies, matrix network chain density is estimated using the Flory-Rehner equation [121]. However, as noted by Planes et al [106], this equation depends on a constant coefficient f describing the network functionality, and the Flory–Huggins polymer–solvent dimensionless interaction term. However, the network functionality is decreased as a result of material ageing, and the value of the Flory–Huggins parameter is also difficult to estimate after material degradation. To compound this problem, the result calculated from the Flory-Rehner equation is strongly sensitive to the Flory–Huggins parameter. Valentin et al. [122] also agree with this assertion. They have shown that certain approximations used in the Flory-Rehner equation fail in both the description and the prediction of the rubber network behaviour. They conclude that the Flory−Rehner equation is only useful as a qualitative evaluation of crosslink density. Given these observations only the soluble fraction data is considered in this work as an indicator of crosslink density and additive leaching.

Accelerated Life Testing

Accelerated life testing is an important and necessary step in the development of new material sets and new material applications in a range of industries. Several methods are available for extracting useful data which describes actual operation from accelerated testing data [123,124]. Tang and Chang [125] use the Eyring model to explain degradation measure dependence on accelerated factors. Park and Padgett [126] describe a method for extracting information from accelerated degradation testing with multiple degradation factors. By applying these methods, it is possible that the collected data can be used to develop models of component failure, as the accelerated life data informs the first modelling steps during the product design and development phases. However, care must be given to ensure that the failures seen during accelerated testing are analogous to real-world failures. Accelerated testing conditions can result in fault modes which only occur under the accelerated conditions.

'Corrodere' is the Latin term for gnawing or slow degradation, which can gradually lead to the loss of physical and/or mechanical properties in polymers and cause problems such as leaks, requiring costly repairs, particularly in safety critical industries such as in the mining, gas and oil industries. Polymers which are used for corrosion protection can themselves become a main feature of corrodere. Coatings, liners, umbilicals, O-rings, seals or other protective systems can all be attacked in a slow but insidious way. Hydrolysis of the polymer is one of the most common breakdown mechanisms, which applies to polymers such as nylon, polyurethanes, and polyesters that have hydrolysable linkages in the main chain. Other mechanisms include oxidative degradation, particularly if air can gain access, and biodegradation of the polymer. Accelerated aging tests followed by mechanical testing and molecular weight analysis are the most useful general methods for appraisal of the likely future state of the polymeric material [127].

Using a combination of the EPDM degradation test methods described above, several researchers have investigated accelerated life testing of polymers to help product development and characterisation. Deepalaxmi and Rajini [81] exposed EPDM and Silicone Rubber to gamma/electron beam irradiation for their use as seals in Nuclear Power Plants, in order to forecast long-term performance. Dixon and Boyd [128] investigated the effects and underlying mechanisms of ageing of poly(ether block amide) used in angioplasty balloons. They recommend the use of accelerated testing protocols at temperatures of up to 45°C to generate room temperature shelf life estimates. Hamid and Amin [129] carried out natural and artificially accelerated weathering trials on low-density polyethylene samples used for agricultural and disposable purposes. They found that the confidence level of predicting lifetime on the basis of artificially accelerated exposure trials is dependent on many parameters, which include time, material, equipment, etc. The authors do not recommend a particular testing methodology which is superior. Conversely, Miyano et al [130] developed an accelerated testing methodology based on the time-temperature superposition principle for the prediction of long-term fatigue life of polymer matrix composites. The authors demonstrated that their methodology was a robust way of long-term strength and life prediction for the polymer matrix composites, and summarised the detailed procedure for formulating the master curves of creep and fatigue strengths for the composites. These curves can be used by other authors as the master curves for the the analysis of micromechanics of failure. Le Gac et al [131] investigated the durability of polymer coatings used as thermal insulation of steel pipes in the offshore oil and gas industry, a major issue for this industry. The authors characterised polymer evolution during ageing using both mechanical (tensile test and DMTA) and chemical (FTIR) analyses. Lee et al [132] investigated the tribological properties of a fluorocarbon elastomer seal with the aim of developing suitable accelerated wear test conditions. Their accelerated life testing method could serve as a good reference for development of accelerated life testing methods for other types of elastomers and seals to later be used to aid in life prediction.

2.4 Statistical analysis techniques for reliability model development

One of the essential technical pillars which has supported the rise of reliability engineering as a scientific discipline is the theory of probability and statistics. The developments within statistical reliability approaches have been driven by a cultural shift from the traditional industrial economy, valuing volumetric output, to the modern industrial economy centred on service delivery, i.e. product performance. This change of view has led to increased attention of system availability and the development of techniques for its quantification. Statistical analysis techniques within reliability engineering have been challenged by three fundamental tasks: system representation and modelling, system model quantification, and uncertainty modelling and quantification. Given the complexity of modern industrial systems, an integrated approach in which the hardware, software, and human elements of the systems and their dynamic interdependences are taken in to account are required in combined frameworks [133].

2.4.1 Survival and hazard functions

Two critical functions for describing data within reliability analysis are the survival function $S(t)$ and the hazard function $h(t)$.

The survival function is the probability that a component or system survives longer than some time t, formally:

$$S(t) = P(T > t) \tag{2.4.1}$$

where T is a continuous random variable describing the time elapsed until component failure. The survival function is therefore the inverse of the cumulative distribution function $F(t)$ of T, i.e.:

$$S(t) = 1 - F(t) \tag{2.4.2}$$

From this it can be seen that $S(t)$ is non-increasing and has the following properties: $S(t) = 1$ for $t = 0$ and $S(t) \to 0$ as $t \to \infty$ [44,134].

The hazard function is defined as the instantaneous failure rate at any time instant t, given that the component survives up to time t. It measures how likely a component is to fail as a function of the age of the component [135]. It is defined as:

$$h(t) = {f(t)}\Big/{1 - F(t)} = {f(t)}\Big/{S(t)} \tag{2.4.3}$$

where $f(t)$ is the probability density function of T [134].

2.4.2 Multi-State degradation models

The basic assumption within traditional statistical reliability techniques is that the failure phenomenon is characterised to a large extent as a random event, more particularly in respect of the 'instant' of failure. Approximating statistical models to characterise failure attributes entails collecting failure data from a population of similar components operating in the field. Based on the time to failure data estimates and number of failures encountered the failure rates are estimated. However this can lead to relatively large levels of uncertainties due to, for example, non-availability of sufficient data, adequacy of the model that represents the data trends, and improper interpretation of the data and models [136]. To reduce these uncertainties, traditional statistical modelling approaches have required the availability of large amounts of historical process data [137]. A commonly adopted assumption underlying the quantitative analysis of system failures by reliability engineering methods is that systems are made up of binary components, i.e. devices that can be in two states: functioning or faulty. However, modern industrial systems are represented more accurately as multi-state systems, meaning the systems overall performance level lies somewhere between 0% and 100% of the nominal system capacity. The difference between the two approaches is illustrated in figure 2.8. The analysis of multi-state systems entails the development of new representation, modelling and quantification techniques [133].

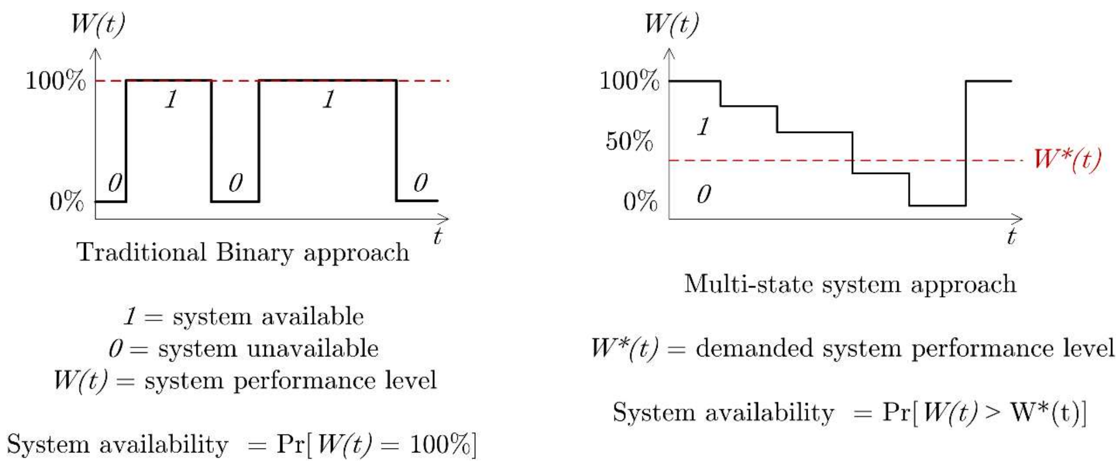

Figure 2.8: Binary and multi-state system approaches in reliability modelling. Adapted from [133].

The multi-state degradation failure model was first introduced by Sim and Endrenyi [138]. Their modelling assumptions were that the system experiences several stages of performance degradation before it fails and the time for the system to stay in each stage was exponentially distributed. While multi-state degradation modelling approaches can be utilised within traditional CBM paradigms, they can also be exploited in industrial situations where no CBM technology exists or is suitable for a given application. One typical source of information that can replace traditional CBM data is provided by the practice of observing the inspected or replaced components and classifying their degradation state into multiple exclusive degradation categories. This allows collecting observations about equipment degradation condition in different instants of its lifetime. This means the model introduced by Sim and Endrenyi can be extended to situations where the system undergoes periodic inspections to determine what degradation stage it is in. At each stage, minor preventive maintenance may be carried out to restore the system to the previous deterioration stage, while major maintenance work restores the system to 'as good as new' [42]. Multi-state degradation modelling can be employed to statistically treat this type data via the discretisation of the equipment degradation process into three or more states, each one associated with a certain range of values of suitable degradation indicator variables. Examples of this approach are numerous in the literature. Compare et al [139] investigated oxidised areas in gas turbine nozzle systems. Baraldi et al [140] investigated electrical resistance values in electrical power switches. Moghaddas and Zuo [141] studied the linear extent of wear in bearing shells. Liu et al [142] developed a Bayesian framework to assess the reliability and performance of multi-state power generating systems. The main advantage of the multi-state modeling approach over the widely used binary model lies in its ability to more accurately fit the sequential phases of degradation, which may even be physically different to one another [143].

2.4.3 Parametric distributions within reliability analysis

The most common parametric model used in reliability analysis is the Weibull distribution, despite the fact that statisticians initially chose the exponential distribution to model life data because the statistical methods for it are relatively simple [18,28,144]. Despite being easier to model, the exponential distribution is limited in applicability because it has only one parameter, the scale parameter λ, also known as the characteristic life of a component or system. By adding a shape parameter β, the distribution becomes considerably more flexible. The generalisation of the exponential distribution to include the shape parameter is the Weibull distribution [134]. With regards to multi-state degradation models, the transition times from one state to another are often assumed to be Weibull-distributed [141,145]. This choice is due to the flexibility that the Weibull distribution offers in the variability of its parameters, as well its ability to retain 'memory' of previous degradation states. This means the time spent by a component in a particular degradation state can influence the next stochastic state transition time [146]. The cumulative distribution function $F(t)$ of the Weibull distribution $W(\lambda,\beta)$ is [134]:

$$Fw(t|\lambda,\beta) = 1 - e^{-\left({}^{t}/_{\lambda}\right)^{\beta}} \tag{2.4.4}$$

where $\geq 0,\ (\lambda,\beta) \in (0,\infty)$. The density function $f(t)$, also known as the failure distribution, is [134,147]:

$$fw(t|\lambda,\beta) = {}^{\beta}/_{\lambda}\left({}^{t}/_{\lambda}\right)^{\beta-1} e^{-\left({}^{t}/_{\lambda}\right)^{\beta}} \tag{2.4.5}$$

The hazard rate and survival function of the Weibull distribution therefore are, respectively, the two parameter models [18,28,134]:

$$h(t) = {}^{\beta}/_{\lambda}\left({}^{t}/_{\lambda}\right)^{\beta-1} \tag{2.4.6}$$

and:

$$S(t) = e^{-\left({}^{t}/_{\lambda}\right)^{\beta}} \tag{2.4.7}$$

The Weibull distribution is extremely flexible in its ability to model numerous forms of reliability data. It allows for the modeling of components with decreasing failure rate as a function of time when $\beta < 1$, for components with constant failure rates when $\beta = 1$, and components with increasing failure rates when $\beta > 1$ [28,134]. When $\beta = 1$ the Weibull distribution becomes the exponential distribution, when $\beta = 2$ it becomes the Rayleigh distribution, while for $3 \leq \beta \leq 4$ the Weibull distribution can be approximated via the normal distribution. For large values of β, typically ≥ 10, the Weibull distribution can be approximated as the smallest extreme value distribution [134]. Different Weibull probability density, hazard rate, and survivor function curves are shown in figure 2.9, representing different values of the shape parameter β with a fixed scale parameter $\lambda = 1$. Note how the hazard rate for $\beta = 0.5$ begins elevated, signifying high infant mortality rates, which then decreases as time continues. This trend is reversed for $\beta = 2$ and $\beta = 4$. Note also how the hazard rate for $\beta = 1$, i.e. the exponential distribution, remains constant. Constant failure rates are also known as 'hard' failures in the sense that the system fails abruptly under such circumstances, rather than gradually worsen over time. Gradual degradation failures are also known as 'soft' failures [42].

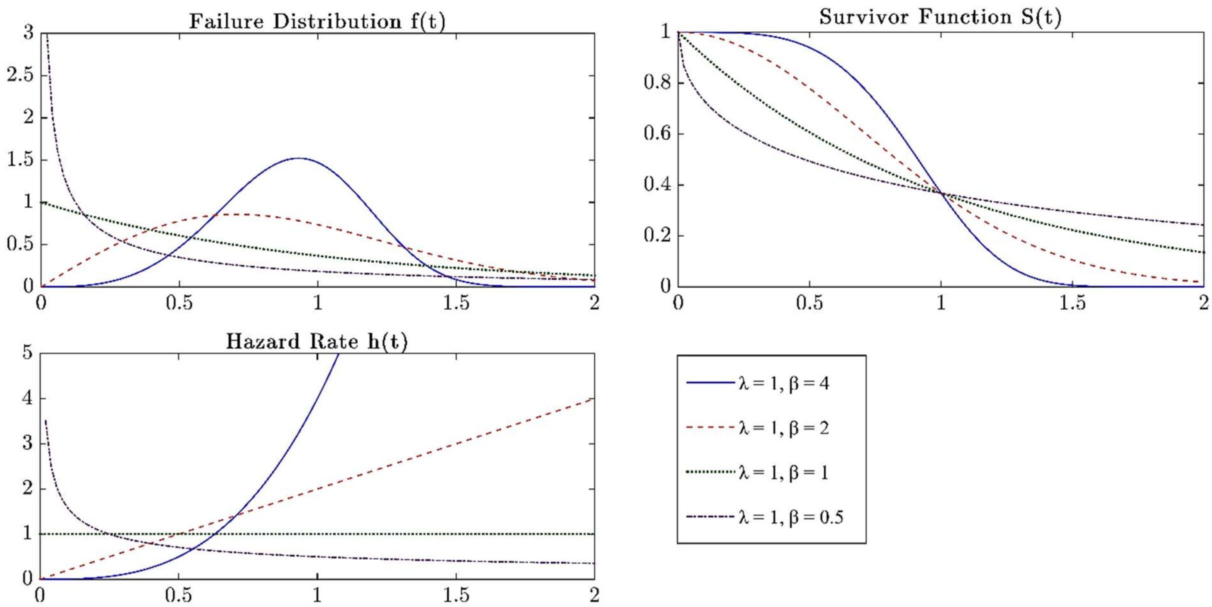

Figure 2.9: Weibull failure f(t), survivor function S(t), and hazard rate h(t) distributions for different shape parameters

In industrial applications, systems and components exist within complex environments described by a multitude of both operational and ambient conditions. It is expected that equipment operating under harsh conditions will fail earlier than equipment operating under more mild conditions. To improve the reliability estimation of systems and components, reliability lifetime modelling approaches need to encode these different influencing conditions. This need leads to the development of degradation models including explanatory variables that describe the operational environment [18]. Particularly in industrial applications where system downtime must be minimised, it is necessary that as many significant factors as possible, describing the operational and environmental conditions in which the system is operating, are taken into account. These operating conditions, known henceforth as covariates, can remarkably influence the degradation process of a system. It is of course intuitive to consider usage conditions, both past and future, when estimating the RUL of a system. Methods which commonly fall into this category include regression analysis with prognostic monitors, Markov Chain models, physics- of-failure models, and Life Consumption models [28].

Despite their being numerous models available with which to encode the effect of covariates on component lifetime, the two classical approaches proposed and used in a wide range of applications are the Accelerated Life and Proportional Hazards Models, both of which have proven to be effective [148]. Both approaches consider a baseline probability model, or hazard rate, describing the evolution of the degradation process under a single operating condition, often labelled as a 'time' variable. This can be any function such as calendar time, hours of operation, time under a certain environmental condition etc. Additional covariates are then introduced to the model which refines the modelling of the degradation process by taking into account further conditioning aspects of the component life, such as environmental exposures, static and dynamic loadings etc. The additional covariates influence the equipment hazard rate, which can also mean the rate of transition between degradation states [149]. Both accelerated life and proportional hazards methods build on the baseline probability model which describes the failure state transition times when all the considered covariates are null. The difference between the accelerated life and proportional hazards models lies in the modelling of the dependence of the aging process on the covariates: multiplicative factors in the failure rates are used in proportional hazards models to model the effects of covariates [150], whereas the covariates impact on time to failure in accelerated life models [151–153]. Conveniently however, the accelerated life and proportional hazards models coincide when the baseline function is parameterised into a Weibull distribution, taking advantage of both models [148]. As covariates can easily be incorporated into Weibull proportional hazards models and their effects on the hazard rate evaluated, this is highly advantageous over other statistical approaches in modelling times to failure [154].

Proportional Hazards Model

The Cox Proportional Hazard Model is a well-known method capable of including additional stress information related to the environmental and operating conditions which modifies the baseline, 'average' hazard rate [18,150]. Specifically, Cox assumed that the survival distribution satisfies the condition [134]:

$$h(t|x) = h_0(t)e^{\sum_{j=1}^{q}\gamma_j z_j} \tag{2.4.8}$$

where the additional stress information is represented by the multiplicative covariates Z_j. Failure data collected at different covariate conditions are used to estimate the coefficients γ_j, typically by ordinary least square algorithms [18]. $h_0(t)$ is called the baseline hazard function, because it is the value of the hazard function when $Z_j = 0$ [134]. The coefficients γ_j tune the effects of the selected covariates on the multi-state transition times. The Weibull distribution can be incorporated into the Cox proportional hazards model via the parameterisation of the baseline hazard function where the value of $h_0(t)$ is dependent upon the Weibull scale λ and shape parameters β, such that:

$$\stackrel{h_0(t)}{\Longrightarrow} h(t|\lambda, \beta, Z = 0) = {}^{\beta}/_{\lambda}\left({}^{t}/_{\lambda}\right)^{\beta-1} \tag{2.4.9}$$

which, when the covariates and their coefficients are included, yields:

$$h(t|\lambda, \beta, Z = 0)e^{\sum_{j=1}^{q}\gamma_j z_j} = h(t|\lambda, \beta, \gamma, Z) \tag{2.4.10}$$

From equation (2.4.10) it can be seen that the updated hazard function, which takes into account the effects of the covariates, is proportional to the corresponding baseline hazard function. This proportionality is a function of the time-independent multiplicative factor $e^{\sum_{j=1}^{q}\gamma_j z_j}$. The time independency of this multiplicative factor means that coefficients γ and covariates Z do not depend on time.

Under this hypothesis, usually referred to as the proportional hazards assumption, the Weibull baseline hazard model yields a modified Weibull proportional hazards model such that:

$$h(t|\lambda, \beta, \gamma, Z) \approx Weibull\left({}^{\lambda}/_{e^{\left(\sum_{j=1}^{q}\gamma_j z_j/\beta\right)}}, \beta\right) \tag{2.4.11}$$

Logistic regression

Regression techniques have been widely used by researchers within data-driven diagnostic and prognostic algorithms [155–157]. Within non-probabilistic techniques, some of the best RUL estimation results have been obtained by using one of neural networks, Bayesian networks, and regression [158]. For example, Yan et al [159] employed a logistic regression model to calculate the probability of failure of assets given certain condition variables, and Wang [160] developed a model that can be used to determine the optimal critical level in CBM techniques based on a random coefficient growth model where the coefficients of the regression growth model are assumed to follow known distribution functions. Within data-driven models, regression techniques are considered as numerical techniques, distinct from machine learning techniques such as neural networks or decision trees [156]. Logistic regression techniques in particular have been adopted by several researchers in establishing proportional hazards models. Modelling a proportional hazards model is similar to the process of regress analysis, whereby a set of significant covariates is found and only these significant covariates are included in the model. However, proportional hazards models modelling differs from regular regression analysis in that there are no observations for the hazard rate $h(t)$ and instead observations are available as event data [7]. Liao et al [161] used the proportional hazards and logistic regression models to relate multiple degradation features of sensor signals to specific reliability indices of a component, and subsequently predict its RUL. Their approach modelled multiple correlated degradation features of an individual unit, taking into account the multiple degradation features simultaneously. Their study focused only on the case where historical data under optimal operating conditions was available. A natural extension of their proposed models would be to extend them by considering the effects of different operating conditions. Despite this, they report that that the models are capable of providing accurate RUL predictions.

Logistic regression models can be utilised in degradation analyses to relate the probability of an event to a set of covariates [161]. Unlike linear regression, logistic regression can directly predict probabilities which are well-calibrated when compared to the probabilities predicted by other classifiers, such as Naive Bayes. The coefficients of the model also provide evidence of the relative importance of each input variable [162]. Binomial logistic regression attempts to predict the probability that an observation falls into one of two categories of a dichotomous dependent variable based on one or more independent variables. The dependant variable Y undergoes a logit transformation such that [163]:

$$log\left(\frac{Y}{1-Y}\right) = logit \tag{2.4.12}$$

where $Y = P(X)$.

The logistic regression model assumes that the log-odds of dependant variable Y can be expressed as a linear function of the K input variables x such that [162]:

$$log\left(\frac{P(X)}{1-P(X)}\right) = \sum_{j=0}^{K} b_j x_j \tag{2.4.13}$$

Taking the exponent of both sides of the logit equation yields [162]:

$$\frac{P(X)}{1-P(X)} = e^{\sum_{j=0}^{K} b_j x_j} = \prod_{j=0}^{K} e^{b_j x_j} \tag{2.4.14}$$

where the value e^{b_j} relates how the odds of the response being true increase or decrease as x_j increases by one unit, all other things being equal. Adapting equation (2.4.14) for reliability analysis, where the degradation covariates $Z(t) = x$, we assume the odds ratio between the survival function $S(t|Z(t))$ and the cumulative distribution function $F(t|Z(t)) = 1 - S(t|Z(t))$ is [161]:

$$\frac{S(t|Z(t))}{1-S(t|Z(t))} = e^{\alpha+bZ(t)} \tag{2.4.15}$$

where $\alpha > 0$ and b are the model parameters to be estimated. Finally, the survivor function can now be expressed as [161]:

$$S(t|Z(t)) = \frac{e^{\alpha+bZ(t)}}{1+e^{\alpha+bZ(t)}} \tag{2.4.16}$$

Parameter Likelihood Estimation

The estimation of the model parameters and the characterisation of the corresponding uncertainties are fundamental to properly set and use multi-state degradation models. To do this, different approaches have been proposed in the literature, which mainly depend on the available knowledge, information and data. Namely, when a substantial amount of collected data is available, techniques from statistical analysis can be adopted, which may be purely analytical, e.g. Giorgio et al [164], or numerical, e.g. Compare et al [139]. On the contrary, situations characterised by scarcity of data are common in industrial applications, particularly with very highly reliable components, newly introduced technology etc. In these instances, domain expert knowledge and opinion become valuable source of information to be taken into account. Within this context, different approaches have been proposed within both probabilistic and non-probabilistic theoretical frameworks. Probabilistic approaches are typically based on the elicitation of subjective expert judgements about the probabilities of occurrence of single events, or about the probability distributions of certain quantities of interest [165]. Often, the elicitation process is oriented to obtain a suitable prior distribution to be updated in light of the available data, according to the Bayesian paradigm [166]. Within the non-probabilistic approaches, Possibility Theory has been used to address the situation in which the knowledge regarding the Weibull parameter values is available in terms of a set of nested intervals with corresponding confidence levels provided by an expert [167,168]. Similarly, the Dempster-Shafer theory of Evidence has been applied to develop a semi-Markov degradation model where an interval that is believed to contain the unknown parameter value is asked to each member of a team of experts [145]. Fuzzy logic and imprecise probability have also been used with the same aim [169].

Although many different methods of estimating the parameters and important functions of the parameters, for example quantiles and failure probabilities, have been suggested, maximum likelihood and median-rank regression methods are the most commonly used today. The maximum likelihood estimation function indicates how likely the observed sample is as a function of possible parameter values. Therefore, maximising the likelihood function determines the parameters that are most likely to produce the observed data [170]. Regarding the proportional hazards model, in order to estimate the parameters, it is necessary to have historical data collected under the given operating conditions. Typical data will consist of aging times, feature sample paths, and indicators of events, for example exact failure times or censored data. Then the log-likelihood function of the collected data is given by [161]:

$$\mathcal{L}(\lambda,\beta,\gamma|DATA) = \prod_{j\in\varphi_F} ln\big[h\big(t_j\big|Z(t_j)\big)\big] \times \prod_{k\in\{\varphi_F\cup\varphi_S\}} \int_0^{t_k} h(\tau|Z(\tau)\{\tau\colon 0\le\tau\le t_k\})d\tau \tag{2.4.17}$$

where φ_F is the set of failure times, φ_S is the set of surviving times, t_j is the failure time of the j^{th} component, t_k is either the failure or the surviving time of the k^{th} component, and $ln\big[h\big(t_j\big|Z(t_j)\big)\big]$ is the natural log of the hazard rate. The integration of the data can implemented using a method such as the adaptive Simpson quadrature rule [161].

The goal of logistic regression is to estimate the unknown parameters b_j in equation (2.4.14). This again is done with maximum likelihood estimation which entails finding the set of parameters for which the probability of the observed data is greatest. The maximum likelihood equation is derived from the probability distribution of the dependent variable, which in the case of logistic regression is the binomial distribution [171]. The log-likelihood function of the logistic regression model can be expressed as [162]:

$$\mathcal{L}(X|P) = \sum_{i=1,y_i=1}^{N} ln\{P(x_i)\} \times \sum_{i=0,y_i=0}^{N} ln\{1-P(x_i)\} \tag{2.4.18}$$

where (X,y) is the set of observations. If K is the set of the input variables x, then X is a $K+1$ by N matrix of inputs where each column corresponds to an observation, y is an N-dimensional vector of responses, and (x_i,y_i) are the individual observations.

In reliability applications, data sets are typically small or moderate in size. Simulation studies show that in small sample designs where there are only a few failures, the maximum likelihood estimation method is better than the least squares estimation method, commonly used in other types of regression analysis. With heavily censored datasets, the maximum likelihood estimation method uses the information in the entire data set, including the censored values. The least squares estimation method ignores the information in the censored observations. Typically, the advantages of the maximum likelihood estimation method outweigh the advantages of the least squares estimation method [170].

When sample sizes are large, it is harder to reject more complex models because the chi-square test statistics are designed to detect departures between a model and observed data. Therefore, adding more terms to a model will always improve the fit, but with a large sample it becomes harder to distinguish between actual improvements in fit from trivial ones, with of course the added danger that model overfitting is present. Likelihood-ratio tests alone often lead to the rejection of acceptable models, and models become less parsimonious than they need to be. Therefore, information measures such as Aikake Information Criterion (AIC) have become increasingly popular. The AIC proposed in Akaike [172] is a measure of the goodness of fit of an estimated statistical model. It is grounded in the concept of entropy. The AIC is an operational way of trading off the complexity of an estimated model against how well the model fits the data. The basic idea is to compare the relative likelihood of two models as opposed to finding the absolute deviation of observed data from a particular model. AIC essentially has an in built penalty for including variables that do not significantly improve model fit.

The AIC method is defined as [172]:

$$AIC = -2 \times log(likelihood) + 2k \tag{2.4.19}$$

where p is the number of model parameters, k = 1 for exponential models, k = 2 for Weibull, log logistic, and log normal models [173].

Particularly with large samples, information measures can lead to more parsimonious and adequate models. Another advantage of information measures is that you can compare the fits of different models, even when the models are not nested. This is particularly useful when you have competing theories that are very different. The smaller the value of the statistic, or the more negative the value is, the better the fit of the model [174]. A commonly used check of the goodness of fit of a logistic model is the pseudo-R^2 measure proposed by Cragg & Uhler [175] and Nagelkerke [176]:

$$\psi := R_{CU}^2 = \frac{1 - \left(\frac{\mathcal{L}_0}{\mathcal{L}}\right)^{2/N}}{1 - (\mathcal{L}_0)^{2/N}} \tag{2.4.20}$$

where $\mathcal{L}_0$ is the likelihood of the logistic model without covariates, and $\mathcal{L}$ is the full model with covariates.

It is necessary to reduce the number of model parameters as parametric prognostic models require non-negligible amounts of data to estimate the model parameters. This means that the larger the number of covariates, the larger the number of parameters, and accordingly the larger amount of data required to tune the model. This is a critical consideration, as the selection of the most influential covariates can have a significant impact on the effectiveness of the resulting degradation model, since irrelevant and noisy covariates tend to unnecessarily increase the complexity of the model and thus degrade modelling performance. With these considerations, variable selection is strongly beneficial for analysis based on a small amount of data [146]. Methods used to select relevant variables from a larger set of alternatives can be divided into filtering and wrapper methods [177–180]. Filtering selects the significant covariates independently from a model used for prediction, based on heuristics that significantly reduce the computational burden. Filtering approaches work well within frequentist probabilistic frameworks, and the use of frequentist analysis to perform filtering selection does not entail a loss in prior information about the effect of the covariates, as there is no other source of information about the effects of the covariates available. Wrapper methods look at the improvement on predictive performance of the final model using combinations of the filtered subset of covariates [177]. For smaller datasets, filtering methods have a distinct advantage in that they avoid overfitting of the model and the heavy computation required to analyse the full initial dataset.

Degradation-based prognostic algorithms are the only true individual-based estimation methods. Making RUL estimates based on actual component condition is considered the ultimate goal for high risk and high value systems. Because these algorithms involve trending some measure of component degradation, also known as a prognostic parameter, identification of an appropriate prognostic parameter is critical. However, prognostic parameters do not have to be directly measured phenomenon. They could be obtained through a function of several measured variables that provide a quantitative measure of degradation. Thus, several measures of key degradation sources may be combined to provide a robust prognostic parameter for estimating RUL. Commonly, identification of prognostic parameters is left to expert analysis and engineering judgment. If any first-principle, or physics of failure, information is available about the system, this knowledge can also be used to inform parameter identification. In the absence of any specific engineering knowledge of the system, however, parameters are typically identified through visual inspection [28].

2.5 Soft-sensors

To accurately predict the remaining useful life of systems and components, prognostic frameworks presume that there is predictability in the failure time of the system. Although the most reliable approach to lifetime prediction is the use of precise first-principle models, such models are not available in most newly developed processes and modelling of a complex industrial process is very difficult and time-consuming. In particular, it is difficult to build precise first-principle models that can explain why defects appear in components. To circumvent this problem, operational data can be used in a data-based approach to monitor and control numerous process variables [181]. To achieve an accurate data-driven prognostic model, failure event model uncertainty must be reduced through the identification and inclusion of as many system variables as possible. Typical industrial case studies however often involve failure events where little failure data is available and where the component degradation process is not well characterised or understood. The problem for maintenance decision makers in establishing maintenance plans in these circumstances is exacerbated for components which cannot be assessed by traditional CBM methods, meaning the actual degradation state of the system at any time t cannot be determined. This can occur due to there being no technology developed to monitor the condition of the component in question, the inability to interfere with the process stream with additional sensorisation suites, the failure mode condition that requires monitoring may not be known, or the requisite technological knowledge may not be available or be too expensive [44]. In these circumstances a 'soft-sensor' approach can be utilised. Soft-sensors act as inferential system health estimators via proxy process indices. Models devoted to the estimation of other variables are known either as inferential models, virtual sensors, or soft-sensors [26,44]. Soft-sensors are essentially mathematical models which relate operating conditions to component condition using multivariate statistical techniques [181]. The basic idea of soft sensing is therefore to estimate the outputs of primary variables by easily measured secondary variables, which are correlated to the primary variables [182]. Soft-sensors offer a number of advantages in situations where it is impossible to install online measuring devices due to limitations in measuring technology [26]. These include [26]:

- Soft-sensors are a low-cost alternative to expensive hardware devices, allowing the realisation of more comprehensive monitoring networks
- Soft-sensors can work in parallel with hardware sensors, thereby giving useful information related to fault detection tasks
- Soft-sensors can be implemented using existing hardware and retuned when system parameters change

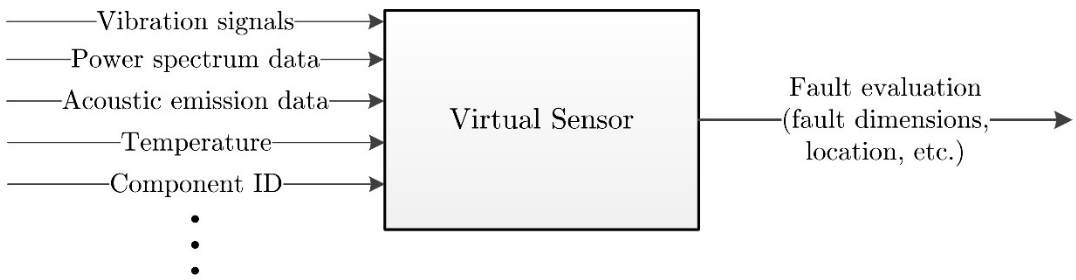

Figure 2.10: Schematic representation of soft-sensor development. Adapted from [44]

Designing a soft-sensor exploits the concept of gathering and combining numerous measurable quantities or features as inputs, and outputting the time evolution of a fault pattern [44]. A schematic representation of a virtual soft-sensor is shown in figure 2.10.

Soft-sensors, modelled as latent variables, have revolutionised industrial multivariate statistical process control by improving early fault detection capabilities over univariate methods [183]. Latent variable methodologies exploit the main characteristic of process databases, namely that although they consist of measurements of a large number of variables, these variables are highly correlated and the effective dimension of the space in which they exist is very small. Latent variable methods that exploit the correlation of process variables, and therefore model the structure of the process space, are extremely powerful when dealing with two common problematic characteristics of industrial historical databases, namely missing data and low content of information in any one variable [183]. The most commonly cited methods for constructing latent variables using multivariate statistical methods are principal component analysis and partial least squares, and both have attracted wide research interest [182,183]. For example, Kresta et al [184] utilise two case studies from distillation column control to demonstrate the general development of inferential models via partial least squares, Mejdell and Skogestad [185,186] implemented both principal component analysis and partial least squares estimators' of product compositions within distillation columns, and Lin et al [187] utilise both principal component analysis and partial least squares to develop a systematic approach for soft-sensor development. The key issue of soft-sensor design and multivariate statistical process control is not only selection or usage of modelling methods but selection of process data suitable for modelling, and selection of input variables necessary for estimation and monitoring. In practice, most efforts are devoted to such preparation. An efficient and robust procedure needs to be developed for adequate data pre-processing and model adaptation [181]. Statistical methods also become extremely powerful when combined with process-related knowledge. Therefore, utilising contextual knowledge can help determine which variables to include, as well as transform raw data into useable information, and decide on the frequency of data sampling. It is therefore important that domain expert knowledge from industry always be exploited when developing predictive models. Specific process knowledge, as well as general technical knowledge of the unit operations, can be utilised to convert the raw process variables to meaningful variables appropriate for modelling [188].

The core of a soft-sensor is the generation of a virtual measurement to replace a real sensor measurement. Soft sensing modelling is a problem of signal estimation, interpolation and prediction [182]. Models based on first principles, known as phenomenological or white box models, are often not available due to the complexity of industrial processes. As a result, data-driven, or black box, models are the most popular with which to develop soft-sensors. The problem of empirical modelling is to find a model with the best generalisation and prediction performance, given the empirical data. Currently, empirical soft sensing modelling techniques include multivariate statistics, Kalman filters, artificial neural networks, regression models, fuzzy logic, and hybrid methods [182]. The process of utilising mathematical techniques and industrial process knowledge to develop soft-sensor solutions is outlined in figure 2.11.

Figure 2.11: Overview of soft-sensor development in the process industry. Adapted from [27]

Historical process data can be exploited using data driven soft-sensors developed using statistical and machine learning techniques to obtain additional information that can be used to make decisions towards more efficient and safe process operation. This kind of information can be an instant prediction of the variables that are related to the product quality, or the estimation of a current process or system state, which can be achieved using process monitoring and fault detection soft-sensors [26,188,189]. However, model building in this context is not a trivial task, because historical data are often data rich but information poor [190]. Data-driven based soft-sensors are developed when no detailed knowledge is available about the process being modelled. Therefore, process data is used to build statistical models to determine the relationship between the inputs and outputs. In this regard statistical regression methods have become increasingly popular techniques for process modelling and are used for both fault detection and quality estimation [191]. Data-driven and model driven approaches can also be combined, creating what has been termed as a ‘grey-box’ approach [27]. For example, a statistical model can act as the input to a physical model in the form of differential or algebraic equations. Outputs of physical models can also be transformed by a statistical model, or the difference between measured and calculated variables can act as the inputs of a statistical model used for correction [191]. An example of where this grey-box approach would be useful is where there is a need to build a semi-Markov degradation model in an intermediate situation between that of having a sizeable amount of field data (which would justify the application of traditional statistical techniques in the frequentist probability framework) and the opposite, of having no data available (which has been historically treated with non-probabilistic techniques that avoid information commitment). The objective is to fully exploit all the available sources of information in a coherent way. To do this, one can resort to the Bayesian statistics framework, which allows combining the prior knowledge of experts with the evidence coming from field data to build a degradation model useful for maintenance applications [139,192]. The proposed methodology allows the elicitation of the prior distributions of the model parameters, avoiding possible commitment of prior information provided by an expert.

The general procedure of data-driven soft-sensor development, defined by Abonyi et al [191], is shown in figure 2.12.

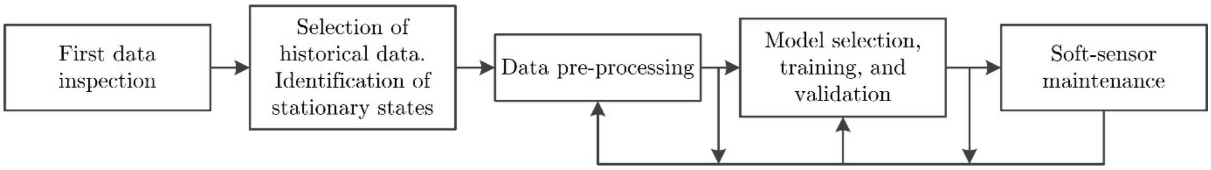

Figure 2.12: Data-driven soft-sensor development methodology. Adapted from [191].

1. *Data inspection*: Specification of the critical unmeasured variables, how to calculate them from measured data, and an overview of the data structures
2. *Selection of historical data and identification of stationary states*: Data to be used for the training and evaluation of the model are selected. Stationary segments of the data have to be identified and selected
3. *Data pre-processing*: Includes normalisation of data, handling of missing data, outlier detection, and selection of relevant variables.
4. *Model selection, training and validation*: Selection depends on the application, nature of the data, and personal preferences. If possible simpler models should be developed first, with model complexity gradually increasing as long as significant improvement in performance can be observed.
5. *Validation and testing*: After finding the optimal model structure and training the model, evaluation of the model performance is needed.
6. *Maintenance*: When a soft-sensor is developed, its performance may deteriorate as process characteristics changes. Soft-sensors should be updated to follow these changes.

As is often the case, no one statistical method can be described as better than all others for all situations or for all criteria [193]. This relates to the well-known 'no free lunch' theorem of Wolpert and Macready, who state that "if an algorithm performs well on a certain class of problems then it necessarily pays for that with degraded performance on the set of all remaining problems" [194]. It is often necessary therefore to use several approaches and base conclusions on a combination of analysis results [193].

2.5.1 Soft-sensors in the process industries

Soft-sensors have been widely used in industrial process control to improve the quality of the product and assure safety in production. Several methods have been proposed for constructing soft-sensor models. Yan et al [182] proposed a soft sensing modelling method based on support vector machines and the Bayesian evidence framework to estimate the freezing point of light diesel oil in a distillation column, due to it being impossible to measure online given the limitation of both process technology and measurement techniques. The authors develop the soft-sensor model using process data records and laboratory analysis results. The authors do not comment on the models' stability or robustness. Kano et al [195] present a partial least squares regression approach to develop a soft-sensor to estimate the product compositions of multi-component distillation columns from online measured process variables such as tray temperature, reflux flow rate, reboiler heat duty, and pressure. The authors claim that inferential models can be greatly improved by using dynamic time-series based models, as opposed to steady-state models. Kadlec et al [189] agree with this assertion, claiming that the performance of static models starts to deteriorate during their online operation. All data used for model development was simulated. Recently, Ruilan et al [196] utilised genetic algorithms to optimise the parameters of a support vector machine to estimate the melt index in polymer manufacture. They do not report on the industrial application of the model post-development. Lin et al [187] presented a systematic approach to build data-driven soft-sensors partly to predict emissions due to cement kiln processes. Due to the low signal-to-noise ratio of industrial operations data, they demonstrate that data pre-processing is an essential step. The authors used statistical techniques to extract the relevant process information in the presence of outlying observations. While an industrial case study was used, the model is not implemented in an industrial application.

Soft-sensors are particularly suited to chemical processing industries, such as biopharmaceutical production, due to the lack of reliable online sensors which can detect important state variables, the nonlinear and time-varying nature of the production systems, and the slow response of the process, in particular for cell and metabolic concentrations [197]. Sterility requirements within the biopharmaceutical industry also make online mass sensorisation difficult. Cheruy [198] states that a common bottleneck in bioprocess monitoring and control is often caused by the lack of reliable sensors, raising the need for soft-sensor development. Guenard and Thurau [199] further outline some of the important considerations for sensorisation implementation within chemical processing industries such as biopharmaceutical production. These include instrument deployment in a hazardous processing environment, regulatory requirements for implementation in a current good manufacturing practice (cGMP) setting, and data management and interface with plant systems. Operation of instruments and systems in strict chemical processing cGMP environments also necessitates development of standard operating procedures and procedural workflows including instrument qualification and change control. More recently skid-based process and instrumentation configurations have been developed. However, the actual location of sensors in the system has been shown to have a significant impact on measurement ability and accuracy due to issues such as sensor fouling, especially for heterogeneous systems [200]. Sensorisation in this industry can therefore be problematic. While a high degree of sensor sensitivity is typically required, a key condition for reliable measurements is that all instrumentation should be robust enough to endure the typical variations of a chemical process environment [201].

Soft-sensors are particularly widespread in the pharmaceutical industry in connection with Process Analytical Technology where they are used to generate online quality estimates based on online analytical measurements [191]. De Assis and Filho [202] review the use of soft-sensors in the biopharmaceutical industry for predicting process variables such as those relating to cell product concentrations, cell mass, etc. The authors suggest that two models particularly suited to biopharmaceutical processes are the Kalman filter and artificial neural networks. However, the authors also state that the Kalman filter requires a large design effort and a priori estimates of measurement noise and model uncertainty characteristics, while large amounts of experimental data are needed to train neural networks. In a practical setting, this may hinder the industrial use of such models. Desai et al [203] present a machine learning based modelling formalism known as support vector regression for the development of soft-sensor applications in fed-batch biopharmaceutical processes. The authors allude to the difficulty of direct sensorisation within biopharmaceutical processes given the lack of available sensorisation technology, making it particularly suited to soft-sensor development. The authors opine that empirical modelling approaches are most suited to biopharmaceutical processes given the complex nonlinear process dynamics. All data used in the model development was simulated.

2.5.2 Data fusion in soft-sensor development

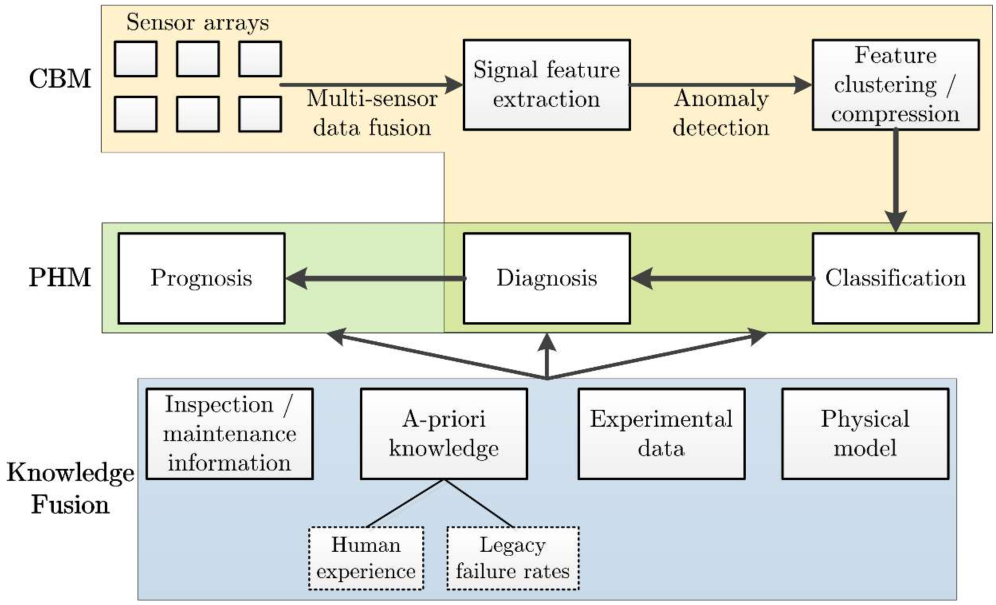

Figure 2.13: Knowledge fusion approach to system reliability prediction. Adapted from [44]

Within traditional system health monitoring, fusion technology plays a significant role [44]. The incorporation of external data can yield more information and lower the variance in the parameter estimates of predicted response variables [193]. The combination of multiple sensors in a multi-sensor data array to validate signals and create features is common in modern industrial applications. For example, multiple sensors can be used to create time-synchronous averaged signals. At a higher level, fusion may be used to enhance diagnostic information. An example would be the use of vibration sensor information concurrent with data on lubrication oil particle count in a bearing. The combined result enhances the confidence about the bearing health prediction. Developing this methodology further within a PHM framework allows for a total knowledge fusion approach. This approach combines experience based information such as legacy failure rates, reliability testing data, and a-priori human knowledge with traditional signal based information from sensor data [44]. This approach is outlined in figure 2.13.

Bayesian inference for knowledge fusion

Bayesian approaches to estimating uncertainty are common because they naturally incorporate information about the current system with prior knowledge, for example expert opinions, results of past analyses etc. [204]. The basic idea of model selection within the Bayesian framework is to maximize the posterior probability of parameter distribution to obtain the optimal parameter. According to the Bayesian theory, the most possible parameters value and optimal model are obtained at the point where posterior of these parameters distribution are maximum [182].

The Bayesian rule can be described as:

$$Posterior\ probability = \frac{likelihood\ x\ prior\ probability}{evidence} \tag{2.5.1}$$

Bayesian inference can be used to determine the probability that a particular fault diagnosis is correct given priori information.

Analytically, this process is described as [44]:

$$P(f_1|O_n) = P(O_n|f_1)\,.\,P(f_1)\Big/\sum_{j=1}^{n}(O_n|f_1)\,.\,P(f_1) \tag{2.5.2}$$

where $P(f_1|O_n)$ is the probability of fault f given the diagnostic output O, $P(O_n|f_1)$ is the probability that the diagnostic output O is associated with the fault f, and $P(f_1)$ is the probability of the fault occurring. Another use of the Bayesian concept is for scale parameter λ and shape parameter β estimation of Weibull models. This concept considers that prior knowledge exists, tacit or explicit, on the shape parameter β when it is fitted to a given set of data. This is particularly useful when dealing with small sample sizes and some prior knowledge is available. Therefore, numerous authors have focused on the elicitation of a joint prior measure $f(\lambda, \beta|t_n)$ that formalises prior expert knowledge on the system under investigation [144]. This model is formalised as [144]:

$$f(\lambda,\beta|t_n) = \mathcal{L}(t_n;\lambda,\beta).f(\lambda,\beta)\Big/\iint_0^{\infty}\mathcal{L}(t_n;\lambda,\beta).f(\lambda,\beta)\;d\lambda d\beta \tag{2.5.3}$$

where $\mathcal{L}(t_n;\lambda,\beta)$ denotes the data likelihood.

Kadlec [189] and Kano [195] emphasise the importance of building adaptivity into soft-sensor design, meaning creating dynamic inferential models that include feedback about model performance or changing process conditions. Adaptive soft-sensors rely on various techniques for their online adaptation. Often cited methods include moving window techniques and recursive updates of the least squares, principal component analysis and partial least squares methods. The soft-sensor is first developed using some data pre-processing. Then, available expert process knowledge is applied to the historical data and as result a soft-sensor is obtained [189]. During the operational phase the soft-sensor is adapted using three facets of information: online data, expert knowledge, and performance feedback [189].

Another aspect playing a role in the development and updating of adaptive soft-sensors is the implementation of process knowledge into the soft-sensor model. Traditionally, the application of expert knowledge in soft-sensors is limited to the selection of critical process variables [187,205]. In the case of adaptive soft-sensors, any available expert knowledge about the dynamics of the process can be used for selecting appropriate values for model attributes related to the adaptive operation [189]. For example, Ibargüengoytia et al [25] developed a soft-sensor Bayesian network to estimate the fuel oil viscosity thermo-electrical power plants using related variables, such as historical data and expert advice. Building soft-sensors using Bayesian frameworks allows for an adaptive approach whereby model performance and updated data sources can be fed into the model to refine it.

An obstacle preventing statistical methods being used in practice is the refusal of engineers and operators to do so. The validation of a statistical model is a difficult task. To win operators' trust, models and systems need to be understandable and consistent with process knowledge. In addition, models and systems need to be easily maintained [181].

2.5.3 Uncertainty in decision support systems

The ultimate goal of PHM, CBM, and soft-sensors is to increase component availability, reduce maintenance costs, minimise unscheduled shutdowns, and increase safety. The importance of uncertainty quantification in this context should not be understated. Monitoring the health state of systems, subsystems, and components, the classification of the different types of faults that may occur in these components, and estimating the RUL along with other prognostic metrics such as the End-of-Prediction time index can be extremely helpful to support decision makers in assessing whether maintenance intervention is necessary or not. In ever more complex environments, operators need to quickly make thousands of decisions to maintain optimal decision performance. Although this challenge can be overcome by enabling a decision support system to perform select operations with human consent, without quantifying the associated uncertainties, remaining life projections have little practical value within decision support systems [206,207]. It is the comprehension of the corresponding uncertainties that is at the heart of being able to develop a business case that addresses prognostic requirements. The assumption of data monitoring without uncertainty is particularly problematic in the process industry, as this forces maintenance planning to become an exercise in decision making under uncertainty with sparse data [208].

As stated previously, PHM systems are usually implemented in three stages of a health state management framework for a component of interest: detection, diagnosis, and prognosis. Several methods have been widely developed in the last few decades to increase the reliability of PHM systems. Within the varied fault detection, diagnosis, and prognosis methodologies there exists different sources of uncertainty which may influence the performance of the PHM system, causing false or missing alarms. In the former case, the output of the PHM system indicates that a healthy component is experiencing abnormal conditions, causing potential unwarranted downtime. In the latter case, the output of the PHM system indicates that an unhealthy component is operating under normal conditions, potentially leading to catastrophic unexpected failures of the component/system with associated large downtimes, high cost, as well as possible safety and environmental implications [209]. For these reasons, it is necessary to manage the different sources of uncertainty that may arise in the PHM system stages. In practice, the possible sources of uncertainty that may arise in a PHM system are:

- Uncertainty in the signal measurements
    - Incomplete, noisy, and imprecise measurements
- Uncertainty in the models adopted at each data processing stage
    - Un-modelled phenomena, approximations, simplifications, hypotheses, assumptions, etc.
- Uncertainty due to the inherent stochasticity of the physical processes
    - Stochasticity in the current and future states of the system, unforeseen future loads and environmental conditions etc.
- Human errors relating to human interaction with both the PHM system and the physical process system

Essentially, the inherent uncertainties which propagate through PHM systems mean that the PHM output can never be perfectly reliable [7]. Even if it were, in practice a PHM system is being applied in a complex industrial environmental context and there will almost always be human interaction at the system interface who may choose not to follow the guidance of the PHM system, because of a possible lack of trust in the system output or because they have knowledge extraneous to the modelled parameters. Context drivers in this regard include financial pressures to delay maintenance activities, unexpected environmental conditions which could affect the reliability/uncertainty of the algorithms, a change in the maintenance policies of the organisation, cost of shutting down at a particular time, resource availability, time available for production intervention activities (including time of the year), audit timing within regulated industries, management interests, corporate politics etc. With this in mind, it is important to consider the application of the PHM system within the overall socio-technical system of the maintenance organisation. Only by providing a PHM system that is calibrated against the actual usage of the system can the full benefit be achieved.

Engel, Gilmartin, Bongort, and Hess [207] argue that the calculation of system RUL in PHM systems alone does not provide sufficient information to form a decision or to determine corrective action. They state that without comprehending the corresponding measures of the uncertainty associated with the calculation, decision support systems outputs have little practical value. In terms of uncertainty quantification research the current focus in both industry and academia is on the shortcomings in the availability of run-to-failure data, accelerated ageing environments, real-time prognostics algorithms, uncertainty representation and management techniques, prognostics performance evaluation, and methods for verification and validation [210]. While prognostic model uncertainty qualification is outside the scope of this work (as this work is focussed on initial data elicitation only), it is critical to keep uncertainty quantification in mind if the results from this work are to be expanded upon. Reducing uncertainty at all stages of the data elicitation process should be a key focus for any model derived from the results of this research. In order to reduce data variable uncertainty, a key approach of this study in this regard is the utilisation of multiple data sources and data validation techniques in a unique hybrid way, such as qualitative, quantitative, and statistical.

Another potential source of uncertainty in predicting the remaining useful life of components is the natural variation in human performance which occasionally results in errors. It is often assumed that when maintenance work is conducted, it is considered that repairs/replacements always restore the system to a ‘good-as-new’ condition, which, in practice, may not be very realistic [43]. The effect of incorrect maintenance or installation has sufficient impact for it to be regarded as a separate source of uncertainty, and therefore useful information in its own right. Most PHM models assume that the work done by a maintenance technician has been completed to a requisite standard, thereby allowing predictive analytics a consistent operational performance benchmark from which to operate. However, in practice this is often not the case, with a large variability in numerous aspects related to the ability of a maintenance technician to effectively carry out their work. In an attempt to address this issue there have been systematic methods developed to improve the performance of human-machine systems, such as human error probability assessments [211]. Incorporating such as human error probability assessments in the development of operational procedures can significantly improve the overall reliability of the system [212]. For this reason the uncertainty around human interaction effects on system health are investigated in this work in chapter 5, and are a key component of the hybrid data elicitation methodology developed.

2.6 Human factors

Human error is defined by Reason [213] as ‘a generic term to encompass all those occasions in which a planned sequence of mental or physical activities fails to achieve its intended outcome, and when these failures cannot be attributed to the intervention of some chance agency’. These variations which can give rise to errors may be influenced by the conditions in which tasks are undertaken, such as environmental conditions, quality of procedures, level of training provided, etc. Human error is an important consideration in the process industry, as it is well established that a significant proportion of human errors occur during maintenance activities [211,214]. Human error is cited as a major cause of pharmaceutical manufacturing failures in particular, with human error being attributed to approximately 50% of recorded incidents [215]. A significant proportion of these errors occur during maintenance activities, costing the industry substantial amounts of time and money [211]. Human error in maintenance may be defined as the failure to perform a specified task, or the lack of compliance with standardised approaches, that could lead to disruption of scheduled operations or result in damage to property and equipment [214]. Maintenance errors can generally be divided into two major classes: failing to detect a problem or the introduction of an error during maintenance, specifically [216,217]:

1. hidden system faults and failures which are not detected during maintenance
2. incorrect activities such as wrong adjustments, further damage done during maintenance, and replacement with faulty parts.

A significant number of catastrophic incidents in industry occur primarily due to human factors [218]. For example, Okoh and Haugen [219] analysed 183 major industrial accidents in the United States and Europe between 2000 and 2011. Their investigation showed that 44 percent of those were related to maintenance. They identify a lack of barrier maintenance, deficient design, organization and resource management, and deficient planning/scheduling/fault diagnosis' as being the most frequent causes of active accidents, latent accidents, and work process errors, clearly highlighting the importance of addressing human factors throughout the life cycle of a process.

Modern industries, such as nuclear, petrochemical, automotive, and pharmaceutical, consist of complex socio-technical systems which include a vast array of system combinations of software, electronic, and mechanical components, all of which require some degree of human interaction in their operation and/or maintenance. Despite many technological advancements in both industrial plant machinery and process and condition based monitoring methods and techniques, failure and breakdown of industrial components remains a threat which has the potential to accrue significant economic losses for an organisation. This is partly due to the recent methodological shift of emphasis from pure volumetric output, to quick maintenance response times, elimination of waste, and defect prevention, which creates a competitive environment in which erratic process yields can create immediate problems [220]. This is particularly evident where no redundancy has been built in to a process, as the desired system-level reliability cannot be obtained as the individual components do not have the necessary reliabilities to limit the effect of a single component failure on the system-level reliability [221]. Environmental protection and human health and safety are also a driver for effective maintenance policies in order to create sustainable production processes [222]. Keeping equipment and facilities in optimal working order are an effective means of creating the sustainable environment required to meet societal demand of pollution control and accident prevention [220].

The safety and effectiveness of complex industrial systems and facilities is therefore determined primarily by the humans and organisations responsible for them during their entire life cycle, from design, to construction, commissioning, operation, and maintenance. To preserve and progress the performance and safety of complex systems, it is important to improve system reliability, availability and maintainability. Just as critical is to take into account the elements influencing the performance of people working with the industrial systems, known as human and organizational factors (HOF's). In the context of maintenance, Rasmussen [223] reports that industrial accidents are more likely to be caused by human errors during maintenance activities rather than by errors occurring during plant operation. Khalaquzzaman et al. [224], in their study on maintenance failures in a nuclear power plant, showed that 50% of reactor scrams occur because of human errors having occurred during maintenance activities. Human errors are intrinsically different from traditional machine failures and require properly developed methods for their treatment. In particular, human errors and HOF's should be properly considered during the planning of maintenance activities. Optimising maintenance schedules can substantially improve system availability as well as decreasing the total cost for performing maintenance which can range from 15% to 70% of total production costs in oil and gas refineries [32,225].

Human factors is defined as *'the scientific discipline concerned with the understanding of the interactions among humans and other elements of a system, and the profession that applies theoretical* *principles, data and methods to design in order to optimize human well-being and overall system performance*' [226]. Within multiple high risk industries such as nuclear, petrochemical, aviation, and the medical domains, there is an existing recognition of the importance of human factors, not just from a safety perspective, but also from a systems performance perspective. A recent directorate of the Nuclear Installations Inspectorate of the Health and Safety Executive of Great Britain outlines how human factors need to be incorporated in all industrial projects in the field, throughout the full project lifecycle, to achieve both the aims of increased safety and reliable energy production [227]. The objective is again reiterated about considering human factors as an integral part of all projects, and not just an afterthought. A common repeated issue is that if the requirements of system operators are only accounted for at the end of system design, then it is unlikely that it will be a useable system requiring expensive retrofits and/or limiting productivity.

2.6.1 Integrating human factors metrics in PHM systems

In contrast to its importance to equipment reliability, the quantification and accounting of human errors during maintenance activities has received insufficient attention in the reliability literature [214]. Human factors, the discipline that aims to optimise human well-being as well as overall system performance, provides some possible approaches to accounting for these variations in an attempt to improve the accuracy of predictive lifetime models [226]. Foremost among the relevant Human Factors approaches is Human Reliability Analysis (HRA), which aims to identify and quantify possible human errors in a system, usually as part of a probabilistic risk assessment [228]. Common HRA tools, such as Technique for Human Error Rate Prediction (THERP) [229], Human Error Assessment and Reduction Technique (HEART) [230], Standardised Plant Analysis Risk-Human Reliability Analysis (SPAR-H) [231], and Technique for the Retrospective and Predictive Analysis of Cognitive Errors (TRACEr) [232], start by identifying possible human errors within a task or system and subsequently use databases to assign an expected error rate to that task, known as a human error probability. This error rate can be modified by performance shaping factors, or error producing conditions, which increase the probability of an error during a task. Performance shaping factors include factors external to the individual such as the environment in which the task is conducted, the work hours, the organisational structure, job and task instructions, equipment characteristics, and task characteristics. More individually, stressors can be both psychological, for example time pressures, distractions, etc., and physiological, for example fatigue, hunger, radiation etc. These stressors can also influence task performance and error rates. The base error rate for a particular task, such as valve diaphragm installation considered in this work, will remain constant for that task regardless of the individual valve. However, the performance shaping factors vary according to the specifics relating to each individual valve and may influence the likelihood of correct maintenance actions. In modelling HOFs in maintenance, one can consider HOFs as another type of 'fault injection' [233].

The application of human factors has traditionally been in safety critical industries, where a variety of methods and techniques are applied to understand human interactions within a system and the potential for human error, and recommendations are made to improve the system, environment, organisation or tasks to improve human performance. It has long been recognised that maintenance tasks are vulnerable to human error, particularly in the aeronautical and nuclear industries [223,224,234–238]. In these instances, human factors principles have been applied in order to reduce both the rate and impact of human errors. Despite this, there has not been a strong input from human factors in the domain of PHM. Most of the PHM literature, when it considers human interactions within the system at all, considers that a benefit of PHM is the potential reduction in required maintenance interventions, thereby reducing the opportunity for human errors in the maintenance process [239]. While true, this view of human factors does not consider the possibility of harnessing human intelligence and reasoning abilities to improve the overall maintenance system, or of modelling human interactions with the system to improve both the prediction of faults and effectiveness of the system output. Zhao, Tian, and Zeng [240], and Yu, Syed Zubair, and Yang [241] have suggested that human factors could be included as an uncertainty in the PHM model itself, although ultimately both works neglected to use human factors as a model parameter. Research in this area has not yet investigated the feasibility of incorporating some of the existing human reliability analysis techniques in a PHM model, or of using a simpler approach of using maintainer/installer feedback to generate a confidence interval for the possibility of human error having occurred.

Although little evidence can be found in the literature where HOF and quantitative machine related system data is concurrently utilised to build system reliability models, some research does exist. Farcasiu and Prisecaru [242] consider the incorporation of HOFs within probabilistic safety assessments using techniques from human reliability analysis such as THERP. Their work aims to identify deficiencies of human performance which can be corrected through the improvement of the organisation/human interface. Chateauneuf et al. [243] focus on the reliability of railway equipment, including imperfect maintenance as a factor affecting reliability which in turn helps determine inspection intervals. Kumar and Gandhi [244] quantify human error in maintenance activities using graph theory, and measure the human error potential involved in the maintenance of systems in order to make the systems less prone to human error. Noroozi et al. [211] highlight the importance of considering human error in quantitative risk analyses via the quantification of human error probabilities during maintenance activities. Asadzadeh and Azadeh [245] propose an integrated systemic model for the integration of human reliability models with CBM optimisation. They calculate the probability of human error occurring during data collection, data manipulation, and algorithm development of CBM models. They also include the physical and psychological abilities of maintainers as well as their experience and skill levels. They use the probability of human error having occurred to adjust the threshold of their prognostic CBM algorithms. However, the assumptions of this study are that the human error probabilities can be perfectly quantified and that human errors cause immediate system defects that can subsequently be detected by CBM technologies. These assumptions may not be widely applicable to industrial case studies. Carr and Christer [233] investigate parametric reliability models describing how inspection windows and system downtime are affected by bad installation practices. However, with a lack of a case study they do not quantify human error or provide a method to estimate the probability of human error having occurred. Kiassat et al [149,154,246–248] consider the inclusion of HOF metrics within a Weibull proportional hazards framework. They consider the case of industrial operators who are in constant manual contact with production equipment, but provide no framework for quantifying the HOF metric to be included in the developed model [246]. This approach would not be applicable to the case of maintenance personal who have intermittent offline access only to a system. The authors focus on how operator skill, education level, and social skills change as new operators initially enter an organisation and continuously manually interact with production equipment. They observe how with increased operator experience, equipment productivity is increased [149].

An issue which has received sparse attention in the literature is analysing industrial datasets using Weibull proportional hazards models where data is scarce, particularly where the root cause of the failure mode being analysed is unknown. For example, Kiassat et al [149] use 3049 records of equipment production to build their proportional hazards model. This is in spite of the fact that scarcity of data is a common situation in industrial practice, for example with innovative and/or highly reliable components, with new technology, systems operating in complex environments, etc. This uncertainty can lead to Weibull proportional hazards models with large unit variance which results in lifetime models that are not fit for practical purpose. An issue not explored in the literature is if the inclusion of HOFs as covariates into Weibull proportional hazards models helps to reduce the variance of lifetime estimations, especially with failure modes where the root cause is unclear or where the influencing covariates are not known or well understood. A full methodological framework to guide the development of a Weibull proportional hazards reliability model including HOF in these conditions has never been proposed. Another issue not explored in the literature is the use of human factors metrics to create dynamic lifetime assessment models for identical components in a single plant operating within different HOF contexts. This would naturally extend the application of Weibull proportional hazards models to treat HOFs as a changing environmental factor like any other in traditional CBM/PHM schemes, such as temperature, pressure, flow rate, etc. The HOF chosen could potentially be any factor derived as relevant from an analysis of the performance shaping factors affecting the maintenance staff during maintenance operations.

Another approach lacking in the literature is developing a Weibull proportional hazards model such that an individual component would have its own instantaneous hazard rate, or failure risk level, derived from its own specific maintenance induced HOF metric. The underlying characteristic of available research is that the latent or critical human error probability is assumed to be a constant parameter based on which the stochastic model of the system under study is developed. With the aid of the stochastic model of the system with incorporated human errors, the impact of human error on system reliability or maintenance decisions is analysed [245]. This approach of providing a single risk level applied to an entire system may be an over simplification which does not take into account varying HOF contexts. One part of the methodology presented in this work details how these varying conditions can be taken into account and how including them as covariates in a Weibull proportional hazards model allows for individual components or sections of an overall system to have different reliability levels as a direct result of differing HOF contexts.

Integrating human knowledge in PHM system design

Despite the advantages to be gained from utilising human knowledge in a knowledge fusion framework, most CBM and PHM systems use only 'machine related' quantitative information available from sensors, and almost no use of quantitative or qualitative information derived from human sources is made [154,249–251]. The practical difficulty of building a common platform to process both quantitative and qualitative data has hindered the use of such a hybrid system. The potential advantages of integrating human sourced data within parametric reliability models include uncertainty reduction of the probabilistic system state estimations. These 'human-in-the-loop' models are particularly pertinent where sparse quantitative data is available and where humans are central to the maintenance and/or operation of the system.

Human interaction with automation as a whole, of which PHM can be considered a branch, and the use of decision support systems has been widely researched in human factors. Many lessons can be learned by PHM system designers from the introduction of automated systems in the aviation industry for example, and there is a large volume of knowledge which exists in the human factors literature on the subject. One of these lessons is whether total system safety is always enhanced by allocating functions to automatic devices rather than human operators [252]. Research on decision support systems information output indicates that decision support systems which indicate the status of a system are preferable to those that advise operators on how to respond, and in general, presentation of status significantly reduces the time required to make a correct decision. The relative superiority of status output is particularly evident when a decision aid is inaccurate. Under these conditions, subjects receiving status information are reported to be unaffected by an inaccurate decision aid [253]. Similar findings in high-risk industries where the information is imperfect suggest that status displays are better than command displays [254]. Decision support systems which incorporate a high degree of decision autonomy have failed frequently in industrial settings. In theory, a decision support system acts as a 'prosthesis' to aid a human decision maker who is purportedly characteristically flawed and inconsistent in their decision making. As such, more precise algorithms are the preferred research objectives of PHM, as opposed to a greater understanding of the power of human cognition [255]. This type of reasoning is common in the PHM literature. However, the level of automation required with such an approach conflicts in reality with the number of situations an algorithm may face. The danger is that a decision support system may make wrong decisions regarding situations it has not been modelled to compute.

With regard to the power of human cognition in the decision making process, the human recognition process relies heavily on context, knowledge, and experience. The effectiveness of using contextual information in resolving ambiguity and recognizing difficult patterns is the major differentiator between the recognition abilities of humans and systems [256]. A fundamental research issue in building intelligent decision support systems should therefore centre on linking the domain-specific knowledge of experts with the normative power of analytical decision techniques to improve the quality of decisions [257]. The complex human decision process largely follows a Bayesian approach, as given a set of information, human decision makers tend to duplicate Bayesian predictions if they are provided adequate information in appropriate representations [258]. The strength of this approach is demonstrated in recent research which illustrated that human reasoning in complex situations, in this case complex ribonucleic acid folding schemes, outperformed specifically formulated ribonucleic acid folding algorithms almost by an order of magnitude. The research focused on allowing humans to construct complex folding patterns for ribonucleic acid through an online crowdsourcing application. Users were able to manually develop better models of ribonucleic acid folding than previous computer algorithms, and design rules formulated by the human interactions with the system have been used to develop a new algorithm, and in some cases represent completely new understandings about ribonucleic acid folding that have yet to be explained mechanically [259].

Formal methodologies have been developed, called knowledge-based expert systems, in an attempt to capture human knowledge to draw conclusions in a formal methodology framework. An expert system is a decision support system that essentially mimics the cognitive behaviour of a human expert. It consists of a knowledge base, a set of if-then-else rules, and an inference engine which searches through the knowledge base to derive conclusions from given facts [260]. This forms a knowledge fusion approach, using information sources like a-priori knowledge about the industrial environment to form human input into a decision support systems [45]. However one issue with this kind of knowledge representation is that it has no intrinsic understanding of the underlying physics of the system, and therefore performance may be slightly degraded in cases where a new condition is encountered that is not defined in the knowledge base [260].

Similarly, Billings [261] describes what he terms as 'human-centred automation' in the aviation industry. Automation systems in Billings definition include systems which have intelligence, or some capacity to learn and then to proceed independently to accomplish a task. Such reasoner systems are evidenced frequently in PHM literature. Billings argues that the quality and effectiveness of an automation system depends largely on the degree to which the system takes advantage of the combined strengths of humans and automation technologies, and equally compensates for the weaknesses of both elements. Though Billings admits that humans are far from perfect sensors, decision-makers and controllers, he argues that they possess a number of vital attributes which automation systems do not. These are that humans are excellent detectors of signals in the presence of noise, that they can reason effectively given uncertainties, that they are capable of abstraction and conceptual organisation, they can cope with failures not envisioned by system designers, they possess the ability to learn from experience and thus the ability to respond quickly and successfully to new situations, and to innovate and to reason by analogy when previous experience does not cover a new problem. Humans thus provide a degree of flexibility with regards to knowledge input and final decision making that cannot be attained by computational decision support systems alone, except in narrowly and well defined, well understood domains and situations. These uniquely human attributes each provide a reason to retain the human in a central position in systems which are neither directly controllable nor fully predictable [261].

The reliability of automation and decision support tools has long been understood to be a key factor in the success of the tool [262]. Madhavan and Wiegmann [263] and Wickens and Dixon [262] both conducted a meta-analysis of research studies relating reliability of diagnostic automation and how this affects the performance of human operators. The main conclusion from both studies indicates that below an optimal threshold of 70% reliability, performance degrades to the point that decision support systems are largely disused. Balfe et al [264] describe a set of principles for automation systems designed for rail automation but applicable to other domains. Among these are the importance of reliability of the automation, and feedback to the human operator in terms of making the base information, raw data that has been transformed in to useful information, visible and providing understandable outputs to the operator. Bechhoefer and Morton [265] explicitly mention the need for end-user confidence in PHM systems to be high in order to preserve the value of the system. They refer to the need to reduce false alarm rates and increase the sensitivity to actual faults. They also specify that to achieve widespread deployment, it is necessary to change end-users' perception by convincing them of the value proposition of supporting PHM. One of the facets enhancing a strong proposition that they note is an improved user interface, greater system reliability, and greater access to more actionable information.

Human interaction with PHM system outputs

PHM systems aim to be highly autonomous up until the point that a decision is required regarding maintenance intervention. In this way PHM systems can assist maintainers to determine the optimum time to perform maintenance given a host of constraints, providing the operator with confidence bounds on the availability of critical assets to meet production schedules. Ideally autonomous diagnostic and prognostic capabilities are to be implemented within an integrated maintenance and logistics system that supports critical complex systems throughout their lifetimes [44]. However, there is little to no evidence that it has as yet proven possible in practice to achieve this level of autonomy, and some degree of human intervention is typically required. In fact, a completely autonomous prognostic health management system still does not exist [210]. There are several authors that consider the issue of the user interface through which PHM analysis is displayed to the maintenance staff. Mathur et al [266] recognise that human factors considerations need to guide the development of interface components and accessibility requirements. They provide an example of a web-based design of servers which support a distributed, multi-platform, three-tier architecture. Saxena et al [210] detail the fact that including metrics based on functionality and usability is important when classifying software requirements. Bechhoefer and Morton [265] studied the lack of adoption of condition monitoring systems in wind turbines. They concluded that as no single condition indicator can detect all failure modes, a user display requirement is necessary to view, threshold, and trend information that incorporates more than just spectral data or one condition indicator. They specify the need for a data reduction methodology that is intuitive and user friendly, citing the use of the health indicator concept, which is the integration of several condition indicators into a single variable. The health indicator provides the health status of the component to the end user. In contrast to these works, which focus on providing a user friendly interface at the end of system development, early consideration of how the operator will interact with a PHM system and its outputs in practice should drive the whole philosophy of the PHM system and hence influences not just the design of the interface, but the decisions on what data to present and at what level of detail.

Tied to this is the fact that removing the responsibility of decision making from human decision makers in high-risk industrial settings may have negative consequences as people will simply blame erroneous decisions on the automation. This phenomenon has been labelled as automation bias. Automation bias is the tendency to over-rely on automation, and has been studied in various academic fields. Although most research shows overall improved operator and system performance with the use of automation, there is often a failure to recognise the new errors that decision support systems can introduce. This problem can result in automation-induced complacency or insufficient monitoring of automation output. User factors which directly influence automation bias include operator trust and confidence in the decision support systems. Environmental mediators include workload, task complexity, and time constraints, which pressurise the cognitive resources of the end users. Mitigating factors of automation bias includes implementation factors such as training and emphasising user accountability, and decision support systems design factors such as the updated confidence intervals of the decision support systems output, and the provision of information versus recommendation [267]. The 'information versus recommendation' degree of automation where the decision maker is used to critique the output of a decision support system has met with more success in terms of industrial integration, particularly in high-risk situations [255]. For example, Guerlain et al. [268] created a decision support system for blood type identification in a blood bank. When used as a critiquing tool, where the decision support system presented the users with different hypotheses regarding the data available rather than defined solutions, the operators made correct decisions 100% of the time. This was in contrast to a decision support system which did not allow the operators to critique the decisions, which led to wrong decision being made between 33% and 63% of the time.

Trust in decision support systems

ISO 9241-210 [269] describes six key principles to ensure that the design of interactive automation systems, such as component reliability models, are user centred. These are:

- The design is based upon an explicit understanding of users, tasks and environments.
- Users are involved throughout design and development.
- The design is driven and refined by user-centred evaluation.
- The design process is iterative.
- The design addresses the whole user experience.
- The design team includes multidisciplinary skills and perspectives.

In terms of addressing the whole user experience, the standard outlines the following*: 'the concept of usability used in ISO 9241…can include the kind of perceptual and emotional aspects typically associated with user experience'*. This is an important point, as for a system to be fully utilised, it has to be more than 'easy to use'. Critical is the operators trust in the system. A review of trust in automation systems was conducted by Balfe [270], of which decision support systems can be considered a branch.

Table 2.1 outlines the key findings from research on the factors leading to operator trust in automation systems. It can be argued that the usage of decision support systems under uncertainty relies on the same tenets to realise integration into the working environment. Balfe concludes that the effect of system uncertainty on trust and subsequent usage has been conclusively proven, and that evidence exists to support the notion of human competence as a key dimension in trust as understanding automation systems can improve the rating of trust.

Table 2.1: Summary of key research on trust in automation. Adapted from [270]

Key Finding	Reference
There is a correlation between trust in and usage of automation.	[271,272]
High reliability and competence are fundamental requirements for trust in automation.	[271,273]
Operator self-confidence and the usefulness of the automation also influence usage.	[274,275]

For complex systems, explicit feedback is required to develop trust.	[276–278]
Trust must be well calibrated to ensure optimal use of automation.	[279,280]
Accurate mental models are important to ensure correct calibration of trust	[281]
Individual differences influence trust.	[282]

Decision making given large uncertainties has been widely studied in the medical literature, many of whose conclusions on decision support systems integration into the working environment agree with those of Balfe [270]. One example of this is evidence based medicine where clinicians integrate individual clinical expertise with the best available external clinical evidence from systematic research. Combining both individual expertise with external evidence allows clinicians to improve the accuracy and precision of diagnoses and prognoses [283]. Evidence based medicine has led to the creation of clinical decision support systems, interactive computer software systems designed to aid doctors with medical decisions, designed to impact clinician decision making about individual patients at the point in time that decisions are made [284]. They are similar in scope and design to their industrial counterparts, albeit the system inputs are clinical metrics related to the human body. This same approach can be utilised by maintenance and management personnel involved in decision making related to defective components or equipment. Uckun, Goebel, and Lucas [285] and Popov, Fink, and Hess [286] draw similar comparisons.

While clinical decision support systems have many proven benefits, their uptake by doctors is limited. Shibl, Lawley, and Debuse [287] researched how and why doctors accept decision support systems via a Unified Theory of Acceptance and Use of Technology based model. The insights into the reasons why doctors do not use decision support systems are transferable to other industries for the development of strategies to enable greater widespread adoption of decision support systems. Shibl et al. conclude that the four main factors influencing decision support systems acceptance and use include usefulness, appropriate training, ease of use, and trust in the decision support systems output. Similarly, Alexander [288] concludes that a clinician's level of trust in decision support systems is affected by how knowledge is represented, the decision support systems ability to make reasonable decisions, and how it is designed. Dreiseitl and Binder [289] investigated how physicians react when faced with decision support systems suggestions that contradict their own diagnoses. They found that physicians were significantly less likely to follow the decision systems' recommendations when they were confident of their initial diagnoses. They conclude that given uncertainties, people are most likely to trust their own judgement. False trust leads to wrong diagnoses, therefore uncertainty quantification is critical. Quality assurance and validation of such systems is therefore of paramount importance.

The challenge of increasing system reliability concurrent with decreasing system complexity allowing greater usability cannot be understated. For while the algorithms and methods behind the three facets of PHM, detection, diagnosis, and prognosis, must become more robust and potentially more complex as they seek to reduce and ultimately eliminate uncertainties, so too must their outputs become flexible, reconfigurable, and subjectively easy to interpret. While one can argue that this approach would dictate the use for a 'black box' style methodology to decision support systems, this too is also not favourable. This is because the end-user perception of potential high missed detection and false alarm rates leads to mistrust and eventual non-use of decision support systems. Consequently, a more open interface is required where PHM outputs are viewed as non-esoteric. This essentially means the transformation of data to usable information, useable information being context driven. As such the management of decision support systems must be addressed to providing the right information in the right form to the right people at the right time in the right place to support maintenance-related decision-making across different organisational levels [290]. Uckun et al. [285] similarly state the need for PHM to become less of an art and more of a science. They conclude that one of the main issues with PHM today is the lack of standardisation governing the research, and that it is often impossible to derive actionable conclusions based on the research results.

2.7 Summary

Maintenance is essential to ensuring the profitability of world class manufacturing organisations. However, maintenance programs are only effective in this endeavor if system intervention is performed at the correct time, taking into account multiple extraneous factors that are difficult to include in a single unified model. Ensuring the correct timing of maintenance actions is further complicated for systems whose components cannot be monitored using additional sensorisation suites. While multiple mathematical and statistical models exist for system lifetime estimation, most of these models depend on adequacy of historical records of component failure data.

In order to estimate the remaining useful life of components which cannot be monitored by traditional CBM techniques, virtual sensors have been an interesting topic of research. Virtual sensors act as inferential system health estimators via proxy process indices, which are typically measured offline. However, in order to develop these models, data inspection, selection of historical data, and data pre-processing must be carried out. However, no holistic methodology exists in the literature for carrying out these functions for components where failure data is scarce and whose health state cannot be monitored online.

Much research work has been performed in the area of smart elastomers, which are potential solutions for condition monitoring of elastomers in industrial scenarios. The potential usage areas of these sensors is large, but the technology is still in its relative infancy and little industrial implementation of these solutions exists currently. In order to develop these solutions further, it is necessary not only to invest in research in the technical solutions around sensorisation, but it is also critical to understand the changing mechanical properties that need to be monitored.

In order to fully encapsulate all significant variables leading to component degradation, it is critical to take into account the elements influencing the performance of people working with industrial systems. As Rasmussen [223] reports, industrial accidents are more likely to be caused by human errors during maintenance activities rather than by errors occurring during plant operation. Despite this importance, few prognostic lifetime algorithms today take in to account human and organisational factor effects. There exists much scope to develop useable solutions to aid maintenance decision makers in this task.

The next industrial revolution, labelled as 'Industry 4.0', has been often cited in the literature over the past 4-5 years [291]. 'Smart Factories', and 'Factories of the Future' have been described as the next generation of industrialisation which is being made possible due to such phenomenon as 'Big Data', Big Data analytics, and modern automation paradigms such as Cyber Physical systems etc. [206]. While absolutely necessary from both a research and industrial perspective, an overlooked fact in many studies is that converting existing industrial plants with often legacy IT frameworks so that they can take advantage of 'Industry 4.0' solutions is not a trivial task. As authors such as Coble [28] have pointed out, much of the academic research today is directed towards ever advanced mathematical solutions to lifetime prognostic algorithms, the vast majority of which are not based on real industrial case studies, do not use industrially sourced data, and do not deal with many of the real-world issues facing the implementation of such advanced analytics. Another barrier to implementation is the lack of understanding, and hence the lack of trust, of maintenance and engineering personnel towards these solutions. As Malik [39] stated back in 1979 "…there is more isolation between practitioners of maintenance and the researchers than in any other professional activity". It can be argued that little has changed in the preceding four decades.

Following from this, one of the issues facing modern analytical solutions in real-world industrial implementation scenarios is a lack of relevant data that can be fed into appropriate models. Despite this obvious challenge, there have been few practical solutions offered in the literature to aid the solving of this problem for commodity status components. This is critical if current manufacturing practices are to evolve to take advantage of 21st century solutions. There is scope therefore to bridge that knowledge and research gap.

Chapter 3

Analysis of process variables contributing to component degradation

Analysis of process variables contributing to component degradation
Chapter 3

- Diaphragms collected and assessed post industrial service
- Service history and environmental exposure data of diaphragms collated
- Statistical selection of significant process variables contributing to degradation

Material characterisation of component degradation
Chapter 4

- Confirmation of significant process variables contributing to EPDM degradation
- Determination of chemical and physical property changes in EPDM diaphragms during degradation

Consideration of human factors contributing to component degradation
Chapter 5

- Methodological framework to create and integrate quantitative human factors metrics proposed
- Developed methodology accounts for human uncertainty during maintenance tasks
- Investigation of impact of incorrect installation on diaphragm degradation

3.1 Introduction

3.1.1 Case study system level description

The components investigated in this case study are elastomer valve diaphragms belonging to numerous connected production vessels within the upstream processing department of a large biopharmaceutical manufacturer, illustrated in figure 3.1. For a more detailed insight into the biopharmaceutical drug production process within the case study facility, please refer to Appendix B.

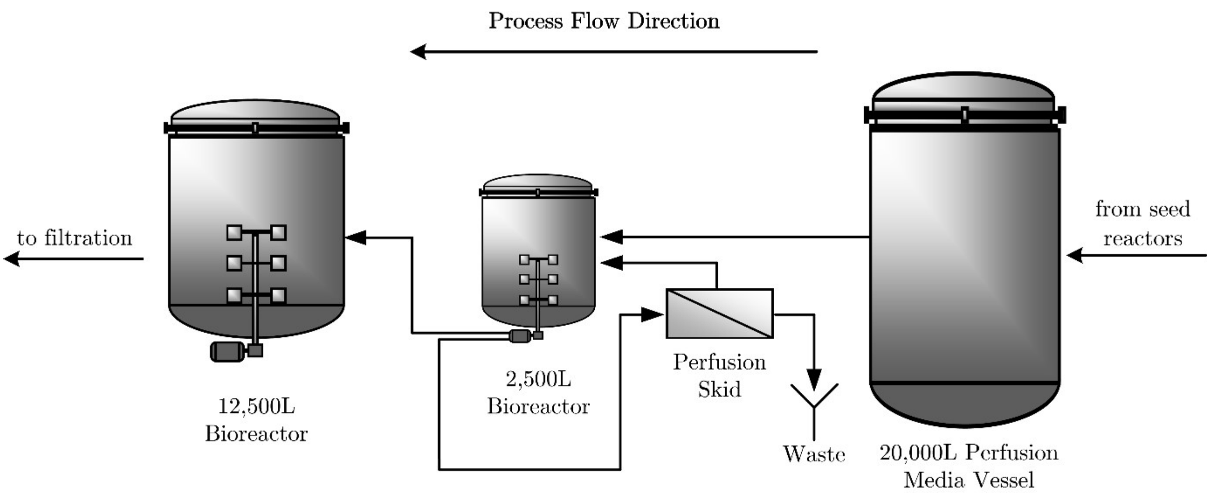

Figure 3.1: Role of the systems in scope of this work

As bioprocesses use living material, they have unique manufacturing challenges, in particular, keeping the product in a state suitable for sustained biological growth via appropriate internal environmental conditions. To accomplish this, there is a need for a vast multitude of auxiliary equipment to be used around bioreactors. Among the most important of these are the valves used to control flow volume, line pressure, and the movement of material into and out of the reactors. The systems in this case study are the largest vessels within the entire process stream, and have the most numerous associated ancillary equipment. They are the key growth reactors in the upstream chain, subject to the most stringent steaming and chemical cleaning regimes. Given their criticality to mission success, these vessels have more in-line process monitoring capabilities than other process equipment. Given the relative availability of diaphragm valves and process data, they afford the best opportunity for targeted data collection. It is worthy to note that the process conditions at these locations have transferability across the industry as a whole.

3.1.2 Equipment level description

The common pneumatically actuated diaphragm valve assembly found in biopharmaceutical operations is described in figure 3.2. The entire valve assembly consists of four parts, the control module, the valve bonnet, the elastomer diaphragm, and the valve weir.

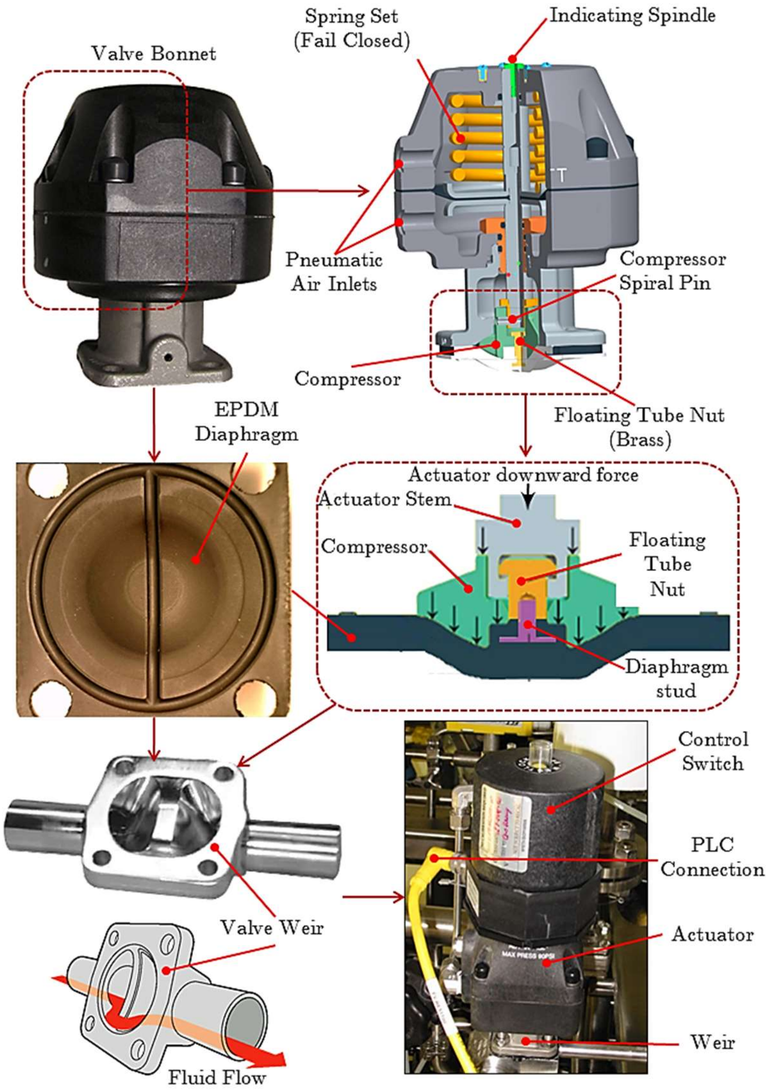

Figure 3.2: Diaphragm valve assembly. Adapted from [292]

The control module is cable connected to the PLC, and controls the pneumatic air supply into the valve bonnet via direct connection. The 6.2 barG pneumatic air supply opens and closes the valve by overcoming the force from a spring set connected to the actuator stem which in turn is connected to the diaphragm compressor. As the actuator stem and compressor move upward, the diaphragm, connected to the compressor via a male threaded stud, also lifts. This allows fluid to then pass through the valve weir. To reduce or stop fluid flow, the compressor forces the diaphragm into the weir cavity. The diaphragm, being malleable, is compressed against the central weir mating element, illustrated in figure 3.3. A moulded finger secures the compressor in the bonnet. The floating tube nut, a female threaded brass connection, is designed to prevent point loading and allow small movement of the diaphragm stud to relieve tensile stress so it is not pulled from the diaphragm. Four fasteners, one in each corner, secure the valve bonnet to the valve weir. The weep hole acts as a leak indicator in case of diaphragm failure

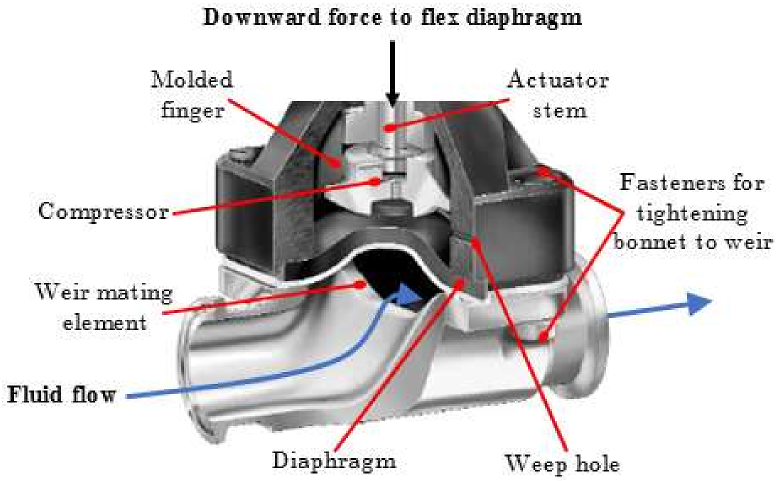

Figure 3.3: Valve assembly, adapted from [292]

3.1.3 Component level description

The components in the scope of this work are peroxide cured compression moulded EPDM valve diaphragms developed specifically for use in the biopharmaceutical industry. For proprietary reasons, all trade names have been removed. The diaphragm is the most critical component of a diaphragm valve. Diaphragms are the valve component that provide positive shut-off between process fluids, protects the process from the environment and protects the environment from the process [292].

The attributes and physical description of the EPDM diaphragms investigated in this case study are given in table 3.1 and figure 3.4 respectively.

Table 3.1: Case study EPDM valve diaphragm attributes

Size		Operating Temperature	Compliance			Shelf Life	Chemical Composition
Inch	DN	°C	FDA	USP	ASME	Years	Relative Quantity (Decreasing Order)
0.25-4	6-100	-20 to +150	Standard 21CFR 177.2600: Rubber Articles Intended for Repeated Use	Standard Class VI, Chapter 87 and 88	BioProcessing Equipment revision 2011 appendix J sub-section J-2 Simulated Steam-in-place (SIP)	6	EPDM Carbon Black Magnesium Oxide Paraffinic Mineral Oil Stearic Acid CAS #61617-00-3 CAS #101-67-7 RM Sulphur Peroxide

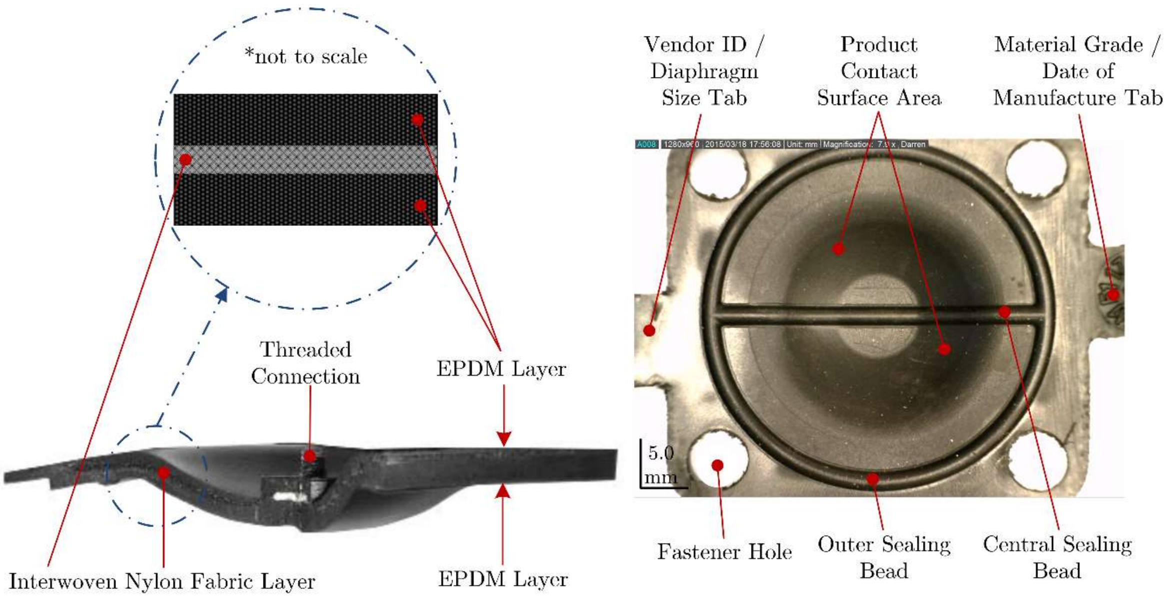

Figure 3.4: Case study EPDM valve diaphragm

The moulded EPDM diaphragm is a sandwich design constructed with two layers of EPDM and a single layer of woven nylon fabric reinforcement. The fabric layer is designed to improve tensile strength and reduce the risk of a full diaphragm split. EPDM diaphragms utilise a threaded connection to the valve compressor [292]. The product contact area consists of the area defined within the boundary of the outer bead, including the central bead. The outer and central beads provide the diaphragm seal as they are compressed against the valve weir. Loss of functionality of either bead will result in loss of sealing ability. The four fastener holes mate with the four fastener holes of the weir and accommodate the fasteners used to tighten the valve bonnet, diaphragm, and weir together. The information tabs on either side of the diaphragm, in the non-product-contact portion of the diaphragm, provide data relating to the date of manufacture of the diaphragm, the specific EPDM material grade used, the diaphragm vendor ID, and the diaphragm size. All diaphragm materials and physical properties are batch traceable via these permanent codes moulded into the diaphragm tabs. The chemical composition of the diaphragms, detailed in table 3.1, were provided by the valve OEM. No other information relating to the chemical composition of the diaphragms or the relative quantity percentages of those chemicals exists in the public domain. Neither does any information relating to the mechanical properties of the components. These issues are explored in greater depth in chapter 4.

3.2 Investigation Methodology

Due to the lack of physics based models describing diaphragm degradation mechanisms, process history data relating to in-situ industrial diaphragm usage was required to facilitate a data driven diaphragm lifetime modelling approach, as described in figure 3.5.

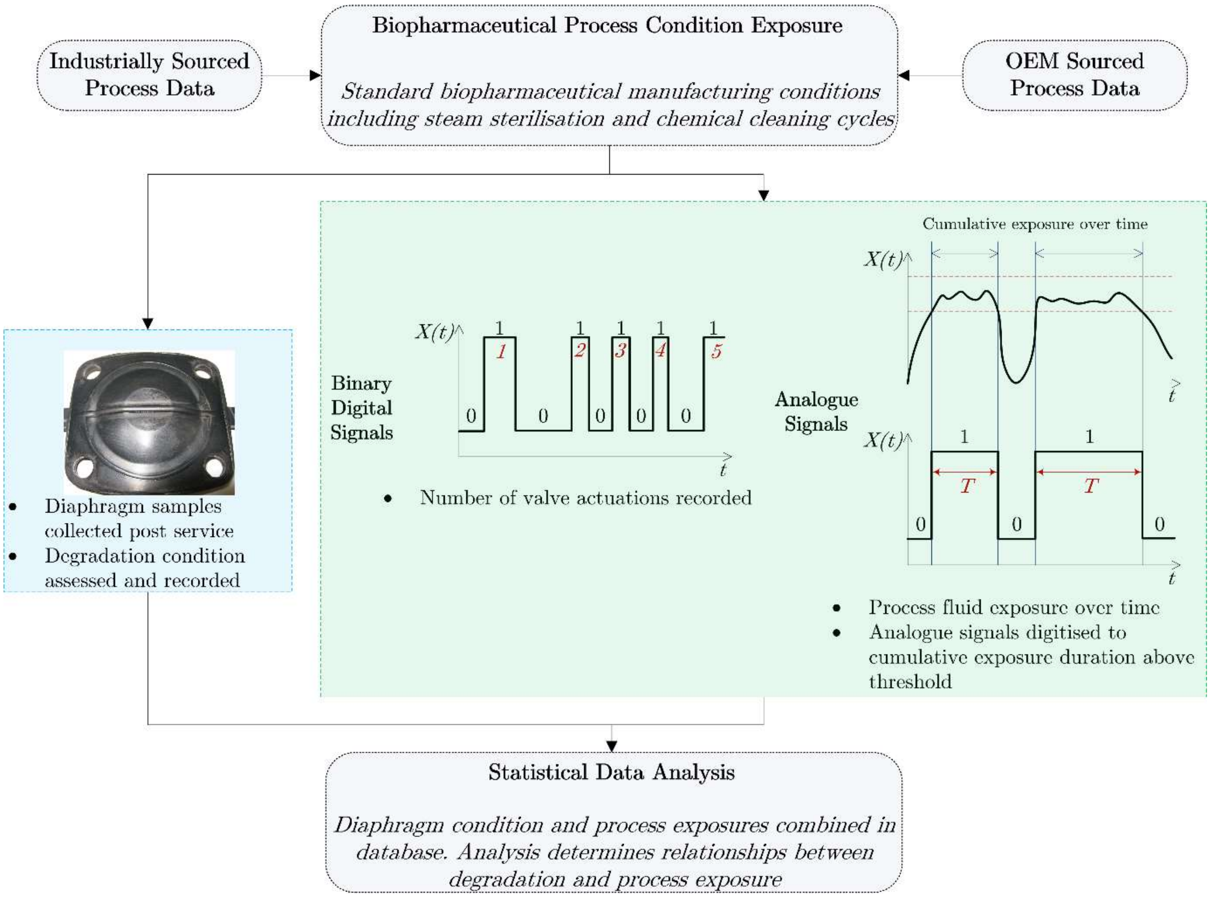

Figure 3.5: Data collection and analysis methodology

The potential for creating accurate physics based lifetime models is limited given the complexities involved with mathematically integrating intricate boundary conditions such as saturated steam, product mediums, and multiple cleaning chemicals exposures, along with multiple poorly understood EPDM degradation and failure modes in this context. Also, as it is not possible to access the diaphragms or assess their degradation state in-situ, a data driven off-line modelling approach would be necessary. However the development of data driven prognostic algorithms necessitates component degradation or failure event data coupled with detailed environmental exposure data. This means that a retrospective analysis of component environmental exposures coupled with component degradation information would be required for model development.

In order to elicit useable information for modelling purposes using limited data resources, the first step was identifying any pre-existing data relating to component lifetimes or environmental exposure histories. A limited dataset of twenty-two samples was available from the diaphragm OEM, comprising of diaphragm lifetime tests conducted using a mock-up of the systems in scope of this work. The OEM testing regime constituted a replication of the industrial usage conditions under investigation, with identical steaming and chemical cleaning conditions with equivalent durations. The testing procedure used by the OEM was designed to replicate worst case scenario industrial exposure conditions of the case study systems. This gives an important insight into diaphragm lifetimes under more extreme process conditions providing data typically difficult to gather in industrial settings. The OEM testing approach was an automated procedure whereby multiple diaphragms were exposed to PLC controlled steaming and chemical cleaning cycles for predetermined durations. Therefore the exact exposure conditions and durations of exposure to those conditions by the diaphragms was known. Each OEM test referred to a virgin diaphragm, and they were removed from service after testing. Initially no information was available to determine the diaphragm degradation state. However access to the OEM tested diaphragms was granted and they were assessed using the developed qualitative methodology, described in detail in section 3.2.2. This degradation data was then combined with the known exposure histories of those samples.

Given the scarcity of information provided by the OEM, additional industrially sourced data was critical in order to enable a comprehensive study of the EPDM diaphragms. To collate this, diaphragms which had been in industrial service for between 6 to 24 months were collected from multiple systems during a biennial scheduled plant shutdown from the systems listed below:

2 x 2500 litre bioreactors
1 x 12,500 litre bioreactor
2 x 20,000 litre perfusion media hold vessels
2 x perfusion skids

Both sets of data are both right and left censored such that the elastomers were exposed to a certain amount of process conditions before being removed from service and their degradation state and exposure history was recorded. This is illustrated in figure 3.6.

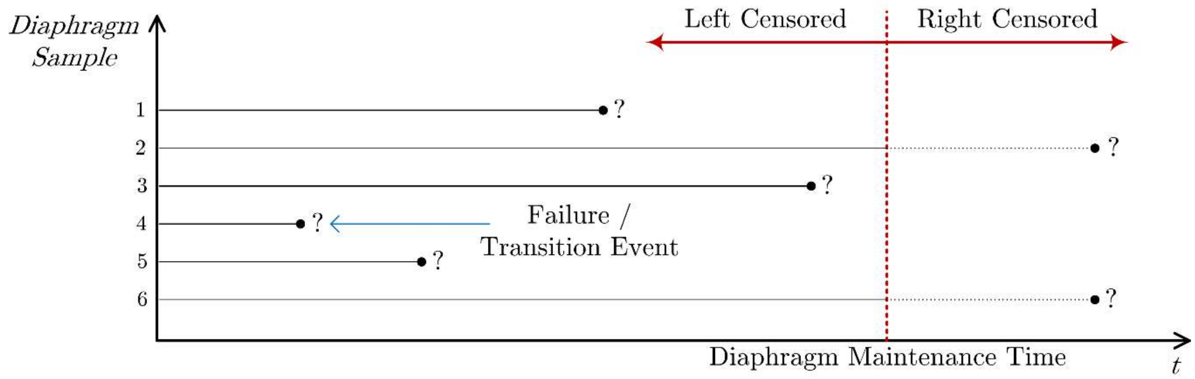

Figure 3.6: Left and right censoring of collected data set

After being removed and collected by maintenance technicians, the diaphragms were individually bagged, sealed, labelled, and stored in a dark, dry, temperature controlled storage environment. This ensured no further degradation mechanisms could propagate as a result of UV or thermal exposure. Each diaphragm sample removed was then assessed and assigned a degradation state. The diaphragms were inspected for any cracks and assigned state membership as having cracked or not. To help determine relationships between the diaphragm degradation and failure states as a function of exposure history, detailed process histories were established for every diaphragm retrieved, from the time of their installation to the time of their retrieval from service. The process history data intended to establish the exact environmental conditions that the diaphragms were subjected to in-situ. It was not possible to automate this process, and instead required a manual data mining approach. The data collection approach used for every individual diaphragm consisted of the following basic steps:

1. Establishing maintenance history records for all systems in order to find the dates of all previous planned and corrective valve maintenance interventions.
2. Mining process history records for the exact number and duration of production batches, clean-in-place (CIP) cycles, and steam-in-place (SIP) cycles processed by each system between these dates.
3. Cumulating the exposures of every individual valve to multiple process and equipment conditions and assembling a bespoke database to capture this information.

In order to create commonality amongst the different data sets, a 'digitisation' approach was developed to convert analogue data sources into cumulative exposure hours over a specific threshold. Using statistical techniques to filter the data into critical and non-critical exposure conditions then allows any cumulative data pertaining to industrial component usage to be utilised as long as those exposure conditions are identical. Further information is available on the thresholds used in determining the cumulative exposure conditions in section 3.3.1. The cumulative data allows the statistical determination of which process conditions contribute to diaphragm degradation mechanisms. If a full parametric degradation model were developed, this step would essentially act as a filtration stage by minimising the number of unnecessary process covariates in the final model.

3.2.1 Diaphragm degradation description

EPDM diaphragms can degrade due to age, environmental and process condition exposure, and handling and installation errors. The valve elastomer diaphragms are subjected to a variety of internal process environmental conditions that affect their rate of degradation, including high pressure saturated steam, cleaning agents and chemical detergents, sparge gases, multiple product mediums, and final purified product. A key issue in the lifetime of the diaphragms is that they are subjected to a variation of these conditions in service, coupled with a wide variety of actuations. In order to describe diaphragm degradation, a qualitative degradation assessment approach was developed in this work. Qualitative signs of gradual diaphragm aging include varying levels of severity of roughening and deformity of the diaphragm surface impacting cleanability and sealability. Signs of sudden diaphragm failure include material cracking and rupturing of the elastomer within the product contact area. The relationship between these two distinct failure modes has been defined in this work for the first time within a three state continuous-time semi-Markov process, illustrated in figure 3.7. The first failure mode is the gradual, stepwise degradation of the component as it is exposed to numerous internal environmental process streams, and is categorised into three phases, from degradation category 1 to degradation category 3. Virgin and minimally aged diaphragms are designated as category 1 degradation. As the elastomer remains in-situ it further degrades over time until it is described as belonging to a category 2 degradation state. The time it takes for a diaphragm to transition from category 1 to category 2 is denoted by T_{1-2}. Category 2 degradation diaphragms are still useable, and this state represents the maximum service life extractable from a diaphragm. The ultimate goal of maintenance optimisation in this regard is to remove diaphragms from service before they transition to degradation category 3, the time of which is denoted by T_{2-3}. Category 3 represents failure mode 1, and occurs when severe deformation has occurred to the diaphragm. In this state, diaphragms have lost their ability to effectively seal and are no longer useable. As noted in figure 3.7 the stepwise degradation mechanisms means the diaphragms must first transition to state 2 degradation and then to state 3 degradation. By definition it is not possible for a diaphragm to immediately transition from degradation state 1 to degradation state 3. The second failure mode is the rupturing or splitting of the diaphragm product contact surface, such that sealing ability is again lost. This failure mode can occur while the diaphragm is in any degradation state, and the transition time is described as $T_{i-C}, i = 1 - 3$.

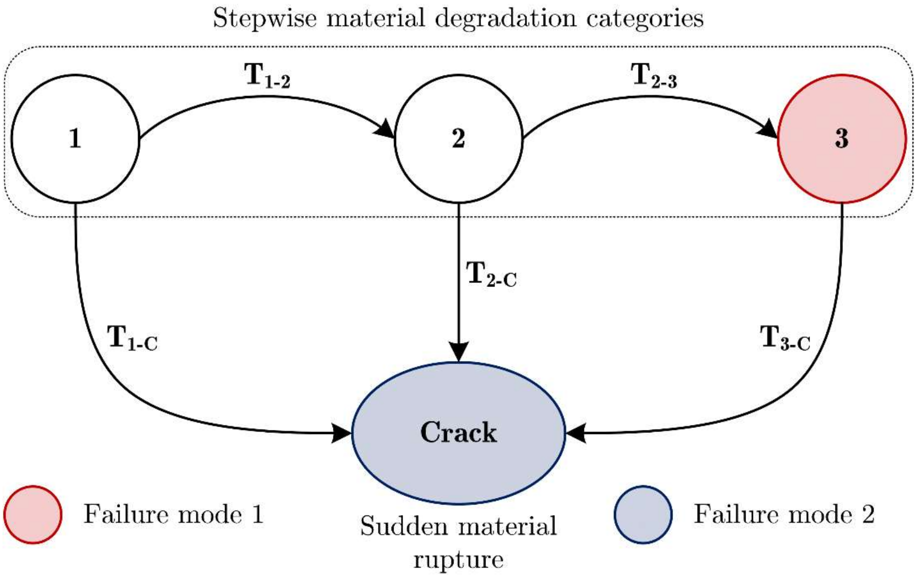

Figure 3.7: Markov chain describing EPDM diaphragm failure modes

Diaphragm degradation category 1

The developed qualitative degradation indications describing state membership of degradation category 1 are shown below in figure 3.8.

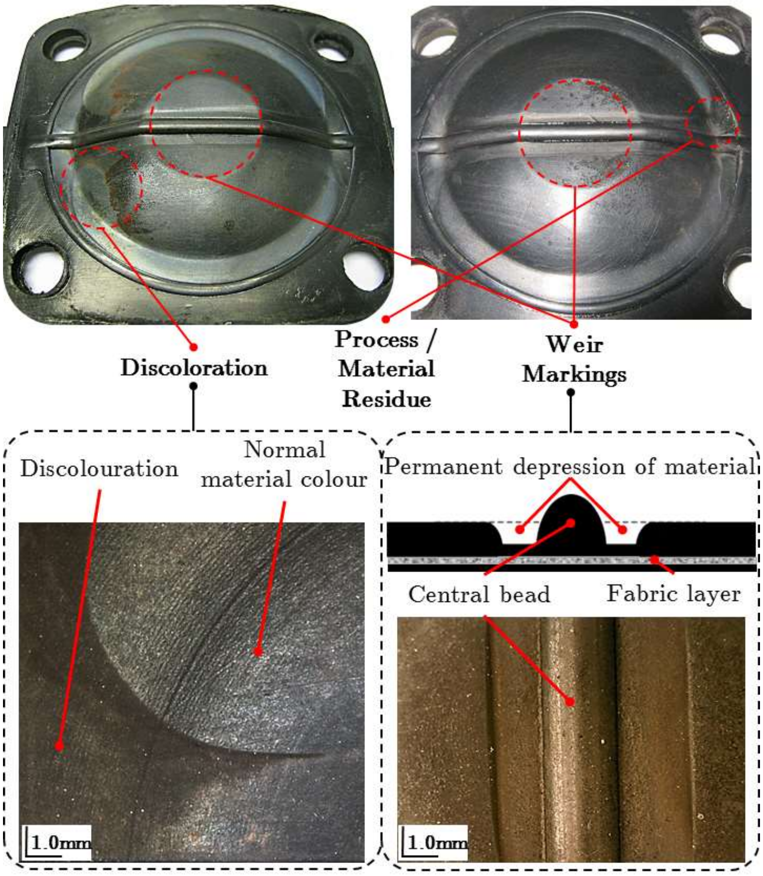

Figure 3.8: EPDM diaphragm degradation state 1

As shown, the three indicators of category 1 degradation are discolouration of the EPDM, process material residue present on the diaphragm surface, and compressive weir markings present on the central and outer beads. None of the above conditions affect the diaphragms' cleanability or sealability, and can be considered as cosmetic damage. The cause of the discoloration was found to be due to surface level oxidative damage, confirmed by FTIR. These FTIR results can be seen in appendix D. This is considered a cosmetic change, as material properties appear unaffected by this change. Once a diaphragm has entered service it is considered as belonging to degradation category 1, therefore it is the lowest level of diaphragm degradation possible. It is not desirable to remove a diaphragm from service in this state, as its useful lifetime has not been fully utilised, and so equipment availability has not been maximised.

Diaphragm degradation category 2

The developed qualitative degradation indications describing state membership of degradation category 2 are shown below in figure 3.9.

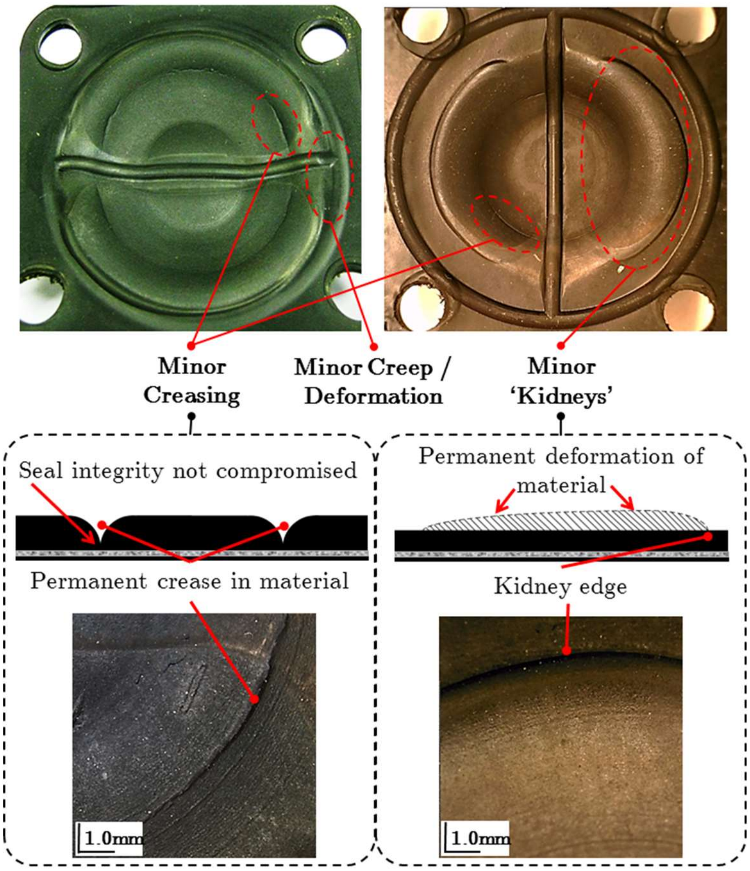

Figure 3.9: EPDM diaphragm degradation state 2

The next stage of diaphragm degradation results in creasing of the EPDM surface, material creep, and deformation of diaphragm features, in particular the central and outer beads, and the formation of 'kidneys'. To be classified as degradation category 2, these conditions must only be present in a 'minor' form, meaning the cleanability and the sealing ability of the diaphragm has not been compromised. Once any of these conditions are present, the damage to the diaphragm is no longer considered cosmetic as the elastomer has flowed from its original moulded state. Continuation of these same degradation conditions will result in the destruction of the usability of the diaphragm. Degradation state 2 represents the maximum useful life extractible from the diaphragms, and it is desirable to remove all diaphragms in this condition.

Diaphragm degradation category 3

The developed qualitative degradation indications describing state membership of degradation category 3 are shown below in figure 3.10.

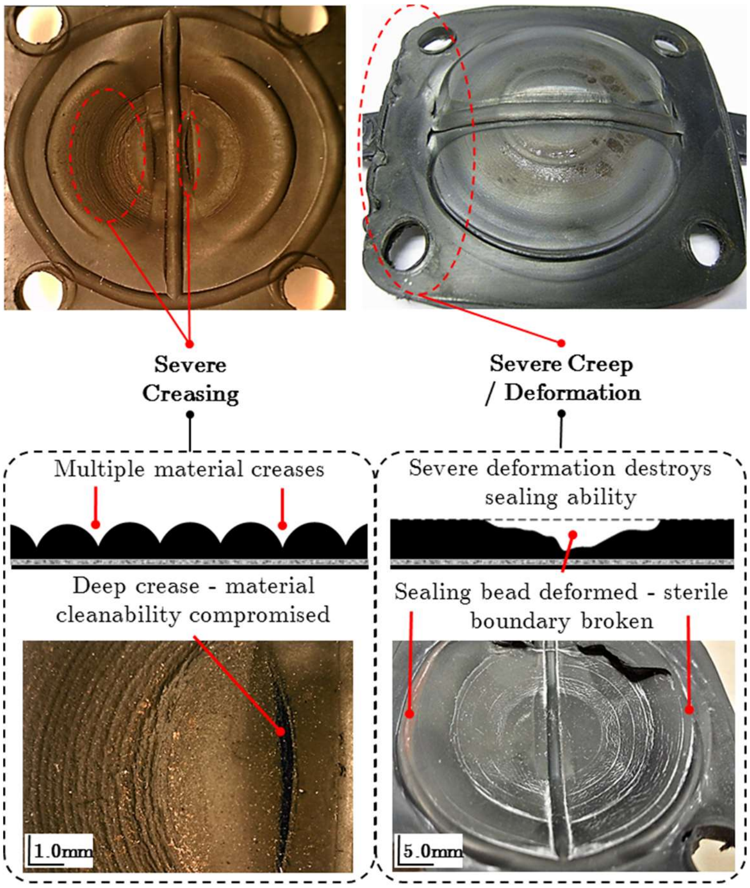

Figure 3.10: EPDM diaphragm degradation state 3

Continuation of the degradation state 2 material deformation mechanisms results in diaphragms that are not fit for purpose due to compromised cleaning and sealing abilities. Both multiple and deep material creases offer an environment for microbiological and endotoxin storage and subsequent propagation. It is important to note that to qualify as a material crease, the split that exists must not penetrate to the fabric layer. Severe melting and deformation of the outer and/or central beads results in complete loss of sealing ability and the hermetic system seal is broken. Microbiological, endotoxin, and chemical ingress can then occur from external and internal sources. Another risk with degradation state 3 diaphragms is physical contamination of the process stream with pieces of elastomer as the diaphragm degrades. Degradation state 3 represents failure state 1.

Diaphragm cracking

The developed qualitative degradation indications describing state membership of a cracked diaphragm are shown below in figure 3.11.

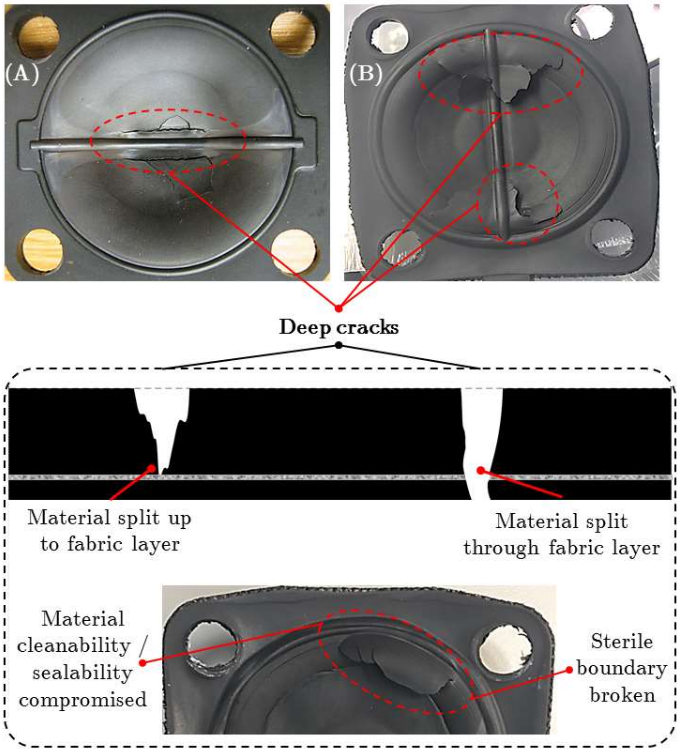

Figure 3.11: EPDM diaphragm cracking

The key difference between a crease and a crack is that a crack has penetrated either to, or beyond, the nylon fabric layer. Once this occurs, the sterile boundary of the system cannot be guaranteed. The sealing and cleaning ability of the diaphragms is also either lost or seriously compromised. The nylon fabric layer is not designed to, and is not suitable for, coming into contact with the process stream. A crack can occur on a diaphragm when it is in any degradation state, despite the presence or absence of any other degradation indicators. For example material creep is not a necessary pre-cursor for state membership. For this reason it is considered as a separate failure mode. Often, a diaphragm crack will have sharp narrow edges and affect a large surface area of the diaphragm, increasing the process integrity risk. Figure 3.11 (A) and (B) show cracks occurring on degradation state 1 and state 2 diaphragms respectively. The diaphragm in figure 3.11 (A) shows mild weir markings and discolouration, while the diaphragm in figure 3.11 (B) shows mild creasing and mild kidney formation. Cracked diaphragms represent failure mode 2, and must be avoided at all cost. As cracking can occur in any degradation state, crack prediction offers a greater prediction challenge than degradation category prediction due to the randomised nature of crack events. To date, little evidence exists for the reason of sudden diaphragm cracking in service. If a crack propagates through the diaphragm in service, the process stream will migrate into the valve bonnet and seep from the weep hole. The weep hole is open to the external atmosphere.

If a diaphragm split occurs, the sterile boundary of the process is compromised and the resultant batch is discarded. The diaphragm is then replaced, and full steaming and chemical cleaning regimes are initiated.

3.2.2 Diaphragm degradation assessment

Given the absence of any formalised method of quantifying diaphragm degradation, in order to effectively categorise the degree of diaphragm damage, a qualitative assessment method was formulated, described in figure 3.12. This involves the organoleptic assessment of the diaphragms after they are removed from service. It is not possible to qualitatively assess diaphragm degradation state in-situ given the closed nature of the production process. A quantitative or condition based assessment method has never been developed. Using the qualitative diaphragm degradation conditions described in chapter 3.2, the below assessment creates a ubiquitous formalised approach towards diaphragm degradation assessment.

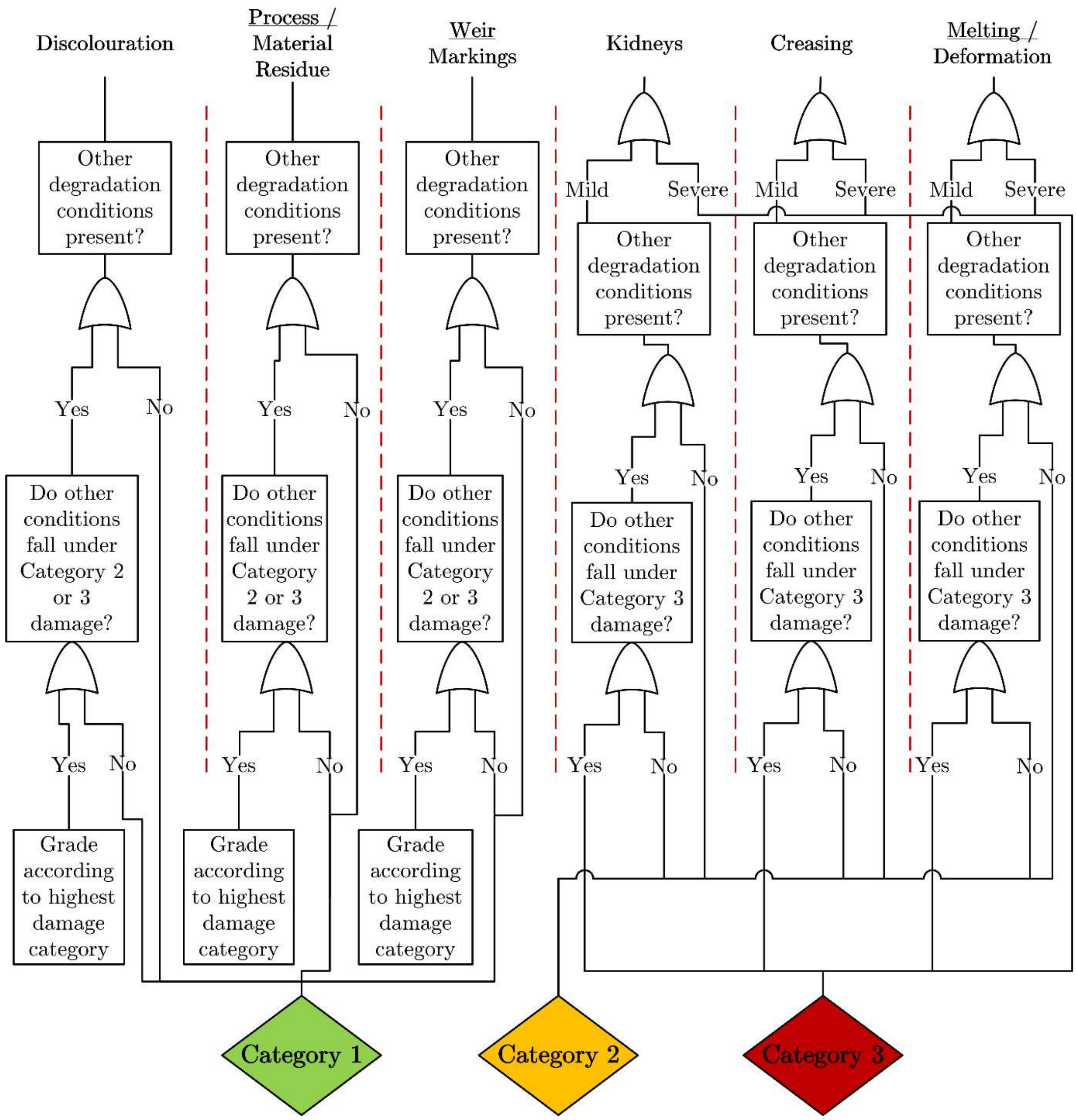

Figure 3.12: Qualitative diaphragm degradation assessment flowchart

3.3 Industrial process history data collection

3.3.1 Degradation database development

The valve sizes are defined by the size of the diameter of the pipework to which the valve is connected, typically given in inches. These valve sizes do not purposefully correspond to any feature on the diaphragm itself. The diaphragms and their sizes collected are given in table 3.2.

Table 3.2: Diaphragm valve sizes in scope of this work

Diaphragm Size (Inch)	Outer Bead Diameter (mm)	Data Set Quantity
0.5	38	67
0.75	48	4
1	56	35
1.5	76	9
2	92	10
3	136	4

Establishing process factor exposures

In order to design effective and thorough reliability frameworks, failure events must be related to their root causes through a systematic study. For this to be coherent, domain knowledge is essential to provide insight into the factors which lead to component degradation [44]. Accordingly, the process factors believed to impact the EPDM material lifetime were identified through domain knowledge experts such as reliability engineers, process technicians, maintenance technicians, and OEM product designers. The basic factors identified as contributing to EPDM diaphragm degradation were identified as per figure 3.13. Each of these factors is included in the full tested dataset, as shown in table 3.13.

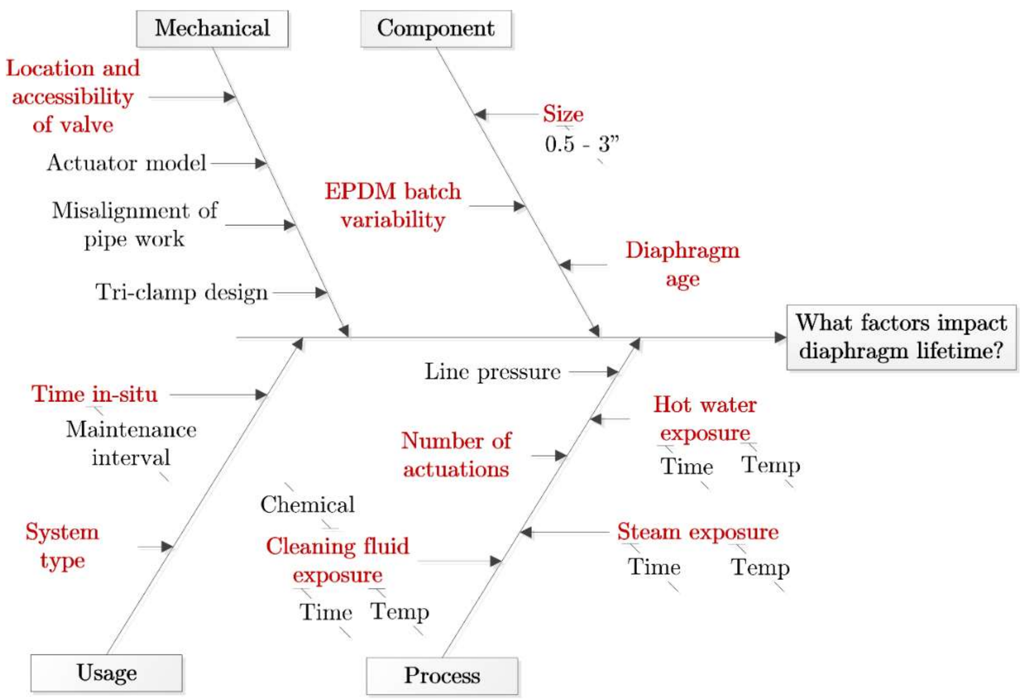

Figure 3.13: Brainstorming of factors impacting EPDM lifetime

Analysis of process variables contributing to component degradation

A number of the factors identified above had already been investigated in terms of their contribution to diaphragm degradation in a limited way by the diaphragm OEM. To expand on this dataset industrial data relating to these and other conditions was also collected. Due to the complex nature of the facility's process control architecture, as shown in figure 3.14, a manual data mining approach was required to build the bespoke database. As illustrated in figure 3.14, the valve solenoid control modules, which control the opening of the valves via control of the pneumatic air flow in and out of the valve bonnets, are connected by a 0.5V, 4-20mA line to control PLC's. The valve solenoid control modules, or switches, being directly connected to the valve actuators act as local control modules.

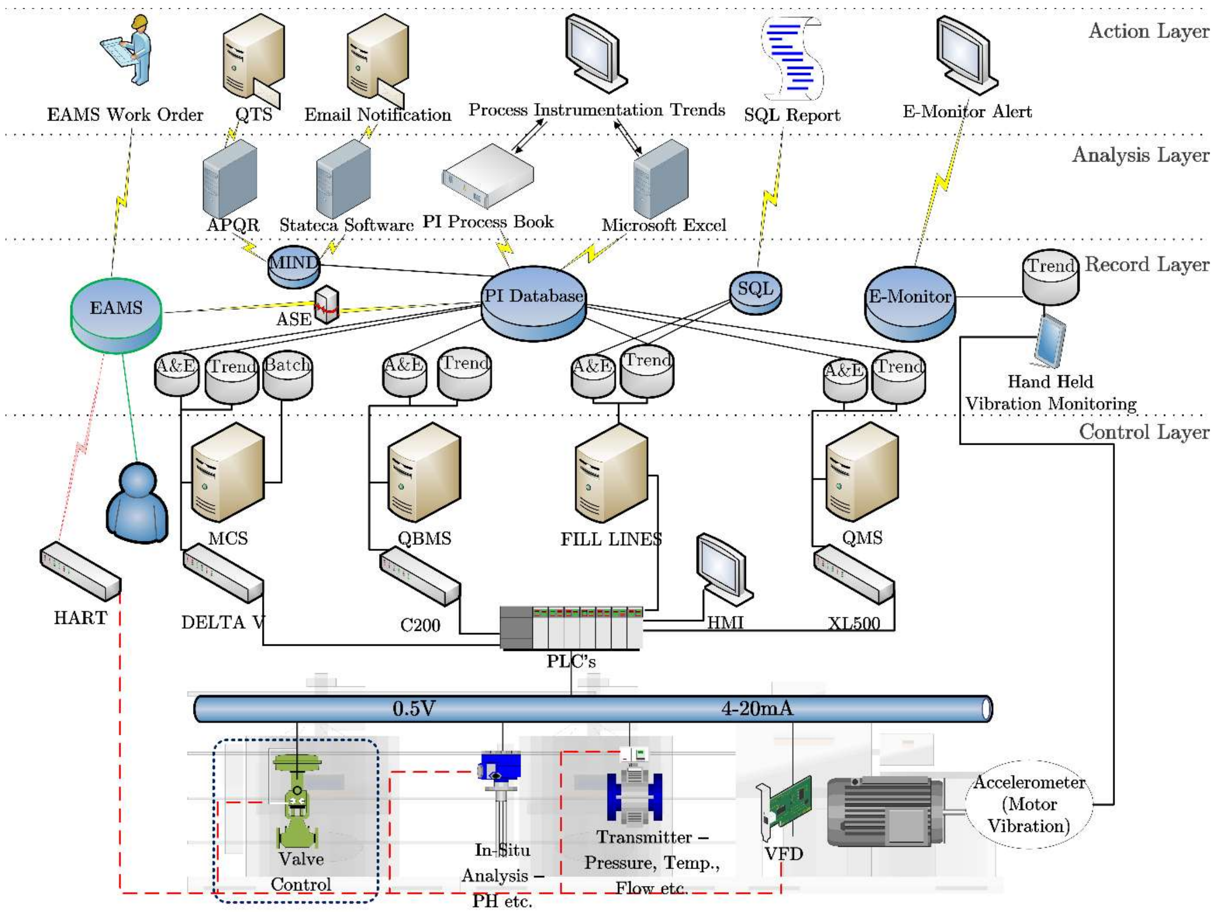

Figure 3.14:Process control system architecture

When the valve control modules pneumatically actuate the valve, this information is recorded within the control module and data is passed back to the PLC. The PLC's are connected to distributed control system modules, which are in turn connected to master control system databases. The master control system database which stores information relating to vessel process history and valve actuations is labelled as MCS in figure 3.14. The QBMS, QMS, and fill lines databases store no relevant data relating to this case study. The master control system databases output alarms and emergency events (A&E), process trends, and batch records of multiple I/O's. The master control system databases are accessible via a cloud database acting as a process data historian, which collates the data from across the site. This cloud is accessible locally on individual workstations via specialised software. This cloud database could be mined to retrieve the cumulative information for CIP, SIP, and production batch history for each vessel, as well as temperature and pressure data from multiple transmitters located throughout the process piping network.

While I/O history is stored in the cloud, work order requests and maintenance history records are stored on a separate enterprise asset management software system, labelled as EAMS in figure 3.14. Data on maintenance interventions and other asset management activities are manually input into the EAMS system, from where work orders are assigned to maintenance technicians against a particular piece of equipment. Separately, within the enterprise asset management software system database, there is a list of spare parts associated with these individual work order requests. The spare parts and work to be carried out is detailed in a document called the maintenance task list. Data relating to diaphragm size and age of diaphragm at installation was established from the diaphragms information tabs, as identified in figure 3.4.

Establishing maintenance history records

The first step in the process data history collection involved identifying which maintenance task list each valve was on. It was critical to track the precise maintenance history of each valve, as numerous valves on the same system are on different maintenance task lists depending on their planned maintenance interval duration. For example, there are 3, 6, 12, 18, and 24-month maintenance task list's developed based on historical valve usage and predicted risk of failure. These maintenance intervals have been set on an ad-hoc basis and represent the current static preventative maintenance approach. When each active valve maintenance task list was correctly identified, the enterprise asset management software system database was searched for maintenance records relating to when these maintenance task lists were conducted. This was in order to ascertain the dates of all previous maintenance interventions on all systems in scope of this work.

It was necessary to ensure that the maintenance task lists and the specific work orders generated in the enterprise asset management software system agreed with each other in terms of the scope of the work actually carried out. Therefore, the list of spare parts used during each maintenance activity was retrieved and cross referenced with the maintenance work order logs. This ensured that the records of the actual parts used matched the parts listed in the maintenance task lists. This step was necessary in case there was any special cause deviation that meant that a particular valve was excluded during a certain work order. This would occur for example if any of the valves in scope had been subject to a corrective maintenance work order, which would typically occur due to the discovery of a failed diaphragm or batch contamination. Between the dates of installation and retrieval of all diaphragms in scope, the enterprise asset management software system was again searched for any corrective work orders carried out on any valve. If a corrective work order had been carried out, the valve identified was noted as having a different installation date than the others on the same maintenance task list.

When the previous maintenance dates for all valves was established, it was necessary to accumulate the precise amount of production batches, steaming cycles, and chemical cleaning cycles each system associated with those valves underwent in the interim time period. This information was available through a separate database, labelled as the PI Database in figure 3.14. A semi-automated method was developed to extract this information, whereby special macro-enabled filters were coded to search the database to find the appropriate records, before each record was manually checked to ensure no anomalies such as recorded double-starts. Once the correct number of production, CIP, and SIP cycles was established, the individual exposure of each valve to different process conditions could be established.

Steam in place investigations

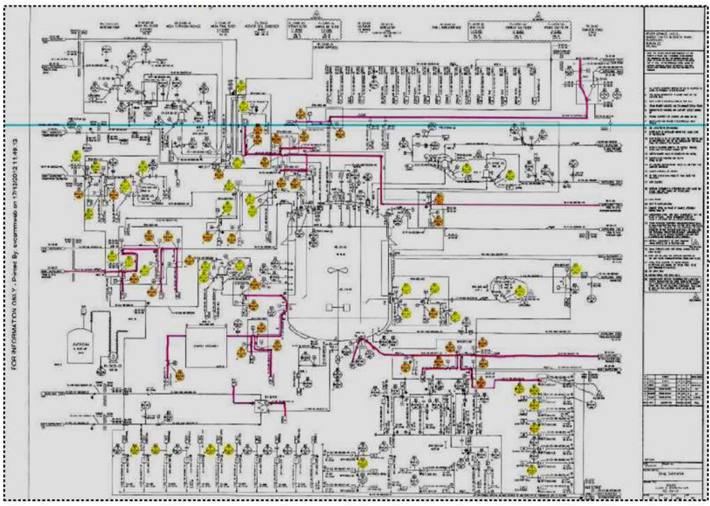

Valves and associated temperature sensors identified from P&IDs

Variable	N	Mean	StDev	Minimum	Median	Maximum
TT-101/102	18	6645	848	4744	6989	7676
TT-001A	18	48.167	3.312	43.000	48.000	53.000
TT-001B	18	48.167	3.312	43.000	48.000	53.000
TT-003	18	6524.2	145.3	6278.0	6536.0	6791.0
TT-004	18	0.000000	0.000000	0.000000	0.000000	0.000000
TT-005	18	0.000000	0.000000	0.000000	0.000000	0.000000
TT-006	18	319.3	163.8	228.0	257.0	927.0
TT-007	18	0.000000	0.000000	0.000000	0.000000	0.000000
TT-008	18	0.000000	0.000000	0.000000	0.000000	0.000000

Temperature records for all transmitters >121.1°C recorded

System Tag	Valve Tag	Cumulated Steam Exposure (Hrs)
RE-51180	FV-150A	0.00
PV-51190	FV-039	16.40
PV-51190	FV-040	16.40
PV-51190	FV-045	16.40
PV-51190	FV-004	16.40

Data accumulated and assigned to each valve

Figure 3.15: SIP data mining methodology

As illustrated in figure 3.15, when the times and dates of all SIPs were established, all possible steam routes for each system were mapped on the appropriate system P&ID'S to assign temperature transmitters to every individual valve. The exposure time of temperatures above 121.1°C for all temperature transmitters monitoring the two types of SIP cycles were retrieved from the PI system. This related to SIPs prior to batch production and SIPs during batch production. The exposure durations above 121.1°C recorded by the controlling temperature transmitters were added together if an individual valve was steamed by both SIP types or was assigned to multiple transmitters.

Clean in place investigations

The main steps in the CIP recipes are listed in sequence in the CIP process map, described in appendix B. To determine the chemical exposure per valve, the functional design specifications for each system and applicable CIP loops were reviewed to determine the programmed time parameters for steps with cleaning media. All cleaning loops were mapped from the P&ID's to identify the flow routes of the cleaning media. When the times and dates of all CIPs were established, the applicable functional design specification timers were assigned to the individual valves and accumulated. The functional design specification timers track the different cleaning media stages through specific parts of the systems by monitoring the fluid conductivity. Conductivity probes determine the ionic content of the process stream, from which the product medium can be determined. To satisfy regulatory requirements, all transmitters on production vessels are strictly controlled and regularly calibrated for conformity.

Valve actuations investigation

When a valve is actuated, a digital response is recorded by the manufacturing control system. These digital records are accessible from the cloud database. The number of valve actuations during both SIP and CIP cycles were collated and counted from the end of one batch to the end of the next batch and allocated to the appropriate process step by cross referencing the time and dates of the SIP and CIP cycles. This allowed the allocation of the number of actuations occurring during each individual process step.

3.4 Statistical data analysis

3.4.1 Data summary

An example of the difference in steam and chemical exposure conditions between the plant data and the OEM data is shown in figure 3.16 below.

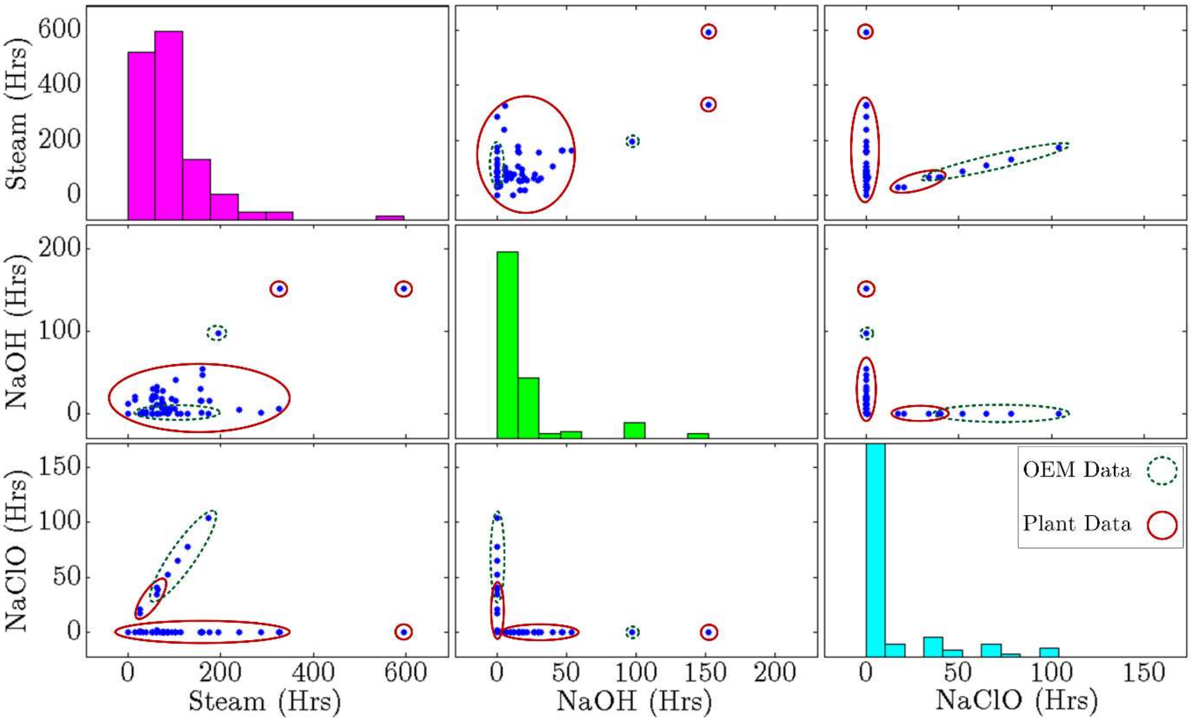

Figure 3.16: SIP, NaOH, and NaClO exposure conditions - industrial data versus vendor test data

Shown in figure 3.16 is each individual sample retrieved from service post-industrial usage or obtained from the OEM. Each sample is represented as a blue dot. It can be seen that there are instances in the data where the plant data represents more extreme exposures than the OEM data, and vice versa. The more extreme exposures, which could be categorised as outliers, are shown as individual samples separated from the larger groups of samples. What is evident is that the OEM data continues and expands upon existing relationships already within the plant data. This demonstrates how the OEM data is representative of the overall environmental interactions, while at the same time in some instances expanding upon those interactions to allow greater insight in to the data in order to aid significant variable selection.

The data collected is composed of two dependant variables and multiple independent variables. The two dependant variables are the degradation category of all samples, coded as a three level ordinal variable from 1 to 3, and the dichotomous variable for the presence of a crack, where "No" is coded as 0, and "Yes" is coded as 1. The number and data type of the independent variables differs across both the production bioreactors and the perfusion skids. The full list of all variables, their data types, role, and parent systems are shown in table 3.3 below.

Table 3.3: All data variables investigated in the initial statistical analyses

Variable Name	Measurand	Data Range	Data Type	Data Role	Parent System
Diaphragm Degradation State/Category	Material Assessment	1 - 3	Ordinal	Dependent	All
Diaphragm Cracking	No/Yes	0 - 1	Dichotomous	Dependent	All
ECO Interval	Hours	0 - 19728	Continuous	Independent	All
Age of Diaphragm at Installation	Hours	1800 - 17616	Continuous	Independent	All
Diaphragm Size	Inches	0.5 - 3	Nominal	Independent	All
Cumulated Steam Exposure	Hours	0 – 594.10	Continuous	Independent	All
Number of Actuations during Steaming	Number of Actuations	0 - 4030	Continuous	Independent	All
Cumulated 80°C Water for Injection Exposure	Hours	0 - 325	Continuous	Independent	All
Number of Actuations during Water for Injection Exposure	Number of Actuations	0 - 4030	Continuous	Independent	All
Number of Actuations during Batch Production	Number of Actuations	0 - 6405	Continuous	Independent	All
Total Number of Actuations	Number of Actuations	0 - 12090	Continuous	Independent	All
Cumulated 65°C Sodium Hydroxide (NaOH) Exposure	Hours	0 – 152.10	Continuous	Independent	Bioreactors
Number of Actuations during NaOH	Number of Actuations	0 - 4030	Continuous	Independent	Bioreactors
Cumulated 60°C Return Osmosis Water Exposure	Hours	0 – 60.11	Continuous	Independent	Bioreactors
Number of Actuations during Return Osmosis Water Exposure	Number of Actuations	0 – 1428	Continuous	Independent	Bioreactors
Cumulated 23°C Phosphoric Acid (H_3PO_4) Exposure	Hours	0 - 9	Continuous	Independent	Perfusion Skids
Number of Actuations during Phosphoric Acid Exposure	Number of Actuations	0 - 420	Continuous	Independent	Perfusion Skids
Cumulated 45°C Sodium Hypochlorite (NaClO) Exposure	Hours	0 - 104	Continuous	Independent	Perfusion Skids
Number of Actuations during Sodium Hypochlorite Exposure	Number of Actuations	0 - 864	Continuous	Independent	Perfusion Skids

After the data shown in table 3.3 was collected, the dataset was assembled into a matrix such that each row represented an individual diaphragm and its associated failure states and covariates, the latter describing the exposure history of each sample in the time interval between installation and retrieval from service. This constituted the bespoke degradation database.

An example of the database data matrix layout is shown in table 3.4.

Table 3.4: Field data degradation database matrix

Diaphragm #	Dependent Variables		Independent Variables (Covariates)		
	Degradation State	Cracking	Steam Exposure (Hrs)	...	Total Actuations
1	1	1	87.3	...	228
2	2	1	103.9	...	2659
...	...	...	...	...	...
129	1	0	195.0	...	12090

A summary of the plant data alone is shown below in table 3.5, while a summary of the OEM data is shown in table 3.6. A summary of the combined data is shown in table 3.7.

Table 3.5: Plant data summary

Crack	0	1	Total
Degradation State			
1	72	6	78
2	21	4	25
3	1	3	4
Total	94	13	107

Table 3.6: OEM sourced data summary

Crack	0	1	Total
Degradation State			
1	17	0	17
2	0	4	4
3	0	1	1
Total	17	5	22

Table 3.7: Full dataset summary

Crack	0	1	Total
Degradation State			
1	89	6	95
2	21	8	29
3	1	4	5
Total	111	18	129

A visual summary of the combined plant and OEM data is shown below in figure 3.17.

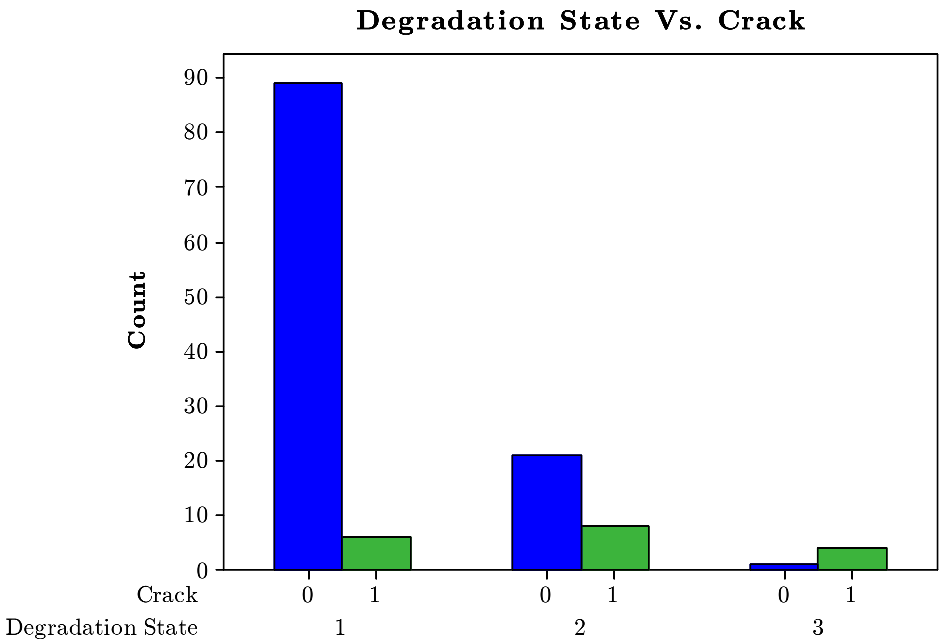

Figure 3.17: Data barchart summary

Table 3.8 and table 3.9 show the full dataset broken down into the individual systems. As shown, the bioreactor type samples account for approximately 66% of the total dataset.

Table 3.8: Bioreactor Type Data Summary

Crack	0	1	Total
Degradation State			
1	56	5	61
2	18	3	21
3	1	3	4
Total	75	11	86

Table 3.9: Perfusion Skid Type Data Summary

Crack	0	1	Total
Degradation State			
1	33	1	34
2	3	5	8
3	0	1	1
Total	36	7	43

A visual representation of the two system types and their associated data sets are shown in figure 3.18. As shown, the number of individual actuations during each exposure type is accumulated to create the variable 'Total Actuations'.

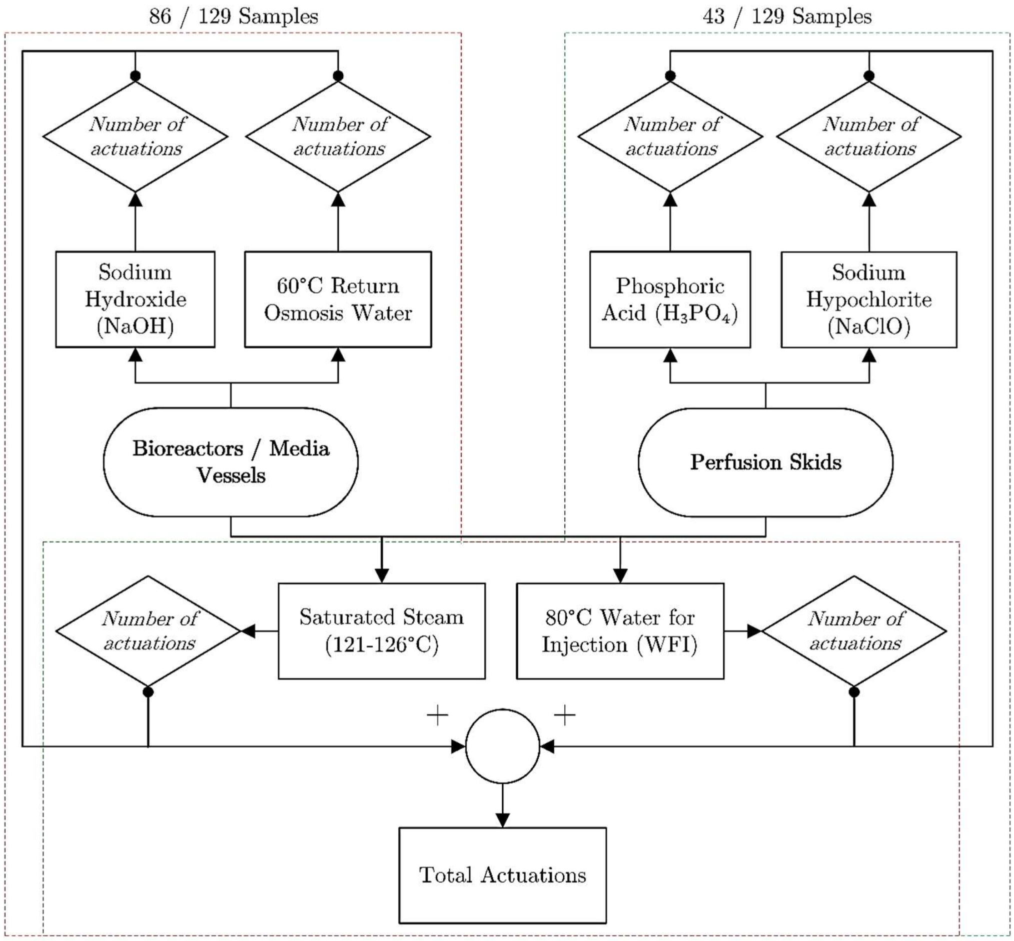

Figure 3.18: Both system types and their associated data

3.4.2 Testing for independence – degradation state vs. crack

In order to determine whether there was any association, i.e. statistical dependence, between degradation state and the presence of a crack, a binomial logistic regression test was conducted. We test the hypothesis:

$$\begin{cases} H0: Degradation\ State\ and\ Crack\ are\ independant \\ H1: Degradation\ State\ and\ Crack\ are\ dependant \end{cases}$$

Independence assessment – binomial logistic regression

It can be seen from the summarised raw data that as the degradation state increases at each step, the ratio between the numbers of cracked to non-cracked parts falls until the number of cracked parts becomes greater in degradation state 3. The degradation state independent variable was treated as a continuous variable because there are not enough incidents of cracking (<10) in each state to test for significance in each state. If there were more than 10 incidents per state then dummy variables could be used for each state [163]. Purely testing for independence, treating the degradation states as a rising continuous variable is valid as the aim is not to identify the strength of relationship of each degradation state, simply whether the probability of a crack increases with increasing degradation. Therefore, the logistic regression model becomes:

$$Logit(\pi(d)) = \alpha + \beta.d, \text{ where } \pi(d) = P(Crack = 1 | Degradation\ State = d) \quad (3.4.1)$$

i.e. the probability of a crack at a particular degradation level. The hypothesis becomes:

$$\begin{cases} H0: \beta = 0 \\ H1: \beta \neq 0 \end{cases}$$

From the output shown in table 3.10 we can reject the null hypothesis of independence (β_0=0) as the coefficient β associated with material degradation category is 1.894 with a low standard error of 0.458 and a significant P value of <0.0005. The overall logistic regression model is statistically significant with a Chi-Square, $\chi^2(2)$, = 20.149, P <0.0005. The model explained 26.1% of the variance in crack events based on the pseudo R^2 metric of Nagelkerke. The model correctly classified 88.4% of cases, however the sensitivity, or true positive value, of crack events was only 22.2%. The change in the odds ratio for each increase in one unit of the material degradation category, e^{β}, is 6.645 with a 95% confidence interval of 2.707 and 16.308. From this information we can conclude that as material degradation state increases, so does the probability of a crack occurring in the material.

Table 3.10: Logistic regression analysis predicting the likelihood of a crack based on material degradation category

	β	S.E.	Wald	df	Sig.	Exp(β)	95% C.I.for EXP(β)	
							Lower	Upper
Material Degradation Category	1.894	.458	17.089	1	.000	6.645	2.707	16.308
Constant	-4.648	.806	33.259	1	.000	.010	*	*

Computing the change in crack probability for each unit change in material degradation category, such that $e^{1.894}$-1 = 6.645 (odds ratio) - 1 = 5.645. Therefore for each unit increase in degradation state the odds of a crack increases by 565%. Extrapolating this relationship shows, depending on the starting probability (P_{Start}), what the new probability of a crack occurring (P_{New}) is given a 1-unit increase in degradation state, as shown in equation (3.4.2) below.

$$P_{New} = \frac{\left(\left(\frac{P_{Start}}{1-P_{Start}}\right)+\left(\left(\frac{P_{Start}}{1-P_{Start}}\right) x\ 5.65\right)\right)}{1+\left(\left(\frac{P_{Start}}{1-P_{Start}}\right)+\left(\left(\frac{P_{Start}}{1-P_{Start}}\right) x\ 5.65\right)\right)} \quad (3.4.2)$$

A graph of the updated probabilities of a crack occurring given a 1-unit increase in degradation state is shown in figure 3.19 below.

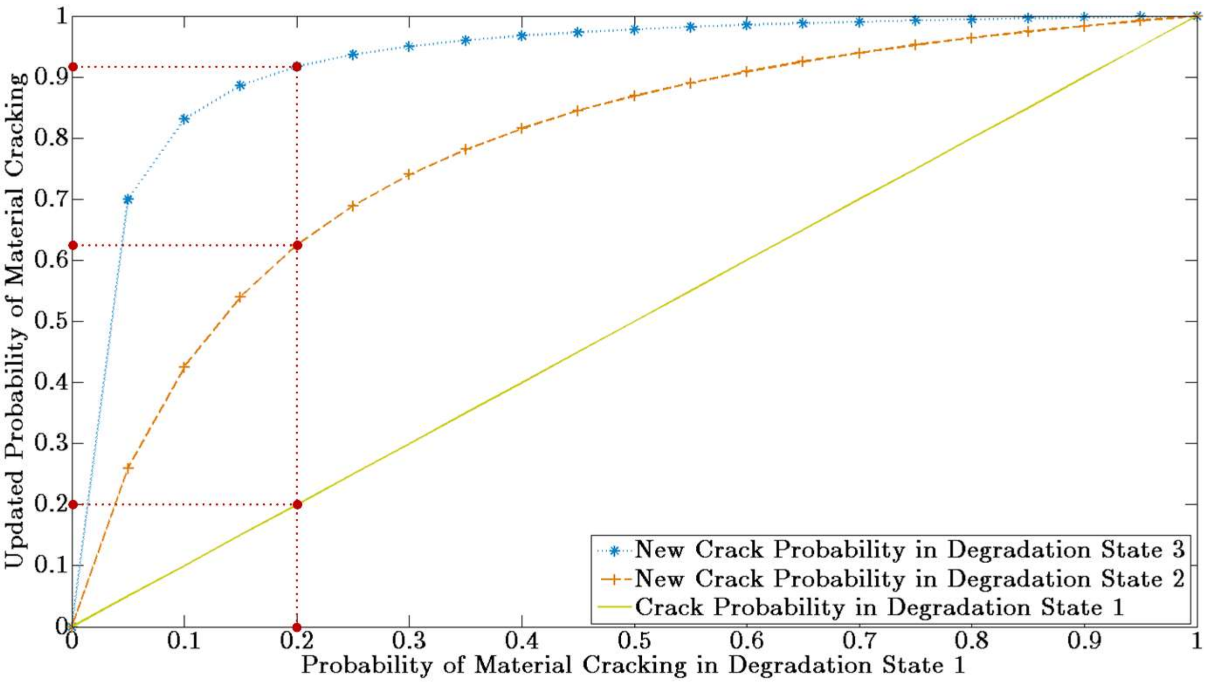

Figure 3.19: Updated probabilities of material cracking as degradation state increases

To illustrate an example, simulated is the probability of a crack occurring during degradation state 1 as being 20%, shown via the broken red line. This probability of a crack occurring during degradation state 1 can be due to a multitude of different reasons. As the component remains in service and changes from degradation state 1 to degradation state 2, now the new probability of a crack occurring in the component 62.4%. If the material further remains in service and transitions to degradation state 3, the new probability of a crack being present in the material is now 91.7%. It is important to keep in mind of course that this relationship shows association, not causation, reiterating the need to predict the initial cracking probability. Although the model correctly classified 88.4% of cases, the model displays poor predictive ability overall, as shown in table 3.11.

Table 3.11: Cracking versus degradation state classification table

Observed		Predicted		
		Crack (Y/N)		Percentage Correct
		0	1	
Crack (Y/N)	0	110	1	99.1
	1	14	4	22.2
Overall Percentage				88.4

While the specificity, i.e. true negative percentage, value of the model is 99.1%, the sensitivity, the percentage of cases of cracking correctly predicted by the model, is only 22.2%. It is likely that as there are relatively few cases of crack events in the data set that this exaggerated the specificity of the model. It is clear there is a need for more insight into the causes of cracking, as due to the complex censored nature of the data, the category 3 diaphragms may have cracked when they were in either state 1 or state 2. However, the statistically dependant relationship established indicates that the longer the material is in service, the greater the probability of the material developing cracks.

3.4.3 Degradation model covariate selection - multivariate binomial logistic regression

In this case study, it is assumed that direct transitions from degradation state 1 to state 3 are not possible, which is typical of degradation processes caused by a cumulative damage, and that the degradation process is influenced by a set of covariates. Furthermore, we consider a case in which the components are replaced after inspection. To ascertain from the full available set of covariates Φ the significant subset $\tilde{p}$ for the prediction of crack events and the material degradation category in the bioreactor and perfusion systems, multivariate binomial logistic regression is utilised [293]. From the developed database, a dataset $(d \in \mathbb{R}^N, X' \in \mathbb{R}^{N\times\Phi}) = \{(d_n, x'_n)\}_{n=1,\ldots,N}$ is available, containing N observations, the generic n-th record reporting the degradation state d_n and the corresponding vector $x'_n = (x'_{n1}, \ldots, x'_{n\Phi}) \in \mathbb{R}^\Phi$ of the values of the Φ covariates initially available. Vectors x'_n form the rows of matrix X'. Since the components are replaced after inspection, every record refers to a different component. To expand on the model introduced in chapter 2, the multi-covariate binomial logistic regression model is defined as [163,293]:

$$ln\left(\frac{\hat{P}_F}{1-\hat{P}_F}\right) = \alpha + \beta_1.\Phi_{F1} + \beta_2.\Phi_{F2} + \cdots + \beta_N.\Phi_{FN} = \alpha + \sum_{i=1}^{N} \beta_N.\Phi_N \tag{3.4.3}$$

Which becomes:

$$\hat{P}_F = e^{\alpha+\beta_1.\tilde{p}_{F1}+\beta_2.\tilde{p}_{F2}+\cdots+\beta_N.\tilde{p}_{FN}} \Big/ 1 + e^{\alpha+\beta_1.\tilde{p}_{F1}+\beta_2.\tilde{p}_{F2}+\cdots+\beta_N.\tilde{p}_{FN}} \tag{3.4.4}$$

where $\hat{P}_F$ is the expected probability that the dependant variable, the dichotomous failure event, has occurred, and $\tilde{p}_{F1}$ - $\tilde{p}_{FN}$ are the significant independent variables associated with that specific failure event.

In this case study, material degradation state fits the definition of an ordinal variable, with the three ordered categories 1 < 2 < 3. Normally, a typical analysis to use in this circumstance would be the cumulative odds ordinal logistic regression with proportional odds [293]. Unfortunately, as is often the case with real world data sets, there is not enough sample cases of degradation state 3 in order to reliably predict both the significance and parameter estimates of the individual covariates for this state specifically. This is because the fewer events per variable available, the less reliable the analysis becomes. Typically, having less than 10 events per variable results in biased or unreliable coefficients [294]. As there are only 5 incidences of degradation state 3 occurring throughout the entire dataset it is not possible to run either a full ordinal regression analysis or a multinomial logistic regression analysis. Instead, a binomial logistic regression analysis is conducted for this failure mode using the degradation states 1 and 2, with degradation state 1 acting as the reference category, and degradation state 2 acting as the event category. It is therefore assumed that whatever process exposure conditions cause the EPDM to transition from degradation state 1 to state 2, are also responsible for the transition between state 2 and state 3. Given the scarcity of information, it must also be assumed that the vector of coefficients β_T = $(\beta_1, \square, \beta_\Phi)$ is independent of the two transition times $T_{1\text{-}2}$ and $T_{2\text{-}3}$ defined in the semi-Markov approach, i.e. that the impact of the covariates on the two transition times is the same. Similarly, for the variable selection for crack events, non-cracked samples are used as reference, with crack events acting as the event.

As the data set in this work is industrially sourced, the amount of data available is limited as the majority of samples only become available after the completion of the 12 or 24-month maintenance intervals. The objective of variable selection is to pick, from the whole set Φ of available covariates, the subset $\tilde{p}$ of those that provide the best predictive performance.

In this work a two-step approach is used for variable selection. Firstly, a filtering approach is used initially to discard from the full list of available covariates those which are not significant in determining the transition behaviour between failure states. This is an unrefined selection based on the binomial logistic regression technique. This method is suitable for situations where the number of covariates is large with respect to the amount of available data, and works like a filter method, as the selection is not based on the predictive ability of a final model. Secondly, a wrapper method, based on the AIC and the Pseudo R^2 measure of Cragg & Uhler and Nagelkerke are applied on the filtered set of covariates $\tilde{p}$ to ascertain if predictive performance of the logistic regression models are enhanced using select subsets p of those significant covariates. With a reduced covariate selection, wrapper methods are advantageous as they help the maximisation of predictive performance in the final model. The aim of using both the Pseudo R^2 and AIC metrics is to find the correct balance between maximisation of the variability explained by the model by maximisation of the Pseudo R^2 value, while minimising model complexity by having too many covariates by minimising the AIC value. Figure 3.20 below shows the developed procedure for selecting the significant covariates for the degradation models using binomial logistic regression analysis, corresponding to the filtering method for selecting the initial covariate subset, and the wrapper methods for verification of predictive model performance using AIC and the Pseudo R^2 measure of Cragg & Uhler and Nagelkerke.

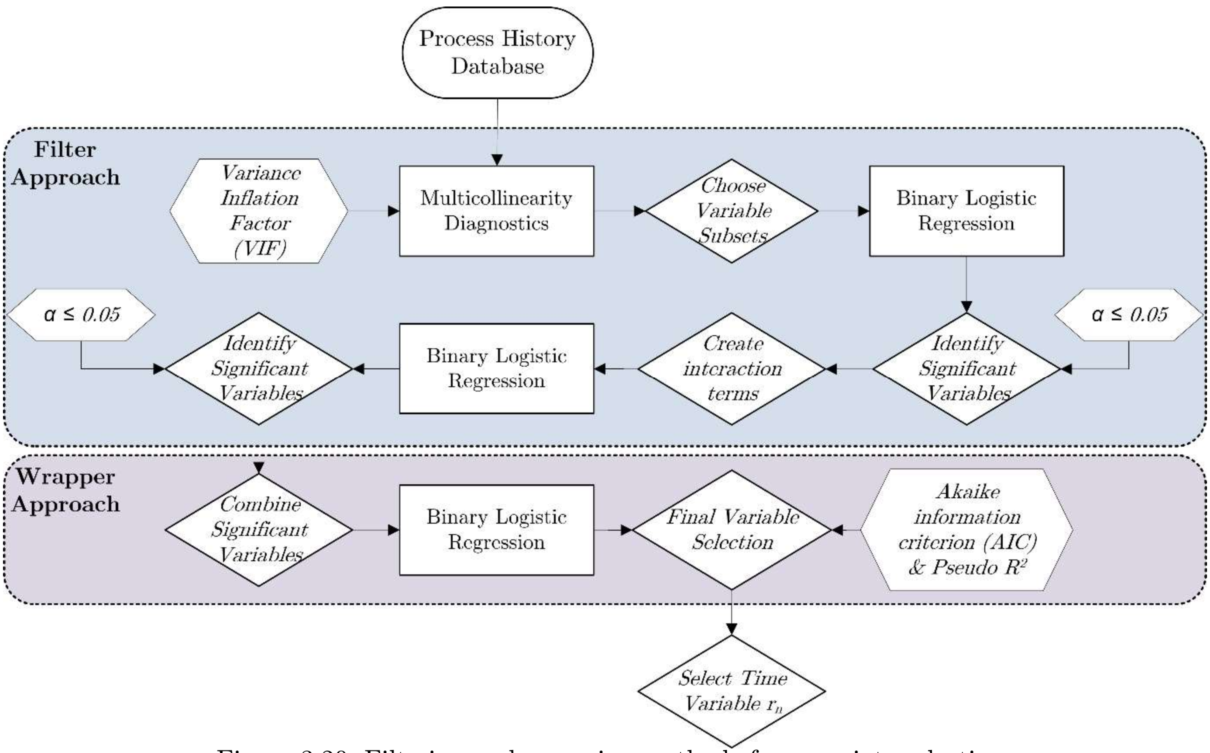

Figure 3.20: Filtering and wrapping methods for covariate selection

Time variable selection

In order to develop dynamic component specific degradation models, it is preferential not to assume the use of calendar time as the most appropriate time variable used to describe diaphragm degradation state transition rates. Rather, the approach adopted here is to use a ubiquitous process variable applicable to all components which also significantly lends to the degradation rate experienced by the components. Therefore the time variable chosen has two constraints: 1) it must be an independent continuous time process variable which all components regardless of system type are subjected to, and 2) it must be the variable deemed most significant with regards to the degradation state transition rates defined within the semi-Markov framework. Formally, within the logistic regression model, the values x' of the full covariate list Φ are used as explanatory variables. Then, among the chosen significant covariate subset $\tilde{p}$ the component 'replacement time' r_n of the final predictive model is chosen, where $r_n = (r_{n1}, \dots, r_{n\mathrm{N}}) \in \mathbb{R}^{\mathrm{N}}$. This way, the final significant dataset later used to develop the degradation model can be defined as $(r \in \mathbb{R}^N,\ d \in \mathbb{R}^N,\ X' \in \mathbb{R}^{N\times\,\tilde{p}-1}) = \{(r_n, d_n, x'_n)\}_{n=1,\dots,N}$ reporting the degradation state d_n in which the n-th component was found at the replacement time r_n, i.e., the 'time' elapsed from installation to replacement. The initial candidate variables satisfying condition 1 above are:

- Maintenance (ECO) Interval (Hrs)
- Cumulated Steam Exposure (Hrs)
- Cumulated 80°C Water for Injection Exposure (Hrs)

Multicollinearity diagnostics

The first step in the filter approach is to choose the initial variable subsets for both system types that minimises the multicollinearity present among the covariates. Once this initial subset has been elucidated, they will be used within the regression models to filter the significant variables. In multivariate binary logistic regression analysis there are a number of assumptions which must be met in order to proceed with using the model, such as independence of cases and that categories are mutually exclusive and exhaustive. The most pertinent to this analysis, given the large number (>10) of independent variables, is that of multicollinearity. Multicollinearity occurs when there are two or more independent variables that are highly correlated with each other, leading to problems with understanding which variable contributes to the variance explained by the model [163]. The first step in the process is to create dummy variables from the categorical variables to be used in the model. A series of dichotomous variables coded either "0" or "1" can be created in such a way that these new dichotomous variables represent all the information from the original categorical variable. This is necessary as logistic regression models do not allow the direct entry of categorical variables into the equation because they will be interpreted as continuous variables [295]. The categorical independent variable used in both regression models is diaphragm size, which is defined in inches according to industrial usage norms. An example of the new coding format of the diaphragm size categorical data is shown in Table 3.12.

Table 3.12: Diaphragm size parameter coding

		Parameter coding			
Diaphragm Size (Inch)	0.50	0	0	0	0
	1.00	1	0	0	0
	1.50	0	1	0	0
	2.00	0	0	1	0
	3.00	0	0	0	1

Multicollinearity must be addressed as it can increase estimates of parameter variance, yield models in which no variable is statistically significant even though the R^2 is large, produce parameter estimates with an incorrect sign and of incorrect magnitude, create situations in which small changes in the data produce large variations in parameter estimates, and prevent the numerical solution of a model [296]. In order to identify highly correlated independent variables we use the Variance Inflation Factor (VIF), defined as [296]:

$$1/_{1-R^2} \tag{3.4.5}$$

where R^2 is derived by regressing the i^{th} coefficient against all other coefficients in the model. Typically, any variable with a VIF greater than 10 can be categorised as having problematic levels of collinearity to other variables [297]. Menard [298] states that a VIF of greater than 5 is cause for concern, and a VIF greater than 10 almost certainly indicates a serious collinearity problem. However Hair et al. [299] suggest that a VIF of less than 10 is indicative of inconsequential collinearity. As such, a VIF limit of 10 is applied here as a cut off point for variables after which further action is taken to reduce model collinearity if present. It is important to note that multicollinearity diagnostics will only be used during the filtering stage in determining the initial significant covariate selection, meaning the issue of multicollinearity will be addressed when partially determining the relative importance of each potential covariate only. This is because multicollinearity doesn't affect the statistical significance of a variable, meaning if a regression coefficient is statistically significant while there is a large amount of multicollinearity present, it is still statistically significant in the face of that collinearity [296]. Therefore once the significant covariates have been selected, potentially correlated covariates can be used together in a predictive model, as multicollinearity doesn't reduce the predictive power of a model as a whole [293].

3.4.4 Variable subset selection - full dataset

Using the date gathered as detailed in figure 3.13, a VIF analysis was performed on the full dataset in order to understand the relationships that exist overall within the data. As a starting point, the full dataset was analysed using regression techniques before the dataset was broken down into the two separate systems. This is to utilise the data in different formats in order to extract the most information. The challenge with the dataset is the limited amount of data available with which to make conclusions about the significance of individual variables. This is particularly true of the perfusion skid dataset as it accounts for only approximately 33% of the total data available. Utilising the full dataset to test for the significance of individual variables in both failure modes is appropriate in this instance to help further guide the final variable selection for the predictive lifetime models. The final conclusions of variable selection will not be based on a single statistical test, but on various sources of information including material characterisation analyses and expert judgment. The VIF analysis of the full dataset is shown in table 3.13.

Table 3.13: Multicollinearity analysis: Full dataset

Model	Collinearity Statistics	
	Tolerance	VIF
ECO Interval (Hrs)	.324	3.085
Age of Diaphragm at Installation (Hrs)	.624	1.603
Cumulated Steam Exposure (Hrs)	.312	3.209
No. Actuations (Steam Exposure)	.124	8.039
65°C Sodium Hydroxide (NaOH) Exposure (Hrs)	.019	53.391
No. Actuations (NaOH Exposure)	.036	27.601
60°C Return Osmosis (RO) Exposure (Hrs)	.044	22.492
No. Actuations (60°C RO Exposure)	.486	2.059
80°C Water For Injection Exposure (WFI) (Hrs)	.019	53.613
No. Actuations (80°C WFI Exposure)	.021	48.161

23°C Phosphoric Acid Exposure (Hrs)	.357	2.801
No. Actuations (23°C H_3PO_4 Exposure)	.442	2.261
45°C Sodium Hypochlorite Exposure (Hrs)	.120	8.325
No. Actuations (45°C NaClO Exposure)	.099	10.080
No. Actuations During Production Batches	.925	1.082
Diaphragm size 0.5 Inch	.655	1.527
Diaphragm size 1 Inch	.469	2.131
Diaphragm size 1.5 Inch	.736	1.358
Diaphragm size 2.0 Inch	.666	1.501

Individual actuations are highly correlated to their respective exposure conditions, and also to the total actuations variable. Unfortunately, including them in the analysis would be ineffective, as it would not be possible to determine their relative importance given the high degree of collinearity present.

When they are removed from the analysis, within the remainder of the covariates there is a high degree of collinearity between:

- 80°C Water for Injection exposure
- Cumulated 65°C NaOH Exposure
- Total Actuations

Removing all other actuations from the model, one of these three variables can be included with all of the following variables:

- ECO Interval (Hrs)
- Age of Diaphragm at Installation (Hrs)
- Cumulated Steam Exposure (Hrs)
- Cumulated 60°C Return Osmosis Exposure (Hrs)
- 23°C Phosphoric Acid Exposure (Hrs)
- 45°C Cumulated Sodium Hypochlorite Exposure (Hrs)
- Diaphragm size 0.5 Inch
- Diaphragm size 1 Inch
- Diaphragm size 1.5 Inch
- Diaphragm size 2 Inch

Diaphragms of size 0.75 and 3 inches are removed from the analysis, as due to their low frequencies only unreliable and unstable coefficients are produced. The frequency of the different diaphragm sizes in the full dataset is shown in table 3.14.

Table 3.14: Frequency of diaphragm sizes in total dataset

Diaphragm Size (Inch)	Frequency	Percentage of Overall
.50	67	51.9
.75	4	3.1
1.00	35	27.1
1.50	9	7.0
2.00	10	7.8

3.00	4	3.1
Total	129	100.0

Using this combination of variables, three separate models can be constructed.

Full dataset - model 1

Table 3.15: The inclusion of 65°C NaOH exposure

Model	Collinearity Statistics	
	Tolerance	VIF
ECO Interval (Hrs)	.465	2.150
Age of Diaphragm at Installation (Hrs)	.643	1.556
Cumulated Steam Exposure (Hrs)	.358	2.794
60°C Return Osmosis Exposure (Hrs)	.328	3.048
23°C Phosphoric Acid Exposure (Hrs)	.787	1.271
45°C Sodium Hypochlorite Exposure (Hrs)	.352	2.843
Diaphragm size 0.5 Inch	.176	5.692
Diaphragm size 1 Inch	.224	4.461
Diaphragm size 1.5 Inch	.481	2.077
Diaphragm size 2 Inch	.394	2.540
65°C Sodium Hydroxide Exposure (Hrs)	.252	3.967

Full dataset - model 2

Table 3.16: The inclusion of 80°C water for injection exposure

Model	Collinearity Statistics	
	Tolerance	VIF
ECO Interval (Hrs)	.432	2.313
Age of Diaphragm at Installation (Hrs)	.646	1.547
Cumulated Steam Exposure (Hrs)	.335	2.983
60°C Return Osmosis Exposure (Hrs)	.409	2.445
23°C Phosphoric Acid Exposure (Hrs)	.741	1.350
45°C Sodium Hypochlorite Exposure (Hrs)	.343	2.920
Diaphragm size 0.5 Inch	.175	5.706
Diaphragm size 1 Inch	.218	4.596
Diaphragm size 1.5 Inch	.483	2.070
Diaphragm size 2 Inch	.393	2.545
80°C Water for Injection Exposure (Hrs)	.387	2.584

Full dataset - model 3

Table 3.17: The inclusion of cumulative total actuations

Model	Collinearity Statistics	
	Tolerance	VIF
ECO Interval (Hrs)	.509	1.963
Age of Diaphragm at Installation (Hrs)	.651	1.535
Cumulated Steam Exposure (Hrs)	.380	2.630
60°C Return Osmosis Exposure (Hrs)	.405	2.468
23°C Phosphoric Acid Exposure (Hrs)	.785	1.273
45°C Sodium Hypochlorite Exposure (Hrs)	.409	2.443
Diaphragm size 0.5 Inch	.173	5.768
Diaphragm size 1 Inch	.217	4.615
Diaphragm size 1.5 Inch	.483	2.071
Diaphragm size 2 Inch	.392	2.550
Total Actuations	.506	1.977

3.4.5 Variable subset selection - bioreactor dataset

The first VIF analysis of the full list of covariates from the bioreactor type dataset is shown in table 3.18. As the variable ‘Total Actuations’ is a linear combination of each of the individual actuations, and therefore linearly dependant on them, it has been dropped from the initial analysis as the collinearity would be so great as to cause the model to fail. As shown, the most highly correlated covariates are:

- Cumulated 65°C NaOH exposure
- Number of actuations during NaOH exposure
- 60°C Return Osmosis exposure
- 80°C Water for Injection exposure

- Number of actuations during 80°C Water for Injection exposure

All other covariates have VIF values lower than 10.

Table 3.18: Multicollinearity analysis: Full bioreactor type dataset

Model	Collinearity Statistics	
	Tolerance	VIF
ECO Interval (Hrs)	.417	2.400
Age of Diaphragm at Installation (Hrs)	.689	1.452
Cumulated Steam Exposure (Hrs)	.359	2.782
No. Actuations (Steam Exposure)	.125	7.977
Cumulated 65°C Sodium Hydroxide (NaOH) Exposure (Hrs)	.022	46.329
No. Actuations (NaOH Exposure)	.019	51.984
60°C RO (Hrs)	.046	21.888
No. Actuations (60°C RO Exposure)	.513	1.942
80°C WFI (Hrs)	.014	72.752
No. Actuations (80°C WFI Exposure)	.008	129.601
No. Actuations During Production Batches	.928	1.078
Diaphragm size 0.5 Inch	.144	6.962
Diaphragm size 1 Inch	.188	5.318
Diaphragm size 1.5 Inch	.366	2.732
Diaphragm size 2 Inch	.282	3.551

As a first step, due to the high VIF values, all actuations during individual exposures were removed from the model and replaced with their linear combination which is the total actuations variable.

Table 3.19: Multicollinearity analysis: Bioreactor type dataset excluding individual actuations

Model	Collinearity Statistics	
	Tolerance	VIF
ECO Interval (Hrs)	.484	2.065
Age of Diaphragm at Installation (Hrs)	.714	1.401
Cumulated Steam Exposure (Hrs)	.375	2.669
Cumulated 65°C Sodium Hydroxide (NaOH) Exposure (Hrs)	.028	36.532
60°C RO (Hrs)	.065	15.597
80°C WFI (Hrs)	.028	35.270
Total Actuations	.109	9.151
Diaphragm size 0.5 Inch	.148	6.784
Diaphragm size 1 Inch	.193	5.188
Diaphragm size 1.5 Inch	.370	2.703
Diaphragm size 2 Inch	.289	3.462

Table 3.19 shows that the cumulated exposures to NaOH and hot water at both 80°C and 60°C are highly correlated. This is also illustrated in figure 3.21 below. Figure 3.21 illustrates also how the OEM exposures are at times more extreme than the industrial process data exposures, with the reverse also being true. The contrast between the two datasets is favourable, as it allows for better distinction between the affect that the two exposures may have on component degradation.

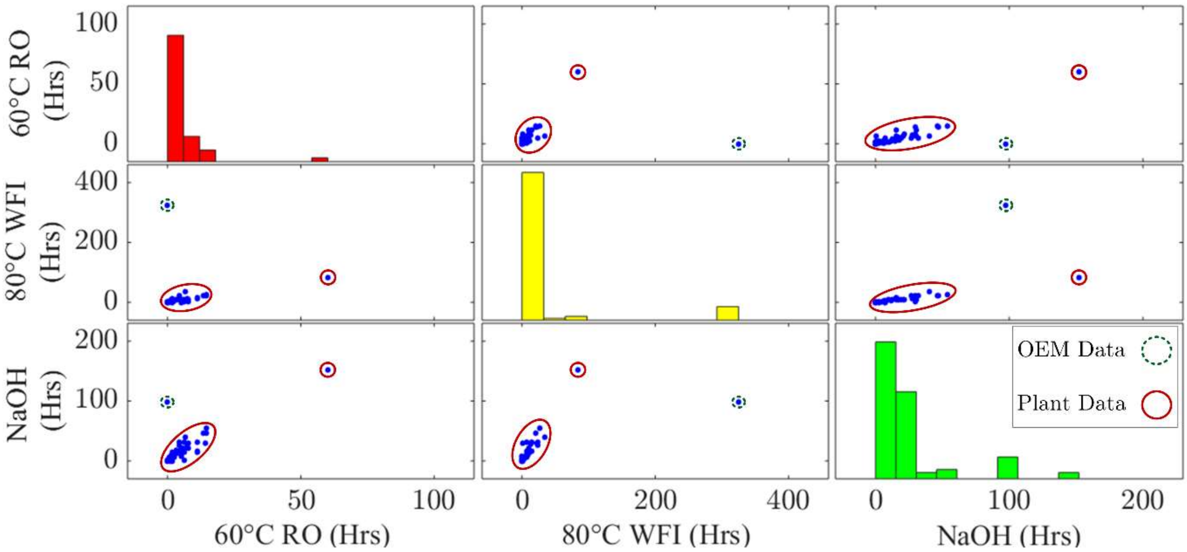

Figure 3.21: CIP exposure conditions - industrial data versus vendor test data in bioreactors

Rather than simply delete the offending chemical exposure variables or create a linear combination of all three of them, it is important to first understand the relationship between them and the roles they play in the overall production process. As shown in figure 3.21, NaOH, 60°C return osmosis water and 80°C water for injection exposure are highly correlated during production runs. However, when included, the OEM data gives greater insight into the role of all three variables as this reduces the correlation between the variables, as shown in figure 3.22. Exploring the relationship between the NaOH and 60°C return osmosis water exposures shows that when the OEM data is not included in the analysis, the adjusted R^2 value of a linear regression between the two variables is 0.9221. This is shown as the solid black line in figure 3.22. This is because they are both only used in the cleaning cycles for bioreactors, as opposed to the 80°C water for injection variable which is used in the cleaning cycles of both the bioreactors and the perfusion skids. This contrasts to an adjusted R^2 value 0.338 when the OEM data is included. This is shown as the broken red line in figure 3.22. The OEM data point shown in figure 3.22 represents multiple samples with identical exposures. The OEM data here provides insight into diaphragm condition given low levels of 60°C return osmosis water exposure but high levels of NaOH exposure. This contrasts to information garnered from the industrial dataset which provides information relating to high levels of both NaOH and 60°C return osmosis water exposures. Either deleting one of the NaOH and 60°C return osmosis water exposure variables, or linearly combining them into a new variable, could potentially cause an important loss of information.

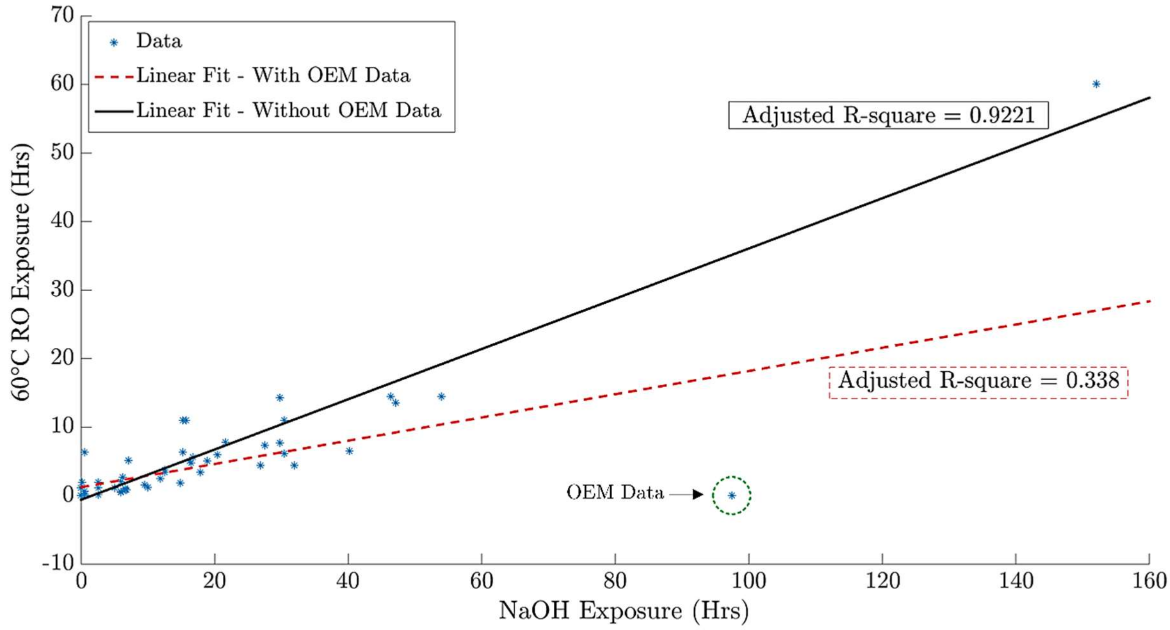

Figure 3.22: Relationship between NaOH exposure and 60°C return osmosis water exposure in the bioreactor systems

As shown in figure 3.23, observing the correlation between NaOH and 80°C water for injection exposure across all systems, it is evident that there is not a strong correlation between the two variables. It is therefore not appropriate to either delete one of these two variables or to merge them into one new individual variable. A theoretical single model unifying all systems would potentially lose critical information due to the loss of one of these variables. The OEM data point here again represents multiple samples, providing additional information not available from the process data about the effect of moderate levels of NaOH exposure but high levels of 80°C water for injection exposure.

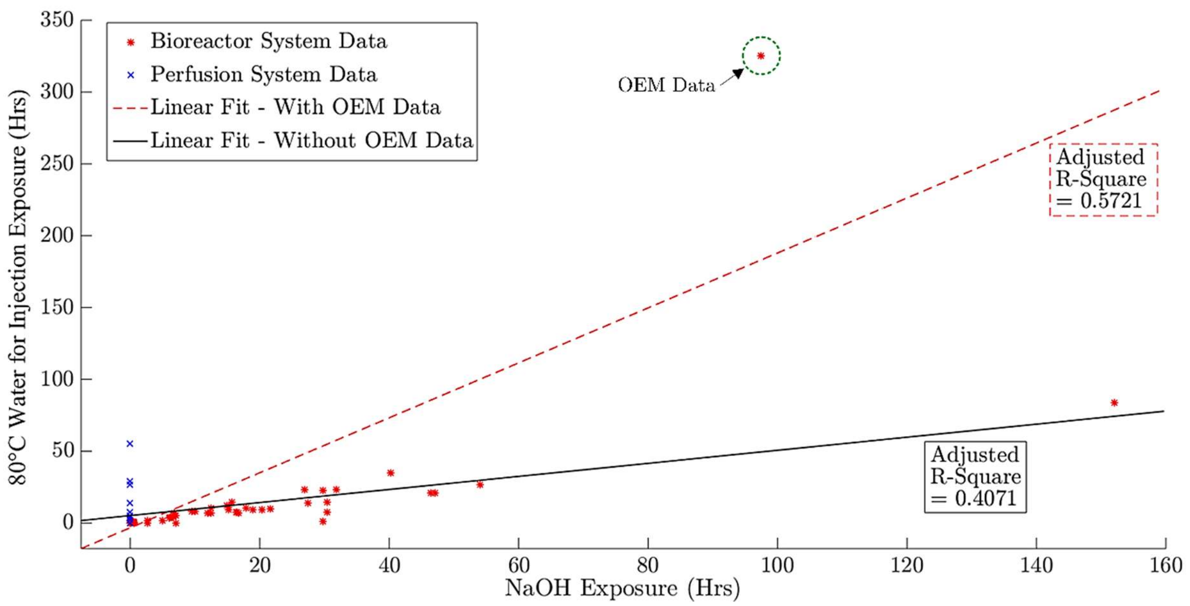

Figure 3.23: Relationship between NaOH exposure and 80°C Water for Injection exposure across all systems

Several combinations of all variables were analysed, however the only combination that produced VIF values lower than 10 were the following eight variables:

- ECO Interval (Hrs)
- Age of Diaphragm at Installation (Hrs)
- Cumulated Steam Exposure (Hrs)
- Cumulated 65°C Sodium Hydroxide (NaOH) Exposure (Hrs)
- Diaphragm size 0.5 Inch
- Diaphragm size 1 Inch
- Diaphragm size 1.5 Inch
- Diaphragm size 2 Inch

Combined with one of the following three variables:

- 60°C Return Osmosis Exposure (Hrs)
- 80°C Water For Injection Exposure (Hrs)
- Total Actuations

For this reason, three separate models will be used for all logistic regression models in the bioreactor dataset. These are the eight variables listed plus one of the three variables listed. If any combinations of two or more of the three variables are used, then the VIF values produced are greater than 10. The three models with the lowest multicollinearity diagnostics therefore are the following:

Bioreactor dataset - model 1

Table 3.20: Inclusion of 80°C water for injection exposure

Model	Collinearity Statistics	
	Tolerance	VIF
ECO Interval (Hrs)	.519	1.926
Age of Diaphragm at Installation (Hrs)	.740	1.351
Cumulated Steam Exposure (Hrs)	.415	2.412
Cumulated 65°C Sodium Hydroxide (NaOH) Exposure (Hrs)	.185	5.414
80°C Water for Injection Exposure (Hrs)	.152	6.567
Diaphragm size 0.5 Inch	.156	6.399
Diaphragm size 1 Inch	.197	5.080
Diaphragm size 1.5 Inch	.387	2.587
Diaphragm size 2 Inch	.304	3.294

Bioreactor dataset - model 2

Table 3.21: Inclusion of 60ﬂC RO exposure

Model	Collinearity Statistics	
	Tolerance	VIF
ECO Interval (Hrs)	.571	1.752
Age of Diaphragm at Installation (Hrs)	.716	1.397
Cumulated Steam Exposure (Hrs)	.407	2.458
Cumulated 65°C Sodium Hydroxide (NaOH) Exposure (Hrs)	.188	5.320
60°C Return Osmosis Water Exposure (Hrs)	.269	3.720
Diaphragm size 0.5 Inch	.165	6.076
Diaphragm size 1 Inch	.223	4.478
Diaphragm size 1.5 Inch	.401	2.494
Diaphragm size 2 Inch	.302	3.306

Bioreactor dataset - model 3

Table 3.22: Inclusion of total actuations

Model	Collinearity Statistics	
	Tolerance	VIF
ECO Interval (Hrs)	.613	1.631
Age of Diaphragm at Installation (Hrs)	.750	1.333
Cumulated Steam Exposure (Hrs)	.414	2.418
Cumulated 65°C Sodium Hydroxide (NaOH) Exposure (Hrs)	.229	4.368
Total Actuations	.276	3.624
Diaphragm size 0.5 Inch	.152	6.576
Diaphragm size 1 Inch	.211	4.739
Diaphragm size 1.5 Inch	.389	2.569
Diaphragm size 2 Inch	.302	3.308

3.4.6 Variable subset selection - perfusion skid dataset

The first VIF analysis conducted was of the full list of covariates from the perfusion type dataset. Again the variable 'Total Actuations' has been dropped from the initial analysis, along with the number of actuations during 80°C water for injection exposure, as they are highly correlated to other variables in the dataset which would cause the model to fail. As shown, the most highly correlated covariates are:

- 45°C cumulated sodium hypochlorite exposure
- Number of actuations during 45°C sodium hypochlorite exposure
- 80°C water for injection exposure
- 23°C phosphoric acid exposure
- Cumulated steam exposure
- Number of actuations during steam exposure

All other covariates have VIF values lower than 10. The results from the first VIF analysis from the perfusion type dataset are shown in table 3.23

Table 3.23: Multicollinearity analysis: Perfusion type dataset

Model	Collinearity Statistics	
	Tolerance	VIF
ECO Interval (Hrs)	.138	7.242
Age of Diaphragm at Installation (Hrs)	.331	3.017
Cumulated Steam Exposure (Hrs)	.029	34.535
No. Actuations (Steam Exposure)	.011	88.775
23°C Phosphoric Acid Exposure (Hrs)	.016	62.812
No. Actuations (23°C Phosphoric Acid Exposure)	.189	5.305
45°C Cumulated Sodium Hypochlorite Exposure (Hrs)	.008	129.490
No. Actuations (45°C Sodium Hypochlorite Exposure)	.052	19.238
80°C Water for Injection Exposure (Hrs)	.011	92.517
No. Actuations During Production Batches	.526	1.902
Diaphragm size 0.5 Inch	.358	2.792
Diaphragm size 1.0 Inch	.658	1.520

Similar to the full and the bioreactor datasets, due to their high VIF values, all actuations during individual exposures were removed from the model and replaced with the total actuations variable, as shown in table 3.24.

Table 3.24: Multicollinearity analysis: Perfusion type dataset excluding individual actuations

Model	Collinearity Statistics	
	Tolerance	VIF
ECO Interval (Hrs)	.281	3.564
Age of Diaphragm at Installation (Hrs)	.397	2.522
Cumulated Steam Exposure (Hrs)	.067	15.017
23°C Phosphoric Acid Exposure (Hrs)	.051	19.710
45°C Cumulated Sodium Hypochlorite Exposure (Hrs)	.040	24.952
80°C Water for Injection Exposure (Hrs)	.052	19.190
Total Actuations	.549	1.823
Diaphragm size 0.5 Inch	.515	1.942
Diaphragm size 1.0 Inch	.410	2.438

This had the effect of considerably decreasing the VIF values across most covariates. However there are still four remaining covariates with VIF values greater than 10. These are:

- Cumulated Steam Exposure
- 23°C Phosphoric Acid Exposure
- 45°C Cumulated Sodium Hypochlorite Exposure
- 80°C Water for Injection Exposure

The high correlation amongst certain combinations of these variables is illustrated in figure 3.24. The most highly correlated variables are highlighted in bold. Among the variables that are not highly correlated, the OEM data again offers an advantageous distinction between the potential effects of the variables on component degradation, reducing high correlation that would have been present if the OEM data were not included.

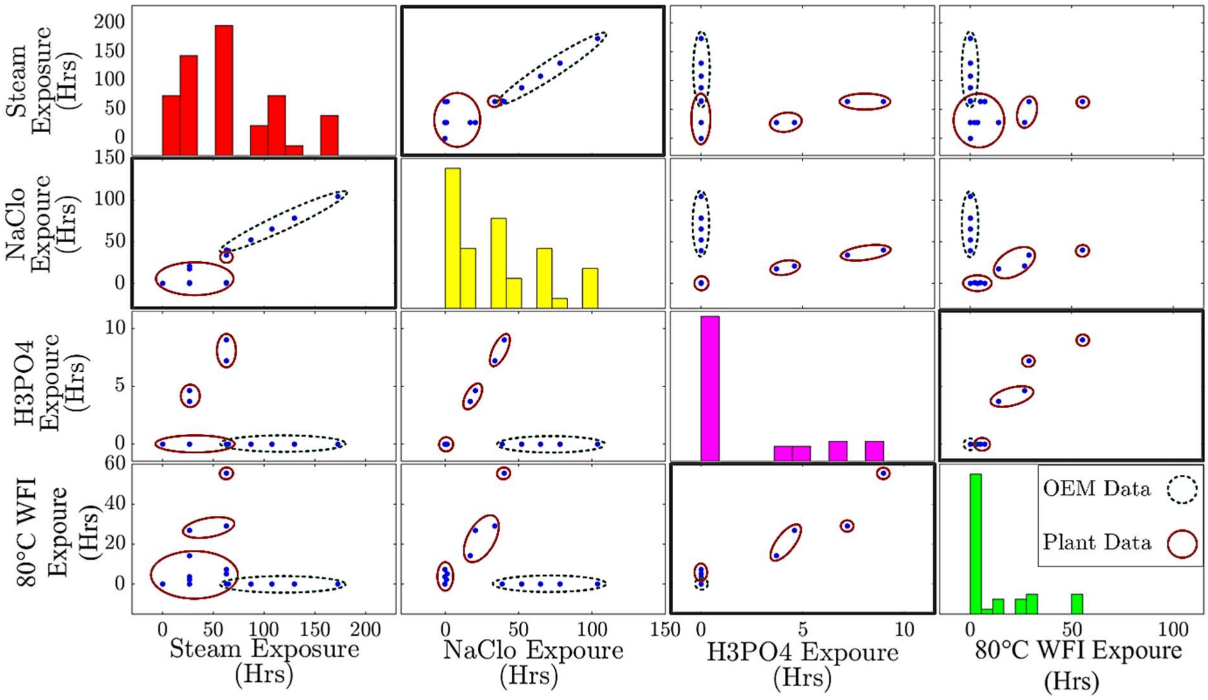

Figure 3.24: Exposure conditions - plant data versus OEM data in the perfusion skids

In further detail, there are two groups of variables that are highly correlated to one another even when the OEM data is considered, which are:

1. Cumulated Steam Exposure & Sodium Hypochlorite Exposure

and

2. Phosphoric Acid Exposure & 80°C Water for Injection Exposure

These relationships are further highlighted in figures figure 3.25 and figure 3.26 below.

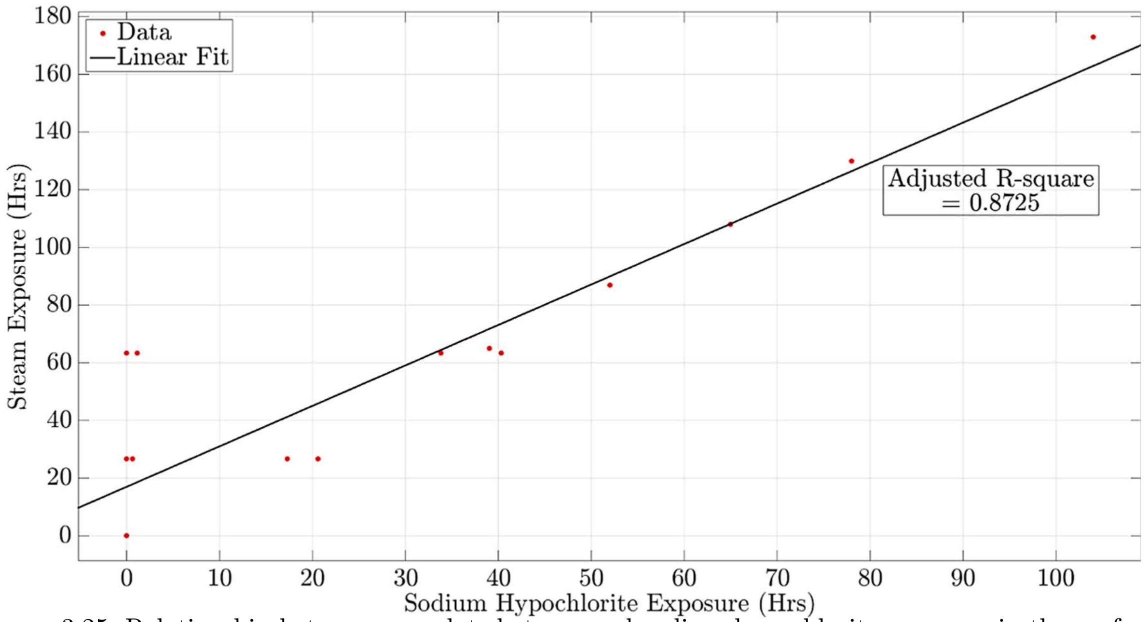

Figure 3.25: Relationship between cumulated steam and sodium hypochlorite exposure in the perfusion dataset

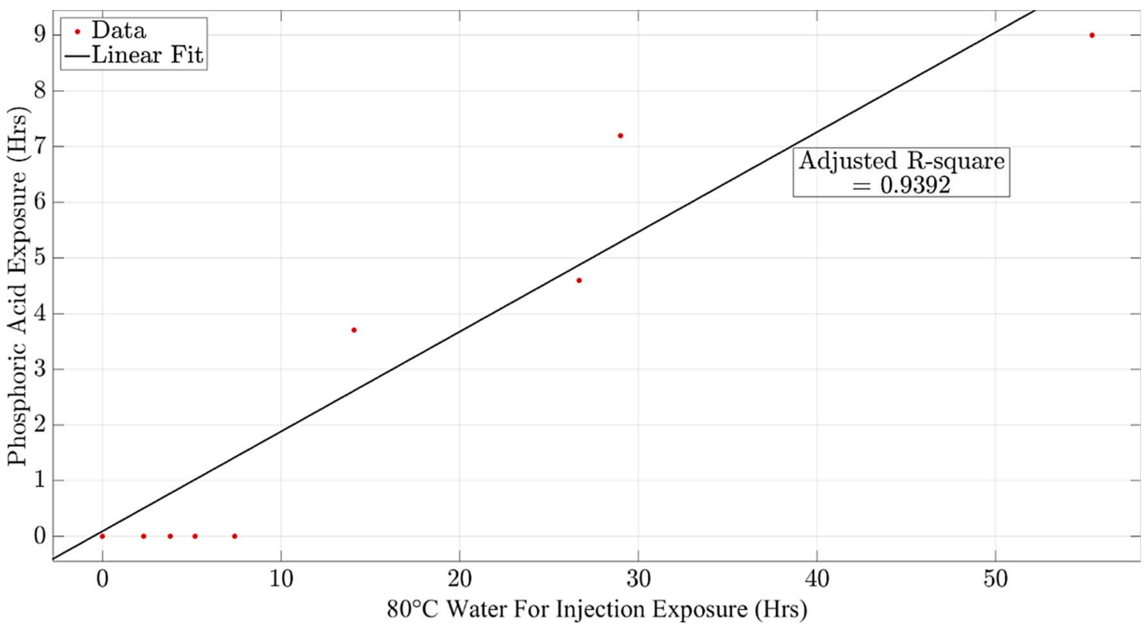

Figure 3.26: Relationship between cumulated phosphoric acid and 80°C water for injection exposure in the perfusion dataset

Again, several combinations of all variables were analysed, however the only combination that produced VIF values lower than 10 were the following six variables:

- ECO Interval (Hrs)
- Age of Diaphragm at Installation (Hrs)
- Total Actuations
- Diaphragm size 0.5 Inch
- Diaphragm size 1.0 Inch

Combined with specific combinations of the following four variables:

- 23°C Phosphoric Acid Exposure (Hrs)
- 80°C Water for Injection Exposure (Hrs)
- 45°C Sodium Hypochlorite Exposure (Hrs)
- Steam Exposure (Hrs)

The six variables listed at the top above act as the base model, with which specific combinations from the correlated four variables listed below them will form the four separate models detailed below. These four models will be used for all logistic regression models in the perfusion dataset. These are:

Perfusion skid dataset - model 1

Table 3.25: The inclusion of steam exposure and 80°C water for injection exposure

Model	Collinearity Statistics	
	Tolerance	VIF
ECO Interval (Hrs)	.320	3.124
Age of Diaphragm at Installation (Hrs)	.565	1.770
Total Actuations	.604	1.657
Diaphragm size 0.5 Inch	.140	7.135
Diaphragm size 1.0 Inch	.130	7.690
Cumulated Steam Exposure (Hrs)	.223	4.487
80°C Water for Injection Exposure (Hrs)	.676	1.479

Perfusion skid dataset - model 2

Table 3.26: The inclusion of steam exposure and 23°C phosphoric acid exposure

Model	Collinearity Statistics	
	Tolerance	VIF
ECO Interval (Hrs)	.319	3.132
Age of Diaphragm at Installation (Hrs)	.561	1.784
Total Actuations	.634	1.578
Diaphragm size 0.5 Inch	.141	7.080
Diaphragm size 1.0 Inch	.130	7.698
Cumulated Steam Exposure (Hrs)	.222	4.506
23°C Phosphoric Acid Exposure (Hrs)	.712	1.405

Perfusion skid dataset - model 3

Table 3.27: The inclusion of 45°C sodium hypochlorite exposure and 80°C WFI exposure

Model	Collinearity Statistics	
	Tolerance	VIF
ECO Interval (Hrs)	.288	3.469
Age of Diaphragm at Installation (Hrs)	.475	2.106
Total Actuations	.674	1.483
Diaphragm size 0.5 Inch	.096	9.430
Diaphragm size 1.0 Inch	.110	9.064
80°C Water For Injection Exposure (Hrs)	.504	1.982
45°C Sodium Hypochlorite Exposure (Hrs)	.140	7.145

Perfusion skid dataset - model 4

Table 3.28: The inclusion of 45°C sodium hypochlorite exposure and 23°C phosphoric acid exposure

Model	Collinearity Statistics	
	Tolerance	VIF
ECO Interval (Hrs)	.281	3.555
Age of Diaphragm at Installation (Hrs)	.462	2.166
Total Actuations	.707	1.415
Diaphragm size 0.5 Inch	.095	9.499
Diaphragm size 1.0 Inch	.108	9.244
23°C phosphoric Acid exposure (Hrs)	.509	1.965
45°C Sodium Hypochlorite Exposure (Hrs)	.134	7.487

The reasoning behind the covariate selection for the four models is straightforward. It is desirable to keep at least two chemical variables in the model to help ascertain the relative importance of each variable. Therefore the two groups of correlated variables were combined, as knowing the significance of one variable can help ascertain the level of significance of another variable in a minimally changed model.

The logistic regression results tables from all statistical analyses investigated can be found in appendix C. These results are discussed below.

3.4.7 Filter approach covariate selection results - cracking failure mode

There are several conclusions that can be drawn from the statistical analysis results in relation to the cracking failure mode, these are:

- Knowing the current degradation state of a component and the initial cracking probability it is possible to predict the updated probability of a crack event occurring in the material
- The probability of a crack occurring increases greatly with increasing material degradation state. For each unit increase in degradation state the odds of a crack increases by 565%. The final crack event probability is however contingent upon the initial probability of a crack event occurring when the component is in degradation state 1

Full dataset

- Maintenance interval time is significant at the 10% level in all three models
- NaClO exposure is significant at the 10% level in model 3

Bioreactor systems

- Maintenance interval time is significant at the 5% level in all three models
- The 1.0 inch diaphragms were statistically significant variables in models 1 and 3 at a significance level of 5%, and at 10% in model 2. It is possible that this size, potentially due to design flaws or other weakness, is more prone to cracking in service in comparison to other sized diaphragms in this environment. They were not significant in the models built using the full or perfusion skid datasets
- The 0.5 inch diaphragms were significant at the 10% level in model 1

Perfusion systems

- No variables were found to be statistically significant in the perfusion system models at either the 5% or 10% significance levels

3.4.8 Filter approach results - gradual degradation failure mode

In relation to the gradual stepwise degradation failure mode, there are several conclusions that can be drawn from the statistical analysis results. These are:

- Cumulated steam exposure is the most statistically significant covariate in terms of predicting the gradual degradation of the EPDM diaphragms. Apart from model 2 of the perfusion skid dataset, in all models from all datasets steam exposure is significant at the 5% level of significance. In model 2 of the perfusion skid dataset steam exposure is significant at the 10% significance level.

Full dataset

- The maintenance interval is significant at the 10% significance level in models 1 and 2, and at the 5% level of significance in model 3, of the models built using the full dataset
- Cumulated NaOH exposure is significant at the 10% level of significance in model 1
- Cumulated NaClO exposure is significant at the 10% significance level in model 3

- No variable among diaphragm size, 80°C Water for Injection exposure, 60°C Return Osmosis Water exposure, actuations, or diaphragm age at installation, was found to be significant in any model, suggesting they play no role in the gradual degradation of the EPDM material
- An interaction variable created between steam exposure and NaClO exposure was found to be significant at the 5% level. Including the steam / NaClO interaction variable increased the true positive predictive ability of the model by 3.4%

Bioreactor systems

- In the bioreactor models maintenance interval is significant at the 5% level in all three models
- Cumulated NaOH exposure is at the 5% significance level in model 3 of the bioreactor dataset. It was not found to be significant in models 1 and 2 of the bioreactor dataset, which included 80°C Water for Injection exposure and 60°C Return Osmosis Water as covariates respectively
- No interaction terms were found to be significant

Perfusion systems

- Cumulated NaClO exposure is significant at the 5% level of significance in models 3 and 4 of the perfusion skid dataset. NaClO exposure was only investigated in models 3 and 4 due to issues with multicollinearity
- Maintenance interval was not shown to be significant in any model
- Although not generally recommended due to a biased estimation of the regression coefficients [300,301], a backwards stepwise elimination of the least significant variables was conducted in model 2 to ascertain if any more variables were highlighted as significant. This was done as the result in this model is the only instance of steam not being found to be significant at the 5% level. Both steam and H_3PO_4 exposure are significant at the 5% level using the backwards stepwise elimination method
- No interaction terms were found to be significant

3.4.9 Wrapper approach results

In terms of the cracking failure mode, only maintenance interval was found to be significant, and then only in the bioreactor models. For this reason only the gradual degradation state covariates will be analysed via the wrapper approach. Based on the filter approach results outlined in section 3.4.8, the following covariates will be used in the wrapper approach models:

Bioreactor systems

- Steam Exposure (Hrs)
- NaOH Exposure (Hrs)
- Maintenance Interval (Hrs)

In order to test all possible nested models with these covariates, 7 unique models were investigated, the results of which are shown in figure 3.27. Detailed results for all models can be found appendix C.

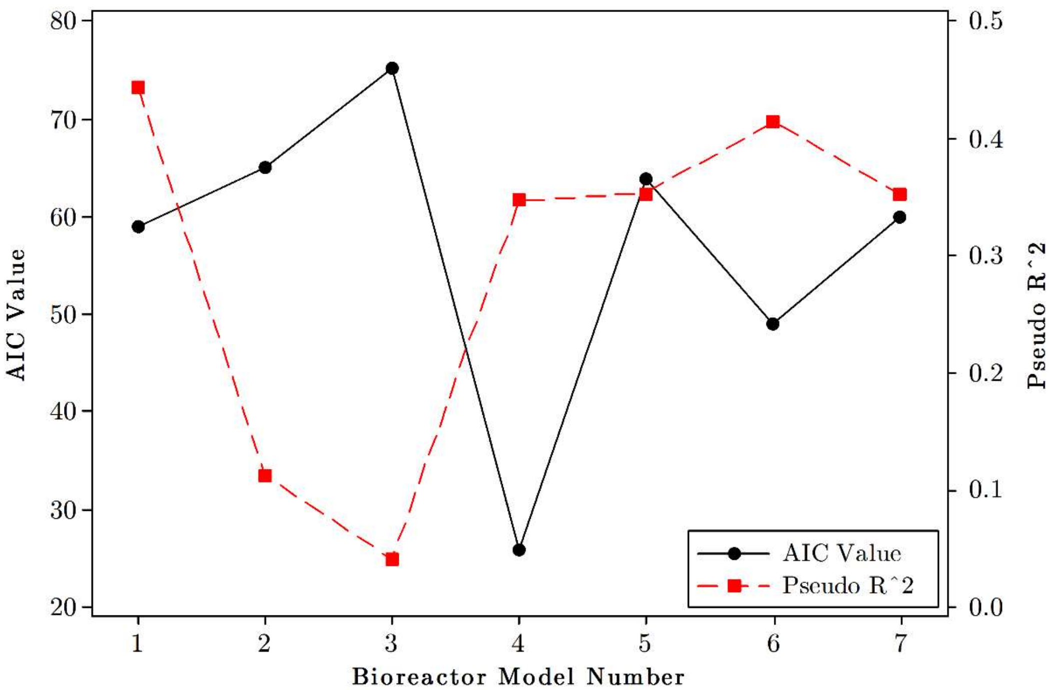

Figure 3.27: Bioreactor system nested models AIC and Psuedo R^2 values

The results from these models suggests:

- The time between maintenance intervals plays a significant role in degradation state transition events
- Inclusion of the steam exposure variable to the maintenance interval covariate model increases the variability explained by the model by approximately 6.7%
- The model with the best predictive ability is the model including all three covariates. However, including the NaOH exposure variable to the steam exposure and maintenance interval variable model increases explained variability by only 2.9%. This modest increase results in a heavy penalisation in the AIC value

Perfusion systems

- Steam Exposure (Hrs)
- NaClO Exposure (Hrs)
- Steam/NaClO Exposure (Hrs) – interaction variable
- H_3PO_4Exposure (Hrs)
- Maintenance Interval (Hrs)

In order to test all possible nested models with these covariates, 31 unique models were investigated. The AIC and Pseudo R^2 values of each model are shown in figure 3.28 below. Details for all models can be found appendix C.

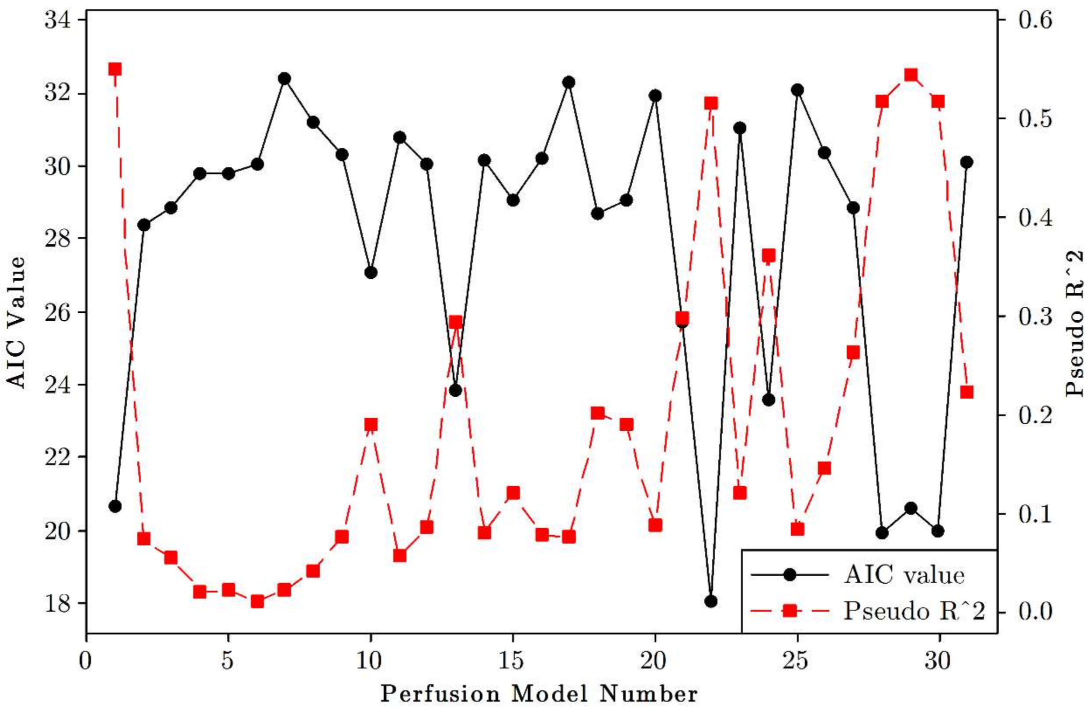

Figure 3.28: Perfusion system nested models AIC and Psuedo R2 values

The results from these models suggests:

- The most important variables are the steam exposure and the steam / NaClO exposure interaction variables
- In terms of predictive performance, the next most important variables appear to be the NaClO exposure and maintenance interval variables
- There is a very minor improvement in model performance including the H_3PO_4 exposure variable along with the NaClO exposure and maintenance interval variables, in addition to steam exposure and the steam / NaClO interaction variables
- Using all variables together results in the model explaining the most variability, with only a modest increase in the AIC value

3.5 Discussion

For both system types, there is overwhelming evidence suggesting that steam exposure is ubiquitously the most significant factor influencing gradual degradation state transition events, and therefore could be used as the time variable in a virtual sensor model. There is some evidence to suggest that maintenance window interval, NaOH exposure, NaClO exposure, H_3PO_4 exposure, and the interaction between steam and NaClO exposures also influence degradation state transition events. Performing a sensitivity analysis on these variables only, as shown in table 3.29, illustrates this point. However, with the current dataset it is not possible to conclude with sufficient certainty whether these variables have a significant effect. For this reason, these exposures will be further investigated using material analysis techniques to determine if and what influence they have on the EPDM diaphragm material.

Table 3.29: Sensitivity analysis of potentially significant variables

	Sensitivity Order	β	S.E.	Sig.	Exp(β)	95% C.I. for Exp(β)	
						Lower	Upper
Cumulated Steam Exposure	1	.023	.008	.008	1.023	1.006	1.040
ECO Interval	2	.000	.000	.009	1.000	1.000	1.000
Interaction variable: Cumulated Steam Exposure * 45°C NaClO Exposure	3	-.001	.000	.027	.999	.999	1.000
45°C NaClO Exposure	4	.101	.046	.028	1.107	1.011	1.211
65°C NaOH Exposure	5	-.033	.021	.123	.967	.928	1.009
23°C H_3PO_4 Exposure	6	-.102	.134	.446	.903	.694	1.175
Constant	*	-4.865	1.031	.000	.008	*	*

Using the current dataset and statistical techniques employed, there is no clear indication as to which variable contributes to crack events occurring, apart from the degradation state of the material and possibly the maintenance interval time. However, these variables may only indicate that the probability of a crack occurring increases the longer the component is in service. As it was not possible to isolate a variable that could reliably predict the onset of cracking with a significant degree of confidence, this failure mode is investigated further using different means, namely a study on the effects of incorrect installation practices on the probability of a diaphragm developing a crack in service. In order to reduce the likelihood of a crack occurring during the lifetime of a component, the initial probability of a crack occurring must be minimised. According to Ohlsson [302], tightly controlling bolt torqueing procedures during component installation will have this affect. Material characterisation analysis will be used to help ascertain if physical or chemical stresses or interactions also contribute to cracks developing in the material, and if material quality is consistent.

Chapter 4

Material characterisation of component degradation

Analysis of process variables contributing to component degradation — Chapter 3

- Diaphragms collected and assessed post industrial service
- Service history and environmental exposure data of diaphragms collated
- Combined with small prior OEM dataset
- Statistical selection of significant process variables contributing to degradation

Material characterisation of component degradation — Chapter 4

- Confirmation of significant process variables contributing to EPDM degradation
- Determination of chemical and physical property changes in EPDM diaphragms during degradation

Consideration of human factors contributing to component degradation — Chapter 5

- Methodological framework to create and integrate quantitative human factors metrics proposed
- Developed methodology accounts for human uncertainty during maintenance tasks
- Investigation of impact of incorrect installation on diaphragm degradation

4.1 Introduction and research rationale

In order to verify one of the conclusions from chapter 3, that NaOH exposure, NaClO exposure, H_3PO_4 exposure, and the interaction between steam and NaClO exposure also influence degradation state transition events, a controlled study of the effects of these variables was necessary to better understand the EPDM degradation process occurring in the case study plant. Therefore, an analysis of the EPDM material pre and post-exposure to varying quantities of the environmental variables they are exposed to in service was undertaken. This ties into the overall methodology by describing the physics of the degradation processes of the components for the first time. The objectives of this chapter therefore are:

1. To determine if exposure to the common CIP constituent chemicals has a degradative effect on the EPDM diaphragms
2. If degradative effects exist, to elucidate the physics of the degradation mechanisms

Unfortunately, at the time of testing it was impossible to expose diaphragm samples to controlled saturated steam conditions matching those seen in industry due to both safety issues and practical issues related to steam generation on a small scale. It was not possible therefore to isolate the effect of steam exposure on the diaphragms. Accordingly, to try and replicate the interaction effects between steam and NaClO, some samples were exposed instead to 100°C H_2O before being exposed to NaClO. This was in an attempt to replicate the thermo-oxidative damage which might occur due to steam exposure.

4.1.1 Testing methodology

In order to address a gap in the available literature, which is to understand the impact that the aqueous chemical solutions detailed in table 4.1 and table 4.2 have on the EPDM material, 24 virgin samples were utilised for testing. The 24 samples were taken equally from four different manufacturing batches from the diaphragm OEM identified in chapter 3, representing the previous 2 years of EPDM diaphragm production. This was in order to clarify if batch differences were responsible for differences in material performance. 12 virgin samples were tested using an array of chemical and physical analysis methods the results of which were collated after every test in order to develop a foundation for the characteristics of the virgin material. The approach was then to expose the remaining samples to an individual chemical under investigation in order to examine the effect that the chemical exposure had on the material. This allowed a direct comparison of the degradation effects attributable to the chemical exposure. All diaphragms were of equal size, and, being virgin components, initially had no cracking or other forms of degradation present. A graphical representation of the adopted methodology is shown in figure 4.1. Table 4.4 and figure 4.54 in chapter section 4.9 summarise the results of each test.

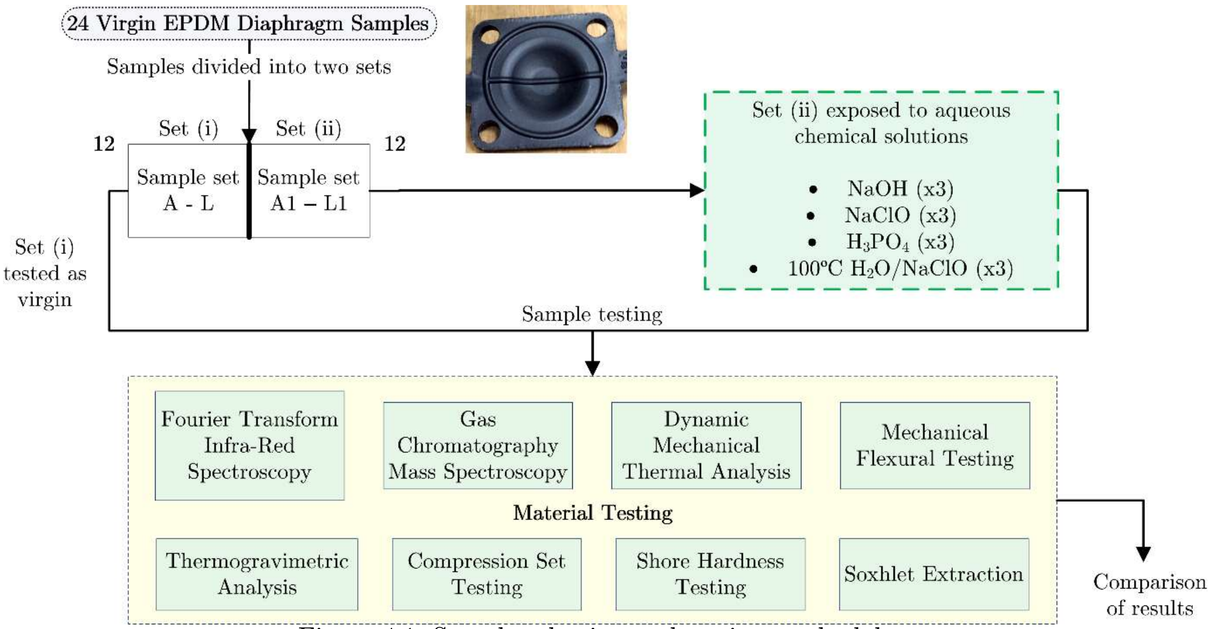

Figure 4.1: Sample selection and testing methodology

The chemical exposures details that sample set (ii) are subject to, represented by the use of the label '1', are shown in table 4.1. The subscript '$_C$' in the sample ID denotes that the sample was exposed to the chemical solution under constant 5mm compression in a valve assembly. One sample from each chemical exposure type was compressed continuously during chemical exposure to investigate if the material degradation is further affected by material compression, for e.g. environmental stress cracking. To achieve this, a bespoke valve assembly was kept in the 'closed position' during chemical exposure. This issue is common in normally opened valves, which comprise 95% of those used within the industrial case study facility, being in the 'closed' position during chemical exposure. Details of this valve assembly set-up are shown in figure 4.9 in section 4.3.

The chemical concentrations, given in units of Molarity (M), the temperatures, and the pH values of the chemical solutions match exactly those used during the chemical cleaning cycles in the case study facility.

Table 4.1: Chemical exposure specifications of set (ii) test samples.

Sample ID	Chemical (Concentration)	PH	Chemical Exposure Duration (Hours)	Exposure Temperature (°C)	Material Compression
A1	NaOH (0.5 M)	13.5	504	65	None
B1	NaOH (0.5 M)	13.5	168	65	None
$C1_C$	NaOH (0.5 M)	13.5	168	65	5mm
D1	NaClO (0.87 M)	10.75	504	45	None
E1	NaClO (0.87 M)	10.75	168	45	None
$F1_C$	NaClO (0.87 M)	10.75	168	45	5mm
G1	H_3PO_4 (0.033 M)	1.5	504	23	None
H1	H_3PO_4 (0.033 M)	1.5	168	23	None
$I1_C$	H_3PO_4 (0.033 M)	1.5	168	23	5mm
J1	100°C H_2O / NaClO (0.87 M)	6.14/10.75	504	100 / 45	None
K1	100°C H_2O / NaClO (0.87 M)	6.14/10.75	168	100 / 45	None
$L1_C$	100°C H_2O / NaClO (0.87 M)	6.14/10.75	168	100 / 45	5mm

The full exposure details of each sample is given in table 4.2.

Table 4.2: Chemical exposure conditions of all samples used for testing

Manufacturing Batch	Sample ID	Cumulated NaOH Exposure (Hrs)	Cumulated H_3PO_4 Exposure (Hrs)	Cumulated NaClO Exposure (Hrs)	Cumulated H_2O Exposure (Hrs)
Set (i) - Virgin Samples					
1	A	0.00	0.00	0.00	0.00
1	B	0.00	0.00	0.00	0.00
1	C	0.00	0.00	0.00	0.00
2	D	0.00	0.00	0.00	0.00
2	E	0.00	0.00	0.00	0.00
2	F	0.00	0.00	0.00	0.00
3	G	0.00	0.00	0.00	0.00
3	H	0.00	0.00	0.00	0.00
3	I	0.00	0.00	0.00	0.00
4	J	0.00	0.00	0.00	0.00
4	K	0.00	0.00	0.00	0.00
4	L	0.00	0.00	0.00	0.00
Set (ii) - Chemically Exposed Samples					
1	A1	504.00	0.00	0.00	0.00
1	B1	168.00	0.00	0.00	0.00
1	$C1_C$	168.00	0.00	0.00	0.00
2	D1	0.00	0.00	504.00	0.00
2	E1	0.00	0.00	168.00	0.00
2	$F1_C$	0.00	0.00	168.00	0.00
3	G1	0.00	504.00	0.00	0.00
3	H1	0.00	168.00	0.00	0.00
3	$I1_C$	0.00	168.00	0.00	0.00
4	J1	0.00	0.00	504.00	30.00
4	K1	0.00	0.00	168.00	30.00
4	$L1_C$	0.00	0.00	168.00	30.00

The exposure durations were chosen in order to ensure that any potential degradation effect would be seen upon material testing. While these are an extreme representation of field exposures, it was important that any chemical and physical changes would occur to their full effect in order to gauge their contribution towards diaphragm degradation. 504 hours, or 21 days, exposure time was chosen in order to discover if further extreme exposures had additional degradation effects, or if full damage had already occurred at 168 hours, corresponding to 7 days' exposure.

It should be noted that a full design of experiments was not conducted as the interaction effects between the four different chemical exposures was not being considered, only the main effects that each individual chemical had on the virgin EPDM. This in accordance with the sparsity-of-effects principle, whereby single factors are considered to have the most significant responses and higher order interactions are regarded as very rare [303]. This rationale was based on the process knowledge gained from chapter 3, whereby not all of the chemicals under investigation interact during the production process. Accordingly, a fractional factorial design was conducted, valid in this case study for its economy and versatility in allowing the elucidation of the physics of the degradation mechanisms of the EPDM material [304]. Accordingly, the statistical significance of the effect of each chemical exposure could not be determined due to the limited sample size. Rather, the results are used as an indicative measure to the effect of chemical exposure on the EPDM material.

In addition, while compressing a subset of the diaphragms during chemical exposure constitute an analogous to the ISO standard bent strip method [305] to discover if environmental stress cracking (ESC) plays a role in early EPDM diaphragm failure, a full study of the structural parameters that govern the ESC phenomenon was not feasible in this work. This is because a full ESC study would need to take into account constant displacement rates, constant loads, and constant displacements for every exposure type, greatly increasing the scope of the testing [306]. Rather, changes in stiffness during tensile displacement was used to indicate if the EPDM material has become susceptible to stress cracking due to increased crosslinking and chain entanglements, as this has been shown to be a fast and reliable indicator for evaluating ESC in polymers [307].

The testing order is outlined in table 4.3 below. This order was designed to minimise the impact of each test on the subsequent tests and the results obtained.

Table 4.3: Testing order and sample type used per test

Test	Test Type	Test Order	Sample Type Used
Fourier transform infrared spectroscopy	Non-destructive	1	Full diaphragm
Shore hardness		2	
Flexural modulus testing		3	
Cyclic compression testing		4	
Compression set testing	Destructive	5	Sample from diaphragm (different sample per test)
Thermogravimetric analysis		6	
Soxhlet extraction		7	
Gas chromatography mass spectroscopy		8	
Dynamic mechanical thermal analysis		9	

The testing conducted is divided into 4 technical areas to fully assess the changing physical and chemical properties of the EPDM composites. Some of the tests involved are a combination of two techniques. All tests and their functional areas are detailed in figure 4.2.

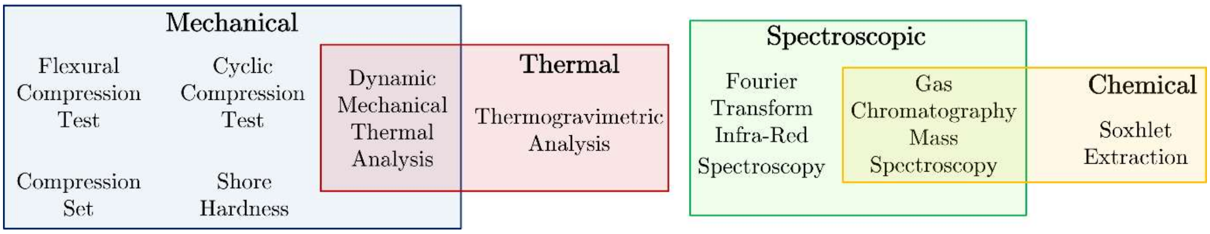

Figure 4.2: Full testing regime conducted during material characterisation

The testing rationales, testing methods, and results for each test are described in detail in the rest of the chapter. A discussion on the details the main findings of each test can be found at the end of the chapter. The sequence of the remainder of the chapter is as follows:

1. Mechanical testing
    a. Shore hardness
    b. Dynamic flexural testing
    c. Compression set testing
    d. Dynamic mechanical thermal analysis
2. Thermal testing
    a. Thermogravimetric analysis
3. Spectroscopic testing
    a. Fourier transform infrared spectroscopy
4. Chemical testing
    a. Soxhlet extraction
    b. Gas chromatography mass spectroscopy

4.2 Shore hardness

4.2.1 Method

The mechanical property of hardness was assessed using a CV Instruments DS series shore A durometer in conjunction with a 1 kg shore bench stand, as shown in figure 4.3.

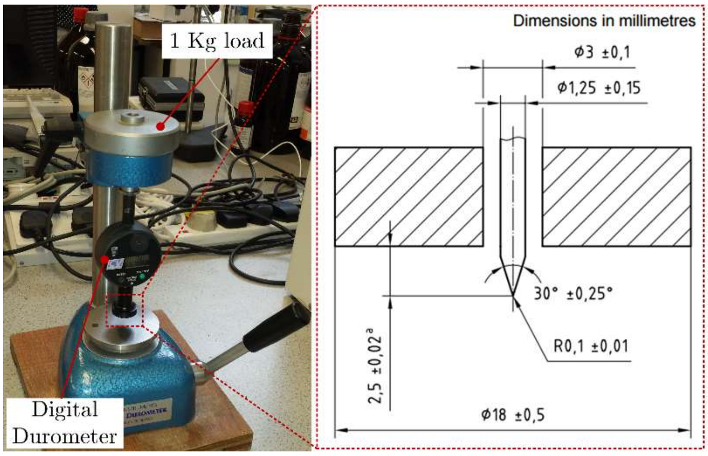

CV Instruments Durometer Digital DS Series	
Load	1 Kg
Scale	Shore A
Manufacturing Tolerance	ASTM D2240 / ISO 868
Test Time	3 seconds
Maximum Indentor Speed	3.2 mm/s

Figure 4.3: Shore hardness scale A durometer test equipment. Adapted from [108].

The testing was conducted according to ISO 7619:2010 [108]. The test piece was placed on the bench stand parallel to the pressure foot which mounts the indenter. Force was applied to the rubber for 3 seconds, after which the reading was taken. In accordance with the ISO standard, five measurements were taken in total on different positions on the sample, the median value of which was used as the final hardness value. The instrument is calibrated internally before every test using six standard rubber blocks in the range of 30 to 90 IRHD (International Rubber Hardness Degrees), using a spring force of 445 mN. The accuracy of the durometer was 0.1 shore A hardness.

4.2.2 Results

The data for the results between batches for all virgin EPDM material, and between virgin EPDM and the chemically exposed EPDM, are displayed in box plots for the remainder of this chapter. Figure 4.4 is a legend to illustrate the meaning of the different components of these box charts.

The differences in the hardness values of the virgin samples as a function of production batch are illustrated in figure 4.5. As shown, there is little variation in the hardness values between production batches within the virgin samples. This means that peroxide crosslinking initiated during production is consistent across production batches. Any additional crosslinking present in the material surface due to increased crosslinking is therefore attributable solely to the additional chemical exposure.

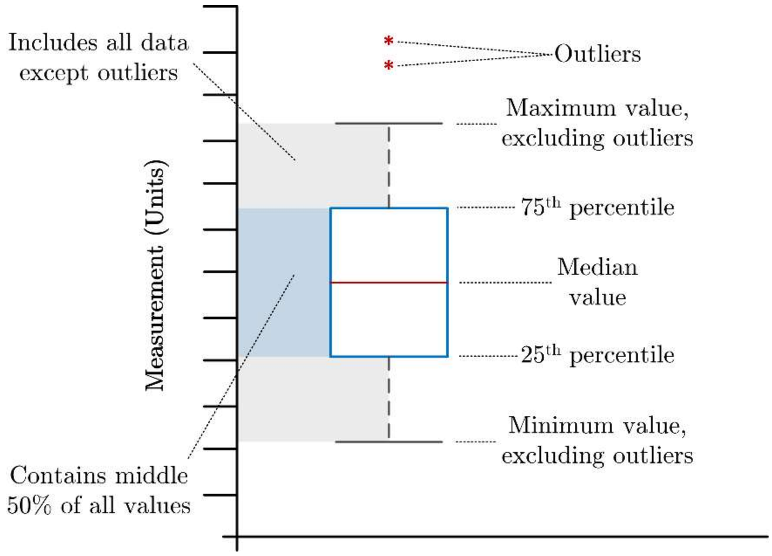

Figure 4.4: Box plot legend

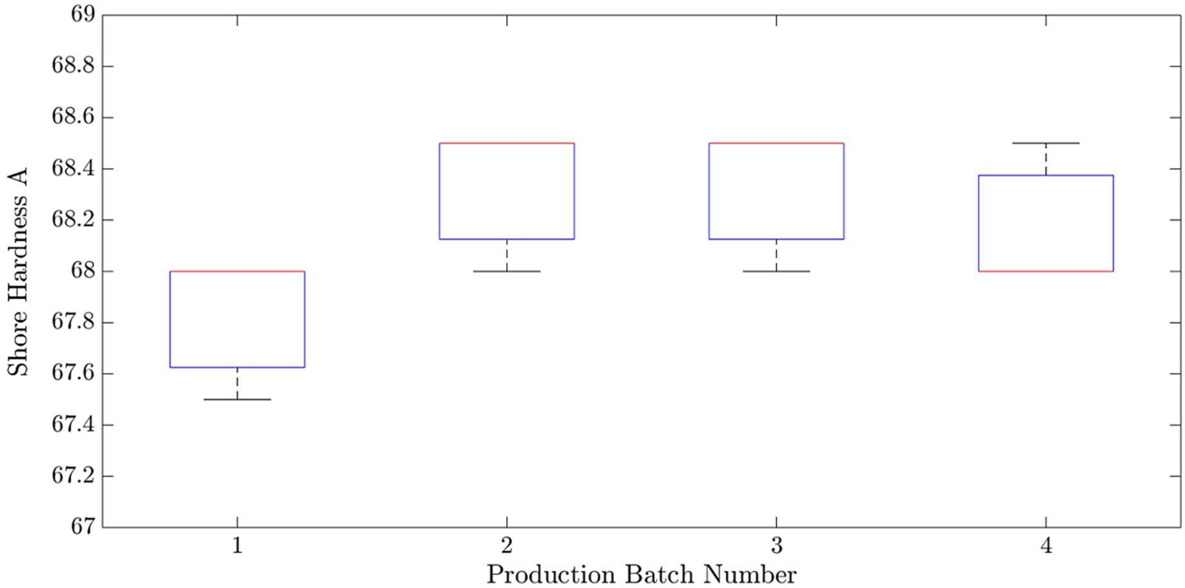

Figure 4.5: Shore A hardness of virgin samples as a function of production batch

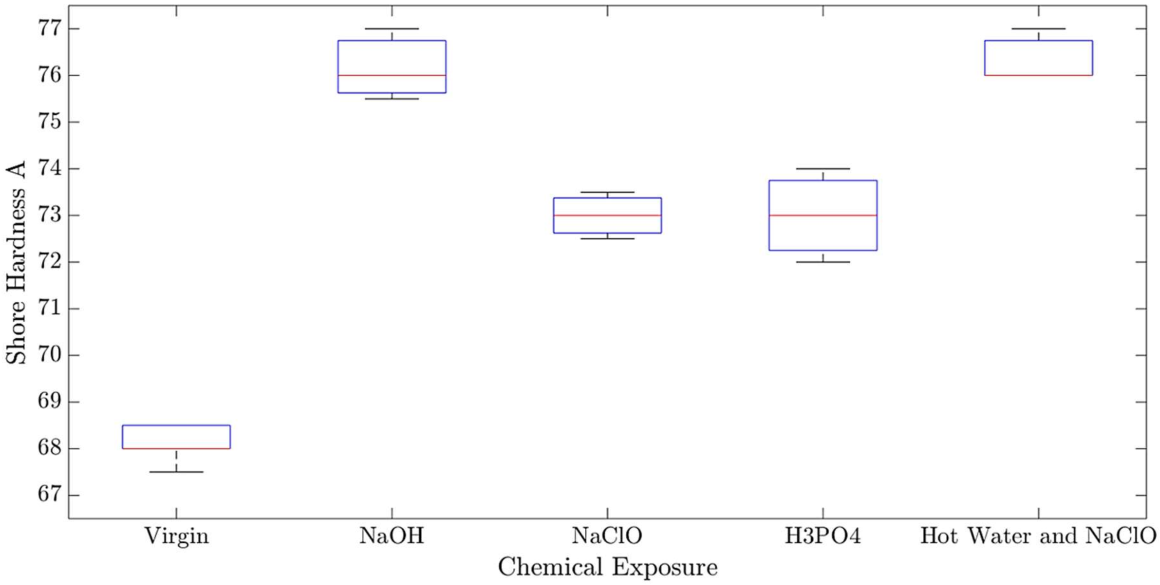

Figure 4.6: Shore A hardness results of all samples as a function of chemical exposure

The results of the variation in hardness values as a function of chemical exposure are shown in figure 4.6. There are clear variations in the hardness values of the exposed samples in comparison to the virgin samples, indicating that additional crosslinking has occurred. It is apparent that NaOH and 100°C H_2O / NaClO exposure have the largest effects on the material in this regard. It is also apparent that the addition of 30 hours 100°C H_2O exposure has had an additional effect on the material in terms of increased degradation, as a result of either increased material oxidation or through the removal of additional plasticiser from the EPDM composite, in comparison with NaClO alone. There is no substantial difference in the hardness values of the NaClO and H_3PO_4 samples.

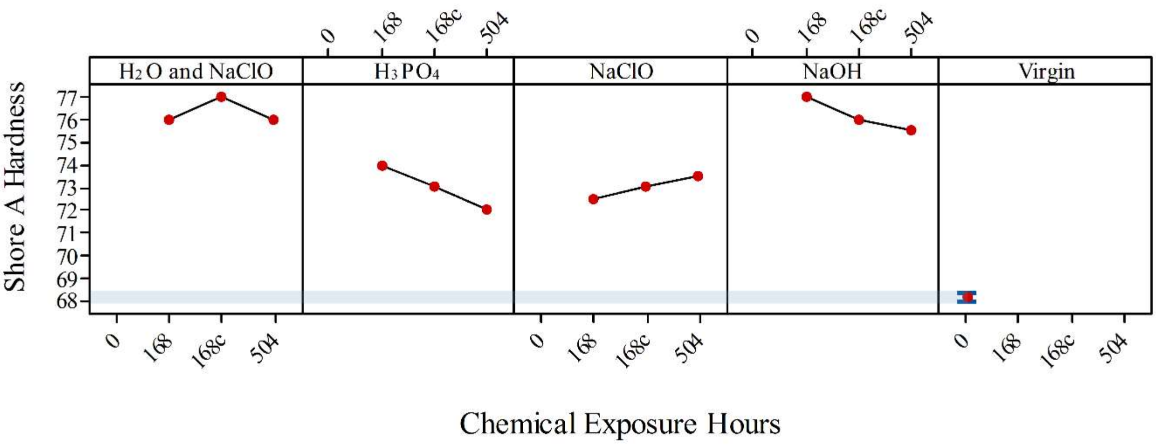

Figure 4.7: Shore A hardness results as a function of exposure type and duration

Figure 4.7 illustrates the differences in hardness values for each sample, based on both exposure type and exposure time. For the NaOH and H_3PO_4 exposed samples, hardness decreases when the material is compressed during exposure, and further decreases when the material is exposed up to 504 hours, in comparison to non-compressed 168-hour exposure. For both NaClO exposures, it appears that material compression results in increased crosslinking. For the 100°C H_2O / NaClO exposed sample the hardness value for both 168 hours and 504 hours is the same, indicating no additional crosslinking or chain scission behaviour after 168 hours. However, the NaClO exposed samples appear to continually crosslink with additional exposure. In the 100°C H_2O / NaClO exposed variables there was no increase or decrease in crosslinking after 168 hours exposure. A small increase was seen however due to EPDM compression at 168 hours. The addition of the 30 hour 100°C H_2O exposure has resulted in increased degradation of the EPDM. The increased hardness of the EPDM surface can result in surface brittleness, which can reduce crack propagation resistance.

4.3 Dynamic flexural testing

4.3.1 Cyclic compression testing

Method

As the EPDM materials under investigation in this work are composite products with multiple layers, traditional tensile testing would not yield satisfactory results as tensile strength and elongation at break would be determined by the strength of the nylon layer rather than the EPDM layers. In order to elucidate therefore if additional crosslinking has occurred due to chemical exposure, dynamic cyclical and flexural compression testing was conducted. Cyclical compression testing was conducted keeping both strain and strain rate conditions constant while observing the changes in the force and the work required to displace the material. The cyclic compression testing was performed using a Lloyd LRX universal testing machine designed for use in dynamic loading applications, as shown below in figure 4.8. In order to measure the force and work required to fully compress the samples, each diaphragm sample was cyclically actuated within an industrially standard valve setup. Using a sine frequency function, this corresponded to fully actuating, from the fully open to the fully closed position, a normally open diaphragm valve. The testing parameters are also given below in figure 4.8. The value of 10,000 test cycles was chosen to represent the average number of actuations the diaphragms in this case study undergo in a typical 24-month period.

Lloyd LRX Universal Testing Machine	
Data sampling rate	8kHz
Force capacity	5kN
Load resolution	0.0001 N
Load cell accuracy	<0.5%
Speed accuracy	<0.2%
Displacement resolution	<0.1 microns
Test displacement rate	200 mm/min
Total test displacement	5 mm
Number of continuous test cycles	10,000

Figure 4.8: Universal testing machine specifications and cyclical compression test parameters

The valve assembly was recreated loyally from those parts used as standard in service, to help ensure the accuracy and transferability of all test results. The final valve assembly is shown in figure 4.9.

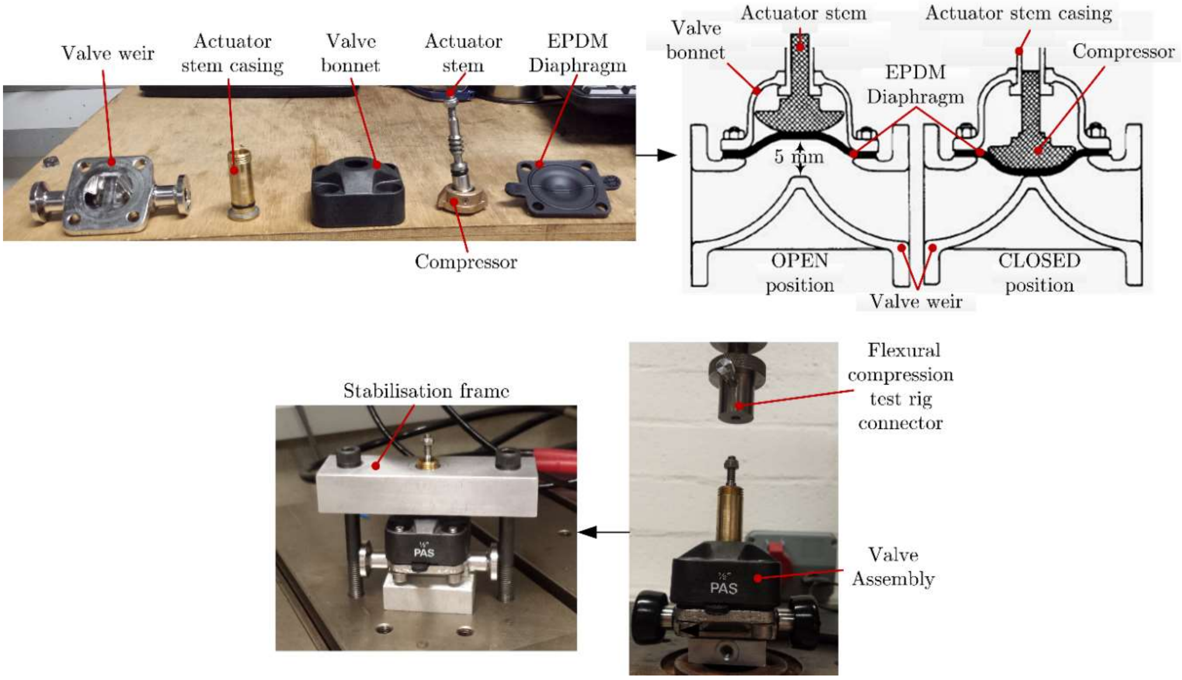

Figure 4.9: Valve assembly flexural test setup. Adapted from [308]

The compressor and actuator stem were placed inside the actuator stem casing, which was then placed inside the valve bonnet. The diaphragm was then screwed into the compressor as per SOP guidelines. Finally, the valve weir was connected via 4 bolts, one in each corner, and torqued appropriately according to manufacturer's specifications. In order for the diaphragm to be actuated into the closed position, the top works of the valve was removed, allowing the actuator stem to protrude from the assembly. This was then manually tightened into a test rig connector. A stabilisation frame was also built to ensure the valve stayed upright and that the diaphragm was consistently normal to the direction of applied force.

Critical to the accuracy of the testing was the bolt/washer/nut combination. To ensure that the clamping force applied to the valve assembly was consistent across each test, new bolts, nuts, and washers were used for every test. This was essential as clamping force has a profound effect on the force required to actuate the valve, as illustrated in figure 4.10 below. The results shown were generated from a different virgin sample to the others being tested. Initially, each bolt was tightened to 2.3Nm torque, the minimum of the diaphragm manufacturers specifications. The diaphragm was then subjected to the standard testing conditions described above. After the completion of each testing cycle, the valve bolts were tightened by a further 0.2Nm, and the test was re-run. The final testing torques used in each M6 bolt was 4.5Nm, the maximum limit of the diaphragm manufacturers specifications. The range of values from 2.3 to 4.5Nm is still therefore within manufacturers guidelines. The results below demonstrate that if the torque was not applied consistently during testing, there was a possibility that the results could be inconsistent or erroneous. This issue is addressed further in chapter 5.

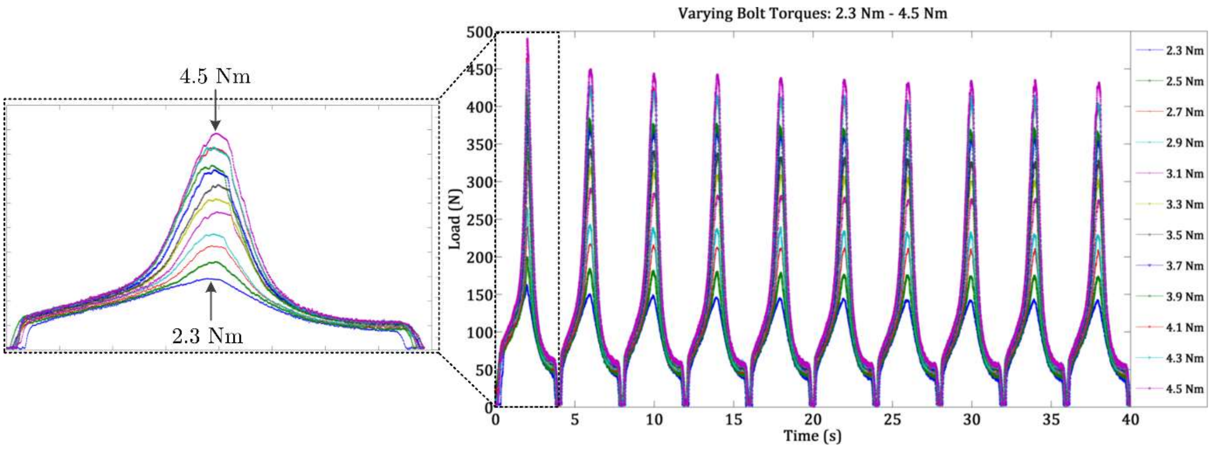

Figure 4.10: Loads required to actuate valve through varying bolt torques

As figure 4.10 illustrates, the full displacement load differences which exist between different bolt torques made it imperative that the torque could be accurately reproduced for every test. This also applies to the installation of the diaphragms in service. The force required to actuate the valve at 4.5Nm is approximately 220% larger than the force required to actuate it when the bolts are tightened to 2.3Nm. Over-torqueing therefore may induce considerable stress into the diaphragms, potentially leading to early failure. The two assembly factors therefore which affect the clamping force the most are the torque of the bolts and the friction coefficient of the threaded interface (μ) between the bolt and nut. In this assembly, the friction coefficient between the nut and valve body (μ_c) was not critical, as the nut was allowed to spin during torqueing. As the nut interfaces with the smooth plastic surface of the valve bonnet the friction coefficient at this location is low. For this application μ_c was estimated to be 0.1, corresponding to a median value of under head friction for a low resilience connection of stainless steel A4 grade with no lubrication [309]. The bolt tightening torque used as standard is 4.5Nm, so the only variability is the friction of the threaded connection. This can be affected in a number of ways, the most pertinent of which is galling of the mating surfaces, resulting in a decrease in clamping force, or accidental lubrication resulting in an increase in clamping force when a torque is applied.

The theoretical clamping force and subsequent axial stress as a function of μ was calculated via the following relationship [310]:

$$T = KF_c d \tag{4.3.1}$$

where T is the torque (Nm), F_c is the clamping force (N), d is the diameter of the bolt (m), and K is the torque coefficient given by:

$$K = \left(\frac{d_m}{2d}\right)\left(\frac{tan\lambda + \mu\, sec\alpha}{1 - \mu\, tan\lambda\, sec\alpha}\right) + 0.625\mu_c \tag{4.3.2}$$

where μ = friction coefficient of the threaded interface, μ_c = friction coefficient between the nut and valve body, and $d_m = \frac{d_p + d_t}{2}$ = mean thread diameter (m) where d_p = M6 pitch diameter (m) and d_t = M6 root diameter (m) given by:

$$tan\lambda = \frac{P}{\pi d_m} \tag{4.3.3}$$

where P = thread pitch and $\alpha = \frac{\varphi_n}{2}$ where φ_n = thread angle (degrees). The values of μ used in the calculation, referenced from BS EN ISO 3506-1:2009 [309] for screws made from A2 or A4 stainless steel and anti-corrosion steel, were ranged from 0.1 to 0.16 for lubricated connections, and 0.23 to 0.5 for unlubricated connections. The clamping force F_c (N) in the valve and the tensile stress σ_t (N/mm^2) experienced by the bolts are proportional, given by:

$$\frac{F_c}{A_t} \tag{4.3.4}$$

where A_t, effective tensile area (mm^2), is given as $A_t = \left(\frac{\pi}{4}\right) \times {d_m}^2$

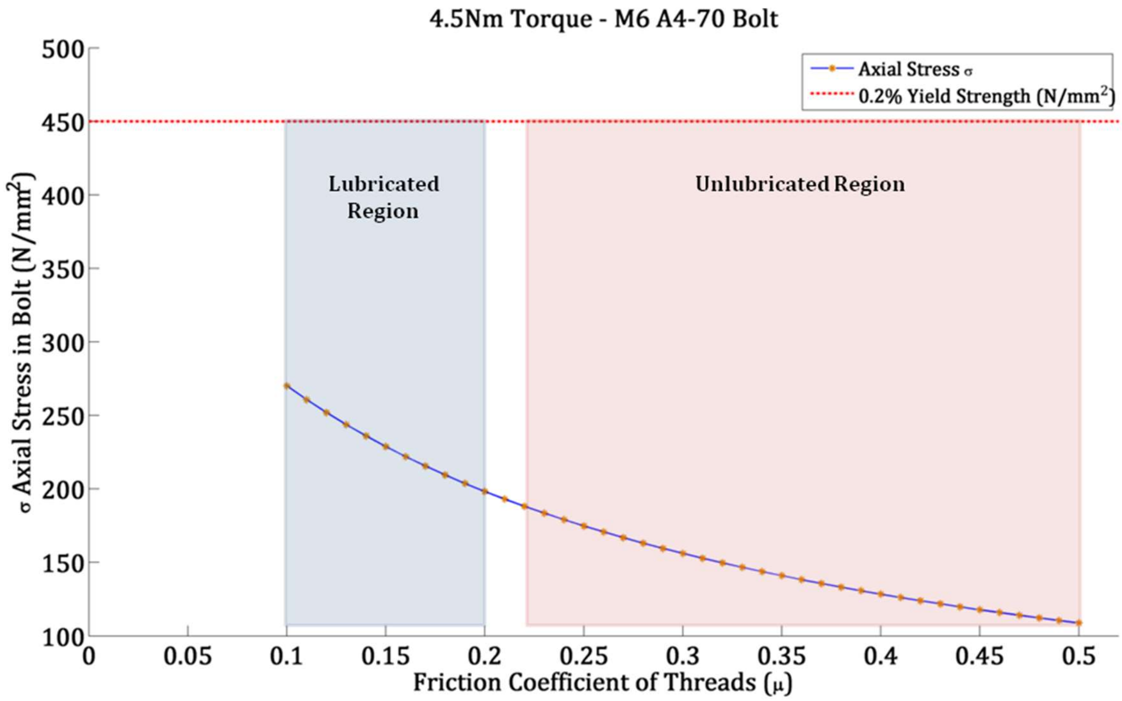

Figure 4.11: Axial stress as a function of friction coefficient of threaded connection

Figure 4.11 demonstrates how the axial stress experienced by the bolts, and hence the pre-load or clamping force, is affected by the friction coefficient of the threaded interface. In the range of friction coefficients between 0.1 and 0.5 the axial stress experienced by each M6 bolt ranges from 24% to 60% of the 0.2% yield strength of A4-70 stainless steel, which is 450N/mm^2, a variability of over 35% [309]. In order to ensure repeatability of the tests, as a control method, new and unlubricated nuts, bolts, and washers were used for all tensile tests.

In order to calculate the average work required to strain the samples between the pre-set strain limits, the areas within and under the curve of the elastic hysteresis loop were determined. In this scenario, displacement of the test samples can be considered equivalent to strain, as the total displacement is measured relative to the null displacement of the sample. As shown in figure 4.12 (a), the first cycle requires the highest force to fully strain the sample. The diminishing maximum stress values eventually stabilise at a constant value, known as the Mullins effect [311]. Therefore, to calculate the average energy, the first 100 cycles are ignored, after which the average area within all hysteresis loops is calculated, as shown in in figure 4.12 (b). The elastic hysteresis loop is a result of the material viscoelasticity, as the rubber exhibits a time delay in returning to its original shape [312]. In figure 4.12 (c), the total average hysteresis loop of all cycles is isolated. Using this, as shown in figure 4.12 (d), the total elastic strain energy, the energy dissipated due to heat, and the useful recoverable energy can be determined. The area within the elastic hysteresis loop, shown in red, is the amount of energy lost in the rubber to due internal friction, this energy is then dissipated as heat. The area underneath this curve, shown in green in figure 4.12 (d), is the remaining energy thereafter, also known as the recoverable energy. The total energy required to strain the sample is therefore the sum of these two energies, corresponding to the total area underneath the loading curve, also known as the work to maximum compression [313]. The average force to maximum load is calculated as the average of all forces required to complete full strain of the samples, again excluding the first 100 values to negate the Mullins effect.

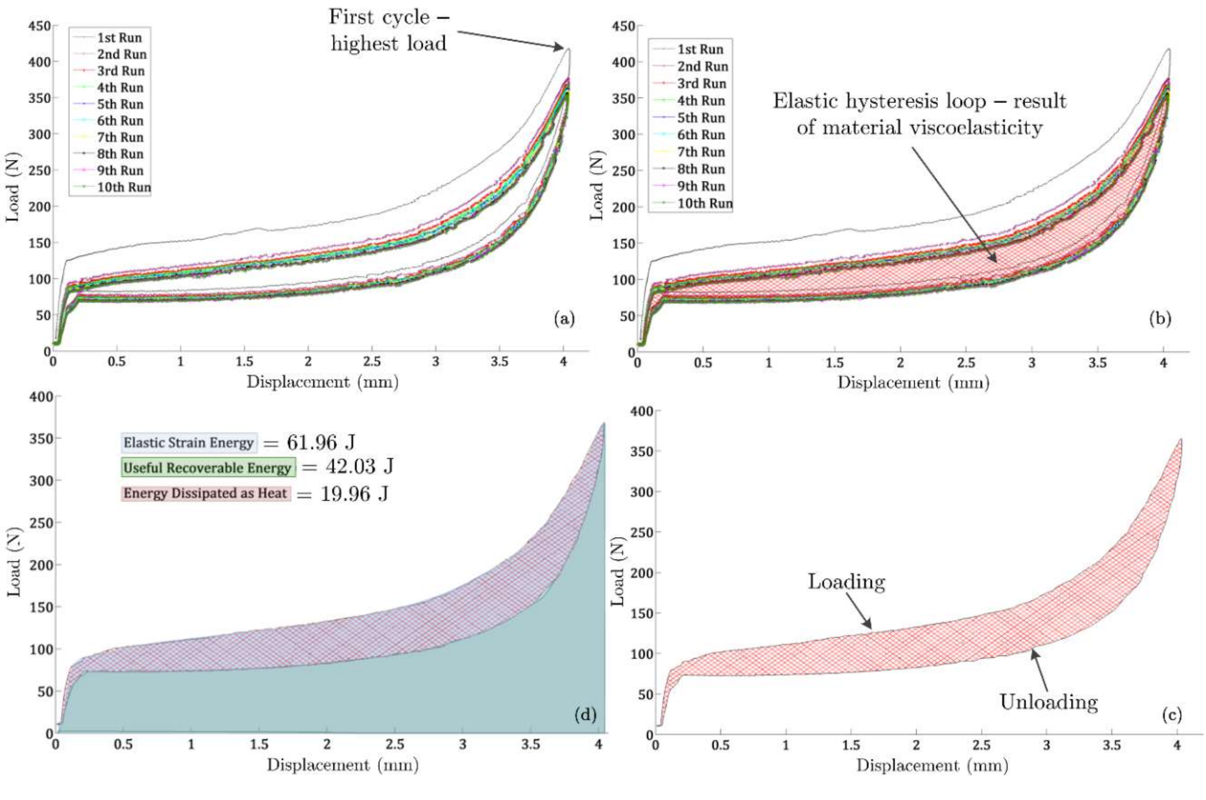

Figure 4.12: Calculation of energy required to strain samples from hysteresis loop

Results

Figure 4.13 and figure 4.14 illustrate the differences in the average work and force required to compress the virgin diaphragms as a function of production batch number respectively. There is some variation in the average work to maximum compression, with production batch 1 needing the least work to compress. Batches 2 and 3 require similar amounts of work for diaphragm compression. Production batch 1 also has the largest variation in force required to actuate, followed production batch 4. Production batches 2 and 3 require the least amount of force to actuate and have less variation.

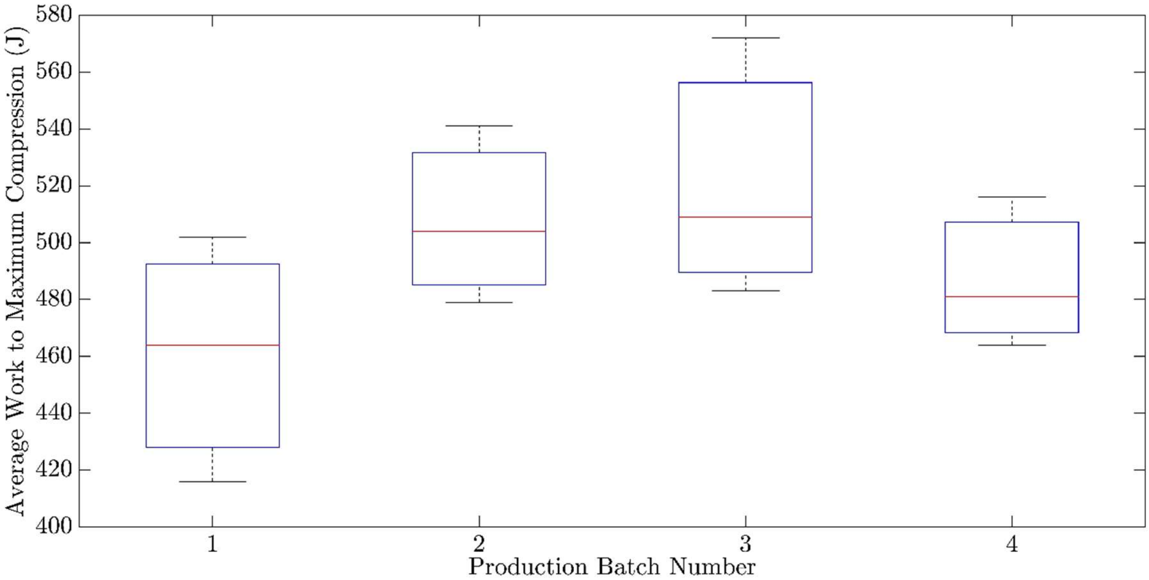

Figure 4.13: Average work to maximum compression of virgin samples as a function of production batch number

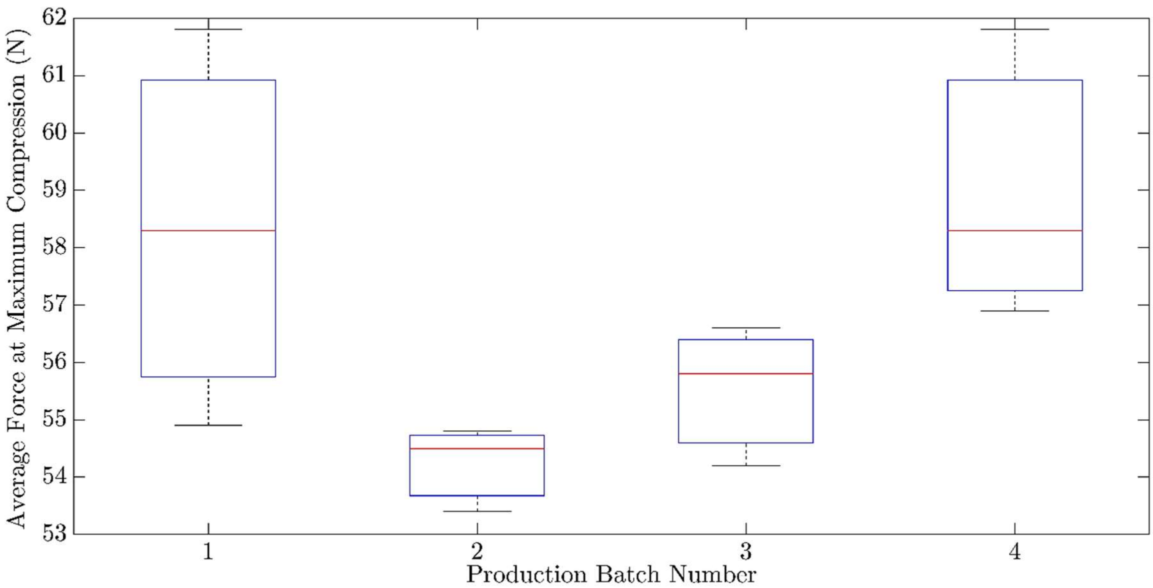

Figure 4.14: Average force at maximum compression of virgin samples as a function of production batch number

Despite the variations in both metrics across virgin production batches, these variations are minor in comparison to the variation elicited as a result of chemical exposure, as seen in figure 4.15 and figure 4.16. As shown in figure 4.15 there is a large increase in the average work required to maximally compress the exposed samples in comparison to the virgin samples, indicating a large increase in crosslinking. All exposed samples require similar energy to compress, although the samples exposed to NaClO alone have a larger variation and may require more energy than the other exposed samples.

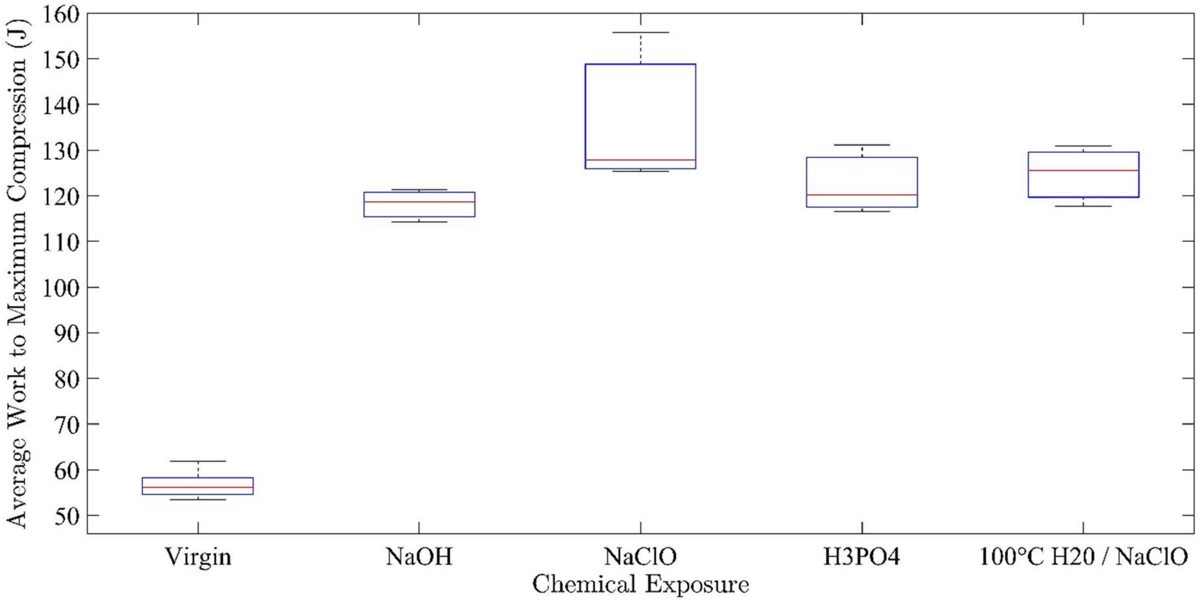

Figure 4.15: Average work to maximum compression of all samples as a function of exposure type

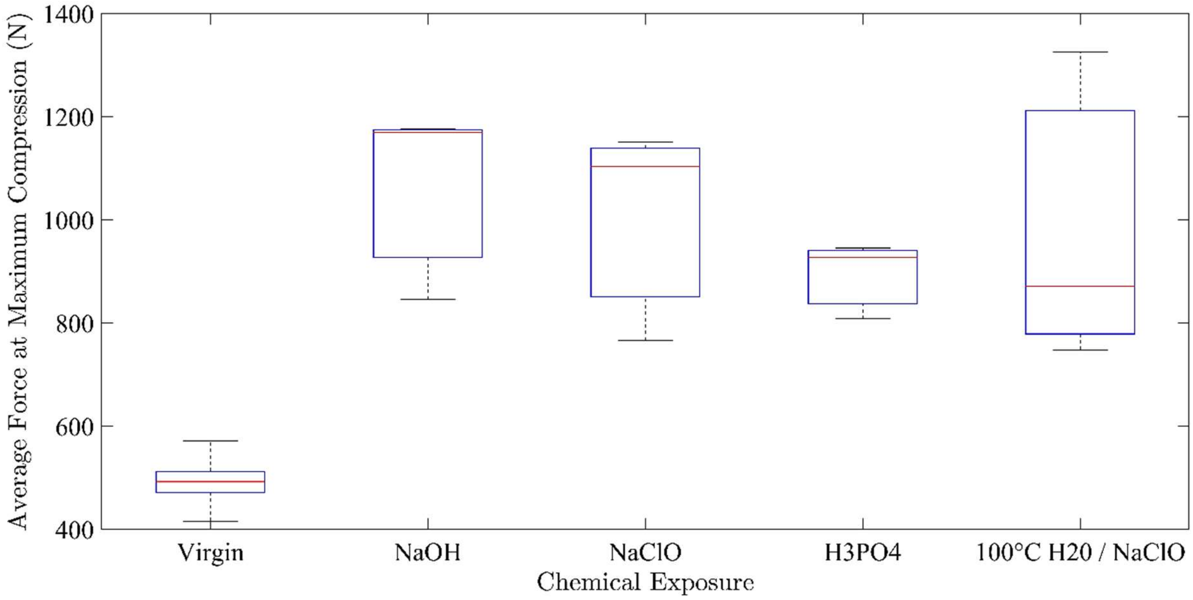

Figure 4.16: Average force at maximum compression of all samples as a function of exposure type

Figure 4.16 illustrates a similar conclusion, whereby there is a large increase in the force required to actuate the exposed samples in comparison to the virgin samples. There is some variation in the average force required to actuate the diaphragms among the exposed samples. The H_3PO_4 exposed samples have a smaller variation than the other exposed samples.

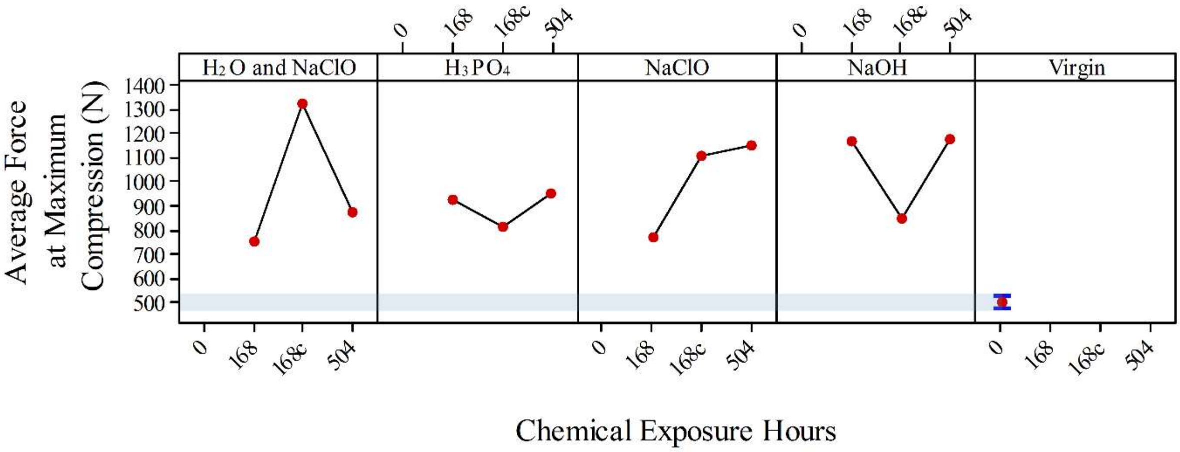

Figure 4.17: Average force at maximum compression of all samples as a function of exposure type and duration

As figure 4.17 illustrates, with both NaClO exposures, that there was a large increase in the average force required to actuate the samples after they had been compressed for 168 hours in comparison with the non-compressed 168 hour exposed samples. There was also an increase in the force required to actuate the 504 hour exposed samples in comparison to the 168 hour exposed samples, although this was less pronounced in the 100°C H_2O / NaClO samples. This signifies that additional crosslinking is occurring in the material upon compression and upon continued exposure up to 504 hours. In both the H_3PO_4 and NaClO exposed samples, compression may have inhibited crosslinking formation, while additional exposure up to 504 hours has had little effect. This would indicate that the rate of crosslinking is accelerated in the H_3PO_4 and NaClO exposed samples, and that crosslinking saturation has already occurred at 168 hours, in contrast with the NaClO exposed samples which have a slower rate of crosslink formation.

Figure 4.18 shows minimal variation in the results, particularly in comparison with figure 4.17. In the NaClO exposed samples of both types, there is a very modest increase in the energy required to compress the samples after they have been compressed for 168 hours, in comparison to the non-compressed 168 hour exposed samples. In the samples only exposed to NaClO, the results agree with those seen in figure 4.17 whereby there is a continued large increase in energy required to compress up to 504 hours. In the H_3PO_4 exposed samples there is a modest decrease in the energy required to actuate the diaphragms after 168 hours of exposure through compression. There is little to no variation in the energy required to compress the NaOH exposed samples across the three test types.

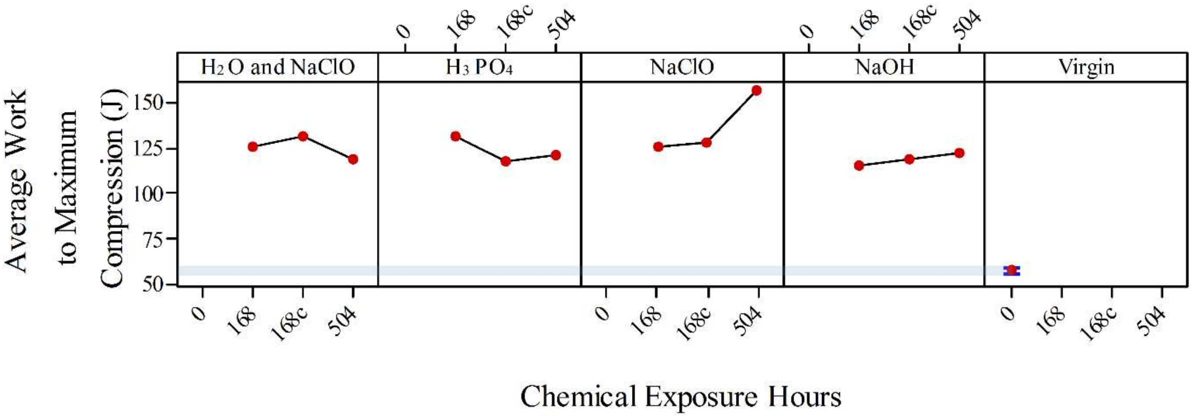

Figure 4.18: Average work to maximum compression of all samples as a function of exposure type and duration

The results shown in figure 4.17 and figure 4.18 correlate well to the shore hardness results. Both the Work to and force at maximum compression indicates increased crosslinking behaviour in the 504 hour exposed NaClO samples and the 168 hour compressed 100°C H_2O/NaClO samples. Likewise, a reduction in force and Work is seen in the NaOH and H_3PO_4 samples exposed under compression and up to 504 hours. This correlates to the reduction in hardness seen in those samples in comparison to the 168 hour exposures. The commonality in the agreement of the results can be attributed to the hardened layer that has been shown to have formed, and how that hardened layer evolves via further crosslinking or chain scissions. The results imply that a heavily crosslinked layer requires more force and Work to strain, indicating that monitoring force and Work during diaphragm use may be a useful indicative measure of EPDM diaphragm degradation.

After the 10,000 actuations of the cyclic compression testing was completed, each sample was visually assessed using the qualitative methodology developed in chapter 3 to evaluate its degradation state and if cracking was present. All exposed samples were classified as degradation state 2, mainly due to slight material deformation. There were no cracks present in any samples, except for the 100°C H_2O / NaClO exposed samples. Each of these samples had significant cracking present. The virgin samples were all classified as degradation state 1, with no material deformations or cracking present.

4.3.2 Flexural modulus testing

Method

The flexural modulus testing was performed using the same Lloyd LRX universal testing machine as detailed in section 4.3.1 in order to help determine the flexural properties of the EPDM samples according to ISO 178 [110]. The test applies to a freely supported beam loaded at mid-span, which is then loaded until the material yields. During this time the loading force is continuously monitored. The test speed, or displacement rate, was kept constant at 200mm/min, the pre-load on the loading edge was set at 5N, and testing temperature was controlled at 22.6°C. The pre-load was necessary to reduce the curvature at the start of the force-displacement region. The sample displacement s (mm), and the flexural modulus (MPa), are given as a function of the load at material yield. As detailed in table 4.3, samples from the EPDM diaphragms were cut out and used to conduct this investigation.

Results

As figure 4.19 and figure 4.20 show, there is little variation in either the flexural modulus or the overall displacement of the virgin samples among the four different production batches. Production batch 2 has the largest variation in flexural modulus.

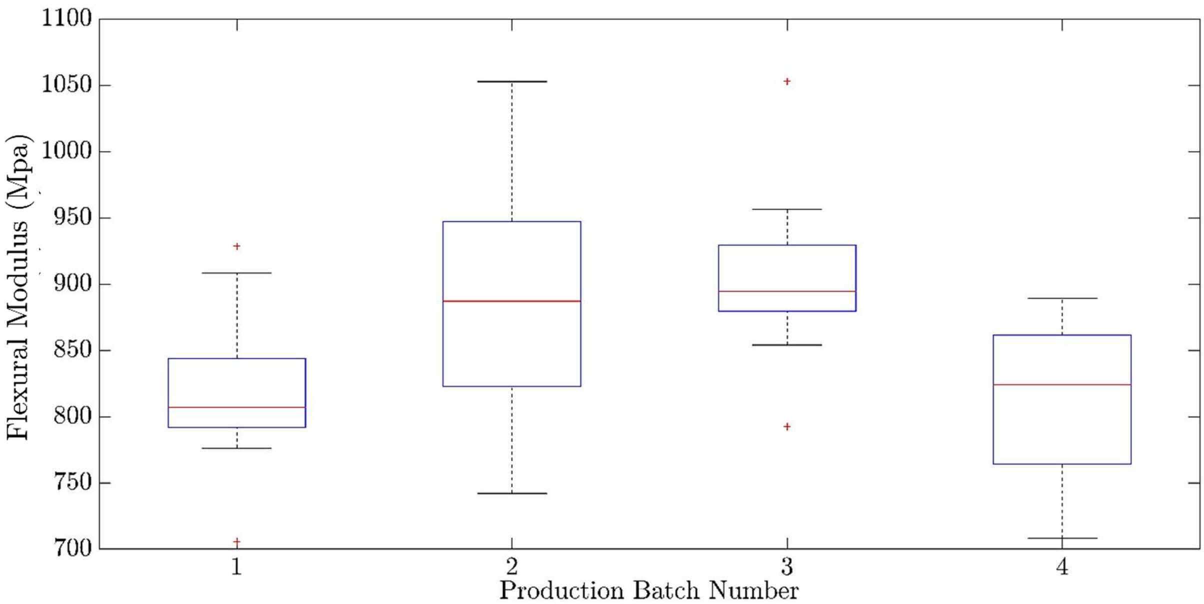

Figure 4.19: Flexural modulus of virgin samples as a function of production batch

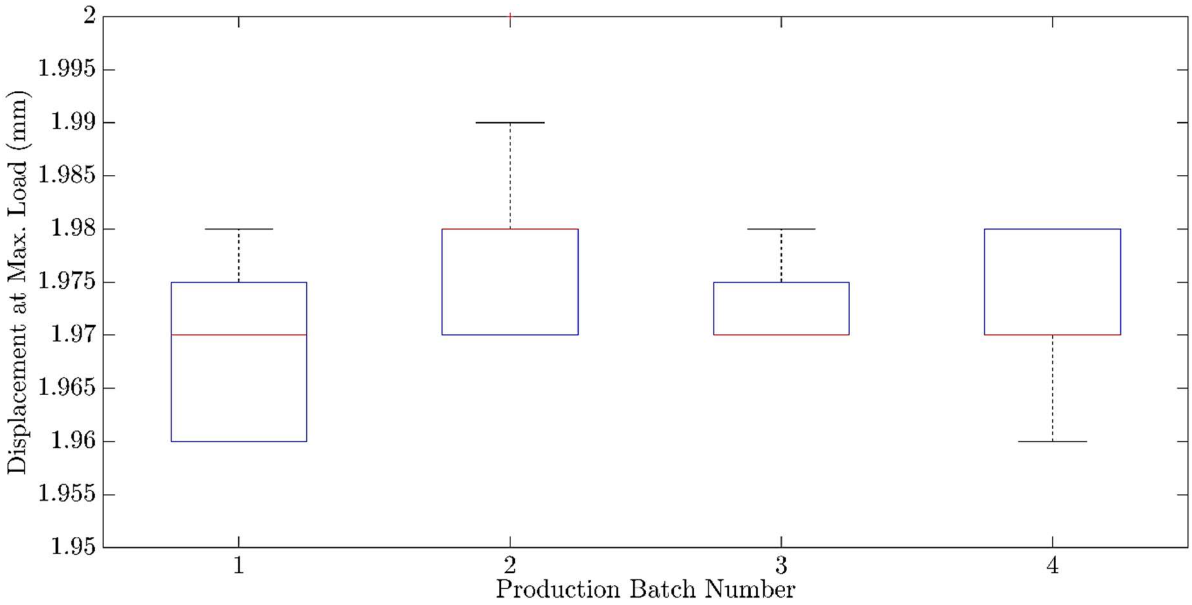

Figure 4.20: Displacement at max. load of virgin samples as a function of production batch

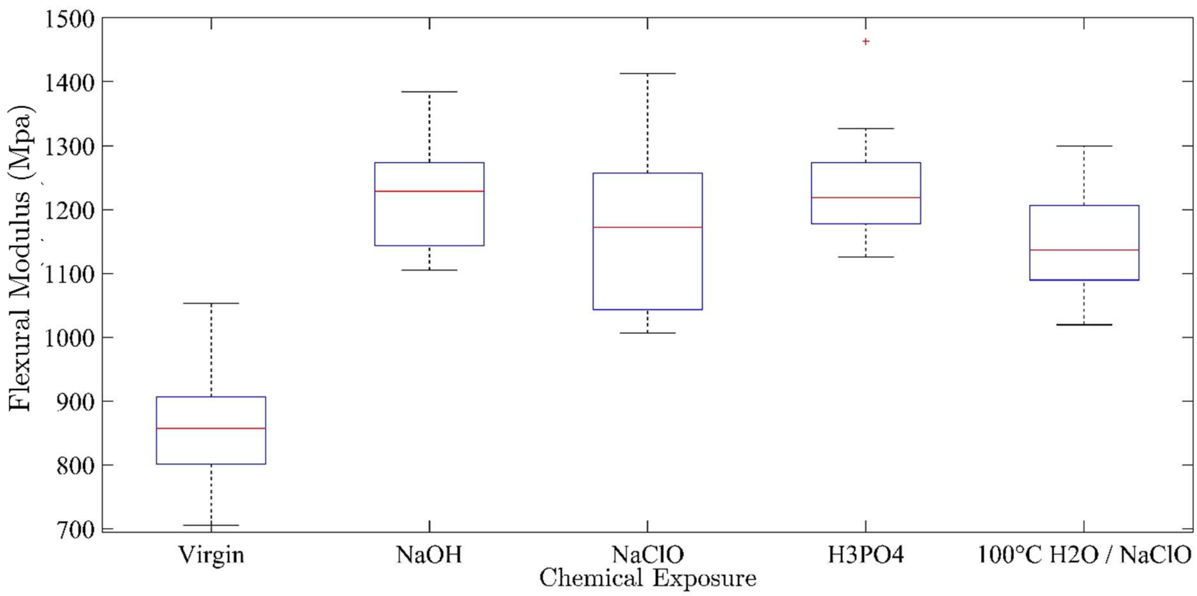

Figure 4.21: Flexural modulus as a function of chemical exposure type

Figure 4.21 illustrates a marked increase in the flexural modulus of the samples post chemical exposure. This corresponds to an increase in the elastic modulus which strongly suggests that the EPDM matrix is more rapidly degraded, likely as a result of crosslinking [106,314].

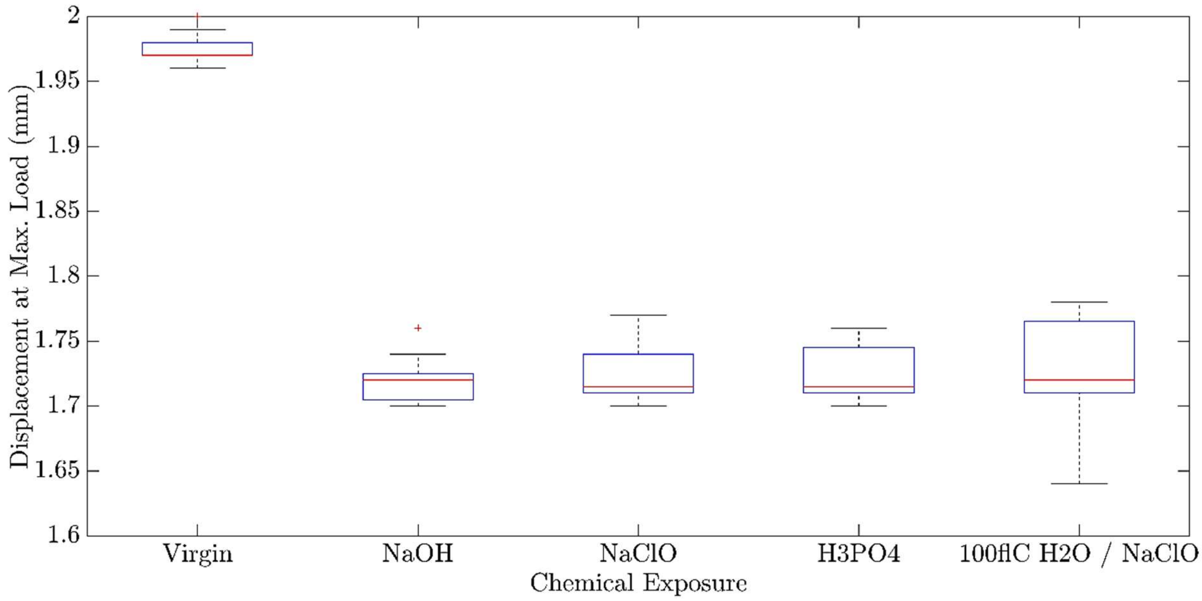

Figure 4.22: Sample displacement as a function of chemical exposure type

In relation to the flexural modulus differences between different exposure durations and types, figure 4.23 shows that the samples solely exposed to NaClO exhibit the largest difference. This is seen as a sharp increase in flexural modulus due to sample compression and to prolonged exposure up to 504 hours. The 100°C H_2O / NaClO and H_3PO_4 exposed samples show a minor increase in flexural modulus up to 504 hours. The NaOH exposed samples have a decreased flexural modulus due to material compression, which again may indicate that compression has inhibited crosslink formation.

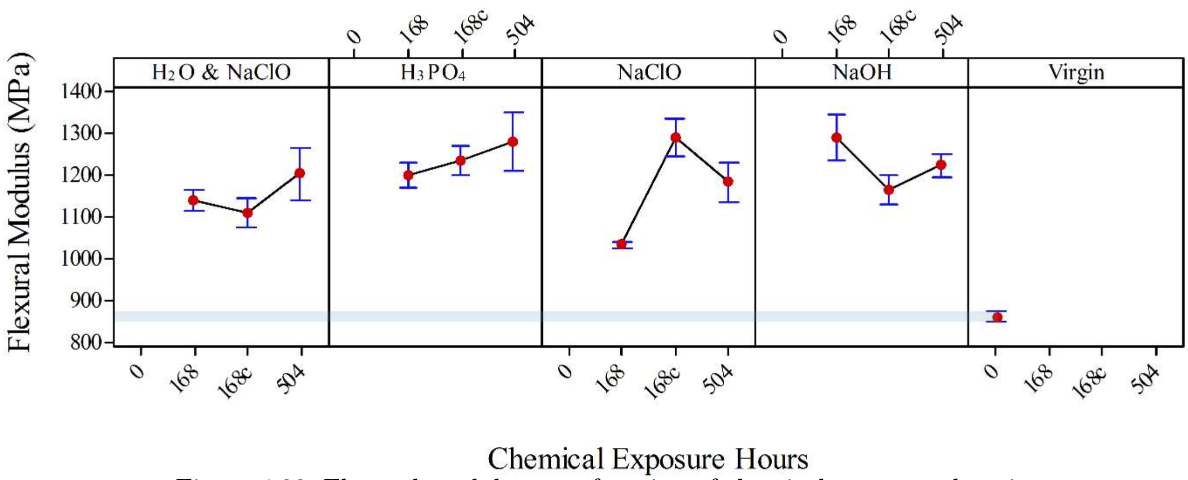

Figure 4.23: Flexural modulus as a function of chemical exposure duration

There is little variation in the displacement of the sample at maximum load between the NaOH and H_3PO_4 exposure types as shown in figure 4.24. There is a modest reduction in the displacement of both NaClO exposure types after material compression, which indicates a possible trend towards increased crosslinking.

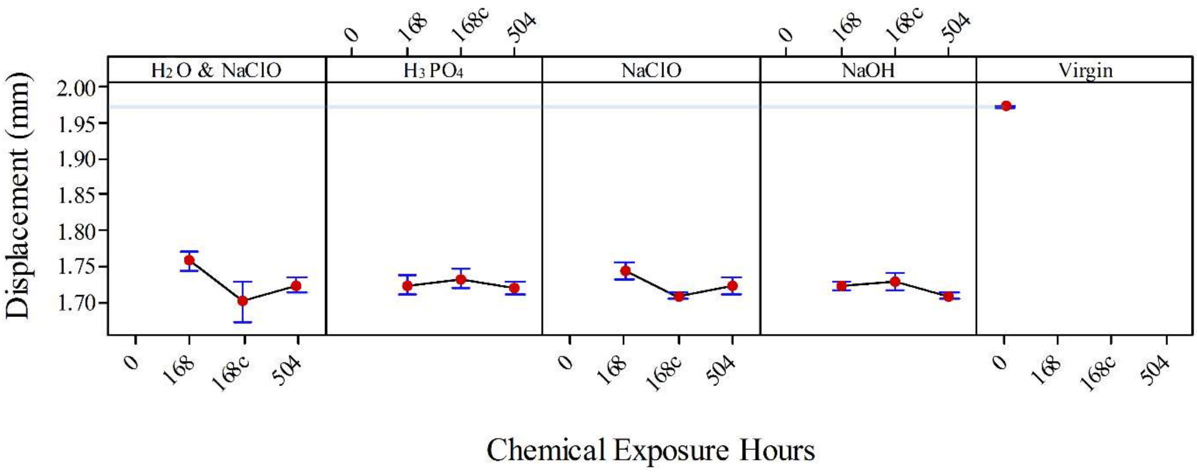

Figure 4.24: Total sample displacement as a function of chemical exposure duration

Chemical exposure during material compression largely seems to have had a negative effect on both the NaClO exposure types with regards to elastomer elongation and flexural modulus, again indicating a higher crosslink density. Continued exposure up to 504 hours also appears to have induced additional crosslinking in both NaClO exposure types. The H_3PO_4 exposed samples show little change in flexural modulus or elongation with regard to continued exposure or compressed exposure, however compressed exposure may have initiated chain scissioning in the NaOH exposed samples due to the decrease in flexural modulus evident. Critically, 100ºC H_2O / NaClO exposure has resulted in cracks developing in the samples exposed to those variables after 10,000 cyclical actuations. As the NaClO exposed samples did not show signs of cracking, it can be concluded that the addition of 30 hours of 100ºC H_2O exposure has had an additional degenerative effect on the samples.

The results of the flexural modulus testing agree well with the cyclic compression testing results. The displacement at max. load and the flexural modulus indicate increased crosslinking in both of the 504 hour and 168 hour compressed NaClO type exposed samples, in comparison to the 168 hour non-compressed exposure. Similarly, a reduction in displacement and flexural modulus is seen in the NaOH exposed samples, indicating that chain scissioning has occurred post 168 hour non-compressed exposure. This is also in agreement with the shore hardness results. The strong correlation of results among the tests is a good indicator of the degradation mechanisms occurring and their evolution in the EPDM material.

4.4 Compression set testing

4.4.1 Method

In accordance with ISO 815 [111], the dimension of the test specimens was measured after which they were compressed by 25% in an ISO creep fixture and held for a duration of 24, 84, and 168 hours at 125ºC. The samples were then removed from the fixture and cooled at room temperature for 30 minutes before their new dimensions were measured. The ISO compression rig setup is shown in figure 4.25.

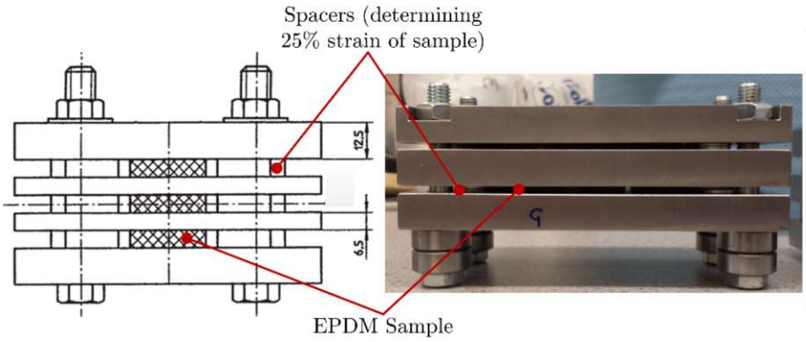

ISO 815 Compression Set Fixture	
Test Strain	25%
Test Temperature	125°C
Test Duration	24, 84, 168 hours
Cooling Temperature	22.6°C
Cooling Time	30 minutes

Figure 4.25: ISO 815 test parameters and creep fixture setup. Adapted from [111].

4.4.2 Results

Figure 4.26 shows the creep results of the virgin samples across the four different production batches. There is some variation in the creep percentage among the batches, particularly batch 3, all of which clearly worsen with time under compression. This indicates that the raw EPDM undergoes strain induced elasticity loss at high temperatures. The potential reasons for this are discussed in section 4.4.2. As shown, there is large variation in the creep percentage results across the three compression durations.

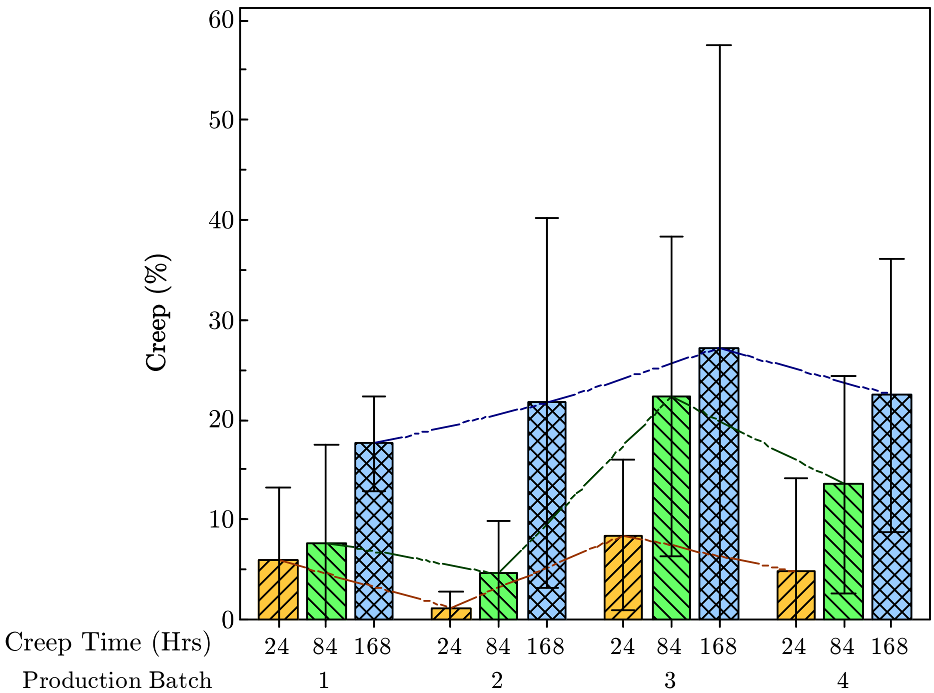

Figure 4.26: Creep percentage results of virgin samples

Figure 4.27 shows the creep results for all samples. After 24 hours compression there is not a large difference between the creep of the chemically exposed samples and the virgin samples. The relative difference in permanent compression between the chemically exposed and virgin samples increases however after 84 hours, and again after 168 hours of compression. It is clear that prior chemical exposure accelerates or aids the degradation mechanism responsible for permanent loss of material elasticity under induced strain. There are some relative differences in the creep between the chemically exposed samples, with the NaOH exposed samples show slightly reduced compression set after 84 hours. There is very little difference in the creep values between the two NaClO variables. It could be foreseen that prior material degradation negatively impacts the materials' ability to withstand further stresses induced under elevated temperatures.

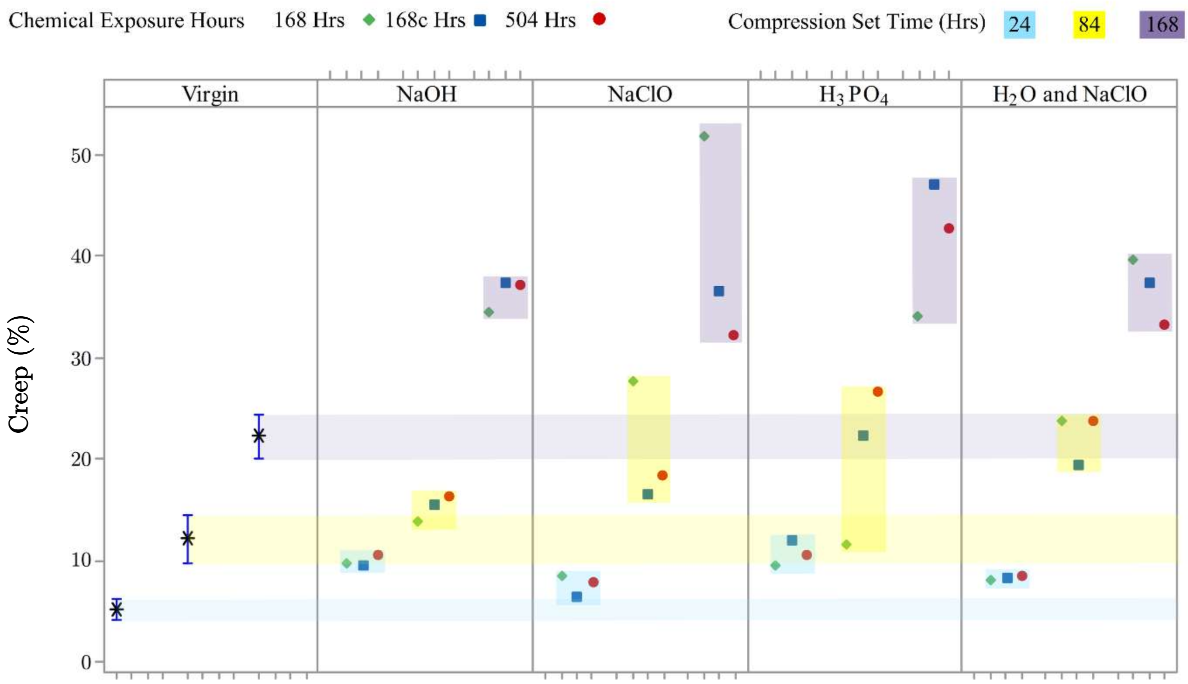

Figure 4.27: Creep % as a function of chemical exposure and type and duration

As shown in figure 4.27, exposure to NaClO under 168 hours of compression prior to creep testing may have had a protectionist effect. The creep percentage of these samples, designated as '168c', is reduced in comparison to those samples which were not-compressed when exposed to NaClO for 168 hours, designated simply as '168'. A similar effect can also be seen with continued NaClO exposure up to 504 hours, particularly evident as compression set testing time is increased. The opposite trend is true of the H_3PO_4 and NaOH exposed samples which show worsening creep in those samples exposed to chemical solutions for 504 hours, and 168 hours in a compressed state, prior to testing.

4.5 Dynamic mechanical thermal analysis

4.5.1 Method

Rheometric Scientific Dynamic Mechanical Thermal Analyser Mk III	
Test Mode	Cantilever
Temperature range	-100°C to 60°C
Heating Rate	2°C/min
Force Amplitude	0.1 N
Frequency	10 Hz

Figure 4.28: Dynamic mechanical thermal analysis testing setup and test parameters

The viscoelastic properties of the samples were measured using a Rheometric Dynamic Mechanical Thermal Analyser Mk III in cantilever mode according to the specification given in figure 4.28.

4.5.2 Results

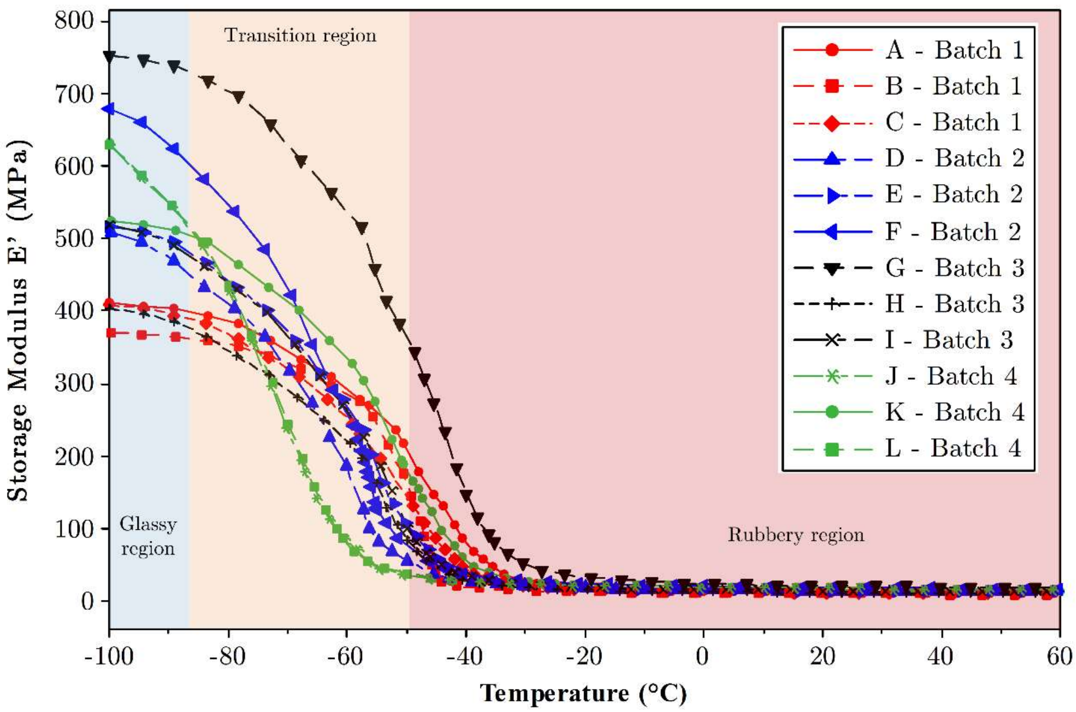

Figure 4.29: Virgin samples storage modulus curves

As shown in figure 4.29, the storage modulus curves of the virgin samples show three distinct regions; a glassy high modulus region where the segmental mobility is restricted, a transition zone where the E' values decrease with increasing temperature, and a rubbery region given by a decay in the modulus with further temperature increase. Sample G from batch 3 has considerably larger crosslink density than the other virgin samples. Note the narrow shoulders of the curves, indicating a narrow transition region.

As illustrated in figure 4.29 there is variability in the storage modulus, and hence crosslinks density, of the virgin samples. In particular, production batch 3 has a large variability in crosslinking, while production batch 1 has low variability and low overall crosslink density.

In figure 4.30, the storage modulus of sample G from batch 3, which had the largest modulus magnitude of the virgin samples, is shown in comparison to the exposed samples. As shown, the total magnitude of the virgin sample is greater in the glassy region below T_g, but this trend starts to changes above T_g in the transition and rubbery regions, beginning above approximately -60°C. As noted, the virgin samples in figure 4.29 largely show narrow bands and quick transitions between phases, while the exposed samples below show broad transitions, with a much larger transition zone, indicating the presence of heterogeneous zones in the polymer matrix [103]. This heterogeneity increase may correspond to a decrease in polymer network swelling, potentially due to a loss of plasticiser in the polymer network due to solvent effects from the chemical exposure, or may be due increased crystallisation of the polymer due to increased chain linking [103,315].

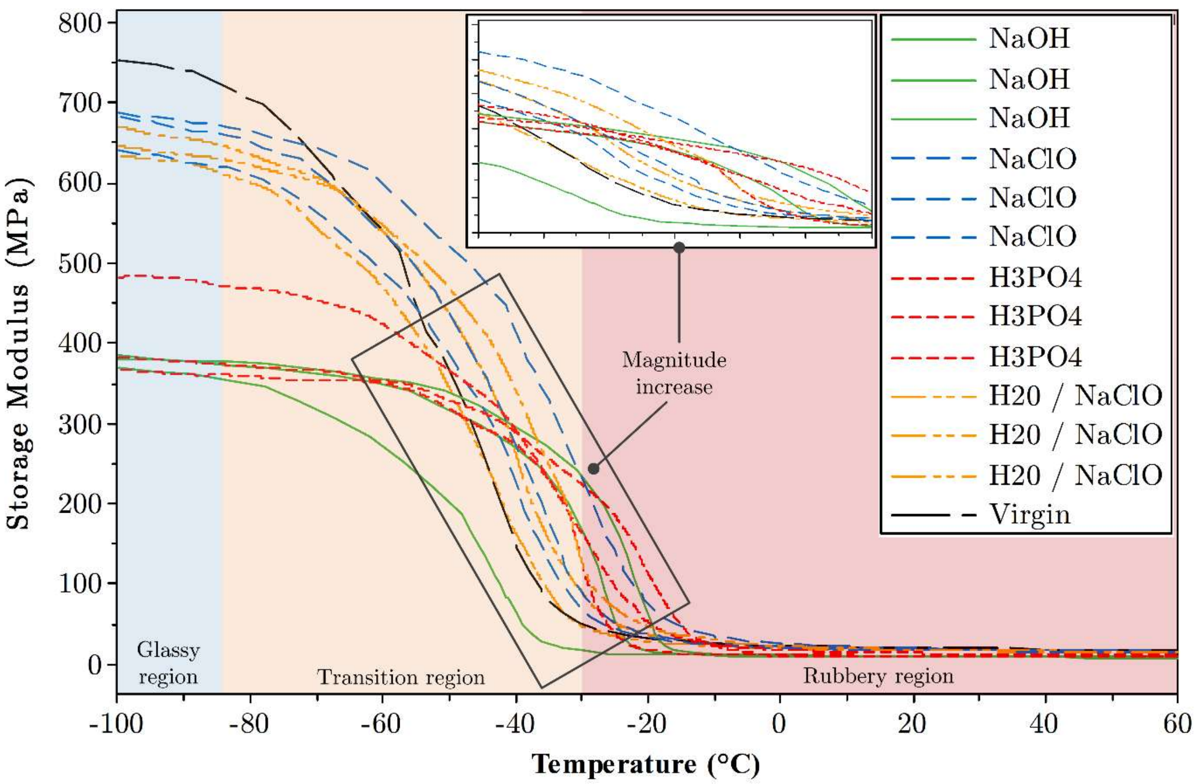

Figure 4.30: Storage modulus of exposed samples

At the interface of the transition and rubbery regions, above T_g, almost all exposed samples show higher storage modulus values. This is important as the modulus in this area is contributed to by the ability of the macromolecules to resist intermolecular slippage which is a function of crosslink density [103]. Investigating the potential shifting of the glass transition temperatures enables the qualification of this more substantively.

Figure 4.31 is an example of the damping factor curves for one sample from each of the virgin production batches and one from each chemical exposure type. It demonstrates how the glass transition temperatures T_g are shifting towards higher temperatures after chemical exposure. As illustrated, the glass transition temperatures correspond to the peak of the damping factor curves.

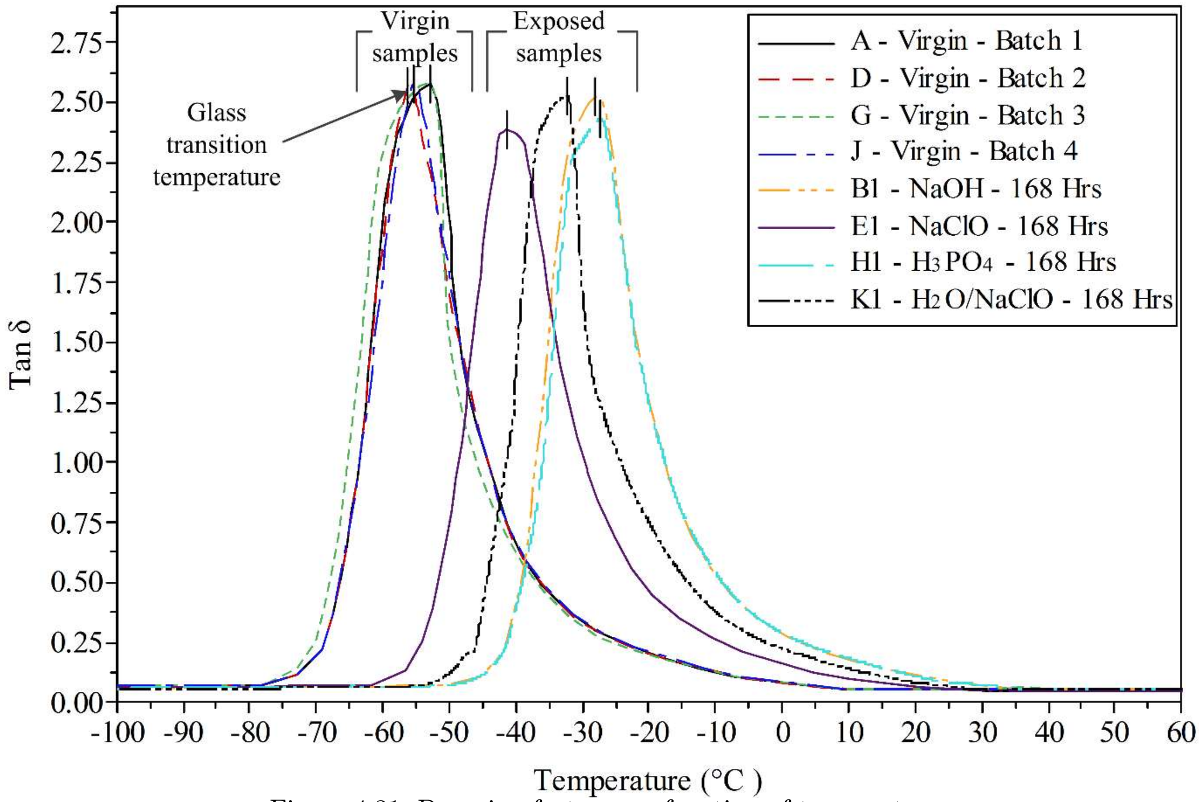

Figure 4.31: Damping factor as a function of temperature

Figure 4.32 shows the glass transition temperatures for each of the virgin production batches. The transition temperatures vary from approximately -52ºC to -58ºC. The transition temperatures of batches 1 and 4 are similar, as are the transition temperatures of batches 2 and 3. Batch 3 has the largest variability in temperature, but still within the range of all other batches.

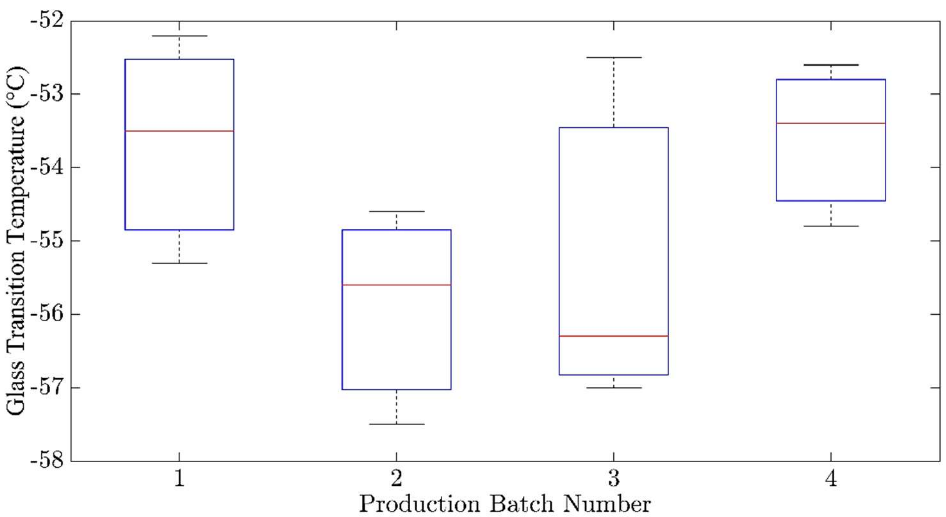

Figure 4.32: Glass transition temperature of the virgin samples

The mean values and variability of the transition temperatures amongst the virgin production batches is dwarfed by the variability and mean values of the chemically exposed samples, as shown in figure 4.33. The glass transition temperatures of all the exposed samples has increased substantially, from approximately -40ºC to -20ºC. The NaOH and H_3PO_4 exposed samples have slightly higher transition temperatures than either NaClO exposures. The addition of 100ºC H_2O to NaClO has had a modest affect, increasing the glass transition temperature slightly and decreasing the overall variability.

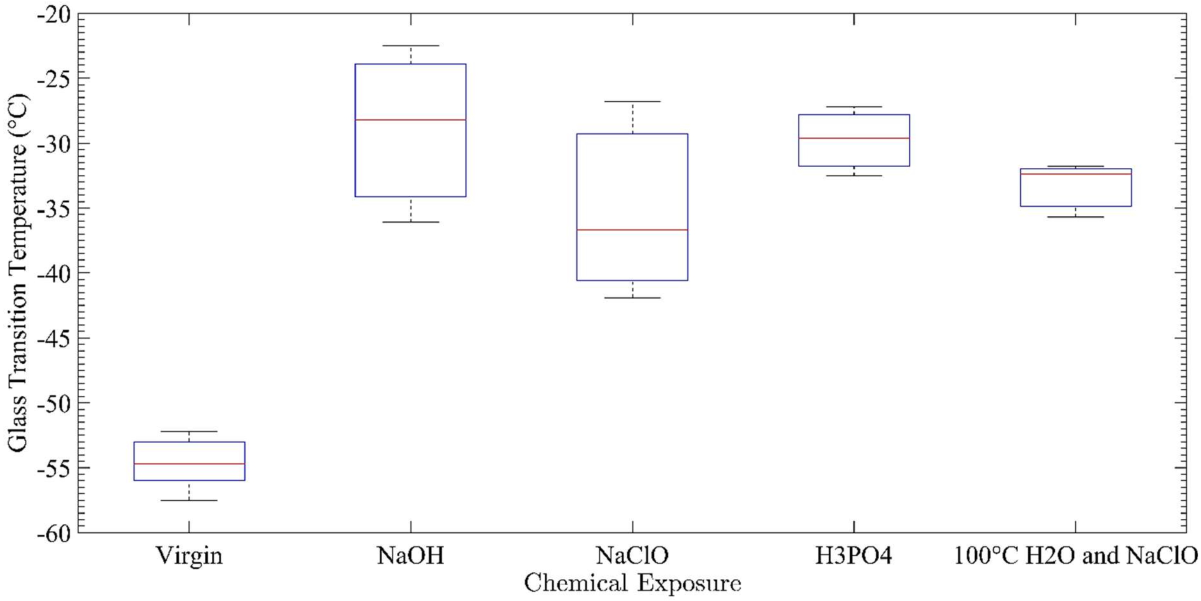

Figure 4.33: Glass transition temperature of all samples

Figure 4.34 shows the variability among the glass transition temperatures as a function of chemical exposure type. The 100ºC H_2O / NaClO exposed samples show a minor increase in transition temperature due to material compression and continued exposure up to 504 hours. The samples only exposed to NaClO however show a large increase in glass transition temperature due to compression and continued chemical exposure. This indicates that continued exposure and exposure during compression to NaClO results in increased crosslink density. The 100ºC H_2O exposure may have accelerated the crosslinking reactions, which is why a smaller difference is observed in these samples, as the samples may be closer to crosslink saturation. There is an additional increase in T_g, and crosslink density, of the compressed NaOH sample, but the crosslink density appears to lessen upon further exposure up to 504 hours. The same is true of the H_3PO_4 exposed samples, which all show decreasing T_g and crosslink density. This may signify that crosslink density has reached a peak in these samples, and continued exposure is now resulting in chain scission reactions within the polymer matrix.

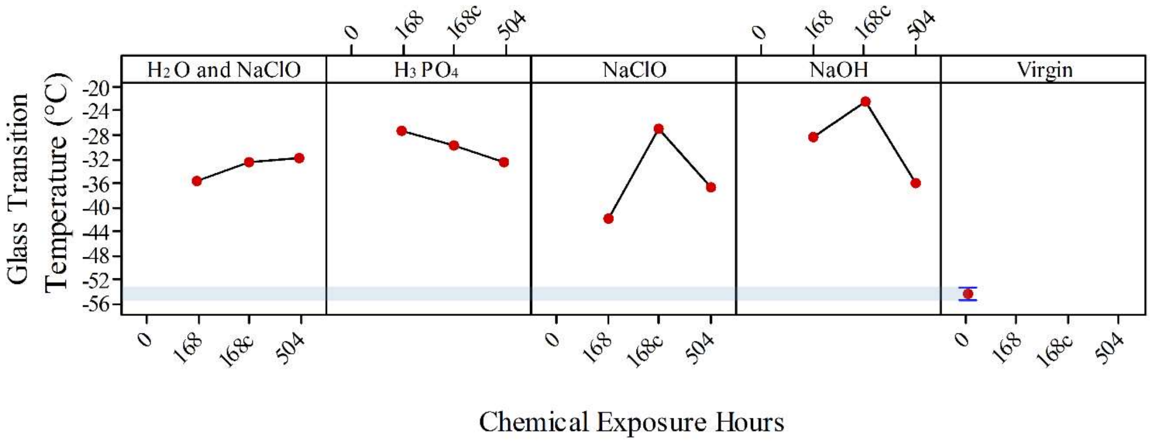

Figure 4.34: Glass transition temperature as a function of chemical exposure type and duration

4.6 Thermogravimetric analysis

4.6.1 Method

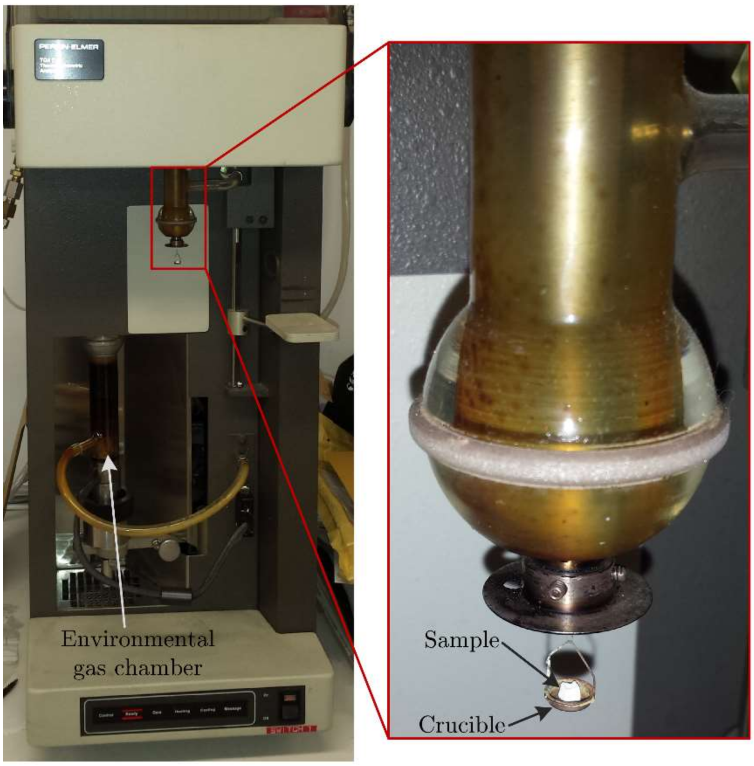

Perkin Elmer TGA 7	
Crucible	Alumel
Reference standard	30% glass-filled polypropylene
Sample starting weight	10-12 mg
Step 1	
Heating Rate	160°C/min
Starting temperature	30°C
Final temperature	600°C
Gas	Nitrogen
Step 2	
600°C hold time	3 min
Gas	Nitrogen
Step 3	
Heating Rate	160°C/min
Starting temperature	600°C
Final temperature	750°C
Gas	Nitrogen
Step 4	
750°C hold time	5 min
Gas	Oxygen

Figure 4.35: Thermogravimetric analysis experimental setup and test parameters

It was important to perform compositional analysis in these investigations to ensure that the ratios of carbon black and solid filler materials to pure polymer content was not partly responsible for any of the mechanical property differences seen in other tests. The TGA testing is divided into two distinct phases; the test is performed firstly under nitrogen to decompose the organic matter within the polymer, and then the test is finished under oxygen to burn the remaining carbon content [116]. Firstly, samples weighing between 10-12 milligrams were placed in an Alumel crucible enclosed in an oxygen free atmosphere of N_2. Compounded polypropylene with a 30% glass-filled concentration acted as the calibration reference material pre-test. The samples were then isothermally heated to two distinct pre-set temperatures, firstly to 600ºC, and then to 750ºC, via a linearly increasing temperature rate of 160ºC/min. The samples were kept at the target temperatures for a set amount of time to ensure all volatile matter was thermally decomposed. The isothermal 750ºC temperature hold was performed under oxygen to halt pyrolysis. The weight loss of the samples was monitored continually throughout the test as the samples thermally decomposed. From the resulting thermograms, the composition of the samples and their thermal stabilities were concluded [73,102].

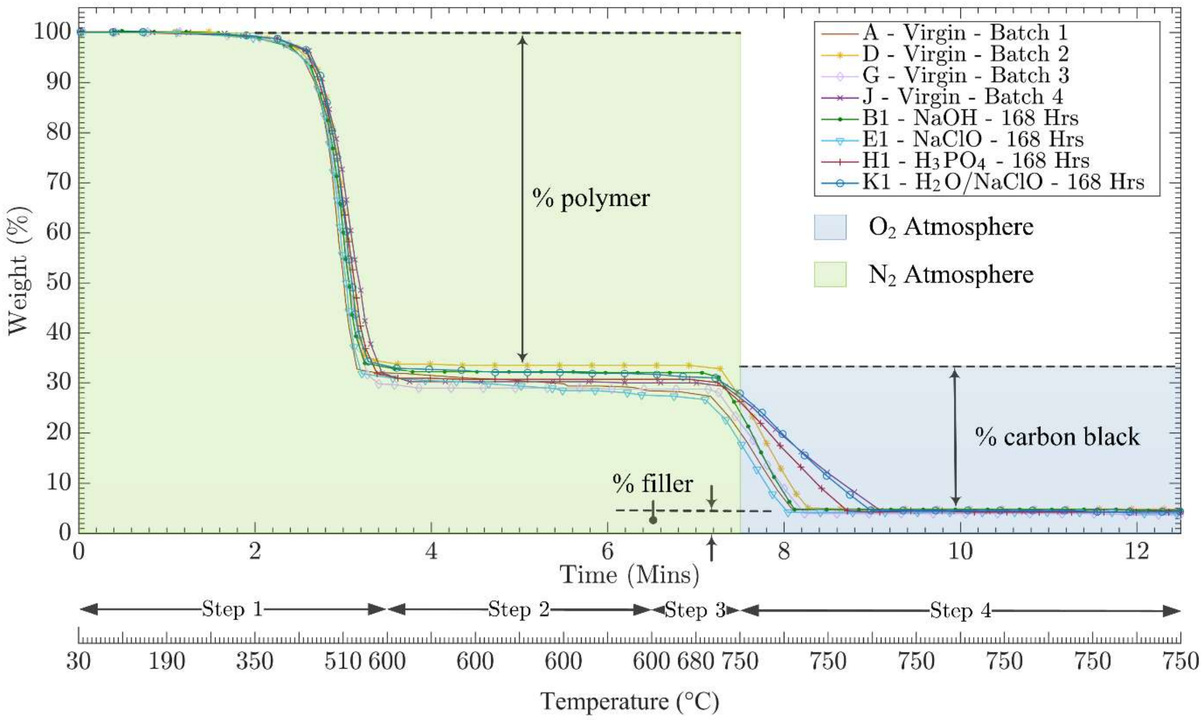

Figure 4.36: TGA thermograms of multiple samples

Figure 4.36 shows the weight loss of multiple samples, both virgin and chemically exposed, as a function of time and temperature. Regarding the testing stages, step 1 of decomposition up to 600ºC results in the loss of oils, waxes, and pure polymer, the 600ºC hold of step 2 ensures all polymer content is decomposed, the temperature increase from 600ºC to 750ºC in step 3 initiates the decomposition of carbon black, which is then accelerated and ensured by the 750ºC hold and oxygen exposure of step 4. The change in weight percentage during each step is then measured. The remaining char at the end of the test corresponds to the percentage of solid filler, likely metallic oxides, which were in the polymer matrix.

4.6.2 Results

Shown in figure 4.37 are the relative weight loss percentages of the constituents of the virgin samples as a function of production batch. As illustrated, the batches have almost identical relative amounts of constituents as one another, with little difference in the relative amounts of pure polymer, additive carbon black, and filler material. This is evidence of the conformity of the diaphragm production process over a two-year period. As weight loss of the polymer content is dependent on the thermal stability of the polymer blend, it can be concluded that there is no thermal history in any of the virgin samples, which could have arisen due to poor storage conditions for example [115].

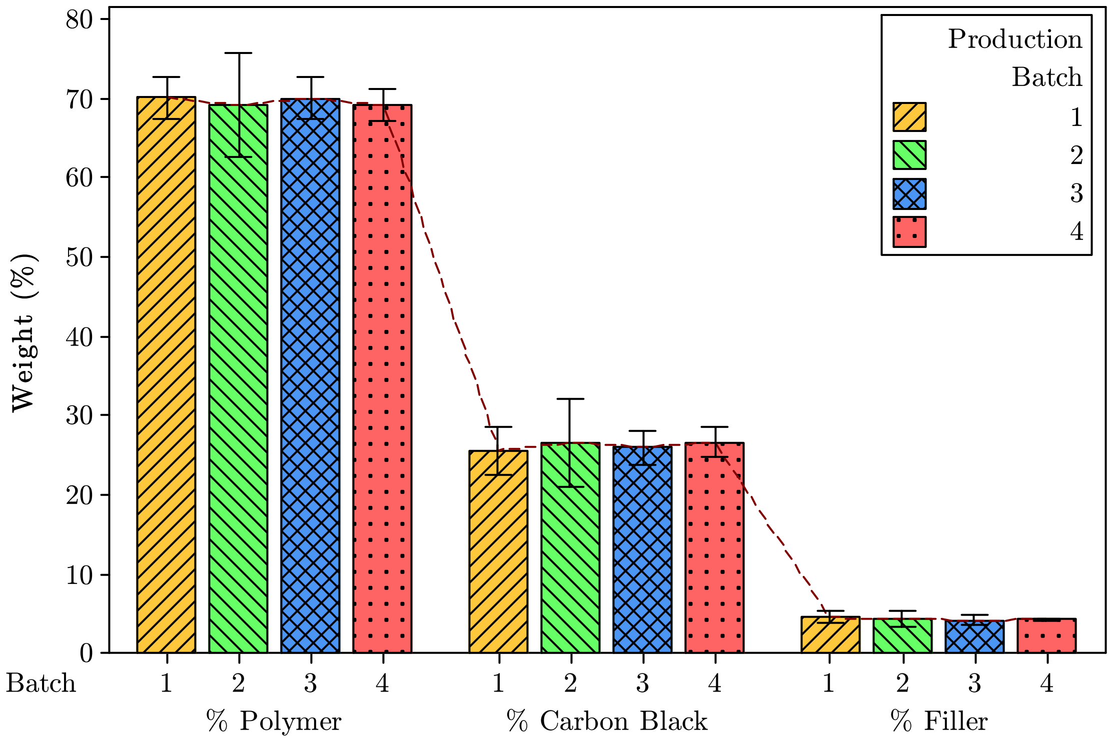

Figure 4.37: Constituent weight loss percentages of virgin samples

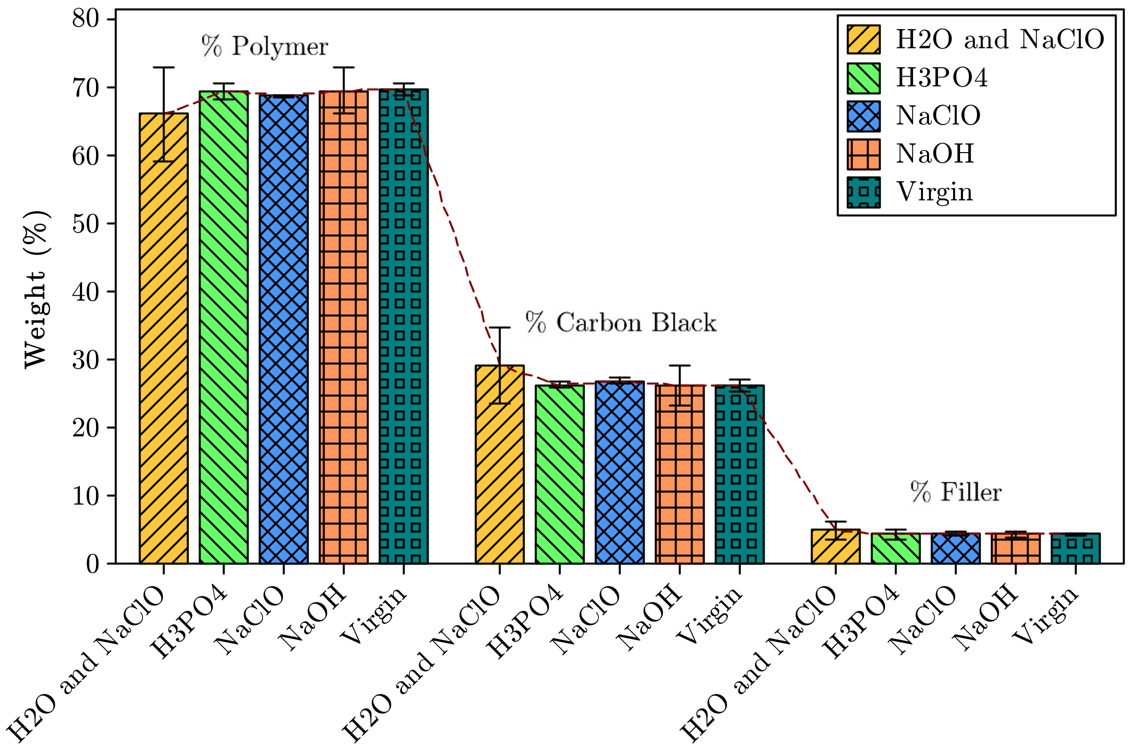

Figure 4.38: Constituent weight loss percentages of all samples

Figure 4.38 shows the relative weight loss percentage of the constituent parts of all samples. As shown, all samples have almost identical relative weight losses of polymer, carbon black, and filler content. The 100°C H_2O / NaClO exposed samples show more variation in the amounts of pure polymer and carbon black content in comparison to the other samples, likely due to the increased thermal stability of the polymer blend induced from the 100°C H_2O exposure, as pure NaClO exposure has not had a similar effect.

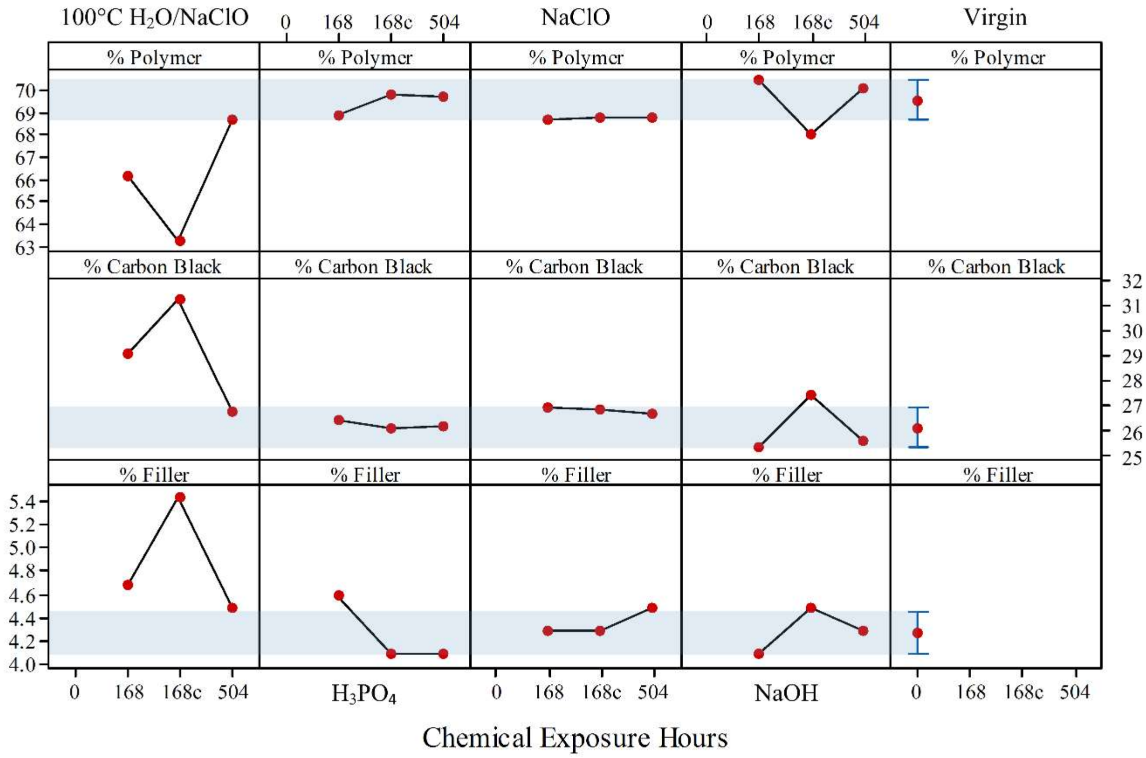

Figure 4.39: Constituent weight loss percentages of all samples as a function of exposure duration and type

According to figure 4.39 there are large differences in the relative weight losses of polymer, carbon black, and filler content of the 100°C H_2O/NaClO exposed samples in comparison to the virgin samples. Again, this is contrary to the NaClO only exposed samples, indicating that the 100°C H_2O exposure has had a thermal impact. This indicates that some thermal degradation, leading to increased thermal stability, has occurred in the material. In the 100°C H_2O/NaClO exposed samples there is a large reduction in the polymer content loss due to compression during exposure. This has resulted in a relative increase in both the carbon black and filler contents. A similar phenomenon is seen in the NaOH exposed samples, which also exhibits a loss of polymer content during compression, but not as much as the 100°C H_2O/NaClO exposed samples.

4.7 Fourier transform infrared spectroscopy

4.7.1 Method

Fourier transform infrared spectroscopy (FTIR) coupled with a 45º single reflection Germanium attenuated total reflection (ATR) crystal with a spectral range of 4,000 – 650 cm^{-1} was chosen to aid the characterisation of the change in surface chemistry due to changes in the chemical functionalities of the EPDM samples, to elucidate the interfacial chemical degradation mechanisms.

The FTIR-ATR spectroscopy analysis was conducted using the exposed side of the samples. The samples were clamped in place using a load-limiting ratchet system available on the test equipment. The load-limit ensured no damage would occur to the crystal. Testing was conducted under ambient conditions. Before each reading, the spectrometer was cleaned and background calibration was conducted with no sample in the ATR holder. The ATR sampling accessory utilised software correction. The tests were conducted using a Perkin Elmer Spectrum One FTIR with a 100 scan per sample cycle and a resolution of 8 cm^{-1}. The spectrometer is calibrated annually.

PerkinElmer FT-IR-ATR Spectrum One spectrometer	
General	Vibration isolated baseplate
Interferometer	Michelson interferometer. Self-compensating for dynamic alignment changes due to tilt and shear
Beamsplitter	Multi-layer potassium bromide
Detector	Electrically temperature-stabilized fast recovery deuterated triglycine sulfate
Wavelength Accuracy	0.1cm^{-1} at 1600cm^{-1}

Figure 4.40: FTIR-ATR Perkin Elmer Spectrum One spectrometer specifications

In order to determine the degree of polymer degradation due to oxidative damage that has occurred within the material post exposure, it is necessary to calculate the oxidation index (O_I), also known as the carbonyl index, of each sample. The method adopted in this work for calculating the O_I is adapted from Blackmore et al [76] and Su et al [65]. The oxidation index can be defined as the ratio of the peak height, i.e. the absorbance intensity, between 1800 and 1500cm^{-1} (A1800–1500), typically peaking between 1730 to 1780 cm^{-1}, and the absorption of the peak of the hydrocarbon C-CH2 scissoring region between 1500 and 1400cm^{-1} (A1500-1400), which typically peaks at approximately 1460 to 1450cm^{-1} [65,76,316]. The C-CH2 scissoring region is used as a stable internal reference representing sound polymer [76].

The oxidation index (O_I) of each individual sample can be written as:

$$O_I = {}^{P_C}/_{P_H} \qquad (4.7.1)$$

where P_C is the peak height of the Carbonyl region and P_H is the peak height of the hydrocarbon region. The peak heights are calculated as the height above the two separate tangential base-lines located on either side of the measured peaks at A1800–1500 and A1500-1400, as shown in figure 4.42. The calculation of the oxidation index is based on Beers law, which assigns a relationship between the ratio of peak heights in an infrared spectrum and the concentration of the functional group responsible for that peak. Beers law is described as [76]:

$$A = abc \tag{4.7.2}$$

where $A = log_{10}(I_O/I)$ is the absorbance of an infrared peak, with I_O and I being the intensity of the incident and transmitted radiation respectively. The absorptivity of the functional group is given as a, while b is the thickness of the sample, and c is the concentration [76]. In this work, the thickness of all samples are identical. Assuming that absorptivity remains constant with concentration, the changes in the relative concentrations of functional groups present in the infrared spectra in this work are therefore independent of the sample thickness value.

Different methods have been suggested for calculating the oxidation index. For example, Wang et al [316] use the peak height of the CH3 symmetrical stretching band at 1376cm^{-1} as the internal reference, instead of the C-CH2 scissoring band used in this work. Similarly, Pourmand et al [105] use an aluminium trihydrate band centring at 800cm^{-1} as the internal reference in their work. Pourmand et al also calculate the total area under the curve of the respective regions, rather than calculating absorbance intensity using the peak height method which is most commonly used. The authors offer no potential advantages for the use of this method.

4.7.2 Results

Shown in figure 4.41 is the FTIR spectrum of the unadulterated EPDM samples A, D, G, and J representative of the four virgin batch samples. As shown, there is very little chemical difference between each batch, demonstrative of the chemical consistency of the product over a two-year period. The bands shown, typical for EPDM, include asymmetrical stretching of the CH3 and CH2 groups at 2952cm^{-1} and 2,921 cm^{-1} respectively, symmetrical stretching of the CH2 group at 2,850 cm^{-1}, symmetrical stretching of the C=O bonds at ~1600cm^{-1}, scissoring of the C-CH2 bonds at ~1,450 cm^{-1}, and symmetrical C-H stretching of CH3 from the propylene unit at 1,375 cm^{-1} [79,85,94,317]. The lower peaks, in the region of 1152 cm^{-1} and 1100 cm^{-1}, possibly represent the asymmetric and symmetric vibrations of C-O-C, respectively, however it is more probable that a coagent such as triallylcyanurate (TAC) has been used to facilitate peroxide crosslinking for greater heat resistance properties [85]. TAC suppresses the chain scission associated with the presence of tertiary hydrogen in the main EPDM backbone during peroxide curing, and forms crosslinks through its reactive double bonds and reacts with the scission products, resulting in better crosslinking efficiency. The presence of TAC explains the lower bands at 1152, 1100 and 855 cm^{-1}, which would be due to C-N-C, N-CH2 and C=C stretching vibrations, respectively, arising from the TAC domains associated with crosslinks [94]. The presence of TAC also explains the existence of the broad bands between ~1600cm^{-1} and ~1750cm^{-1}, as a result of N-(C=O)-N stretching vibrations from crosslinks associated with TAC domains which may be present as a part of the EPDM crosslinked domain. [65,73,94].

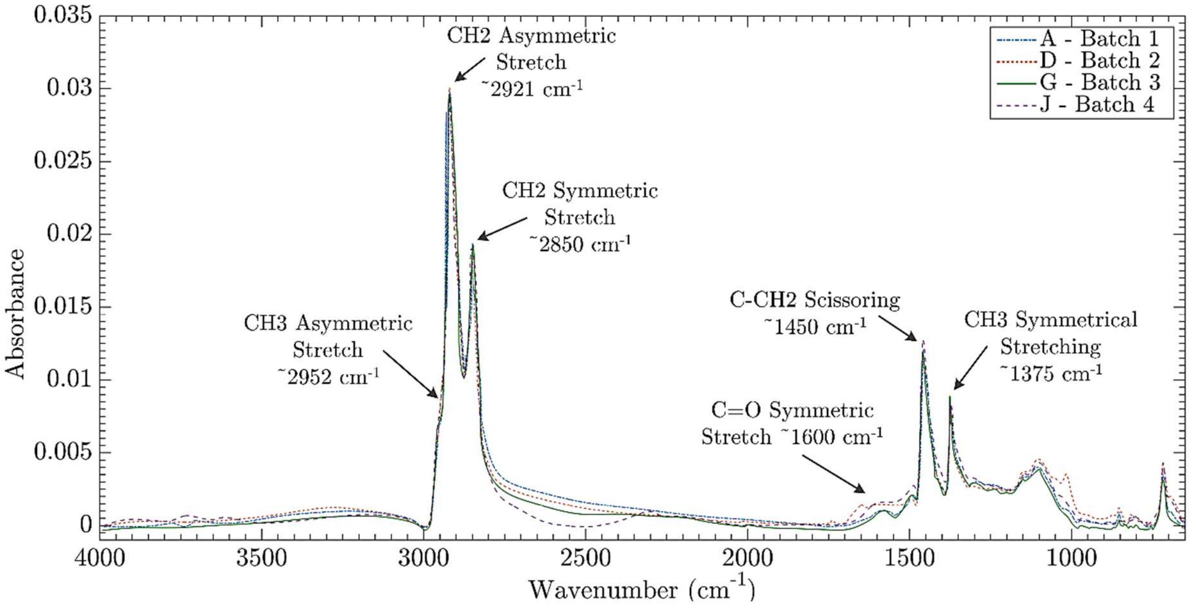

Figure 4.41: Chemical structure of virgin EPDM samples

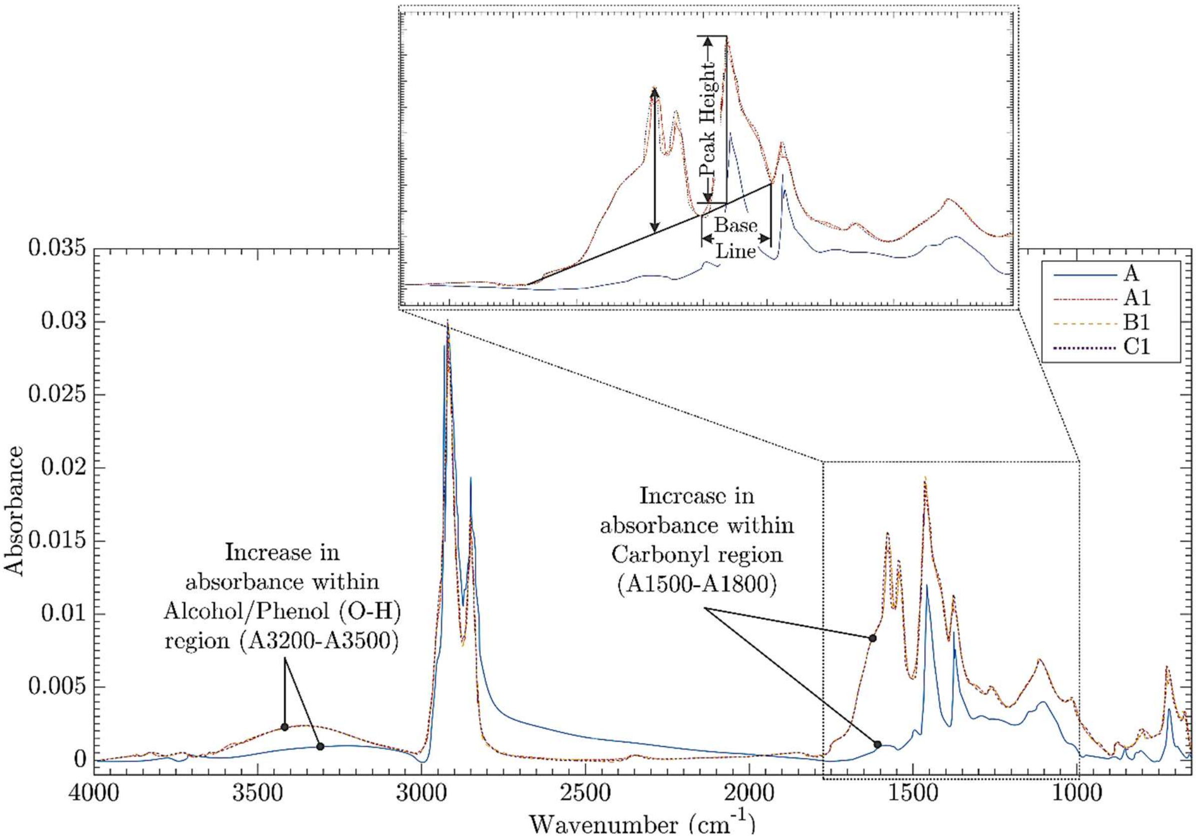

Figure 4.42: Increase in absorbance within Carbonyl and Phenol regions due to oxidative damage

As illustrated in figure 4.42, there are two distinct areas where oxidative damage is occurring in the EPDM material post chemical exposure. These are the Alcohol/Phenol (hydroxyl O-H) region between 3200 and 3500cm^{-1}, and the Carbonyl (C=O) region between 1500 and 1800cm^{-1} [65,66,73,79,118]. Figure 4.42 illustrates the damage occurring after exposure to NaOH at 65°C, in comparison with virgin sample A, representative of all virgin samples. Formation of the hydroxyl groups can possibly be attributed to the dissociation of the peroxide curing agent and can account for the very broad yet weak bands in the region of 3200 to 3500cm^{-1} [94]. The decrease in intensity of ~1460 cm^{-1} is associated with the change in the allylic group associated with TAC [94]. It is apparent that two maxima form in the Carbonyl regional, at approximately 1580 and 1540cm^{-1}. The band at 1540cm^{-1} may be due to the absorption of vulcanisation products present on the material surface [87]. The peak at 1580 cm^{-1} is characteristic of the presence of O=C-C carboxylate groups, and in the presence of aqueous mineral acids, O-H and O=C-C groups could possibly combine to form ester (C-O-C=O) or ether (C-O-C) groups [92]. Mitra et al [94] linked the presence of ester and ether linkages to the recombination of macro oxygenated species combining with each other to form new crosslinks. The same authors state that the chain scissions and crosslinking reactions could compete with each other throughout the degradation process.

Figure 4.43 shows the oxidation indexes of each of the virgin sample production batches. As shown, there is little difference in the degree of base oxidation levels, although batches 3 and 4 have slightly wider distributions.

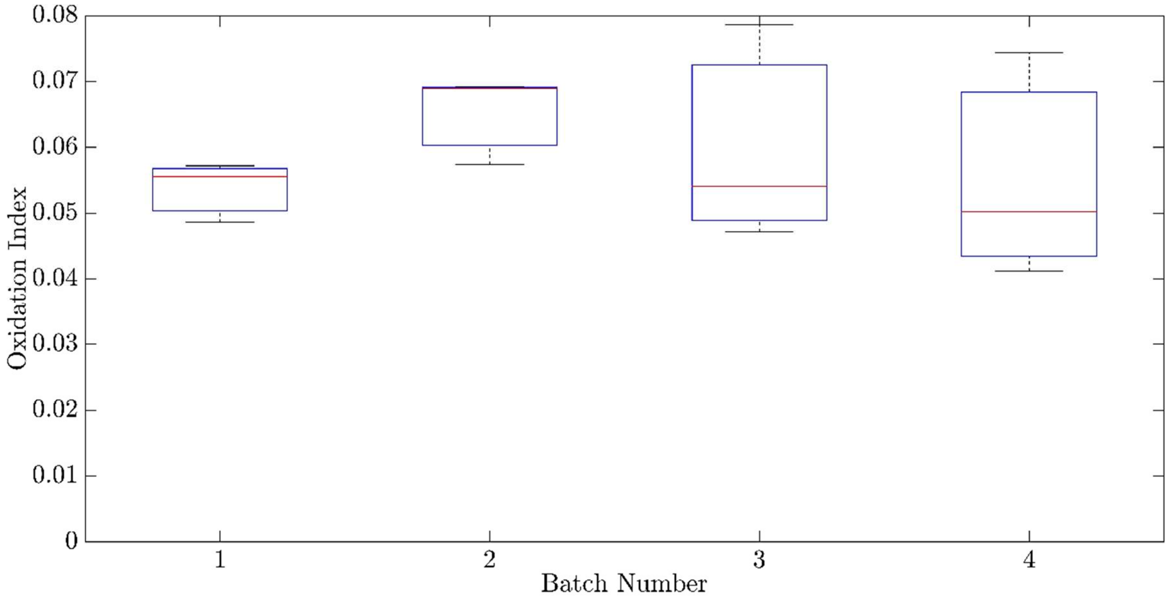

Figure 4.43: Oxidation index as a function of virgin sample production batch

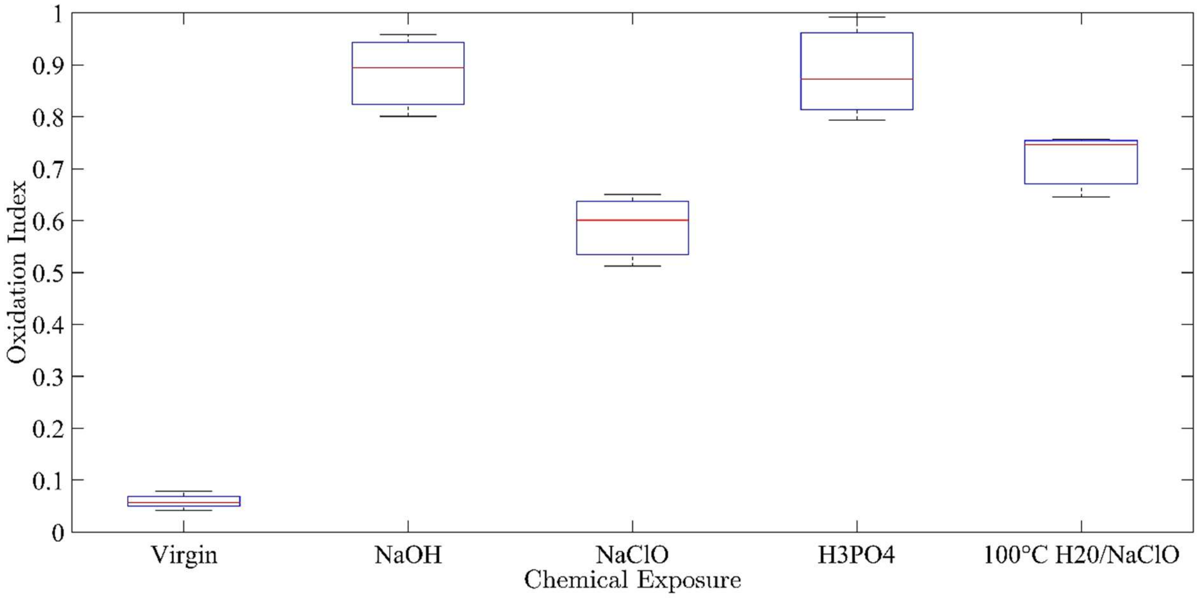

Figure 4.44: Oxidation index as a function of chemical exposure type

In contrast, in figure 4.44, the oxidation indexes for each chemical exposure is compared against the virgin samples. It is apparent that all of the exposed samples have considerably higher oxidation indexes than the virgin samples, indicating that considerable oxidation products are present in the exposed material. The NaClO exposed samples have accrued the least oxidative damage of the exposed samples, followed by the 100°C H_2O / NaClO samples. There is little difference between the NaOH and H_3PO_4 samples. There is a small amount of overlap between the two NaClO exposures, but it is likely that the addition of the 30 hour 100°C H_2O exposure has resulted in further damage to the material. There is little to no separation of the data between the H_3PO_4 and NaOH exposure indexes.

This same relationship in terms of degree of oxidation is observed in figure 4.45. As shown, the relationships hold regardless of the length of duration of chemical exposure, or whether the material was compressed during exposure, although it would appear that the 100°C H_2O / NaClO sample has been particularly negatively affected due to compression in comparison the NaClO exposed sample. Note how there is a large separation of the data between both NaClO samples and the NaOH and H_3PO_4 samples at 168 hours, which decreases with continued exposure. This suggests that the NaOH and H_3PO_4 samples become degraded at an accelerated rate compared to the samples exposed to NaClO.

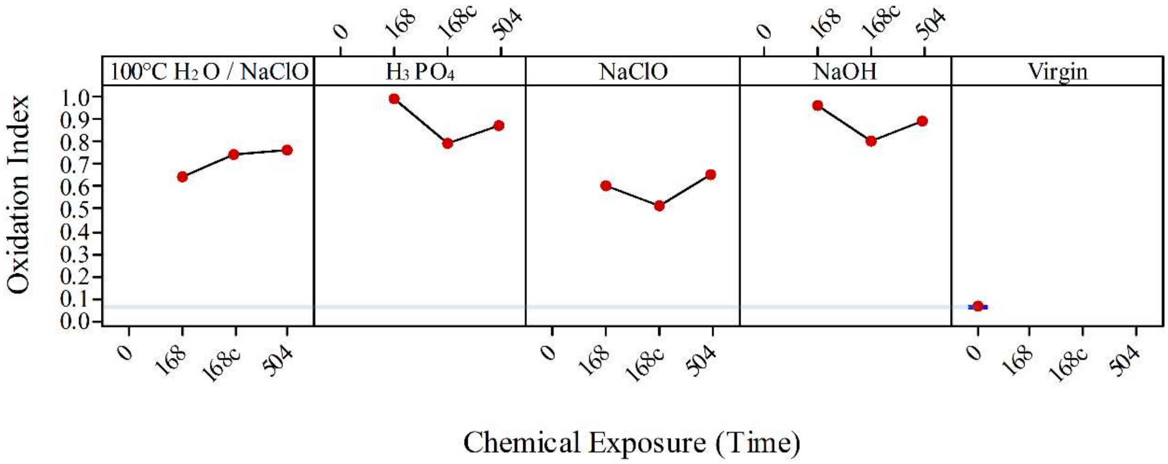

Figure 4.45: Scatterplot of oxidation index as a function of chemical exposure hours

For the NaOH, NaClO, and H_3PO_4 exposed samples, oxidation is reduced during compression. The 100°C H_2O / NaClO exposed samples have increased oxidative products during compression, which remains constant up to 504 hours' exposure, indicating no further damage to the material. For the NaClO exposed samples, 504 hours of exposure produces more oxidation than the 168 hour compressed samples. However, in the H_3PO_4 and NaOH exposed samples, the 504-hour exposure exhibits less oxidation products than the 168 hour exposed samples. As stated, this is not true of the NaClO samples, which shows continued oxidation with continued exposure.

4.8 Soxhlet extraction

4.8.1 Method

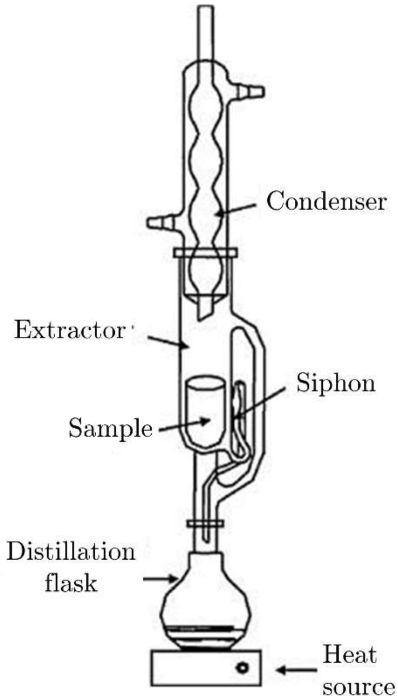

Soxhlet Extraction Setup	
Extraction Solvent	Pentane
Heat Source Temperature	55°C
Extraction Time	120 Hrs
Drying Temperature	40°C
Drying Time	To constant weight

Figure 4.46: Soxhlet extraction apparatus setup. Adapted from [119]

In order to evaluate the changing soluble fractions of the samples, Soxhlet extraction was employed. The soxhlet extraction setup and test parameters are shown in figure 4.46. Pentane was used as the extraction solvent to remove all non-polar substances, such as oil, plasticisers, and non-crosslinked polymer residues. The samples were then dried in a vacuum oven at 40ºC and were weighed until constant weight was achieved, meaning no further substantial amounts of solvent could be extracted. The mass of the samples was determined pre and post extraction using a calibrated analytical balance. After the soluble fraction was extracted, its chemical composition was characterised via FTIR-ATR as described in section 4.7.

4.8.2 Results

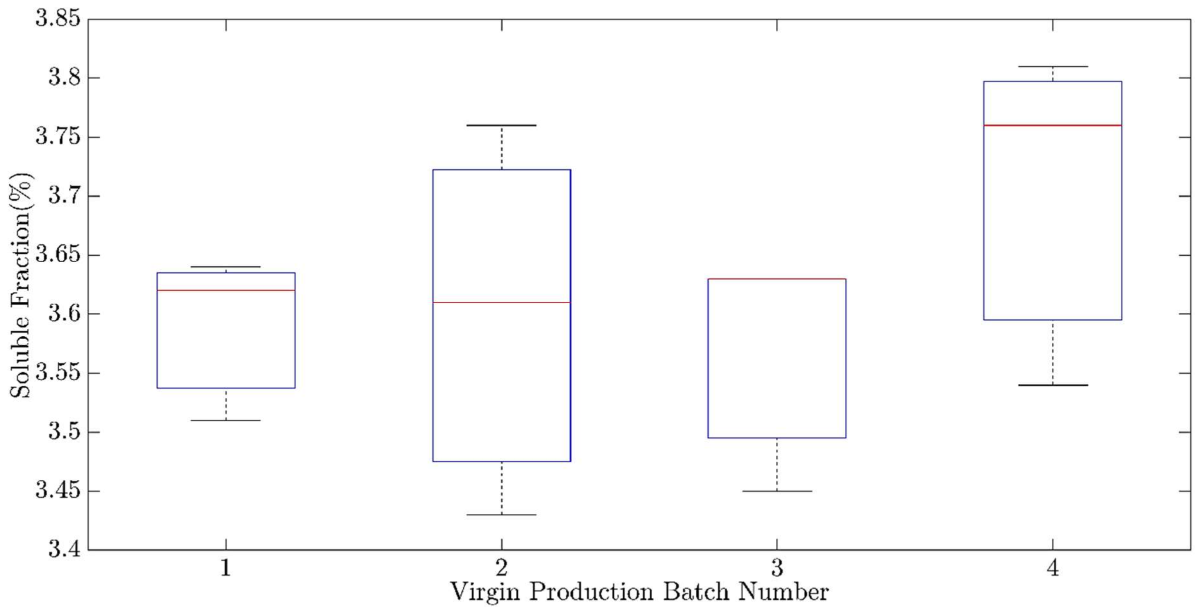

Figure 4.47: Soluble fraction of virgin samples as a function of production batch

As shown in figure 4.47 there is little difference in the soluble fractions of the virgin samples. Batch 4 either has slightly higher amounts of additives or slightly lower levels of vulcanisation leading to fewer initial crosslinks, but the difference is marginal.

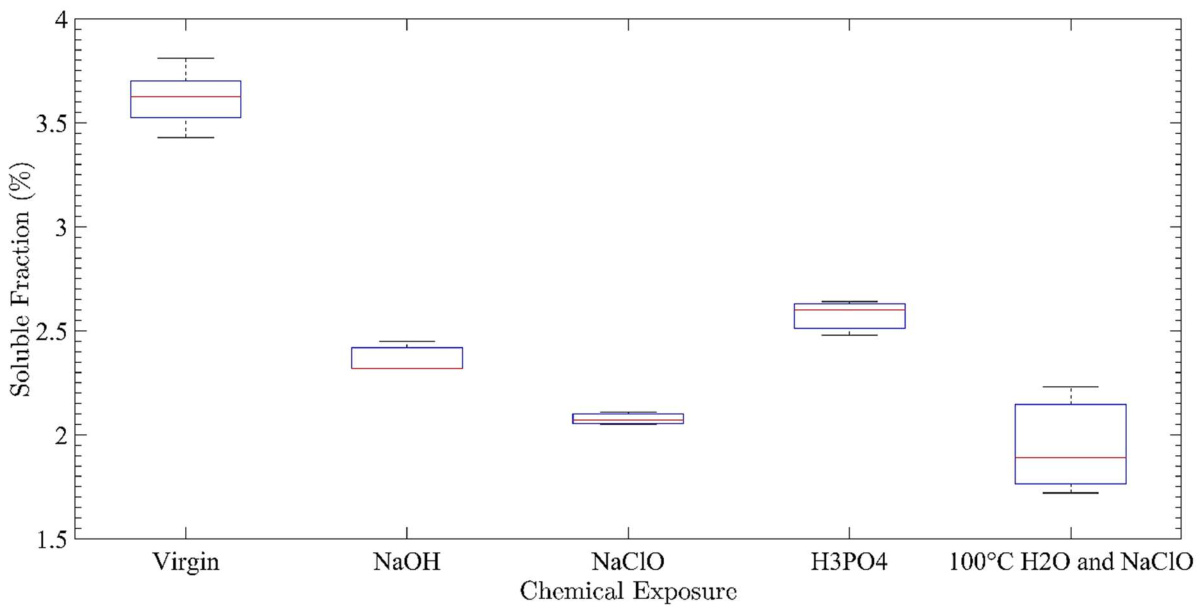

Figure 4.48: Soluble fraction of all samples as a function of chemical exposure

There is however a large decrease in the soluble fraction of the exposed samples in comparison to the virgin samples. The 100°C H_2O/NaClO exposure had the largest insoluble fraction, followed by the NaClO only exposure, both of which had greater insoluble fractions than either H_3PO_4 or NaOH.

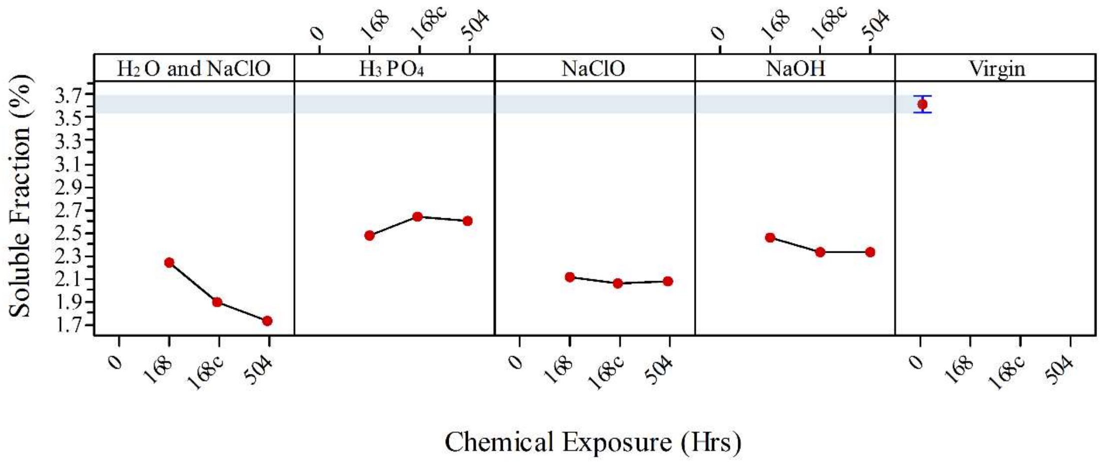

Figure 4.49: Soluble fraction as a function of exposure type and duration

Figure 4.49 shows that there is very little variation in the soluble fraction for all exposure types apart from the 100°C H_2O/NaClO exposed samples. This suggests that for this exposure type there is continued crosslinking and oil leaching due to material compression and due to continued exposure up to 504 hours. The H_3PO_4 exposed samples show a mild decrease in crosslinking and oil extraction due to both compression and continued exposure.

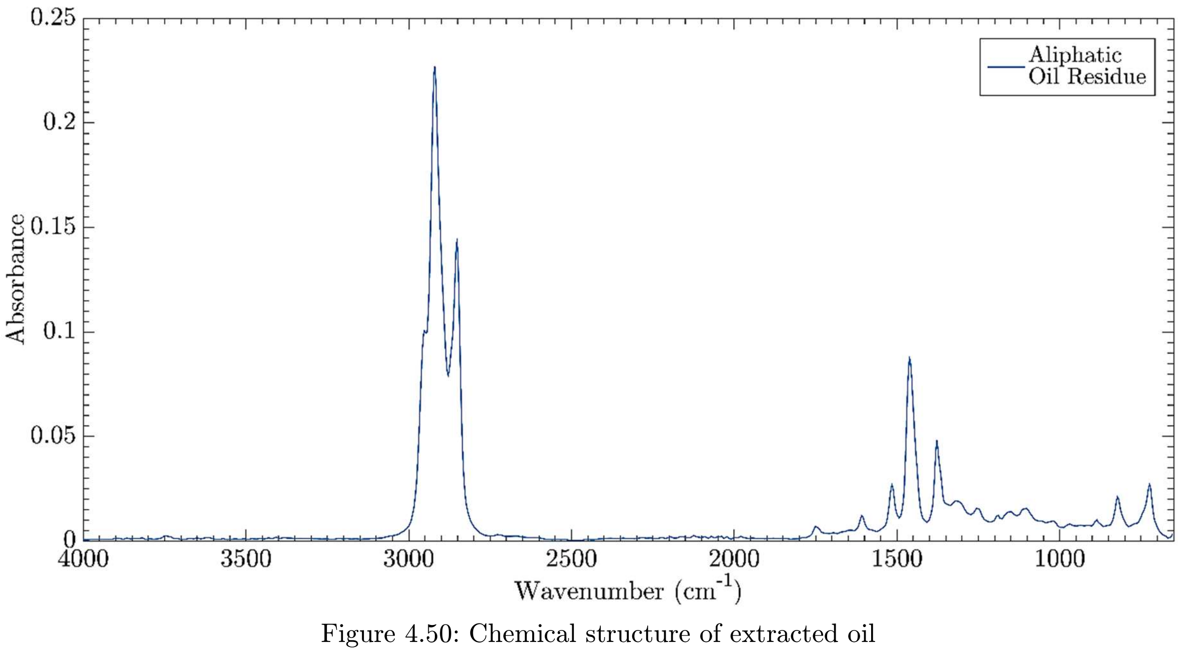

Figure 4.50: Chemical structure of extracted oil

As figure 4.50 shows, there are a considerable numbers of peaks from 650 to 1800cm^{-1} which constitute the bulk of the extracted oil. The oil was identified as an aliphatic hydrocarbon via the chemical matching database. The typical aliphatic hydrocarbon bands of the CH_3 and CH_2 groups are easily identified at 2952cm^{-1} and 2,921 cm^{-1} respectively [318].

4.9 Gas chromatography mass spectroscopy

4.9.1 Method

The oil residue extracted during Soxhlet extraction was identified as an aliphatic hydrocarbon. To confirm the chemical composition of the oil residue and to gain further insight into the exact type of oil being lost during chemical exposure, gas chromatography mass spectroscopy (GCMS) was utilised. GCMS separates the constituents of an analyte in a wound column according to the mass and volatility of those constituents. The wound column is held in an oven which in which controlled temperature increases gradually occur. As the oven temperature increases, those compounds that have low boiling points elute from the column sooner than those that have higher boiling points, aiding in component separation. As compounds are separated they enter a spectrometer which detects each individual constituent, from which a chromatogram is created. From the chromatogram, the chemical can be identified via reference to an online or offline database.

First, the EPDM samples were placed in a known quantity of the non-polar solvent pentane for 72 hours. Then, four parts of this solvent were mixed with one part of the internal standard solution and analysed in the GCMS.

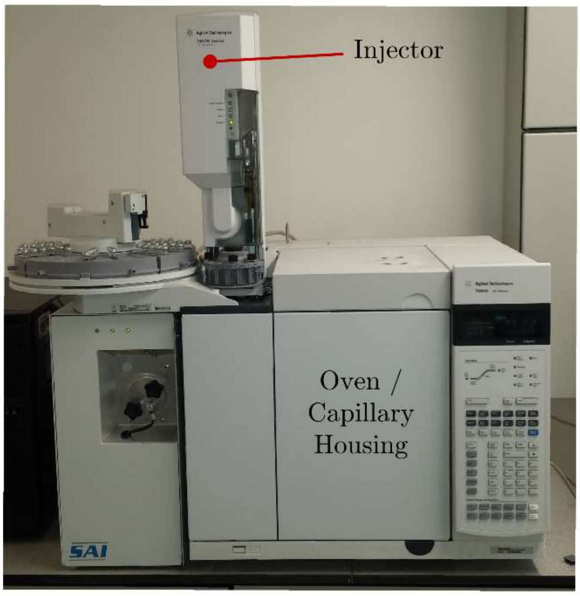

HP5890 Series II GCMS with HP Autosampler Extraction Sample Delivery System		
Injector Temperature	250°C	
Ion Source Temperature	270°C	
Oven Temperature	50°C	235°C
Hold Time	2 mins	5 mins
Oven Heating Rate	10°C/min	
Non-polar Solvent	Pentane	
Internal Standard	2-Nonanone	
Capillary Column Length	30 m	
Capillary Column Internal Diameter	0.25 mm	

Figure 4.51: Gas chromatography mass spectrometry test specifications

4.9.2 Results

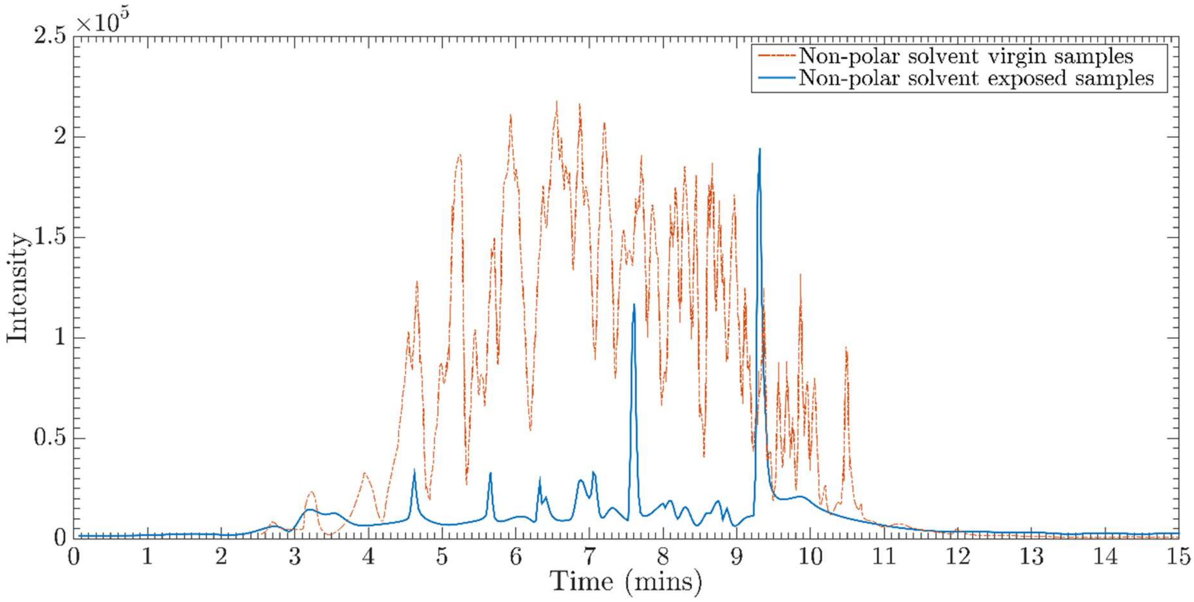

Figure 4.52: Chromatograph of non-polar solvent analyte pre and post chemical exposure

Figure 4.52 shows the chromatographs of the analytes extracted both pre and post chemical exposure. The virgin samples exhibit more peaks of a higher intensity than the exposed samples. This indicates that the exposed samples may have lost numerous additives due to their chemical exposures. The location of some of the major peaks are however consistent, indicating commonality between the extracted masses.

4.10 Discussion

4.10.1 Per test

In this work we consider two bases, NaOH and NaClO, and one acid, H_3PO_4. The main findings and the implications of the findings from each test performed are discussed in detail below.

Shore Hardness

Overall there was a clear increase in the hardness of all samples up to 168 hours exposure, therefore it is apparent that additional crosslinking has occurred in the exposed samples. The large increases seen in the hardness may indicate that severe brittle characteristics have been induced on the surface of the EPDM due to chemical exposure [88]. It is also apparent that chain scissions have occurred in the NaOH and H_3PO_4 exposed samples indicating an additional degradation type due to continued chemical exposure. This decrease in hardness can be attributed to chain scissions within the EPDM, as reported by Khan and Heinrich [319]. It is not clear if the reduced hardness due to compression may be as a result of less crosslinks forming due to compression, or as a result of chain scissions taking place due to compression. As the NaClO exposed samples do not show this behaviour, it is possible that crosslink saturation has occurred already at 168 hours of chemical exposure in the NaOH and H_3PO_4 exposed samples, indicating a higher rate of degradation due to these chemicals than NaClO. NaClO exposure on its own appears to have a continual crosslinking effect over time, although this effect may be minor.

Dynamic flexural testing

The cyclic compression testing signified that for both NaClO exposure types, additional crosslinking occurs in the material when they are compressed for 168 hours during exposure, in comparison to the non-compressed 168 hour exposed samples. The mechanism responsible for this behaviour may be that compression during exposure leads to higher molar mass phases developing in the material. Greater levels of higher molar mass phases and long chain branching results in more crosslinks developing under identical conditions in comparison to lower molar mass EPDM with lower levels of chain branching [94]. In these samples additional crosslinking continues up to 504 hours of exposure. Contrary to this, compression appears to have either inhibited crosslinking in the H_3PO_4 and NaOH exposed samples, or initiated chain scissioning. The rate of crosslinking may therefore be slower in both NaClO exposure types, meaning crosslink saturation has not occurred at 168 hours of exposure. In these samples crosslinking appears to have reached saturation at 168 hours, indicating that the rate of crosslinking is higher when the EPDM is exposed to H_3PO_4 and NaOH.

In the flexural modulus test, an increase in the elastic modulus was observed in all samples. There is a large decrease in the displacement of each sample before material yield is achieved. This suggests that the material has become more brittle and that the softness and the flexibility of the elastomer has been reduced [320]. An increase in the elastic modulus corresponds to the preponderance of crosslinking [106,314]. A strong increase in the modulus increases the stress level at given strain [314]. As the average values of fracture stress and modulus for the exposed samples are higher while sample displacement was reduced, this implies that exposure increases the crosslink density and reduces both the softness and the flexibility of the elastomer [73,320]. It is well known that crosslinking leads to a decrease in the elongation at break of elastomers, of which this can be considered an equivalent [73]. The elongation at break of an elastomer is therefore an indicator of the state of its degradation, with a reduction in elongation to 50% of its absolute considered as a failure criterion [73,80]. The exposed samples in this work had a reduction in elongation of approximately 10 to 15%, well below this figure. Despite this, degradation has occurred in the elastomer, as noted by the sharp rise in the elastic modulus.

Compression set testing

It is evident that the EPDM samples have lost elasticity due to chemical exposure, producing higher permanent set due to compression, or lack of spring back after the release of compressive force. It is known that the density of chemical crosslinks largely determines the elastic behaviour of EPDM. This is because physical network junctions are not efficient in bearing the applied forces during compression, therefore the force will be carried mainly by chemical crosslinks and trapped chain entanglements. Therefore an increase in the density of chemical crosslinks is required for improvement of the elastic recovery [321]. Most linear polymer molecules assume the shape of a coil which can be distorted upon application of mechanical stress. The factors affecting the response to mechanical stresses include molecular weight, chain composition and flexibility, degree of interchain attraction, degree of crosslinking and entanglement, presence of plasticisers, and the temperature at which the measurements are recorded. Upon applied stress, chain slippage occurs as a response to force and deformation on a supramolecular level. At the microscopic level, voids, cavitation, and crack formation take place along with large scale viscoelastic deformation [113]. As detailed in the literature, upon stretching of the EPDM matrix network breakdown occurs, the crosslink density decreases, and the network becomes looser [67].

While higher creep percentage indicates a loss of crosslink density, i.e. chain scission has occurred, the cause of the increased sample creep seen here may have a more complex mechanism. It is important to remember that the technique employed here measures macroscopic, or volume-average properties. However, as indicated by both the shore hardness and dynamic flexural testing results, crosslinking at the polymer surface has occurred creating a hardened layer. The creep results seen here indicate however that chain scissions have occurred in the polymer matrix, as creep is increased in the exposed samples in comparison to the virgin samples.

This contradictory information can be qualified by treating the hardened crosslinked layer as having created a sandwich, or composite, structure type in the samples whereby two different layers in the polymer exist with each layer having slightly different bulk properties. As seen with the dynamic flexural testing results, the flexural modulus of the exposed samples has increased due to crosslinking. However, under constant strain, the flexural modulus of the crosslinked layer may result in proportionally less strain being applied in the hardened layer, but instead the majority of the induced strain may be dissipated into the remainder of the unhardened, less crosslinked, polymer bulk. This would ultimately result in more compressive stress being induced in the bulk, initiating strain induced chain scissioning, worsening the 'sandwich' effect. This hypothesis would explain why compression set worsens due not only to chemical exposure, but also due to continued static strain, as the hardened polymer layer continues to affect the stress distribution within the polymer under longer durations of compression. Unfortunately, mechanical tests alone do not allow for the determination of these factors for compressive force [321]. It is also apparent that continued chemical exposure up to 504 hours and chemical exposure under compression for 168 hours has an impact on the EPDM, whereby creep under these conditions worsens due to H_3PO_4 and NaOH exposure, and improves under both types of NaClO exposure.

Dynamic mechanical thermal analysis

A shift in the glass transition temperatures to higher temperatures was noted, meaning the viscous contribution in the elastomer behaviour has decreased, a sign of crosslinking [87]. This result is confirmed by the magnitude increase of the storage modulus above the glass transition temperature towards the rubbery region. It is plausible that NaOH and H_3PO_4 exposure results in accelerated crosslinking in comparison to NaClO exposure. It is also possible that NaOH and H_3PO_4 exposure beyond 168 hours results in chain scission reactions, seen as a reduction in the glass transition temperature. Compressing the samples during exposure has varying effects on the different samples.

Thermogravimetric analysis

With increased thermal stability of a polymer blend, less relative weight loss of the polymer occurs in comparison to the carbon black and filler contents [115]. A reduction in weight loss of the polymer content in the 100°C H_2O exposed samples indicates that these samples have been affected due to their thermal exposure. The NaOH exposed samples may also have been thermally degraded, which is in accordance with the fact that the NaOH exposure is conducted at 65°C. This indicates that chemical temperature has an additional effect on the material. Material compression during the 100°C and 65°C exposures has increased the thermal degradation effect, whereas continued exposure past 168 hours non-compressed has not had as noteworthy an impact.

Fourier transform infrared spectroscopy

It is clear that there is oxidation occurring in the samples during exposure to the various chemicals, the degree of which varies modestly among the exposure types. The reason for the occurrence of the observed oxidation has been discussed by several authors. It is reported that radicals are first formed through the abstraction of tertiary hydrogen molecules which easily react with oxygen to produce polymeric peroxy radicals. These polymeric peroxy radicals then react further with one another to form ketones and many other types of oxidative products such as carboxylic acid, alcohols and ester [65,89,322]. It has been reported that aqueous chemical solutions attack the olefinic double bonds (C=C) bonds of the ENB diene and the presence of hydroxyl, carbonyl and carboxylic derivatives here justify this [94].

From the results obtained it can be concluded that NaOH and H_3PO_4 have a stronger oxidative effect compared to NaClO. It is possible that the rapid oxidation and hardening of the EPDM surfaces exposed to NaOH and H_3PO_4 suppressed the additional diffusion of oxygen molecules [88]. A similar phenomenon was also observed by Blackmore et al [76]. It is possible that oxidation saturation has already occurred in the H_3PO_4 and NaOH exposed samples at 168 hours. After 168 hours, the diffusion of oxygen molecules, which is confined to the top 1.5-2mm of EPDM composites, appears to decrease [88,105]. It has been reported that low pH acidic particles within EPDM rubber composites can promote the formation of oxidative products such as ketones. It is possible that the formation of oxidative products is accelerated within EPDM composites by extreme pH environments [65]. This could partly explain why H_3PO_4 and NaOH exposures have a stronger oxidative effect on the EPDM material.

This was not true of the NaClO exposed samples, which showed worsening oxidation with continued exposure. It is also apparent that the addition of 30 hours 100°C H_2O exposure in combination with NaClO exposure has had an additional oxidative effect. Compressing the samples during exposure reduced the oxidation levels for all samples except the 100°C H_2O/NaClO exposed samples.

Soxhlet Extraction

It can be seen that there is an increase in the crosslink density in the polymer matrix and that a substantial amount of additives and oil, ~62% on average, has been leached from the samples upon chemical exposure. It is possible that additional crosslinking in the polymer matrix may subsequently increase the polymer molar mass which in turn may lead to additive loss. It is also possible that the chemicals, particularly NaClO, have a solvent type effect on aliphatic oils in such a way that they leach the oil as a non-polar solvent would. This seems to be exacerbated when the samples are exposed to 100°C H_2O in addition to NaClO.

Whatever the mechanism, both loss of oil and an increase in crosslink density will have a negative impact on the functional characteristics and physical properties of the components. In agreement with other testing, it is apparent that there is continued crosslinking and oil leaching with compression and continued exposure to NaClO, though in this case just to 100°C H_2O/NaClO. Also, compression during H_3PO_4 exposure appears to lessen the leaching and crosslinking effects. There are several explanations for this. It is possible that NaClO has greater leaching ability than the other chemicals. It is also possible that there are more crosslinks in the NaClO exposed samples due to NaOH and H_3PO_4 having accelerated aging effects on the material, and that continued degradation due to these exposures has led to chain scissions after crosslinks were formed.

Gas chromatography mass spectroscopy

The peaks from 1 to 12 in both extracted samples, when compared to the internal reference, were identified as aliphatic straight chain hydrocarbon species from C_{10} to C_{32}. Aliphatic compounds are petroleum hydrocarbons that do not contain benzene rings [323]. As shown in figure 4.53, the number of candidate additive oils is large. It can be concluded that there has been a loss of this oil due to chemical exposure, in agreement with the Soxhlet extraction results.

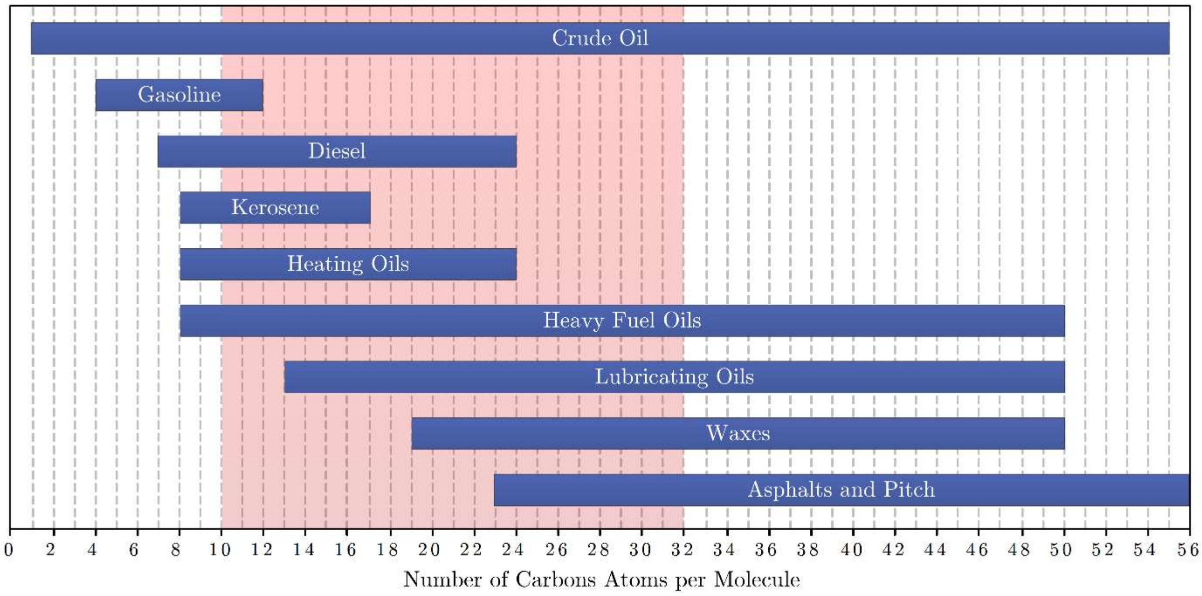

Figure 4.53: Petroleum fractions by carbon range. Adapted from [323].

4.10.2 Overall summary

It is clear from the results discussed above that there is an overwhelming body of evidence to suggest that the virgin EPDM, upon chemical exposure regardless of exposure condition, degrades primarily due to the formation of new crosslinks in the top 1.5 to 2mm. Knowing that crosslinking is the dominant degradation mechanism, it is important to observe the difference between the amount of crosslinking present in the 168 hour exposed non-compressed samples, and those exposed for 504 hours and 168 hours in a compressed state. Therefore observing the difference in degradation mechanisms among the different exposure conditions is a more important consideration than observing the difference in crosslinking between the different exposure conditions and the virgin samples. The difference among exposure conditions informs us how the degradation mechanisms evolves depending on exposure condition / duration.

The results from all tests regarding the additional affect that compression during exposure and continued exposure had on the EPDM material (in comparison to 168-hours of non-compressed chemical exposure) are summarised and visually represented in table 4.4 below. For every test in the discussion above, if the evidence from that test alluded to a further increase in crosslink density in comparison to the 168-hour non-compressed exposure, then the test is represented by a black dot. Conversely, if the evidence from that test alluded to a decrease in crosslink density in comparison to the 168-hour non-compressed exposure, then the test was represented by a white dot. An X was used if the result from the test showed no difference.

Table 4.4: Summary of results of all tests. Comparisons to 168 hour non-compressed exposure

Test	NaOH		NaClO		H_3PO_4		100°C H_2O/NaClO	
	504	*168_C*	*504*	*168_C*	*504*	*168_C*	*504*	*168_C*
Shore hardness	○	○	●	●	○	○	X	●
Cyclic compression testing (Work to max. compression)	X	X	●	X	○	○	X	●
Cyclic compression testing (Force at max. compression)	X	○	●	●	X	○	●	●
Flexural modulus testing (Displacement at max. load)	○	○	●	●	X	X	X	X
Flexural modulus testing (Flexural modulus)	X	X	●	●	X	X	●	●
Compression set testing (Creep at 24 hours)	X	X	X	●	○	○	X	X
Compression set testing (Creep at 84 hours)	○	○	●	●	○	○	X	●
Compression set testing (Creep at 168 hours)	○	○	●	●	○	○	●	●
Dynamic mechanical thermal analysis (Glass transition temperature)	○	○	●	●	○	○	●	●
Fourier transform infrared spectroscopy (Oxidation index)	○	○	●	○	○	○	●	●
Soxhlet extraction (Soluble fraction)	○	○	X	X	○	○	●	●

Increase in crosslink density ● Decrease in crosslink density ○ No change in crosslink density X

As shown in in table 4.4, there is very good agreement among the different tests as to the degradation mechanisms involved and their evolution during the different exposure conditions. There is strong agreement among the tests that continued NaClO exposure beyond 168 hours results in increased crosslink formation, and that continued NaOH and H_3PO_4 exposure results in chain scissioning. Similarly, exposure during compression has the same impact with these chemicals, showing good agreement in all tests. The fact that compressed exposure shows the same trend as the continued long exposure indicates compression accelerates the underlying degradation mechanism. This could be a significant contributor to environmental stress cracking.

Mitra et al [94] and Nandakumar and Kurian [95] both report that in the presence of aqueous acid solution crosslink density of EPDM blends decreases up to 7 weeks exposure, and upon further ageing the crosslink density rapidly increases up to 15 weeks exposure. The main findings of this work appear initially to be in contrast to that of Mitra et al and Nandakumar and Kurian, whereby it can be concluded from the gathered evidence that crosslink density off all samples increases up to 168 hours, or 7 days, exposure time. However, the different chemicals under investigation coupled with the reduced exposure times in this work, which much more closely match real world conditions for biopharmaceutical applications, compliments the work of previous authors. For example, the evidence suggests that upon continued exposure up to 504 hours, or 21 days, both NaOH and H_3PO_4 exposure then results in chain scission reactions, in agreement with those authors. It is plausible that different acids and bases, particularly at different temperatures, have different effects on EPDM composites. However, it is apparent that the NaClO exposed samples continually form new crosslinks upon continued exposure, with no evidence of chain scission. This is evidence that NaOH and H_3PO_4 exposure results in an accelerated rate of crosslinking than NaClO in the early stages of exposure, thereby potentially degrading the EPDM material worse in relation to industrial exposure durations and practical applications. The effects due the chemical exposures seen in each test is discussed in detail below.

To visualise the overall impact that each chemical exposure had, again in reference to the 168 hour non-compressed exposure, the result of each test as described in table 4.4 was assigned a numeric value. If the result indicates an increase in crosslink density, then the test outcome is assigned a value of 1. If the result indicates a decrease in crosslink density, then the test outcome is assigned a value of -1. If the result indicates no change in crosslink density, then the test outcome is assigned a value of 0. The overall results for each exposure type were then averaged, to see if the accumulated evidence signifies an increase or a decrease in the crosslink density due to that chemical exposure duration and type. For example, if the calculated average for an exposure type is greater than 0.0, the evidence suggests that this exposure results in increased crosslink density. If the calculated average is below 0.0, the evidence suggests that this exposure results in decreased crosslink density. The results are illustrated in figure 4.54 below.

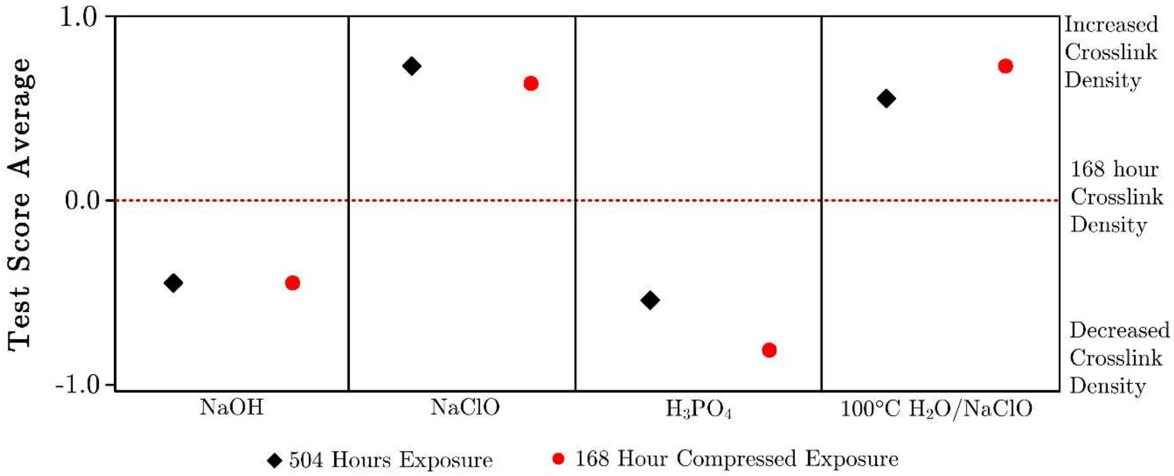

Figure 4.54: Average evidence test scores for chemical exposure type and duration

As shown in table 4.4 and figure 4.54, the accumulated evidence from all tests indicates that NaOH exposure during material compression, and upon continued exposure up to 504 hours, results in a decrease of the crosslink density. Similarly, H_3PO_4 exposure beyond 168 hours up to 504 hours results in a decrease in crosslink density, as does compressing the material during exposure. Material compression during exposure has a crosslink reduction effect in the H_3PO_4 exposed samples. This decrease may be due to the initiation of chain scission reactions occurring after 168-hours of non-compressed exposure. Conversely, evidence from all tests suggests that NaClO exposure results in increased crosslink density due to exposure during compression and continued exposure up to 504 hours. Compression during 100°C H_2O/NaClO exposure has a stronger crosslinking effect than NaClO exposure alone. This is evidence that 100°C H_2O exposure has an additional degradative impact on the EPDM.

The mechanism responsible for crosslink formation is likely due to carboxylate (O=C-C) and hydroxyl (O-H) group formation. Both of these group formations are evident in the FTIR-ATR spectra. These formed oxygenated species plausibly combine, resulting in crosslinking through ester formation by reaction between C-O-O-H and O-H groups, and/or ether (C-O-C) formation through self-condensation of the O-H groups [92,94]. The reason for different crosslink densities, potentially due to chain scission having occurred, can be explained as follows. In a vulcanised rubber matrix, a mixture of different types of crosslinks are formed, for example poly, di, and mono-sulphidic bonds. In a chemical environment, poly-sulphidic bonds may undergo hydrolysis faster than di-sulphidic and mono-sulphidic linkages. The different rates of hydrolysis for the different kinds of crosslinks due to chemical degradation would change the crosslink density over time depending on the initial types of crosslinks present [95]. It is therefore possible that NaOH and H_3PO_4 exposure results in poly-sulphidic bond creation, whereas NaClO exposure may result in di or mono-sulphidic bonding. It has been reported that the degradation in an aqueous acidic environment initiates at the weakest links of the polymer matrix, and propagates from there [8].

In addition to crosslink formation, it is apparent that loss of plasticiser and thermo-oxidative degradation mechanisms are also partly responsible for the reduction in desirable mechanical properties. The interaction effects due to these mechanisms may be very complex to model from a first principles perspective. However, an understanding of these effects offers a potential for condition based monitoring to be developed for this application.

According to Kwak and Choi [88] and Mitra et al [92], degradation of the EPDM surface alone is found to be enough to affect the macroscopic behaviour of EPDM to a considerable extent. Also, Pourmand et al [105] showed that after approximately 1.5mm depth, EPDM oxidation markers from degradation returns to virgin sample levels, i.e., no further degradation occurs at deeper levels. This same mechanism can be explained here, whereby a hardened surface layer has impacted the bulk mechanical properties, a theory corroborated by the compression set testing results. Given that the surface of the EPDM diaphragms is degraded due to crosslinking, the tear strength of the diaphragms will also be reduced, as tear strength reduces with increasing crosslink density [99]. This phenomenon may be a contributory factor in relation to sudden material cracking.

In conclusion, it is apparent that each of these four variables has an impact on the degradation of the EPDM diaphragms, and each should be included in a model describing diaphragm lifetime. Modelling these variables may be challenging however, as given the lack of other data sources relating to them appropriate parameters may be difficult to calculate. While beyond the scope of this work, an appropriate solution may be to initially use modest, best guess estimates of the degradation parameters, and model the degradation for example within a Bayesian framework, or some other suitable method which updates the model over time as new evidence becomes available.

Chapter 5

Consideration of human factors contributing to component degradation

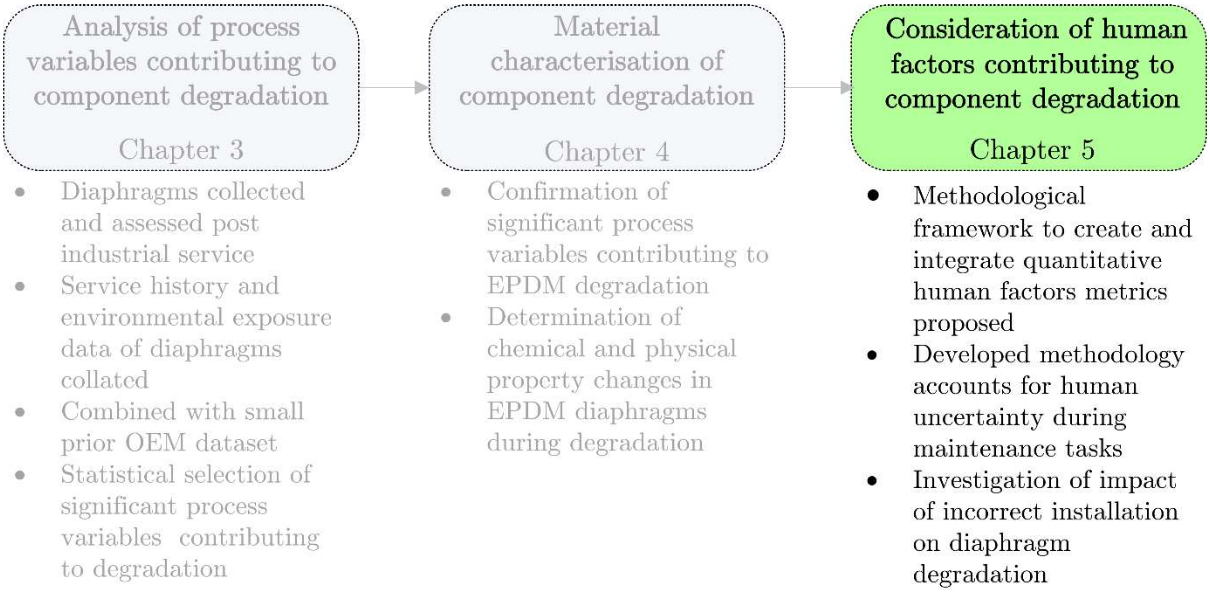

5.1 Introduction and research rationale

This section of the work investigates human error during valve maintenance activities as one variable contributing to component failure events, and explores how such human errors can be accounted for within the reliability modelling process. Existing reliability modelling approaches lack any real methodologies to take account of human maintenance actions in predicting system failure probability. One drawback of many modern modelling approaches therefore is the over-reliance on machine related data, which does not describe the full set of operating conditions in which systems are operating.

The hypothesis is that including HOF metrics derived from the PSFs influencing the maintenance task can reduce the predictive uncertainty of the developed model, provided that the PSFs are found to be significant predictors of the failure event.

In relation to the industrial case study, over-tightening of the valve bolts during torqueing procedures after diaphragm installation is investigated as a root cause of diaphragm cracking. In chapter 4 it was shown how different bolt torques leads to large variation in the force required to actuate the diaphragms. Therefore, this failure mode is investigated further via a study on the effects of incorrect installation practices on the probability of a diaphragm developing a crack in service. It is hypothesised that incorrect valve torqueing is caused partly due valve access difficulty encountered by maintenance technicians during service. This factor is show in figure 5.1. This would allow for individual components or sections of a system to have different instantaneous hazard rates as a direct result of differing PSFs that may exist.

Following from this, the scope and objectives of this section are to:

1. define a methodological framework for the elicitation and quantitation of HOFs
2. demonstrate the developed methodology within the industrial case study
3. demonstrate the integration of significant PSFs alongside process related data sources to derive parametric models of diaphragm lifetime

This work does not constitute a full human factors study, rather the presented methodological framework is limited to simply allowing the elicitation of HOFs as quantitative covariates which could then be used in a prognostic model. As such, human performance modelling is not investigated.

There are several areas of novelty regarding this approach. Other authors, in particular Kiassat et al [149,154,246–248], consider the case of industrial operators who are in constant manual contact with production equipment, and provide no framework for quantifying a HOF metric [246], while this work considers the case of maintenance personal who have intermittent offline access only to the systems and present a clear methodological approach for HOF quantification. Kiassat et al also focus mainly on how operator skill, education level, and social skills change as new operators initially enter an organisation and continuously manually interact with production equipment. They observe how with increased operator experience, equipment productivity is increased [149]. This work focuses on HOFs specifically relating to offline maintenance activities, and critically considers the case where operator skill level is assumed to be consistent and stable across maintenance teams, and thereby does not significantly impact equipment reliability.

In this scenario, one must consider a broader approach to the inclusion of HOFs, therefore this work acts as an extension to those developed models and aims to help bridge the research gap with the presented framework. As a point of clarity, this assumption was driven by the case study, and not the methodology, as records of which individual technician installed which valve wasn't available. However, if such data were available, the methodology could easily extend to including such individual factors.

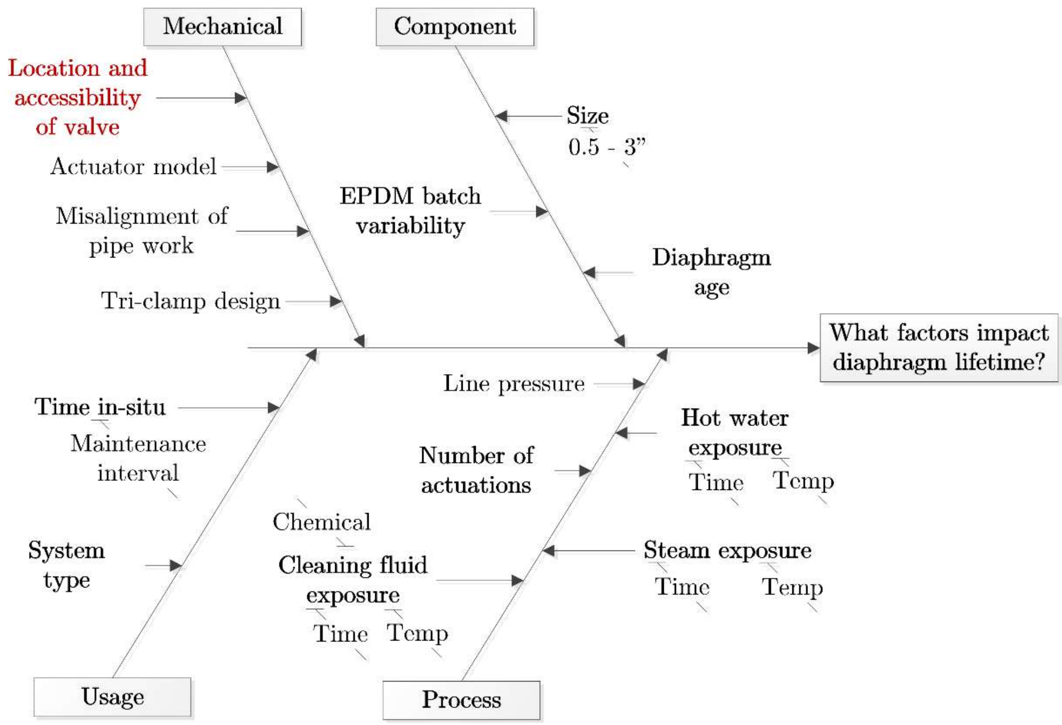

Figure 5.1: Brainstorm of factors contributing to component degradation

The methodology outlined here is intended to provide a framework for maintenance decision makers to identify, assess, and encode any HOFs potentially impacting component reliability into a quantitative covariate for use in system lifetime estimation models. The full procedure is outlined in figure 5.2.

1. If it is suspected that during a maintenance task a HOF influences the ability of the maintenance technicians to effectively complete a maintenance action, and therefore impact system lifetime, a full procedural task analysis (PTA) must be completed
2. The PTA must then be reviewed and corroborated by a task expert, who is asked to identify the critical task(s). These are the steps identified as being the most significant in terms of component reliability, such that an incorrect maintenance action here is likely to have an undue effect on compononet lifetime
3. Using the THERP classification, or another appropriate list of PSFs, all PSFs related to the entire PTA are identified
4. Of that full PSF list, those that are not measurable are excluded from further analysis. The reason for non-measurability might be that particular records are not kept, or that there are legal or practical reasons why it is not possible to measure a particular metric. For example the measurement of a persons ability to complete a task. If the HOF is considered to be potentially significant, procedures may be put in place to gather the required information for future model development.
5. From the measurable PSFs, select those that have the greatest potential influence on the critical maintenance steps. This elicitation can be conducted via interviewing appropriate subject matter experts
6. With the filtered PSF list, identify those that are directly measureable and those that are not. If the metric is directly measurable, continue to step 8. Otherwise continue to step 7
7. A proxy measurement must be created in order to measure the PSF. It is recommended to use a scale which uses 'anchor points' describing PSF severity at intervals along the scale, as outlined in the work of Baraldi et al [324]
8. Measure the PSF, either online or offline depending on the metric. Online measurements are typically time dependant, while offline are time independent
9. Combine the PSF metric with historic failure data or with indices of component health, such as CBM measurements in a database
10. Using the combination of failure data and the PSF metric, determine the significance of the PSF metric. The final modelling choice related to significance determination should be left individual experts working on a particular case study, and is dependant on the context of the case study. Therefore, there is no definitive recommendation made here as to model selection
11. If the PSF is significant, it can be immediately utilised in a covariate driven reliability model developed for the system, such as a Weibull proportional hazards model. If not, continue to step 12
12. System walkdowns and interviews with subject matter experts should be conducted in order to determine if all procedures are being adhered to during maintenance tasks. PSFs can only work in a system degradation model if there is consistent compliance with SOPs
13. If there are issues with non-compliance, then staff retraining should be initiated to ensure future compliance and understanding of maintenance procedures
14. If there are no issues with task compliance, then the maintenance decision maker has two options:
    a. proceed to develop the model without including HOF metrics
    b. re-evaluate the system reliability and the assumption that HOFs have an impact on system lifetime

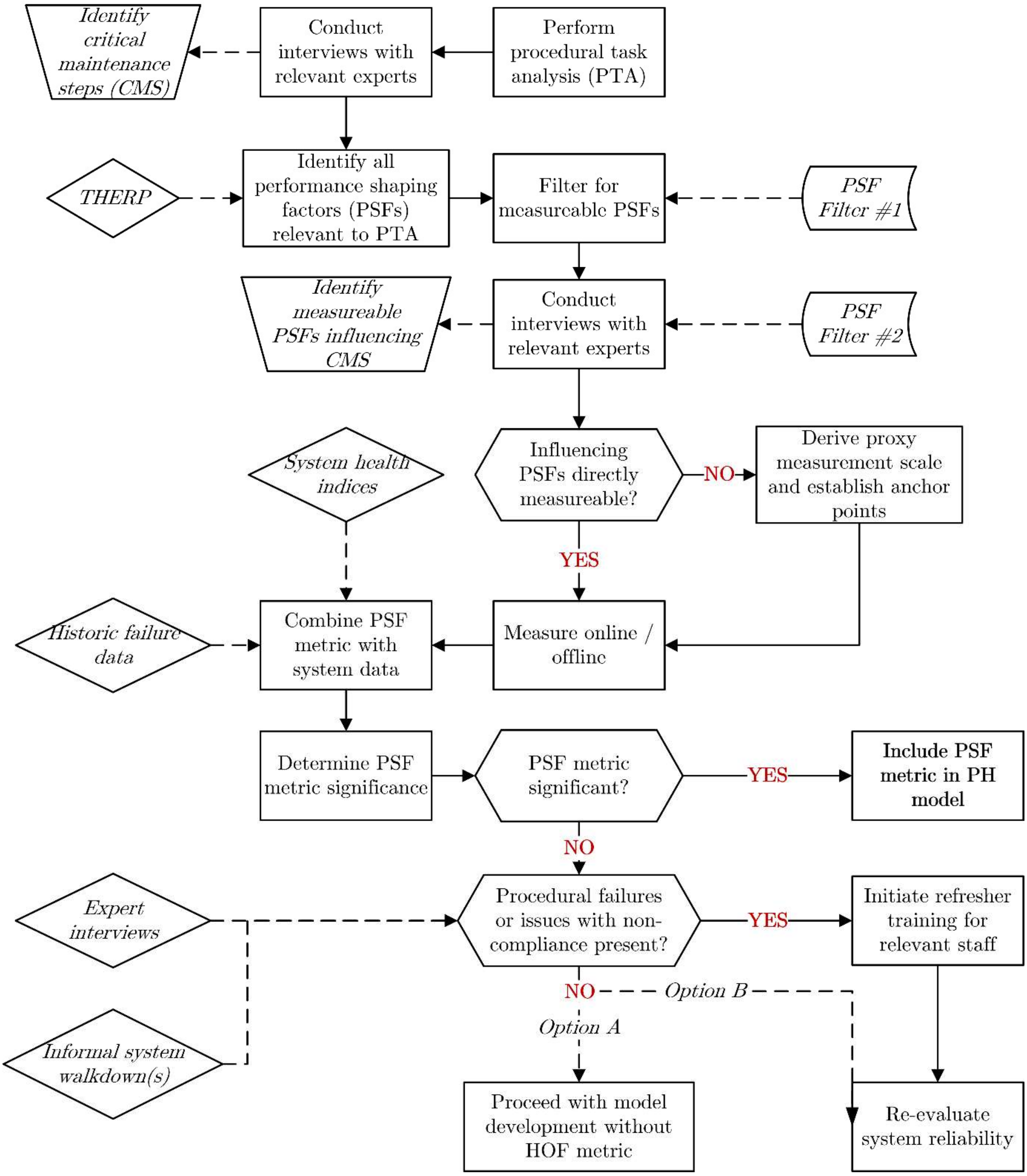

Figure 5.2: Full methodological framework for the inclusion of HOFs in Weibull distributed proportional hazards lifetime models

5.1.1 Determination of PSF metric significance

The method used to determine covariate significance in relation to failure events is the same filter and wrapper binomial logistic regression approach outlined in chapter 3.

5.1.2 Covariate parameter likelihood estimation

For the estimation of the covariate parameters, the maximum likelihood estimation method is utilised which is discussed in chapter 2.

5.2 Application of developed methodology within industrial case study

5.2.1 The Role of Maintainer Competence

The organisation involved in this research has previously identified maintenance technician competence as a key area for improvement in order to improve valve elastomer reliability. After investigating specific issues observed in the field, believed to be responsible for high infant mortality rates of the diaphragms due to EPDM cracking, multiple root causes for leaking valves were identified as elastomer failures from actuator, fastener, and installation issues. Following this, an optimised maintenance technician training program was designed and implemented. The revised diaphragm installation training scheme was introduced in an attempt to reduce errors and thereby reduce the variability of random failure events. The previous training had not been revised for several years prior. The revised training focused on the following:

- inappropriate tooling and maintenance practices, specifying in detail all components and auxiliary equipment to be used
- revised and detailed flow diagrams of the work to be carried out in a step-wise fashion
- valve and elastomer design issues, previously resulting in valve failures, addressed via the introduction of new designs in conjunction with valve suppliers
- fastener replacement initiated site-wide

The responsibility of updating the maintenance training material on a bi-annual basis and communication of any changes made was handed over to maintenance technicians ensuring the ownership of the training material. Subsequent data showed an improvement in key metrics with failure and infant mortality rates more closely matching data from valve supplier led laboratory-based testing, specifically:

1.

- a reduction of corrective maintenance actions per batch by ~25%
- a ~35% reduction in investigations related to damaged diaphragms and leaking valves
- a ~270% increase in the number of successful batches with no quality investigations needed
- a 95% batch success rate even at increased production rates
- a reduced maintenance cost per batch
- a ~12% decrease in potential batch contamination issues

Despite the promising results from the pilot study, there was scope for further improvements due to the continued observance of sudden early stage random cracking failures of the components in service. The increase in component reliability due to increased maintenance technician training and investment partly led to the investigation explored here; whether further HOFs were responsible for reduced service life and unexpected failures. This work therefore explores the PSFs that may influence accurate and reliable completion of diaphragm installation procedures.

It was critical to assess the difficulty of valve installation, as incorrect assembly and tightening of the actuator, diaphragm, and valve body is reported as being one of the main reasons for failure and leakage of diaphragm valves [302]. The valve assembly requires four bolts to be tightened to specific values, depending on valve size, in a crisscross pattern over three passes. If one or more bolts are torqued to a greater value than the others, the clamping force will be unevenly distributed over the diaphragm. Critically, this can result in uneven forces on the diaphragm, leading to premature and unforeseen cracking of the diaphragm, most likely due to uneven stress distributions within the EPDM [302].

In line with the developed methodology, a full PTA of the installation process was conducted. As the author was based fulltime in the biopharmaceutical company for the duration of the research, it was possible to employ an ethnographic approach to data collection [325]. Participant observation was used to gain a detailed understanding of the context and specific issues associated with the valve installation and this was formalised in the PTA. The PTA was validated with senior engineers in the organisation in order to identify the critical process steps. The next task was to identify the PSFs that may influence these critical tasks. A review of PSFs in THERP [229] was undertaken and the contextually relevant PSFs were identified. These were then used to develop a semi-structured interview format. The interviews were designed to identify the factors that increase the difficulty of component installation, and to develop an installation difficulty metric which could be applied to each component in the study. The full PTA is shown in figure 5.3.

Table 5.1: Plant data summary

Crack	0	1	Total
Degradation State			
1	72	6	78
2	21	4	25
3	1	3	4
Total	94	13	107

Logically, the developed methodology could only be applied to those valves within the industrial organisation. Therefore, the relevant dataset to use was the data exclusively retrieved from the plant itself. The breakdown of the samples retrieved from service after industrial usage of between 6 and 24 months in this case study is shown in table 5.1. As shown, there are examples of cracking in each of the three degradation states, validating the need to treat the cracking failure mode separately.

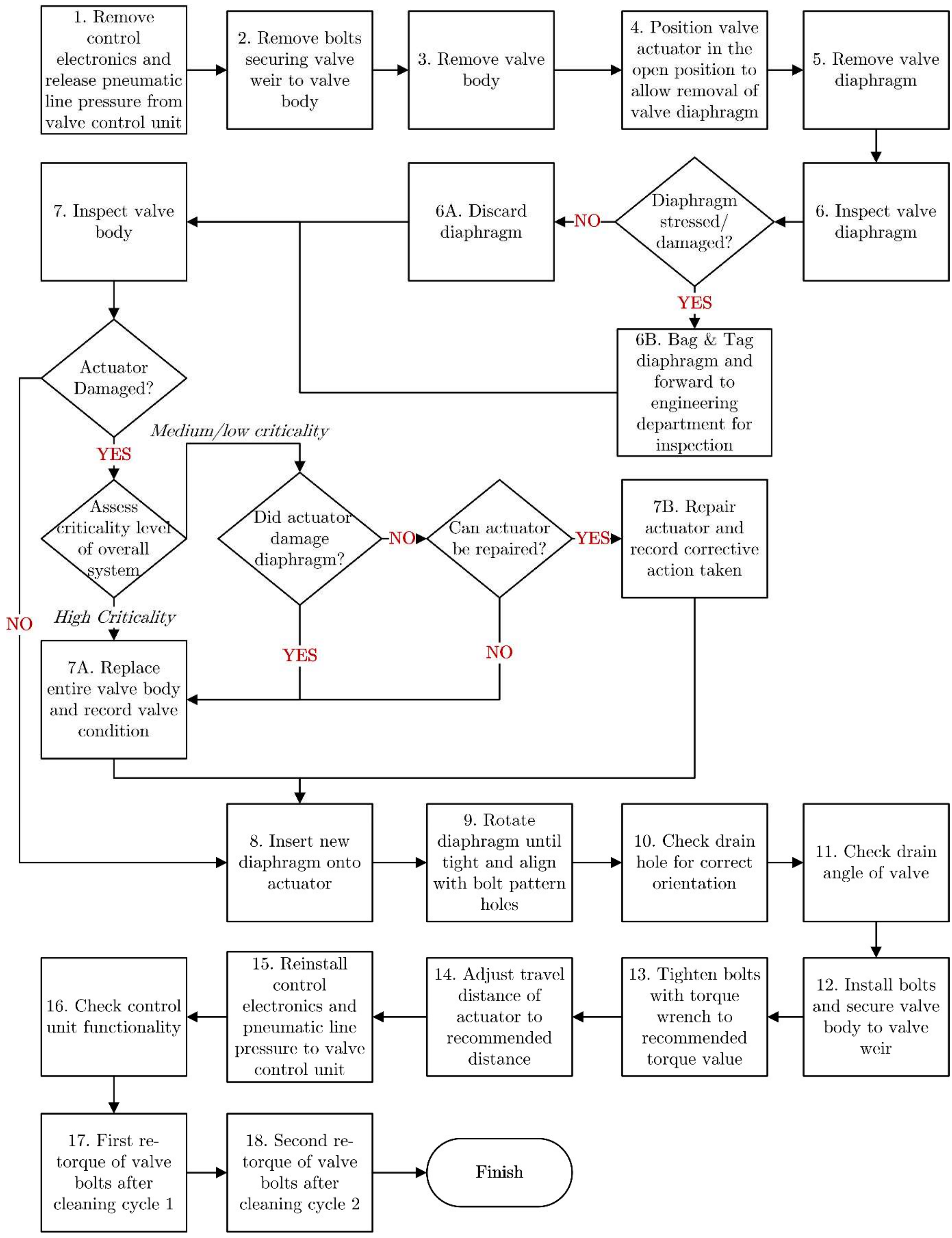

Figure 5.3: Full procedural task analysis of component installation

5.2.2 Identification of performance shaping factors

A review of external PSFs in THERP [229] was undertaken to identify those PSFs that may be relevant to the valve installation task. THERP was used as it contains the most comprehensive set of performance shaping factors among the numerous human reliability analysis methods. The following PSFs were identified as relevant to this case study:

- Quality of the environment, e.g. temperature, humidity, lighting, noise
- Work hours / work breaks
- Availability / adequacy of special equipment, tools, supplies
- Frequency and repetitiveness of tasks
- Task speed
- Task load
- Distractions
- Fatigue
- Movement constriction
- State of current practice or skill

Some of these PSFs had to be disregarded, as it was not possible in this study to identify individual technicians or collect data on their individual state while installing the specific valves used in the case study, as this work was completed before the research started and accurate records were not available. This corresponded to the PSF filtering stage 1. Therefore, work hours, task load, distractions, and fatigue were not further investigated. The remaining PSFs were investigated in more detail in a set of interviews with the technicians responsible for the installation task.

5.2.3 **Technician Interviews**

The basic structure of the interview centred on the following questions, however the interview was structured in a semi-formal manner to help elicit a more natural response from the interviewee:

- What makes maintenance process more difficult from a technician's perspective?
- Could any of the valve components become damaged during installation or maintenance?
- In what ways can a diaphragm be installed incorrectly?
- How much does each of the following factors increase the risk of incorrect diaphragm installation, if at all?
    - Valve assembly complexity
    - Valve size
    - Procedural information for the valve
    - Accessibility of the installation location
    - Lighting in the installation location
    - Noise in the installation location
    - Distractions in the installation location
    - Technician experience level
    - Time available to perform the task
    - Time of day or night

The conclusions reached from the interview was that the enhanced training programs have largely eliminated many of the human factors issued previously encountered, such as procedural information errors, incorrect installation practices, and time pressure issues. However, the interviews with the technicians revealed two key PSFs acting as limiting factors in the successful installation and maintenance of the valve diaphragms. These were the accessibility of the valve location, and the size of the valves. The accessibility was important as this affected the technician's ability to manoeuvre either their bodies or the tooling into the correct position. For example, if the valve is located at height, or behind a bank of pipework, or in a tight crawl space, the ability of the technicians to apply the correct torque values with an appropriate torque wrench to the valve bolts is diminished. Similarly, the size of the valves, with diaphragms ranging from 25mm to 100mm, has the effect of making it more difficult to install if the valve is smaller, due to smaller auxiliary components such as bolts which are more difficult to handle. The technicians felt however that the valve size would have only a minor impact in comparison to valve accessibility. The difficulties posed to maintenance technicians in accessing the valves due to the valve location is illustrated in figure 5.4.

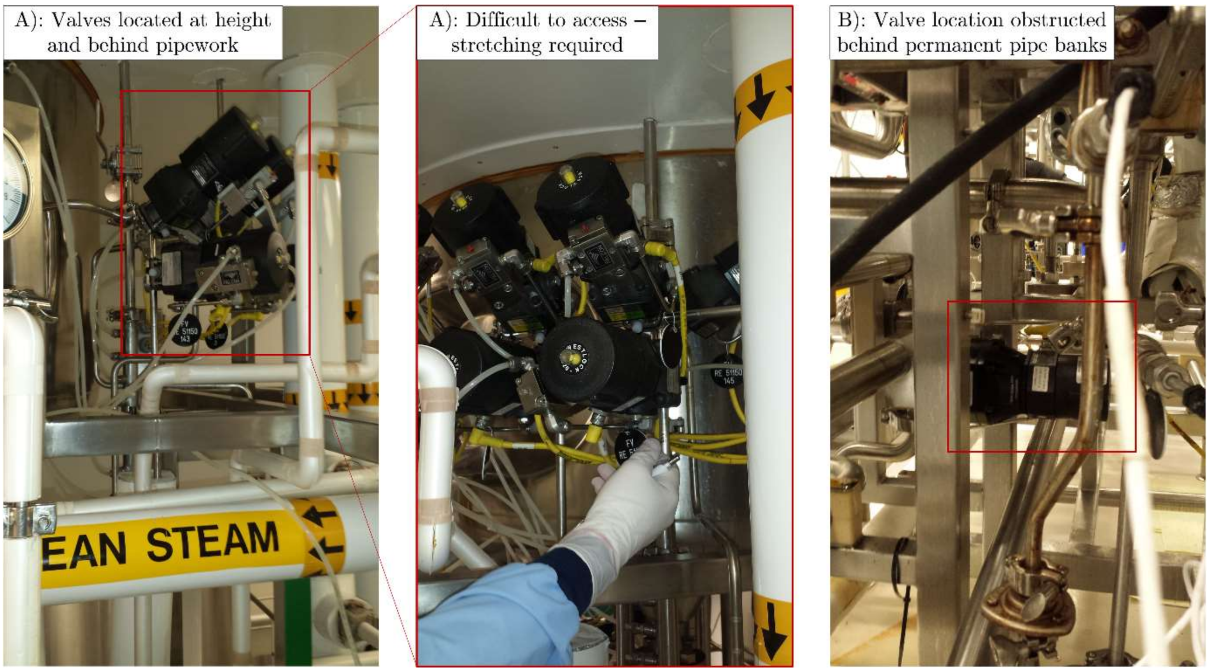

Figure 5.4: Access difficulty of valve locations

Figure 5.4 A) shows a group of valves at height and behind steam line pipework. Due to these factors and the tight grouping of the valves it is difficult to access each of the components adequately with the requisite tooling, in particular the fastener bolts with torque wrenches. This means sub-optimal methods of fastener tightening must be applied, which may have an impact on diaphragm reliability. Figure 5.4 B) illustrates a similar issue, this time with a single valve located behind sterile stainless steel production lines. As these lines cannot be dismantled once the system is operational, valve access is again extremely limited. A human technician would be required to crawl into an appropriate space and then stretch to access the individual valve components. Again, it is believed that sub-optimal maintenance practices here would limit the reliability of the valve components due to inadequate installation methods employed.

When it is not possible to use a torque wrench to apply the correct torque to the valve bolts, many maintenance technicians were observed and reported using older, outdated installation procedures, in particular, a method known as the 'bulge technique'. This entails tightening the valve bolts until the EPDM material deforms and flows from the weir due to being compressed. This method is no longer recommended by the valve OEM due to the stress induced in the diaphragm. An example of a diaphragm tightened using this method is shown below in figure 5.5.

Figure 5.5: EPDM diaphragm 'bulging' due to over-torqueing

5.2.4 Incorrect installation testing

In order to validate the conclusions from the maintenance technicians and that of Ohlsson [302], a maintenance installation testing procedure was designed and implemented. This involved purposefully incorrectly installing several diaphragms into an experimental test rig designed to mimic biopharmaceutical conditions, and subjecting the diaphragms to real world exposure conditions in order to determine if incorrect installation had an effect on component lifetime. The testing procedure involved three scenarios:

1. Ten 25mm diaphragms installed correctly using the correct fastener torque of 7.9Nm
2. Ten 25mm diaphragms installed incorrectly using a mixture of correct fastener torque of 7.9Nm and an incorrect fastener torque of 22.6Nm. In this test, two fasteners are incorrectly torqued while the other two are correctly torqued. This creates an uneven torque profile in the diaphragms
3. Ten 25mm diaphragms installed incorrectly using an excess fastener torque of 22.6Nm

The test sequence for each torque setting is as follows:

1. Install new, unused diaphragm into actuator compressor
2. Torque new, unused bolts up to required value for test, over three passes
3. Open steam inlet valve until desired pressure of 1.05 barG reached in test rig
4. Actuate valve 10,000 times
5. Close steam inlet valve and drain system condensate
6. Remove diaphragm from actuator
7. Record diaphragm condition
8. Repeat test until 10 virgin diaphragms have been tested

The experimental test rig is shown below in figure 5.6.

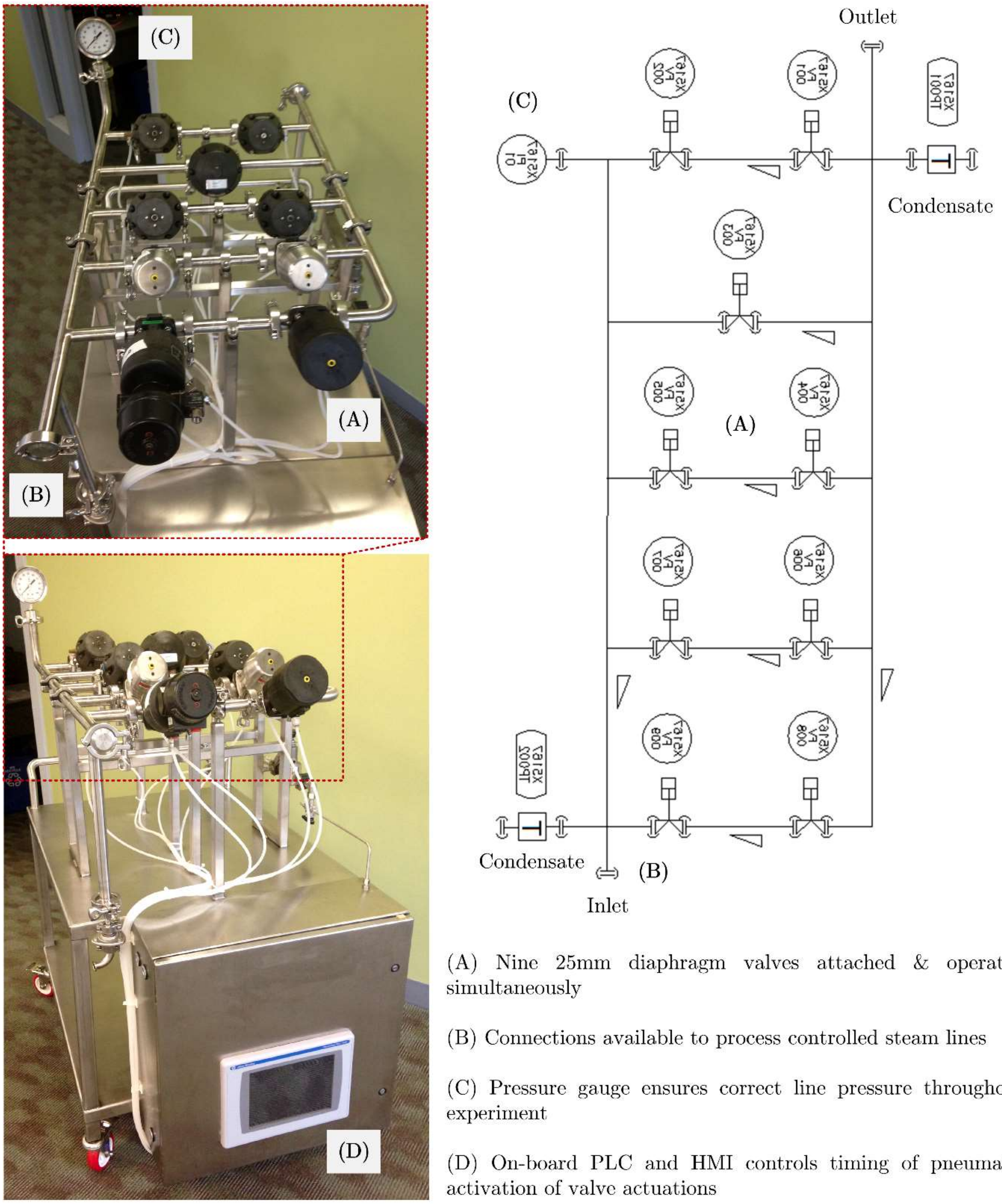

(A) Nine 25mm diaphragm valves attached & operated simultaneously

(B) Connections available to process controlled steam lines

(C) Pressure gauge ensures correct line pressure throughout experiment

(D) On-board PLC and HMI controls timing of pneumatic activation of valve actuations

Figure 5.6: Diaphragm testing rig used for installation torque testing

The following testing conditions were used in order to recreate industrial usage conditions

- Process fluid exposure: Saturated steam at 127°C
- Process fluid exposure duration: 300 min
- Component size: 25mm
- Fastener thread size: M8
- ‘Correct torque’ value: 7.9Nm
- ‘Excess torque’ value: 22.6Nm
- Number of actuations per test: 10,000

Each test used new diaphragms and fasteners to ensure independence of results. The 300-minute test duration corresponds to the average duration of a single steaming sterilisation procedure common in the industry. It was decided to expose the diaphragms to a steaming procedure during testing in order to expedite any damage which might occur due to the over-torqueing. A typical component will be exposed to an average of $30 - 40$ steaming cycles of similar duration during its service life, so the steaming cycle alone should not adversely negatively impact the diaphragms. 10,000 valve actuations corresponds to the average maximum number of actuations commonly seen during service life. This was again included to expedite any potential diaphragm damage. The diaphragms are rated up to 100,000 actuations during service life, so the test value alone should again not adversely affect the diaphragm state. The over-torque value of 22.6Nm was chosen as it was discovered, after multiple bench tests, to be consistently the lowest torque value required to initiate the material flow evident when using the bulge technique. Although it represents a torque value 2.86 times greater than the recommended OEM value of 7.9Nm, it was evident from walk-downs of the systems that this torque was still being applied to valves in certain locations.

Results

As shown in figure 5.7, all components which were correctly installed using a torque value of 7.9Nm were still in degradation state 1 post testing, exhibiting no damage. The unevenly torqued components showed worsening degradation, as four were now considered as having moderate damage corresponding to state 2 degradation. The over torqued components were considerably worse again, with eight being considered degradation state 2 and two considered as degradation state 3 post testing. The degradation state 3 classification meant of course that two diaphragms had severe deformities corresponding to failure. Both of these components were also cracked.

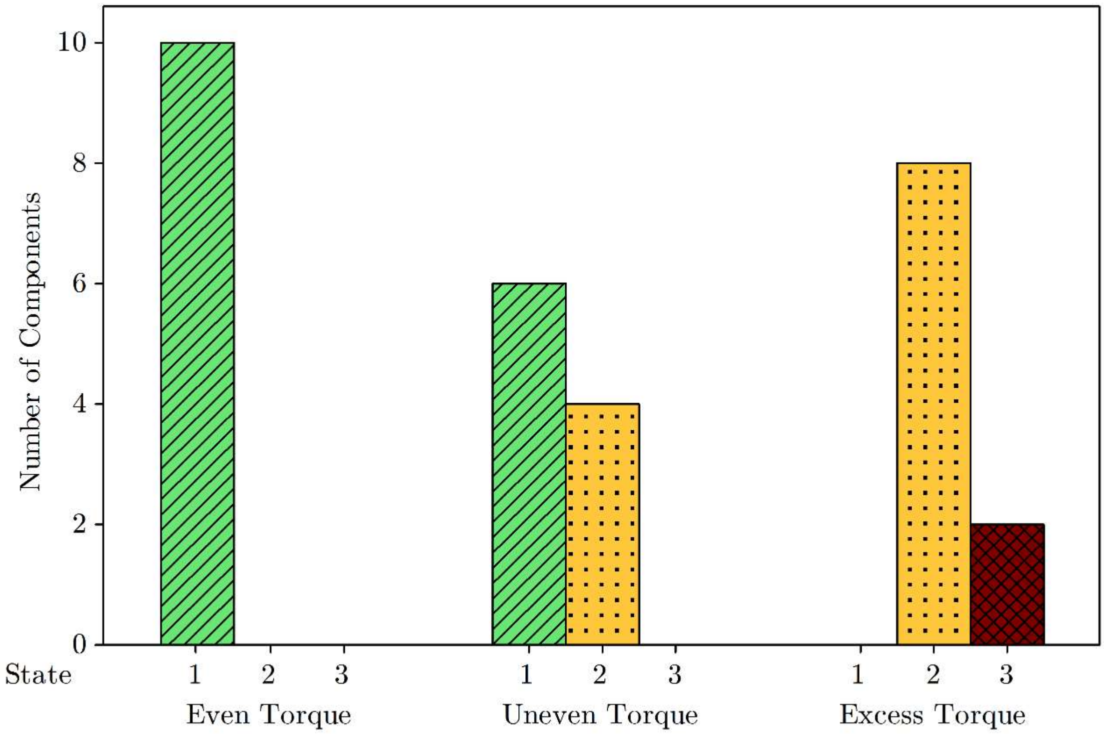

Figure 5.7: Number of components found in different degradation states as a direct result of installation settings

To statistically determine the association between increasing torque values and increasing material degradation a chi-square test for association was conducted between torque setting applied during installation and the degradation state of the component after testing. There was a statistically significant association between torque setting and degradation state, χ^2 (4) = 21.500, p = <.0005. There appears to be a reasonably strong association between torque settings and component degradation state with a Cramer's V value = 0.599, p = <.0005. It is also visually apparent in figure 5.7 that as torque increases, so does the degradation state of the material. Given these results, it was concluded that incorrect torqueing has a negative effect on component lifetime as per interview conclusion, and it was pertinent to investigate HOFs which may influence the ability of maintenance technicians to correctly install the components.

5.2.5 Development of PSF severity classification scale

Similar to the work of Baraldi et al [324] and Zio et al [326] a visual interface was developed for maintenance technicians to assess the PSFs characterising the context in which the maintenance and installation tasks are performed. In this case, the most relevant PSF was the difficulty of accessibility of the valve during torqueing of the bolts at steps 13, 17, and 18 shown in the PTA in figure 5.3. As valve access difficulty is not a directly measurable quantity, the interface was developed in order to elicit a useable quantitative metric to be used as a model covariate. This corresponds to stage 7 of the developed methodology. The intuitive interface supports assessment repeatability across all systems, as demonstrated by Baraldi et al [324]. The proposed interface is based on the use of anchor points that represent particular conditions which are well defined. The allocation of the anchor points on a numerical scale was performed by interviewing maintenance technicians with considerable experience in valve installation and appropriately aggregating their conclusions. The sub PSF allocations defining the anchor points of the scale, defined in conjunction with technicians, are shown in table 5.2.

Table 5.2: Anchor points scale PSF allocation description

Sub PSF Allocation	*Sub PSF Allocation Description*
No Access Difficulty	Valve at an appropriate height, facing towards the technician, with no discernible obstructions in the area
Mild Access Difficulty	Valve at height. Installation or maintenance tasks require auxiliary equipment to reach valve location. Otherwise no obstruction
Moderate Access Difficulty	Valve obstructed by other equipment, such as pipe work, pumps, motors etc., or valve in physically difficult to reach location, such as in a crawl space
Severe Access Difficulty	Combination of two or more of any mild or moderate valve obstruction conditions

The scale is valued from 0 to 100. A value of 0 acts as the first anchor point, 'No Accessibility Difficulty', with a value of 100 acting as the fourth anchor point, 'Severe Accessibility Difficulty'. The second and third anchor points lie in intermediate points along the scale. As the scale measured access difficulty and subsequently associated a single 'difficulty' value to each valve, the scale and subsequent values derived from it became known as the accessibility difficulty metric (ADM). The ADM scale used in the elicitation scale is shown below in figure 5.8.

Figure 5.8: Accessibility Difficulty Metric scale

Each system and valve used in the field data database was then assessed separately via walk-downs of the systems with a lead maintenance technician from the field and an expert from the valve OEM. For each valve they assigned a specific value from 0 to 100 describing the difficulty of torqueing a diaphragm correctly at that location, based on their own experience, with the anchor points continually used as a reference. An example of the values assigned to specific valves, which have been neutralised for publication purposes, is shown in table 5.3.

Table 5.3: ADM data example from four systems

System	Valve ID Code	ADM Expert 1	ADM Expert 2
Size 2 Vessel B	V-005	25	22
Size 1 Vessel A	V-047	10	20
Size 1 Vessel B	V-106	30	21
Filtration System C	V-069	30	22

The hypothesis was that the ADM score can then be incorporated into a probabilistic assessment of both degradation state and diaphragm cracking in service based on valve location. Further combining this information with quantitative service history data would then represent a novel data fusion approach whereby qualitative assessments are combined with traditional process related data sources in order to predict component RUL.

5.2.6 ADM Analysis

The ADM scores obtained from each expert were tested against both the presence of cracking and the transition from state 1 to state 2 for each component to determine whether a statistically significant relationship existed. With regards to the RUL estimation model for the diaphragms, the effect of the covariates is assumed constant across degradation states, so treating the transition between state 1 and state 2 as a failure is valid. The data collected consisted of a continuous real variable, the ADM score, and the dichotomous variable for both the presence of a crack and the two degradation states. To test for independence where the two failure modes act as the dependant variables, binomial logistic regression was used for methodology stage 10. Purely testing for independence, treating the ADM as a rising continuous variable is valid as we are trying to identify whether the probability of component failure increases with increasing ADM score. Therefore, the logistic regression model becomes:

$$Logit(\pi(xi)) = \alpha + \beta.xi, \text{ where } \pi(xi) = P(Failure = 1|ADM = xi) \tag{5.2.1}$$

i.e. the probability of a fail state given a particular ADM score. We test the hypothesis:

$$\begin{cases} H0: \beta = 0 \ (ADM\ and\ failures\ are\ independant) \\ H1: \beta \neq 0 (ADM\ and\ failures\ are\ not\ independant) \end{cases}$$

5.2.7 ADM Results

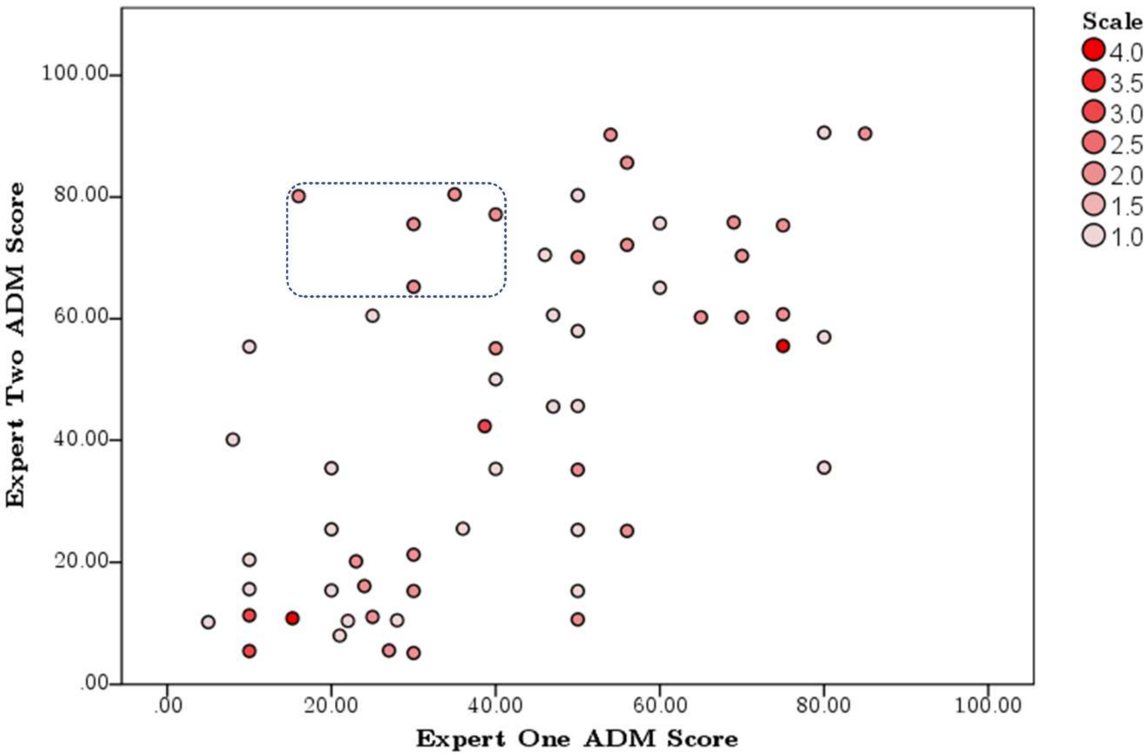

Figure 5.9: Scatter plot of ADM score agreement between the two experts

Shown in figure 5.9 is the scatter plot of the ADM scores attributed by each expert to each data point in the study. Neither variable was normally distributed, as assessed by Shapiro-Wilk's test (p <

.05), however as shown in figure 5.9 the data appears to be monotonically increasing indicating general agreement between the two experts with regards to the location difficulty of the valves. To help clarify the data, it has been binned using the centroid of the agreement points. Those areas of highest colour intensity indicate where there were multiple agreements between the two experts. Despite a general agreement being apparent, there are clear instances where there were multiple large scale disagreements between them, such as the centroids highlighted in the blue dashed line box. For this reason both Spearman's rank-order correlation [327] and Pearson's product-moment correlation [328] were used to test the hypothesis of association between the two variables. Results indicate a strong ($r > 0.5$) positive correlation between the two variables, with a Pearson's correlation $r(97) = 0.615$ ($p < 0.005$) and a Spearman's correlation $r_s(97) = 0.602$ ($p < 0.005$), again indicating general agreement, albeit with notable exceptions as highlighted [329]. To avoid issues with multicollinearity, each individual expert's scores are assessed separately to ascertain their significance and impact with respect to both component degradation and crack events.

Material degradation category

Three regressions were performed to ascertain the effects of component access difficulty on the likelihood that the components have degraded in service. The three covariates investigated were the access difficulty metrics derived from both experts, and an interaction variable between the two. None of the logistic regression models were statistically significant, with no p value for the $\chi^2(2)$ analysis results < .05. The models were only able to explain between 1% to 16%, based on Nagelkerke R^2, of the variance in component degradation level. The three analysed covariates are shown in table 5.4 below.

Table 5.4: Binary logistic regression model predicting likelihood of component degradation state based on ADM score

	β	S.E.	Wald	df	Sig.	Exp(β)	95% C.I. for EXP(β)	
							Lower	Upper
Expert One ADM Score	.002	.011	.033	1	.855	1.002	.981	1.023
Expert Two ADM Score	-.009	.009	1.027	1	.311	.991	.975	1.008
Expert ADM Score Interaction	-.006	.011	.295	1	.587	.994	.974	1.015

In figure 5.10 a greater separation of the data would be expected if the access difficulty of the valve was a significant influencer of component degradation, with two easily defined clusters of category one and category two components. The results of the three seperate binomial logistic regressions reflect this.

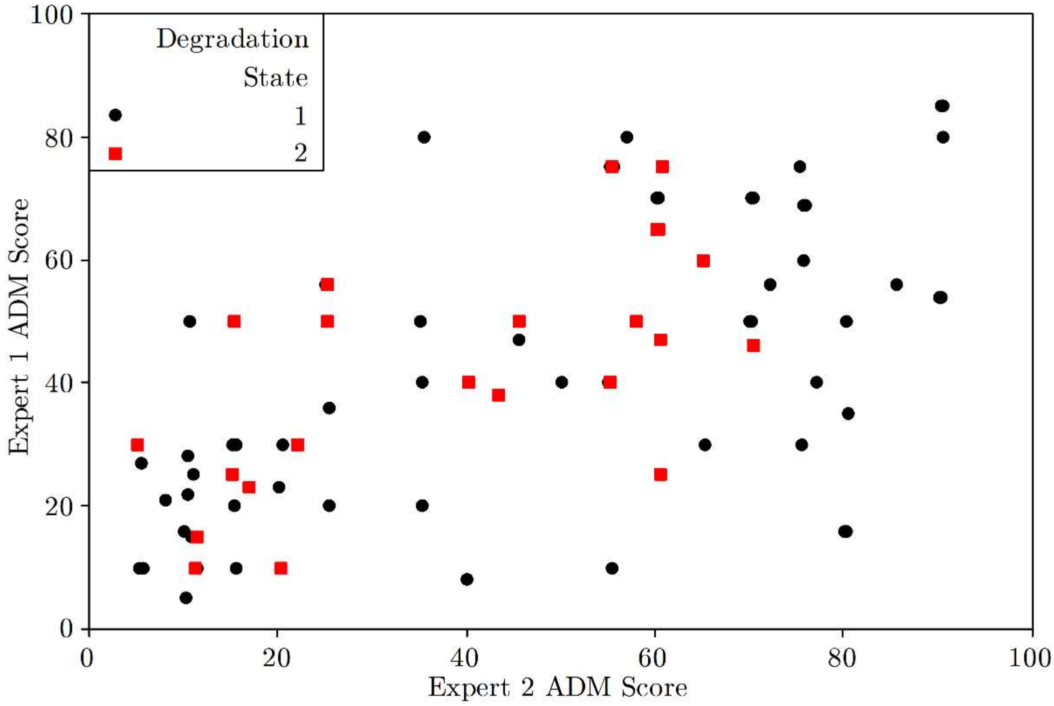

Figure 5.10: ADM score considering component degradation state

Material cracking

Again three regressions were performed with the same covariates to ascertain the effects of component access difficulty on the likelihood that the components have cracked in service. Once more, none of the logistic regression models were statistically significant, with no p value for the $\chi^2(2)$ analysis results < 0.05. The models were only able to explain between 0.5% to 13%, based on Nagelkerke R^2, of the variance in component degradation level. Based on these results it is not possible to reject the null hypothesis $H0: \beta = 0$. Given the independence between ADM scores and the likelihood of both component degradation and cracking in service, it is not possible in this instance to use the ADM score as a covariate within a reliability model. The three analysed covariates are shown in table 5.5 below.

Table 5.5: Binary logistic regression model predicting likelihood of component cracking based on ADM score

	β	S.E.	Wald	df	Sig.	Exp(β)	95% C.I. for EXP(β)	
							Lower	Upper
Expert One ADM Score	-.011	.016	.471	1	.492	.989	.959	1.020
Expert Two ADM Score	.009	.012	.602	1	.438	1.009	.986	1.034
Expert ADM Score Interaction	.002	.015	.022	1	.882	1.002	.973	1.032

Similarly to figure 5.10, figure 5.11 would be expected to show a greater seperation of data if the access difficulty of the valve was a significant influencer of component cracking. Likewise there would be two easily defined clusters of cracked and non-cracked components which would be reflected in the regression results.

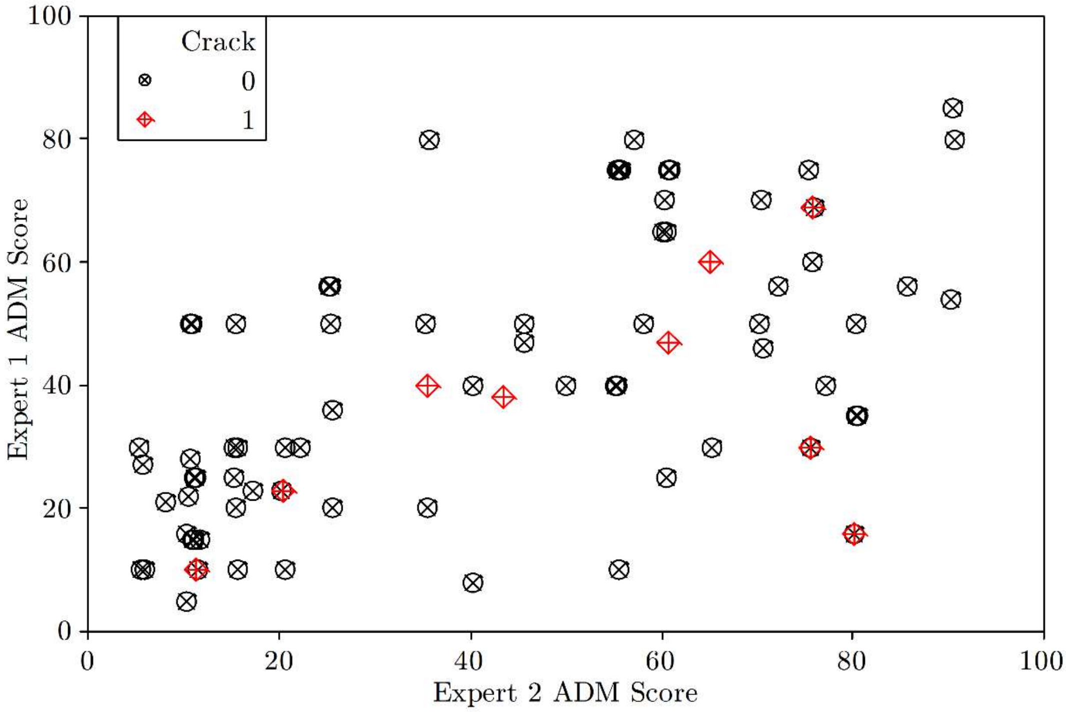

Figure 5.11: ADM score considering presence of component cracking

The reasons for the independence between the ADM score and the likelihood of component failure are discussed in detail in the discussion in section 5.4, but in-short procedural non-compliance was likely responsible for incorrect torqueing of valves, regardless of location. Therefore the overall approach to eliciting and including HOF as covariates in reliability models is still valid, but only when base criteria of compliance with standards can be realistically assumed. In the next section, a synthetic toy example is provided with generated data to demonstrate a complete example of the inclusion of HOF in a proportional hazards model.

5.3 Toy Example

5.3.1 Data Generation

In order to demonstrate the approach, the potential advantages, and the applicability of the developed methodology and of including significant HOF metrics in reliability models, two synthetic ADM score datasets which represent the opinions of two 'experts' were generated. One of the experts is risk averse, the other is less so, labelled as Toy Expert 1 and Toy Expert 2 respectively. The synthetic dataset is created purposefully so that the Toy Expert opinion is a significant factor in the both failure modes of the case study. Toy Expert 1, being risk averse, is more likely to give higher ADM scores to difficult to access valves, while Toy Expert 2 being less risk averse is likely to give slightly lower scores for the same locations. To simulate this, normally distributed random numbers have been generated separately for each 'expert'. The risk averse profiles for both experts were generated for crack events and both degradation states, using normal distributions with the parameters shown in table 5.6.

Table 5.6: Normal distribution parameters used for calculating toy datasets

	Toy Expert 1		Toy Expert 2	
	Mean (μ)	Variance (σ^2)	Mean (μ)	Variance (σ^2)
Crack	85	9	65	9
No Crack - Degradation State 1	30	9	20	9
No Crack - Degradation State 2	60	9	50	9

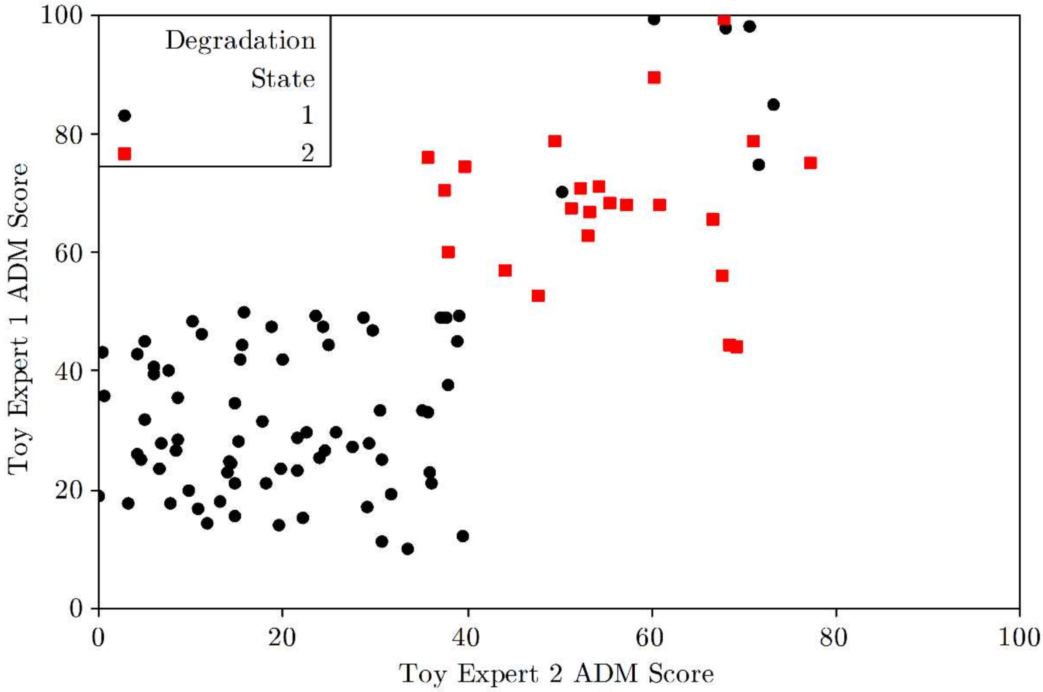

Figure 5.12: Toy ADM score considering component degradation state

Table 5.7: Binary logistic regression model predicting likelihood of component degradation state based on Toy ADM score

	β	S.E.	Wald	df	Sig.	Exp(β)	95% C.I. for EXP(β)	
							Lower	Upper
Toy Expert One ADM Score	.101	.020	24.55	1	.0005	1.107	1.063	1.152
Toy Expert Two ADM Score	.080	.017	22.69	1	.0005	1.083	1.048	1.119
Toy Expert ADM Score Interaction	.001	.000	23.55	1	.0005	1.001	1.001	1.001

In figure 5.12 a greater separation of the toy data is seen in comparison to the corresponding field data shown in figure 5.10 with two easily defined clusters of category one and category two components. The results of the three seperate binomial logistic regressions reflect this. The three regressions were performed to ascertain the effects of component access difficulty on the likelihood that the components have degraded in service. The three covariates investigated were the access difficulty metrics derived from both toy experts, and the interaction between them. All three logistic regression models were statistically significant, with all p values for the $\chi^2(2)$ analysis results < .05. The models were able to explain between 48.4% to 57.5%, based on Nagelkerke R^2, of the variance in component degradation level. The three analysed covariates are shown in table 5.7.

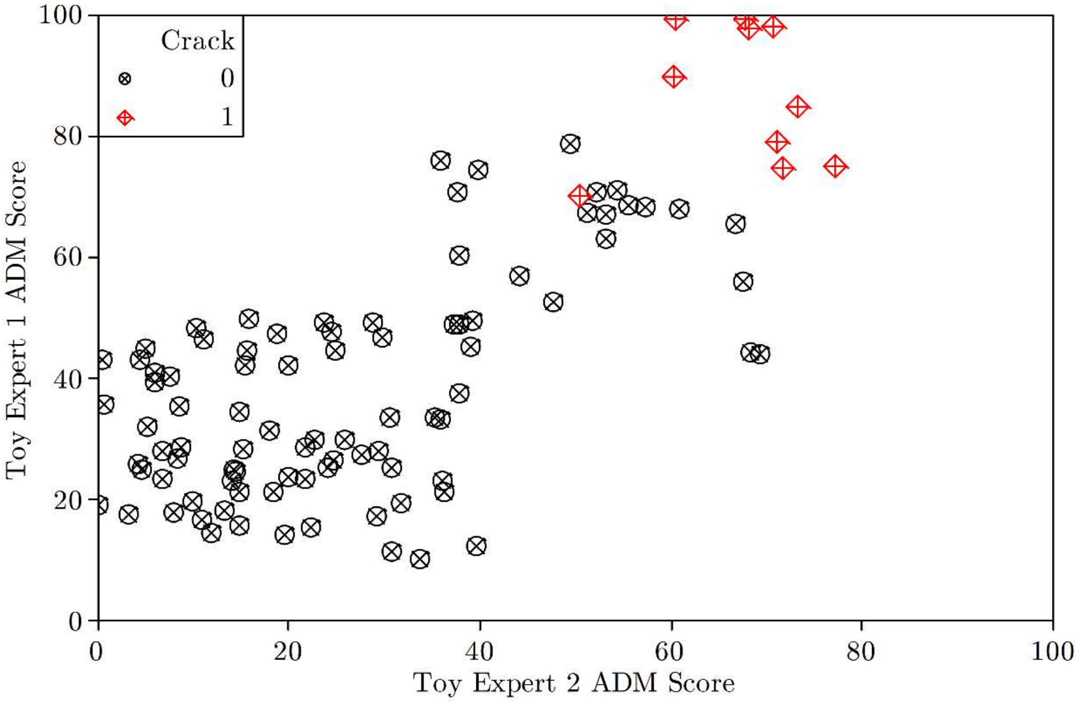

Figure 5.13: Toy ADM score considering component cracking

Table 5.8: Binary logistic regression model predicting likelihood of component cracking based on Toy ADM score

	β	S.E.	Wald	df	Sig.	Exp(β)	95% C.I. for EXP(β)	
							Lower	Upper
Toy Expert One ADM Score	.318	.144	4.88	1	.027	1.374	1.037	1.821
Toy Expert Two ADM Score	.174	.054	10.34	1	.001	1.190	1.070	1.324
Toy Expert ADM Score Interaction	.003	.001	6.28	1	.012	1.003	1.001	1.005

In figure 5.13 a greater separation of the toy data is again seen in comparison to the corresponding field data shown in figure 5.11 with two easily defined clusters of cracked and non-cracked components. The results of the three seperate binomial logistic regressions reflect this. The three regressions were performed to ascertain the effects of component access difficulty on the likelihood that the components have cracked in service. The three covariates investigated were again the access difficulty metrics derived from both toy experts, and the interaction between them. All three logistic regression models were statistically significant, with all p values for the $\chi^2(2)$ analysis results < .05. The models were able to explain between 68.1% to 88.8%, based on Nagelkerke R^2, of the variance in component cracking. The three analysed covariates are shown in table 5.8.

Based on these results it is now possible to accept the null hypothesis $H0: \beta = 0$. Given the dependence between both ADM scores and the likelihood of both component degradation and cracking in service, it is possible in this instance to use the ADM as a covariate, for example within a proportional hazards model. Note that the Toy Expert 1 has higher regression coefficients in both table 5.7 and table 5.8, indicating that a greater likelihood of failure state transition is assigned by this expert to higher ADM scores. The interaction term between the two experts has the lowest coefficients assigned in both regressions. In this instance it is up to the maintenance decision maker which ADM score to use in the model based on the level of operational risk they are willing to assign to the accessibility difficulty. Safety critical industries such as the one in the case study considered here would be typically risk averse and so more likely to utilise the opinion of Toy Expert 1.

5.3.2 Weibull proportional hazards model deployment

The ADM score attributed to Toy Expert 1 is combined with a single machine related covariate in order to demonstrate the impact that the synthetic ADM score has on component degradation state over time. As this example is intended purely to demonstrate the potential for PSF inclusion in a data-driven degradation model, only one machine related covariate is modelled alongside the derived HOF metric. The single machine related covariate chosen was the saturated steam exposure variable, modelled as the time variable t with which the Weibull scale and shape parameters are calculated, in this synthetic instance using the field data alone. As the effect of the ADM covariate does not change depending on degradation state, it is possible to calculate its effect for one transition, about which we have the most information, and use that information to help modify the Weibull curve for the second transition. This means that the ADM scores can still be used to calculate the transition times of both degradation states. This is a significant step given the scarcity of data. Although the convenience of Weibull proportional hazards models accommodating the inclusion of other non-machine related covariates makes the model suitable for the analysis considered here, the justification for the selection of a Weibull model was also performed via parametric distribution function estimation conducted via an Anderson-Darling test [330]. The distribution estimation has been completed using both the field and OEM data. The full dataset, the bioreactor dataset, and the perfusion dataset are tested separately, and are shown in table 5.9.

Table 5.9: Parametric distribution estimation of time to failure data t

Rank	Full Dataset		Bioreactor Dataset		Perfusion Dataset	
	Distribution	*Anderson Darling score*	*Distribution*	*Anderson Darling score*	*Distribution*	*Anderson Darling score*
1	2-Parameter Exponential	143.169	2-Parameter Exponential	115.496	2-Parameter Exponential	31.571
2	Lognormal	143.21	3-Parameter Lognormal	115.51	Normal	31.573
3	Loglogistic	143.229	3-Parameter Loglogistic	115.512	Logistic	31.575
4	Exponential	143.246	Lognormal	115.52	Smallest Extreme Value	31.577
5	3-Parameter Lognormal	143.253	3-Parameter Weibull	115.524	Exponential	31.579
6	Weibull	143.257	Loglogistic	115.536	Lognormal	31.585
7	3-Parameter Weibull	143.269	Weibull	115.564	Weibull	31.586

It is important to note that the Anderson-Darling test was performed using the transition times from category state one to category state two. The results illustrate that the full dataset and bioreactor dataset largely agree, with some small differences in the results of the perfusion system. However, the perfusion dataset may suffer from a lack of data as it is much smaller in size. As shown, each of the datasets fit the exponential distribution well. As discussed previously however, the exponential distribution has a constant hazard rate and is therefore not appropriate for systems that degrade over time. However, as the exponential model is naturally embedded in the Weibull model anyway, using the Weibull model won't discriminate against the exponential model.

The probability plots for the four most common distributions and the Weibull distribution overview plots are shown in figure 5.14 and figure 5.15 respectively.

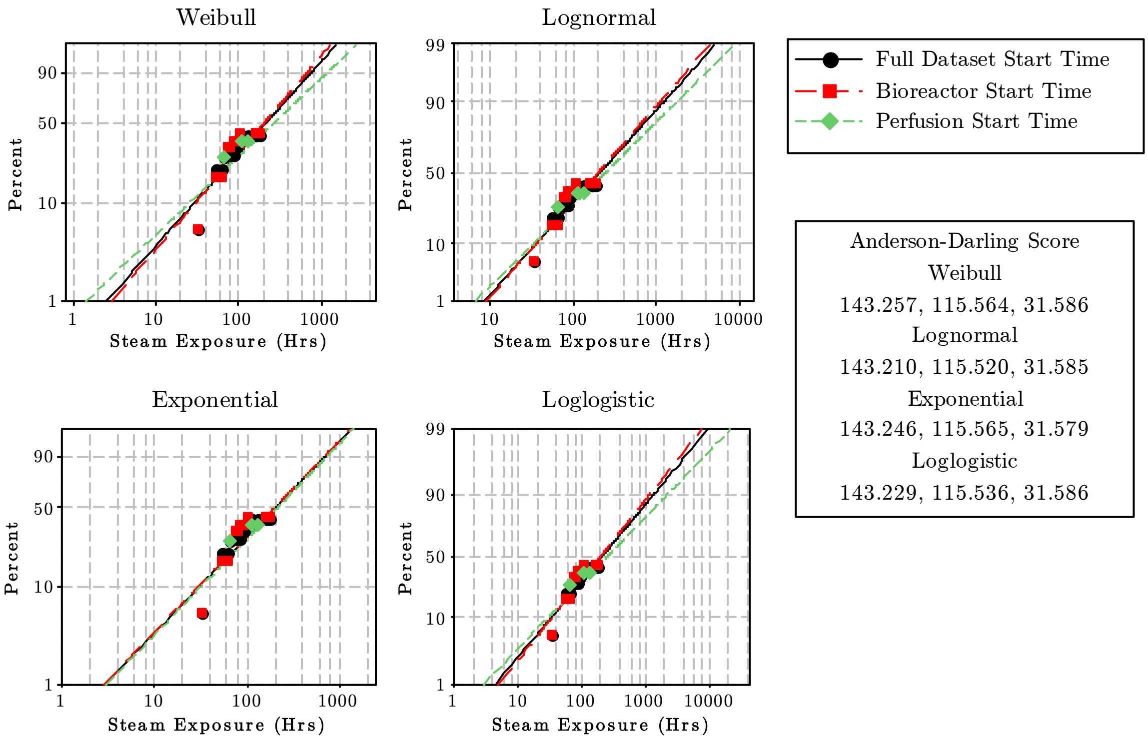

Figure 5.14: Probability plots for all datasets

As shown in figure 5.15, which shows the transition times from state one to state two of the full dataset, the shape parameter β has been estimated at approximately 1.4., with a mean transition time of ~167 hours of steam exposure. This is less than the manufacturers recommendation of ~195 hours of steam exposure. As $\beta > 1$, the hazard function increases over time, while the survival function decreases, which is expected from a system that degrades over time with continued exposure.

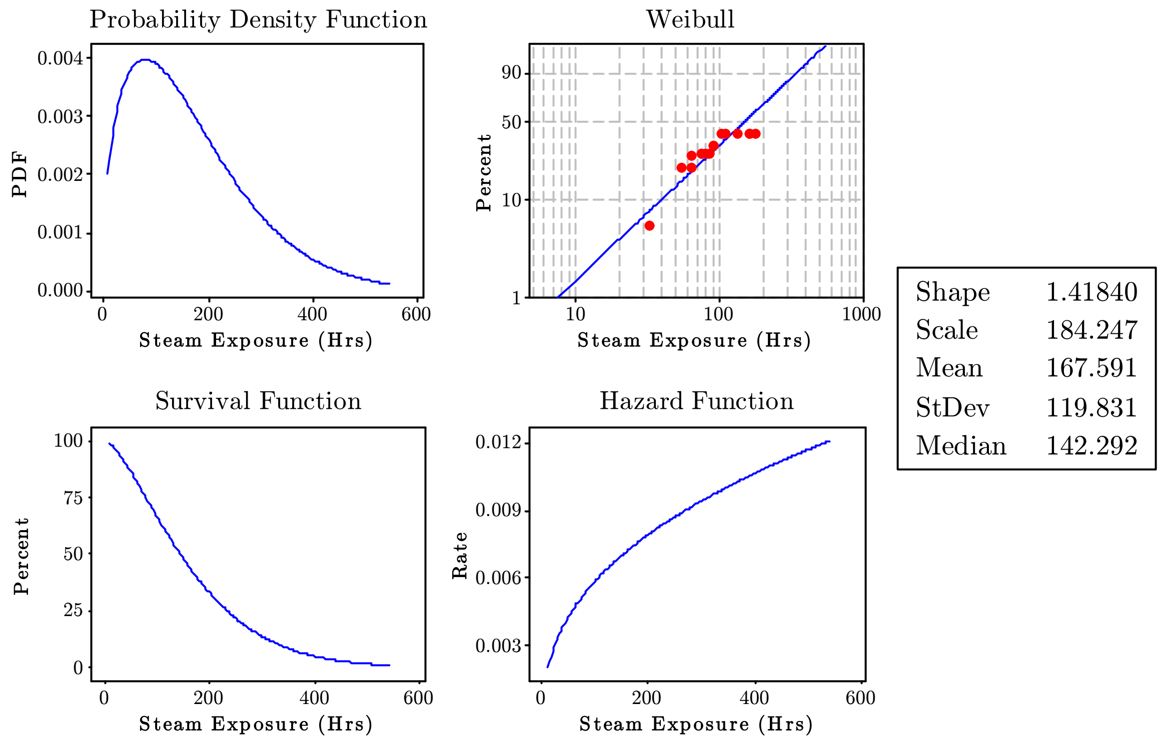

Figure 5.15: Weibull distribution overview plot for full dataset

Following from this, for the baseline model characterising the degradation state transitions, i.e. the model describing system behaviour given a null covariate vector, we assume that the failure state transition times T_{12} and T_{23}, derived from the Markov model illustrated in chapter 3, obey Weibull distributions conditional on the random parameters α (scale) and β (shape) such that:

$$\begin{cases} T_{12}|(\alpha_1, \beta_1, x = 0) \sim Weibull(\alpha_1, \beta_1) \\ T_{12}|(\alpha_2, \beta_2, x = 0) \sim Weibull(\alpha_2, \beta_2) \end{cases} \tag{5.3.1}$$

where $x \in \mathbb{R}^{\tilde{p}}$ is the value of the vector of the significant $\tilde{p}$ covariates identified as the influencing factors out of the full available set Φ, i.e. the covariates selected to be encoded in the analysis. The stochastic transition times from states 1 to 2 and from states 2 to 3 of the n^{th} component, $n = 1, \dots, N$ are indicated by T_{1n} and T_{2n}, respectively. In particular, T_{1n}, $n = 1, \dots, N$ are considered as independent random variables conditional on both parameters α_1 and β_1, and the vector of covariates x_n. Similarly, T_{2n}, $n = 1, \dots, N$ are independent random variables conditional on α_2, β_2 and x_n. The final hazard function of each transition time is proportional to the corresponding baseline hazard function, $h(t_{jn}|\alpha_j, \beta_j, x = 0) = {}^{\beta_j}\!/_{\alpha_j} \left({}^{t_{jn}}\!/_{\alpha_j}\right)^{\beta_j - 1}$, with the final hazard function being a time-independent multiplicative factor of $e^{x_n \gamma}$, as shown in equation (5.3.2):

$$\begin{cases} T_{1n}|\alpha_1, \beta_1, \gamma, x_n \sim^{indep.} Weibull\left(\frac{\alpha_1}{e^{(x_n\gamma/\beta_1)}}, \beta_1\right), n = 1, \dots, N \\ \\ T_{2n}|\alpha_2, \beta_2, \gamma, x_n \sim^{indep.} Weibull\left(\frac{\alpha_2}{e^{(x_n\gamma/\beta_2)}}, \beta_2\right), n = 1, \dots, N \end{cases} \tag{5.3.2}$$

where $\gamma \in \mathbb{R}^{\tilde{p}}$ is the vector of parameters that tune the effects of the selected covariates on both transition times. In this respect, we assume that the effect of the covariates on the two transition times is the same, meaning that the same vector of coefficients γ is used for both transition times. This allows us to reduce the number of parameters to be estimated, a crucial issue given the scarcity of data, not only in the case study but also in many real world scenarios. The vector of coefficients γ can of course differ for both transition times, but enough failure data must exist in order to calculate these. The hazard rate function, $h(t_{jn})$, being proportional to the instantaneous conditional probability of failure at time t, is sensitive to the time variable selected to represent the age of the system. The parameter α, the scale parameter, in the absence of covariates provides the characteristic life of approximately the 63rd percentile of failure data [149]. Finally, vectors $x_1, \ldots, x_n$ are arranged to form the rows of matrix $X \subseteq X'$. The developed Weibull proportional hazards model presented here can include covariates derived from HOF, in addition to traditional MR factors, such as those derived via statistical methods and material analysis as seen in this work. Again, the addition of HOFs as covariates, if significant, allows the maintenance decision maker to calculate their effect on equipment failure risk, which can aid decision makers in the calculation of expected uptime as well as the probability of system failure [149].

The data describing the ADM has been normalised such that:

$$z_i = \frac{x_i - \min(x)}{\max(x) - \min(x)} \tag{5.3.3}$$

where $x =$ the coefficient vector $(x_1, \ldots, x_n)$ and z_i is the i^{th} normalised data.

Weibull proportional hazards model output

The Weibull proportional hazards model outputs derived from the synthetic data for diaphragm degradation state transitions using the maximum likelihood estimation method are shown in below in table 5.10. As shown, the Toy Expert 1 covariate is significant with a parameter γ value of approximately 1.2. This is the amount by which the instantaneous hazard rate increases by for every unit increase in Toy ADM score.

Table 5.10: Weibull proportional hazard model output

	γ	S.E.	Z	Sig.	95% C.I. for γ	
					Lower	Upper
Model Intercept	5.60897	0.253681	22.11	<0.0005	5.11176	6.10617
Toy Expert 1	1.20421	0.341601	-3.53	<0.0005	1.87374	1.0534689

The state transition times modelled using the steam exposure data from the field, with a null covariate vector, are shown in figure 5.16 below. Interestingly, the average time for transition from state 1 to 2 is approximately 120 hours, below the value of 195 hours predicted by the valve OEM.

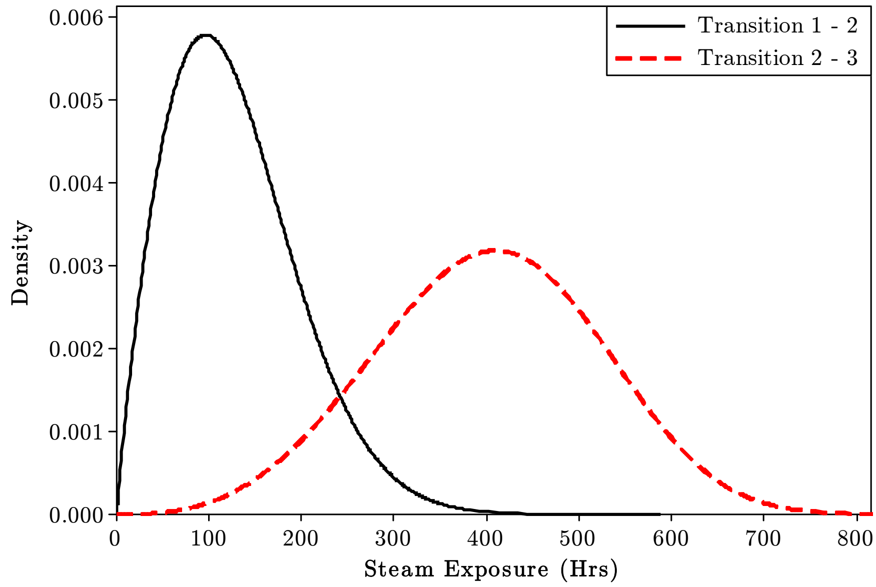

Figure 5.16: Probability density functions of the state transition times T_1 and T_2

The probabilities of a diaphragm occupying each individual degradation state over time *t* with the null covariate vector, in this example an ADM score of 0.0, is shown in figure 5.17.

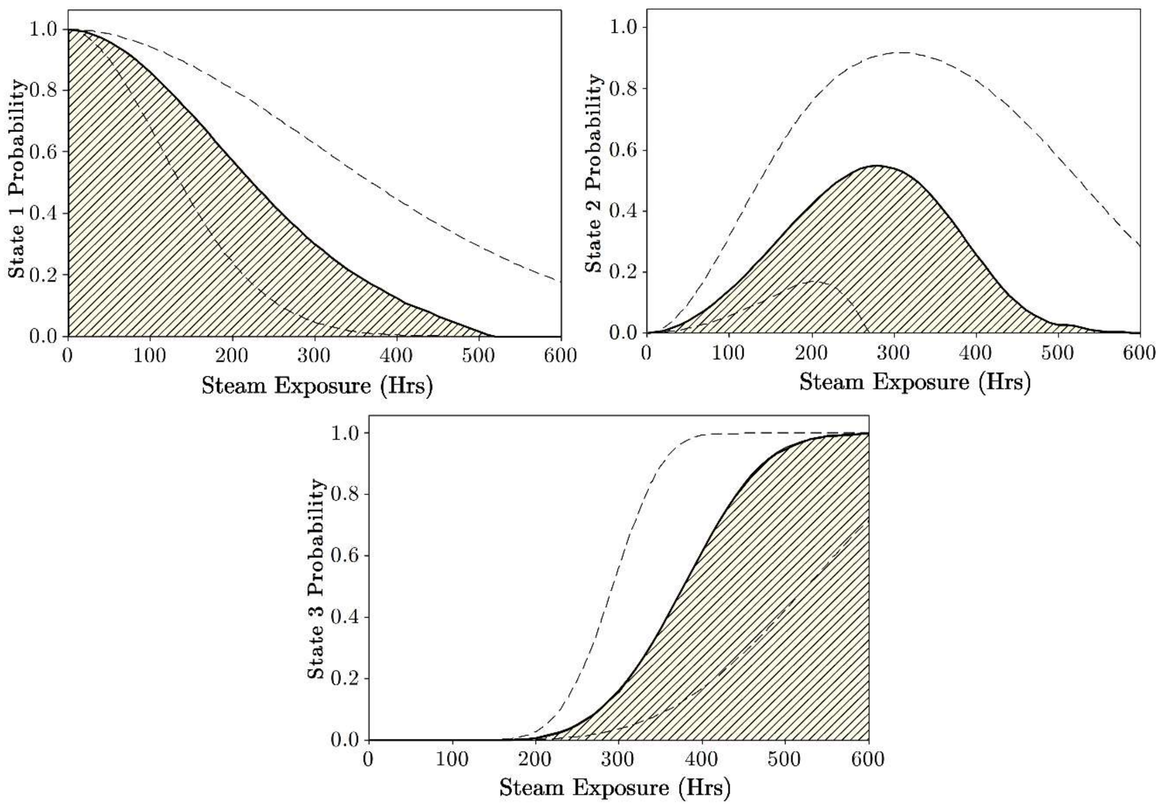

Figure 5.17: State transition probabilities for ADM score of 0.0. The dashed lines represent the 0.05 and 0.95 confidence intervals

Figure 5.18 demonstrates the same probabilities modelled using a diaphragm with an ADM score of 100.

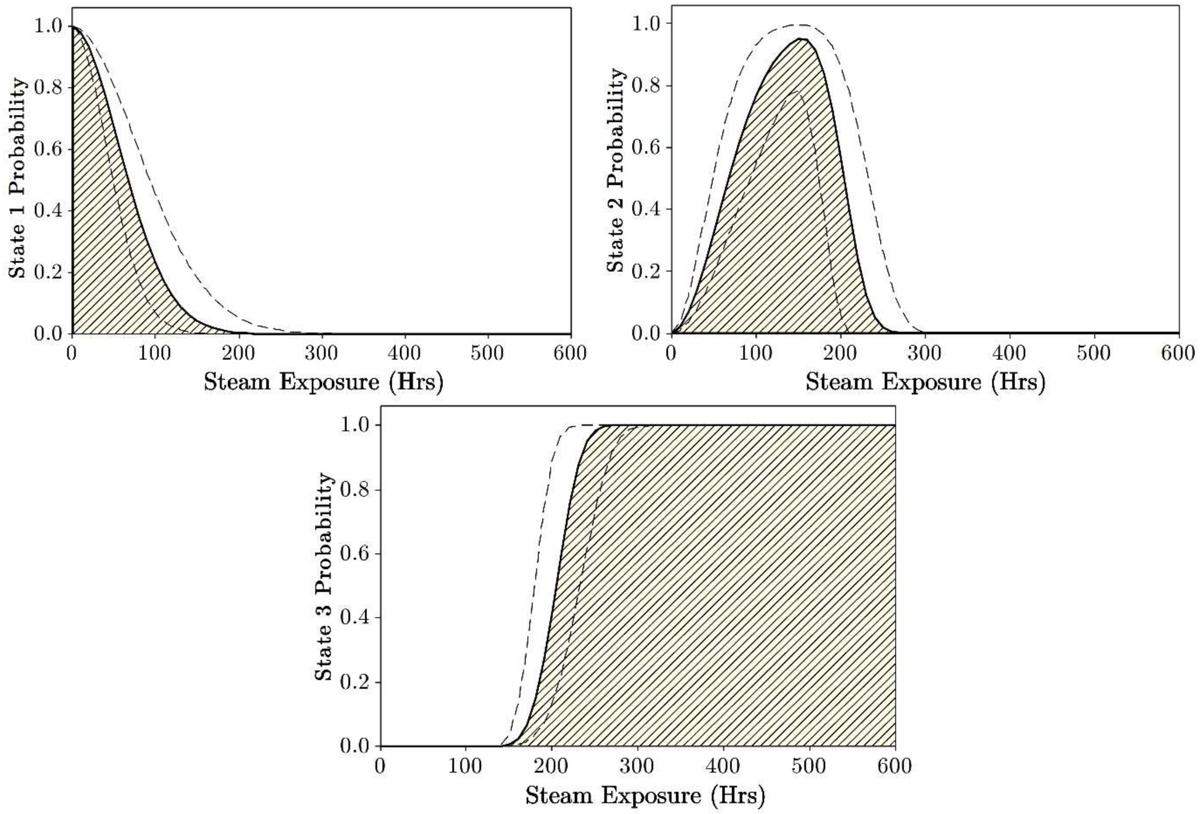

Figure 5.18: State transition probabilities for ADM score of 100.0. The dashed lines represent the 0.05 and 0.95 confidence intervals

What is particularly noteworthy is how the inclusion of the ADM score has dramatically decreased the model uncertainty. This demonstrates how significant HOF metrics can increase the accuracy and thus predictive power of proportional hazards models, thereby increasing system reliability. The amount which the model uncertainty will decrease with the addition of HOF metrics is of course dependant on the amount of model variability explained by those metrics. It is important to note in this synthetic example that the correlation between Toy Expert 1 and the observance of both failure modes is strong, which has exaggerated the model uncertainty reduction. However, it is a useful exercise to demonstrate the potential advantages of including such a derived metric alongside traditional machine related covariates within a Weibull proportional hazards model. Figure 5.19 illustrates the probability of a diaphragm being in degradation state 1 over time for the four ADM anchor points: 0, 35, 75, and 100. As expected, component lifetime decreases with increasing ADM score.

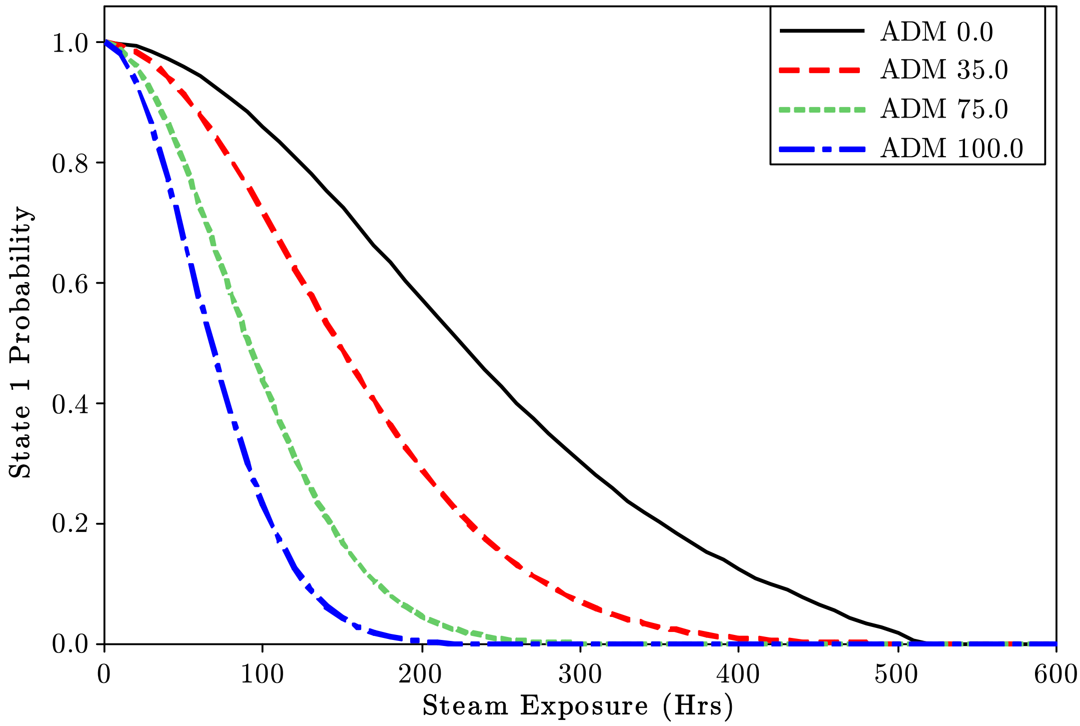

Figure 5.19: Cumulative probability (survival function) of state 1 occupancy of the four ADM anchor points over time

5.4 Discussion

This section of the work has presented a methodological approach to the inclusion of HOF in predictive maintenance models. The parametric Weibull proportional hazards model is used here to demonstrate the methodology. HOF are acknowledged to be a key aspect of system performance but are largely neglected in the literature regarding current prognostic reliability models. This part of the work contributes to the literature in a number of ways. This work outlines for the first time an exact framework for both the elicitation and the inclusion of both quantitative and qualitative HOFs as covariates in parametric prognostic models. This work also illustrates how to incorporate the derived HOF covariate into a Weibull proportional hazards model considering a multi-state degradation profile given scarcity of data. This work focuses on HOFs specifically relating to offline maintenance activities, and critically considers the case where operator skill level is assumed to be consistent and stable across maintenance teams, and thereby does not significantly impact equipment reliability. To reiterate, in this scenario a broader approach to the inclusion of HOFs must be considered, and as such this work acts as an obvious extension to other developed Weibull proportional hazards models found in the literature. Another novelty of the approach in this work is that the parametric model development methodology allows an individual component or system to have its own individual instantaneous hazard rate derived from its own specific maintenance induced HOF metric. An often underlying characteristic of other studies is that the latent or critical human error probability is assumed to be a constant parameter based on which the stochastic model of the system under study is developed.

While the results of the methodology applied to the industrial case study were disappointing in terms of the acceptance of the null hypothesis of ADM score and failure likelihood independence, this also presented the opportunity to fully explore the developed framework. As stated the hypothesis was investigated as to whether there was statistical independence among the component failure modes and difficulty of valve torqueing at specific locations within the manufacturing area. The PSFs identified with experts in the field suggested that the difficulty of valve location would have an impact on the ability of the maintainers to get their bodies, the tooling, or both into the correct location in order to perform the maintenance task effectively. This could then result in incorrect torques being applied which could lead to uneven stress distributions within the elastomer material which has been shown to influence premature cracking of valve diaphragms in service [302]. In this instance there was no evidence to suggest that the valve location had any effect on the probability of component failure in service. Although this result was somewhat unexpected, as per methodology step 12, further interviews with technicians and ethnographic research were conducted to help explain the reasons for the lack of significance in the findings. It is important to note that the hypothesis was built on the assumption that the maintenance staff would only use non-optimal maintenance practices when the valve location negatively dictated their ability to perform the task correctly. In this way the ADM score could be interpreted to mean the ability of the maintainers to appropriately apply the standard maintenance approaches. However, it was subsequently discovered via the continued investigations that in some instances the standard maintenance approaches were not universally applied, even given the presence of no PSFs. This essentially meant that even components which were in optimal locations in terms of ease of access were still not being torqued correctly, negating the influence of the previously determined PSFs. It transpired that certain maintenance technicians were still using the older 'bulge' procedure for component maintenance, which does not explicitly require the use of torque wrenches to accurately tighten the fasteners on the valve bodies. This confounding result was only highlighted through the non-significance of the ADM results. For this reason, the proposed methodology recommends that procedural issues are specifically investigated when developing predictive models of human performance, as full compliance with training and procedures cannot always be assumed for a variety of reasons, for example suitability of the training and procedures, complacency over time, changes to equipment, etc. After it was highlighted that the improved standard maintenance approaches were not universally applied, additional support was provided to maintainers to help re-establish the importance of following the updated procedures as per the developed methodology guidelines. The results of the synthetic example, the Toy ADM analysis, demonstrates the potential positive effects of including HOFs and suggest that further research in this area could greatly improve the provision of parametric predictive models. HOF have the potential to further reduce the uncertainty of parametric reliability models if utilised correctly.

Chapter 6

Summary and Conclusions

6.1 Summary

Modern maintenance methods are dependent upon understanding and monitoring component degradation; however, many industrial situations exist where direct monitoring is impossible, and component degradation characteristics are not well understood. This research explored the hypothesis that data to support Prognostic Health Monitoring (PHM) in practice may be extracted within industrial situations where pre-existing data on component degradation characteristics is scarce and context independence and subject matter understanding is low. In order to investigate this hypothesis, a case-study in the biopharmaceutical industry was followed which attempted to elucidate the significant variables leading to component degradation via a novel hybrid data elicitation methodology. Okoh et al [1] opine that hybrid modelling methodologies can be used to improve prognostic lifetime accuracy, and dataset fusion techniques for remaining useful life estimation may be used where data is available. Abonyi et al [191] outlined the first stages of the development of virtual sensors, a potential modelling solution under these conditions, as data inspection, selection of historical data, and data pre-processing. In addition, ElMaraghy et al [331] intonate that the interaction between human elements and the hardware and software components in manufacturing systems is an important consideration in the overall complexity of systems that should be taken into account. This means that dataset fusion is necessary to adequately model complex manufacturing systems. However a knowledge gap exists to guide the elicitation of the significant variables required for component lifetime modelling under these conditions. To help bridge this gap a holistic methodology is proposed aid in significant data identification and measurement in complex industrial environments where data is scarce, siloed, and disparate.

The case study followed in this work was that of dynamic valve diaphragms used in the biopharmaceutical industry, manufactured from the polymer composite Ethylene Propylene Diene Monomer (EPDM). The central question in this work was therefore, what are the variables, both process and human related, which contribute to EPDM diaphragm degradation and how can their contribution be understood and quantified? In order to answer this question, data from the process level, the system level, the equipment level, and the component level were required. These disparate data sources, including data from both supplier and end-user, each contain valuable information, which needs to be elucidated and then transformed into a common format. The significance of those variables can then be determined, and if significant, this information can be used within remaining useful life prognostic algorithms.

The first step in this work was the modelling of the degradation and failure states of the component within a Markov chain. The semi-Markov approach, a special case of Markov chains where the time spent in the current state depends on both the prior and future states, is useful in this context as no reverse transitions are possible and the disparate data is both left and right censored [332]. The multi-state stepwise nature of the Markov-chain modelling approach of the component degradation states allowed the use of bespoke filter and wrapper binary logistic regression techniques to determine the set of significant degradation process variables. The novel combination of these approaches was developed for this task. If a binary systems approach had been used, there would not have been enough failure data available to estimate the variable significance. The modelling assumption was that any variable responsible for previous state transitions was also responsible for future state transitions. This is achieved by assuming that the vector of parameters that tune the effects of the selected covariates is constant on all state transition times. As more data becomes available to refine the parameters, this assumption can be relaxed and separate parameters chosen for individual transition times if necessary. This critical assumption allows some determination of variable significance, and in effect creates a 'failure' data set, a significant step given the scarcity of data. To enable the multi-state systems approach, a qualitative assessment method was created which categorised the components into different health states for the first time. The initial filtering of non-significant variables allows for further focused investigations into potentially significant variables.

Once the initial list of potentially significant variables had been filtered using the developed method, four key variable interactions were investigated further using multiple material characterisation techniques, a first in the literature. This acted as an additional aid to the selection of the set of significant process variables contributing to component degradation. It was necessary to perform these analyses as the statistical techniques applied to the process history dataset could not identify, with a sufficient level of confidence, which variables should be taken into account when developing models of component lifetime. The analyses examined three different aqueous chemical solutions. Performing the material characterisation analysis developed, for the first time, an understanding of the chemical and physical mechanisms responsible for EPDM degradation that occur during exposure to these variables. An understanding of the physics of failure of the components also acts as a first step in potentially developing condition based monitoring solutions for this application.

To fully encompass all possible sources of component degradation, it was critical to assess if human interaction during maintenance activities played a role in the sudden failure of the components in-situ. To accomplish this, a methodological framework was developed which intended to enable the integration of human and organisational factors as quantitative metrics within degradation models. The developed methodology utilises human knowledge of the maintenance process to transform qualitative assessments of the factors which influence maintenance technician error rates. The hypothesis investigated is that including such a metric could reduce the uncertainty of models developed for system failure probability estimation. The case study investigated whether valve accessibility was correlated with component degradation, but in this case no correlation was found and further investigation suggested that correct procedures were not being following in the valve installation process. A toy example was generated to demonstrate the potential advantages of utilising human and organisational factors in parametric degradation models, where a correlation with degradation is found. However, the discovery of maintenance practice deficiencies resulted in an overhaul of the internal maintenance functions of the host organisation. Modelling the factors which influence technician performance in this way would allow individual components to have their own local hazard rates, a first for human-system interaction effects due to maintenance intervention.

In conclusion, the central hypothesis of this work was substantiated, as useable quantitative data was elucidated from disparate, scarce, siloed data sources via a multi-disciplinary methodology which seeks to unify several sources of information. The gathered data would enable the initial development of prognostic lifetime models for the case study components. It is important to note that the methodological approach of this work is not intended to provide an exact data elicitation solution for all industrial scenarios, as this will change depending on a multitude of extraneous factors related to the case study in question, such as data availability, required resources, time constraints etc. Rather, this work may be interpreted as a template to guide the identification and quantification of variables for inclusion in reliability models which can be adapted as required for different systems.

6.2 Conclusions

6.2.1 Analysis of process variables contributing to component degradation

The first objective in this work was the identification of the significant process variables contributing to component degradation. Firstly, a unique database was established which collated disparate sources of data into a single format. The relationships between and progressions of the failure and degradation states of the components were characterised using a Markov process, a crucial step given the scarcity of data. A bespoke qualitative technique was developed to assess component degradation and failure states. Using heuristic data mining techniques, historic environmental exposure data was collected and combined with the qualitative degradation assessment of every component. Two datasets were sourced, each consisting of two separate system types. One data source was retrieved after the industrial usage of the components, the other was sourced from internal OEM testing. A 'digitisation' approach was developed to convert analogue data sources into cumulative exposure hours over a specific threshold, in order to create format commonality amongst the different data sets. The developed data collection technique enables data fusion from scarce data sources, as any cumulative process exposure data can be collected and tested for significance against intermediate degradation state transition events.

Secondly, using a novel combination of statistical techniques, a two-step approach was developed for determination of which environmental process factors contribute towards degradation state transitions and crack events. Initially, a filtering approach discarded from the full list of available covariates those which were not significant in determining the transition behaviour between failure states. Then a wrapper method was applied on the filtered set of covariates to ascertain if predictive performance of the logistic regression models was enhanced using select subsets of those significant covariates.

Based on the evidence from the developed data collection and significance testing techniques, it can be concluded that:

- Steam exposure is the most significant factor influencing the gradual stepwise degradation of the components
- Material cracking is related to the material degradation state. As the material degrades, there is a higher probability that cracking will occur
- The initial probability of a crack occurring must be minimised to reduce the likelihood of a crack occurring during the lifetime of a diaphragm
- Additional testing is required to determine crack causation
- Additional testing is required to determine if the chemical solutions of NaOH, NaClO, H_3PO_4, and the interaction between steam and NaClO exposure, influence EPDM degradation
- The other process variables investigated do not have a significant degradative effect on the components

6.2.2 Material characterisation of industrial components

The second objective of this work was the characterisation of the industrial components via material analysis techniques, to understand the physics of the degradation processes initiated by exposure to certain process variables. Analysis of the EPDM material pre and post-exposure to varying quantities of these variables was undertaken. The chemical solutions under investigation were aqueous solutions of NaOH, NaClO, H_3PO_4, and the interaction between steam and NaClO exposure. 24 virgin samples were utilised for testing. 12 virgin samples were tested using an array of chemical and physical analysis methods in order to develop a foundation for the characteristics of the virgin material. The remaining 12 samples were then exposed to an individual chemical under investigation and subjected to the same tests as the virgin samples. This was to examine the effect that the chemical exposures had on the material. This allowed a direct comparison of the degradation effects attributable to the chemical exposure. The diaphragm samples were exposed for 168 and 504 hours in an uncompressed state, and 168 hours in a compressed state, in a specially adapted valve rig. The testing consisted of mechanical, thermal, spectroscopic, and chemical techniques. The developed testing regime is the first time EPDM has been tested and characterised under these conditions in the published literature.

Based on the accumulated testing results it can be concluded that:

- Crosslinking is the dominant mechanism responsible for material degradation upon chemical exposure
- Additional crosslinking occurs upon exposure to all investigated chemical exposures
- Oxidative damage and the formation and recombination of free radicals is responsible for the additional crosslinking
- Loss of plasticiser and thermo-oxidative damage are contributory degradation mechanisms
- The hardened surface layer impacts the bulk mechanical properties
- 100°C H_2O exposure has an additional degradative impact on the EPDM
- Compression during 100°C H_2O/NaClO exposure has a stronger crosslinking effect than NaClO exposure alone
- The interaction between 100°C H_2O and NaClO exposure results in material cracking
- NaClO exposure during material compression, and upon continued exposure up to 504 hours, results in an increase of the crosslink density
- NaOH and H_3PO_4 exposure during material compression, and upon continued exposure up to 504 hours, results in a decrease of the crosslink density
- NaOH and H_3PO_4 exposure results in an accelerated rate of crosslinking than NaClO in the early stages of exposure
- As the surface of the EPDM diaphragms is degraded due to crosslinking, it could be foreseen that the tear strength of the diaphragms will also be reduced, a contributory factor in relation to material cracking
- Considering a broader view, an understanding of these effects offers a potential for condition based monitoring to be developed for this application

6.2.3 Consideration of human factors contributing to component degradation

The third objective of the work was the definition of a methodological framework to integrate human and organisational factors as quantitative metrics within parametric degradation models. It was suspected that installation issues are a contributory factor in the early failure of valve diaphragms. This has never empirically investigated or confirmed in the published literature. If significant, it is necessary to capture this information in order to develop accurate component level data-driven degradation models.

A novel framework was developed and deployed for both the elicitation and inclusion of quantitative and qualitative HOFs as modelling covariates. This unique approach allows a component to have its own individual instantaneous hazard rate derived from its own specific maintenance induced HOF metric. From the evidence gathered through the use of this new framework, another novel test was conducted to test the hypothesis that incorrect valve torqueing has a degradative effect on the EPDM diaphragms. The use of a significant derived HOF metric in a prognostic model was demonstrated via a Weibull proportional hazards model.

Based on the findings of the developed framework and the subsequent torque testing regime it can be concluded that:

- Valve access difficulty has an impact on maintenance technicians' ability to perform valve torqueing effectively
- Incorrect torqueing negatively affects the degradation rate of the components

- Incorrect torqueing increases the risk of component cracking
- The developed framework successfully formalises the transformation of qualitative PSFs into quantitative metrics which can be tested for significance in relation to component failure
- Maintenance technicians were not following standard operating procedures in relation to torqueing guidelines. Valves in accessible locations were also being torqued incorrectly
- The non-adherence to SOP's was highlighted through the deployment of the developed framework
- It is justified in the developed framework to recommend that procedural issues are specifically investigated when developing predictive models of human performance, as full compliance with training and procedures cannot always be assumed
- Maintenance technicians were provided with additional support and re-training as a result of the investigations undertaken

6.3 Recommendations for future work

There are several areas where this work could be expanded and developed further. For example:

1. Prognostic degradation models utilising the elucidated significant variables could be developed. In the first instance a virtual sensor approach could be taken, and the significant variables identified in this work monitored in real time. From this real time monitoring a constantly updating remaining useful life estimation for every individual component could be implemented. Given the scarcity of data used to develop the models, it would be beneficial if these models could be updated when new data becomes available which could be fed into the model to improve predictions. These models could also consider possible dependencies between the transition times amongst failure states. As part of this effort other methods for determination of covariate significance should be investigated. For example, future work could focus on the development of a full Bayesian stochastic variable selection, allowing a computationally efficient selection of the most influent covariates, extendable to cases where a large number of them are available.
2. A full factorial design of experiments could be conducted, using a much larger sample size, studying the effects that the chemical exposure conditions have on EPDM degradation. This would constitute a much more substantial body of work than was feasible in this investigation. While this work characterises for the first time the physics of the degradation process and clarifies that the chemicals under investigation do in fact impact material degradation, one of its limitations was the sample size. This did not allow for a more robust statistical determination or ranking of the exposure types in terms of their effects on material degradation. In particular, the effects of material compression during chemical exposure could be expanded to include a full investigation of the environmental stress cracking resistance of EPDM.
3. In addition to virtual sensorisation, condition monitoring techniques for EPDM valve diaphragms can be explored, the output of which could be used in isolation or could be fed into a prognostic model. Given the strict regulatory requirements of the biopharmaceutical industry, an optimal solution would be sensorisation of the non-product contact portion of the valve hardware. This way there would be no additional sensorisation in the process stream, and many quality control regulation conflicts would be avoided. However, sensor stability, and of course cost-benefit analysis, will ultimately determine if such a solution would be effective in the biopharmaceutical industry.
4. In relation to human factors analysis, further research in this area could greatly improve the provision of parametric predictive models. A limitation of this study was the small sample size of technicians used in gathering the data for the model. This was a result of practical considerations and the novelty of the research. Future research should make use of a larger sample size where

possible to capture a wider cross-section of technician abilities and views to achieve a more reliable input to the model. Other methods for collecting the required data from technicians, such as the Delphi technique, could also be explored. If all appropriate PSFs can be quantitatively accounted for within otherwise best practice maintenance procedures, it is the authors' belief that the effect of those PSFs would be highlighted through the suboptimal lifetime of components. It is recommended that further research in this area could also investigate the feasibility of incorporating some of the existing HRA techniques in prognostic models, or could initially use a simplified approach of utilising maintainer feedback to generate a confidence interval for the possibility of human error having occurred which could then be integrated into a probabilistic weighting of early component failure.

References

[1] Okoh, C., Roy, R., Mehnen, J., and Redding, L., (2014), "Overview of Remaining Useful Life prediction techniques in Through-life Engineering Services," *Procedia CIRP*, 16, pp. 158–163.

[2] Roy, R., Erkoyuncu, J. A., and Shaw, A., (2013), "The Future of Maintenance for Industrial Product-Service Systems (Keynote Paper)," Product-Service Integration for Sustainable Solutions: Proceedings of the 5th CIRP International Conference on Industrial Product-Service Systems, Bochum, Germany, March 14th - 15th, 2013, H. Meier, ed., Springer Berlin Heidelberg, Berlin, Heidelberg, pp. 1–15.

[3] Roy, R., and Cheruvu, K. S., (2009), "A competitive framework for industrial product-service systems," *International Journal of Internet Manufacturing and Services*, 2(1), p. 4.

[4] Mobley, R. K., (2002), "An introduction to predictive maintenance," Butterworth-Heinemann, New York.

[5] Roy, R., Shaw, A., Erkoyuncu, J. A., and Redding, L., (2013), "Through-Life Engineering Services," *Measurement and Control*, 46(6), pp. 172–175.

[6] Masood, T., Roy, R., Harrison, A., Xu, Y., Gregson, S., and Reeve, C., (2015), "Integrating through-life engineering service knowledge with product design and manufacture," *International Journal of Computer Integrated Manufacturing*, 28(1), pp. 59–74.

[7] Jardine, A. K. S., Lin, D., and Banjevic, D., (2006), "A review on machinery diagnostics and prognostics implementing condition-based maintenance," *Mechanical Systems and Signal Processing*, 20(7), pp. 1483–1510.

[8] Maggard, B. N., and Rhyne, D. M., (1992), "Total productive maintenance: A timely integration of production and maintenance," *Production and Inventory Management Journal*, 33(4), pp. 6–10.

[9] Garg, A., and Deshmukh, S. G., (2006), "Maintenance management: literature review and directions," *Journal of Quality in Maintenance Engineering*, 12(3), pp. 205–238.

[10] Cholasuke, C., Bhardwa, R., and Antony, J., (2004), "The status of maintenance management in UK manufacturing organisations: results from a pilot survey," *Journal of Quality in Maintenance Engineering*, 10(1), pp. 5–15.

[11] Swanson, L., (2003), "An information-processing model of maintenance management," *International Journal of Production Economics*, 83(1), pp. 45–64.

[12] Swanson, L., (2001), "Linking maintenance strategies to performance," *International Journal of Production Economics*, 70(3), pp. 237–244.

[13] Salonen, A., and Deleryd, M., (2011), "Cost of poor maintenance," *Journal of Quality in Maintenance Engineering*, 17(1), pp. 63–73.

[14] Alsyouf, I., (2007), "The role of maintenance in improving companies' productivity and profitability," *International Journal of Production Economics*, 105(1), pp. 70–78.

[15] Ahuja, I. P. S., and Khamba, J. S., (2008), "Total productive maintenance: literature review and directions," *International Journal of Quality & Reliability Management*, 25(7), pp. 709–756.

[16] Wu, S., Gebraeel, N., Lawley, M. A., and Yih, Y., (2007), "A Neural Network Integrated Decision Support System for Condition-Based Optimal Predictive Maintenance Policy," *IEEE Transactions on Systems, Man, and Cybernetics—Part A: Systems and Humans*, 37(2), pp. 226–236.

[17] Kalgren, P., Byington, C., Roemer, M., and Watson, M., (2006), "Defining PHM, A Lexical Evolution of Maintenance and Logistics," 2006 IEEE Autotestcon, IEEE, pp. 353–358.

[18] Zio, E., (2012), "Prognostics and Health Management of Industrial Equipment," Diagnostics and Prognostics of Engineering Systems: Methods and Techniques, S. Kadry, ed., IGI Global, pp. 333–356.

[19] Rader, R. A., (2008), "(Re)defining Biopharmaceutical.," *Nature Biotechnology*, 26(7), pp. 743–51.

[20] McCamish, M., and Woollett, G., (2011), "Worldwide experience with biosimilar development," *mAbs*, 3(2), pp. 209–217.

[21] Roger, S. D., (2010), "Biosimilars: current status and future directions," *Expert Opinion on Biological Therapy*, 10(7), pp. 1011–1018.

[22] (2014), "Biopharmaceuticals," *IDA Ireland* [Online]. Available: http://www.idaireland.com/business-in-ireland/industry-sectors/bio-pharmaceuticals/. [Accessed: 24-Nov-2014].

[23] Huynh, K. T., Barros, A., and Bérenguer, C., (2012), "Maintenance Decision-Making for Systems Operating Under Indirect Condition Monitoring : Value of Online Information and Impact of Measurement Uncertainty," *IEEE Transactions on Reliability*, 61(2), pp. 410–425.

[24] Souza, F. A. A., Araújo, R., and Mendes, J., (2016), "Review of soft sensor methods for regression applications," *Chemometrics and Intelligent Laboratory Systems*, 152, pp. 69–79.

[25] Ibargüengoytia, P. H., Delgadillo, M. A., García, U. A., and Reyes, A., (2013), "Viscosity virtual sensor to control combustion in fossil fuel power plants," *Engineering Applications of Artificial Intelligence*, 26(9), pp. 2153–2163.

[26] Fortuna, L., Graziani, S., Rizzo, A., and Xibilia, M. G., (2007), "Soft Sensors for Monitoring and Control of Industrial Processes," Springer London, London.

[27] Kadlec, P., Gabrys, B., and Strandt, S., (2009), "Data-driven Soft Sensors in the process industry," *Computers and Chemical Engineering*, 33(4), pp. 795–814.

[28] Coble, J. B., (2010), "Merging Data Sources to Predict Remaining Useful Life – An Automated Method to Identify Prognostic Parameters," University of Tennessee, Knoxville.

[29] James Walker & Co. Ltd., (2011), "Elastomers in bioprocessing EPDM gaskets: What debate?," International Society for Pharmaceutical Engineering Conference, International Society for Pharmaceutical Engineering, Orlando, Florida, p. 37.

[30] Jones, S., (2013), "The Future of Valves and Diaphragms Supply," *BioPharm International*, pp. 32–33.

[31] Keeter, B., (2002), "Managing Availability for Improved Bottom-Line Results," *ARMS Reliability Engineers USA LLC* [Online]. Available: http://reliabilityweb.com/index.php/articles/managing_availability_for_improved_bottom-line_results. [Accessed: 24-Sep-2015].

[32] Zio, E., and Compare, M., (2013), "Evaluating maintenance policies by quantitative modeling and analysis," *Reliability Engineering & System Safety*, 109, pp. 53–65.

[33] Tracht, K., Goch, G., Schuh, P., Sorg, M., and Westerkamp, J. F., (2013), "Failure probability prediction based on condition monitoring data of wind energy systems for spare parts supply," *CIRP Annals - Manufacturing Technology*, pp. 1–4.

[34] Alsyouf, I., (2009), "Maintenance practices in Swedish industries: Survey results," *International Journal of Production Economics*, 121(1), pp. 212–223.

[35] Jonsson, P., (1997), "The status of maintenance management in Swedish manufacturing firms," *Journal of Quality in Maintenance Engineering*, 3(4), pp. 233–258.

[36] Aberdeen Group, (2006), "Collaborative Asset Maintenance Strategies: Redefining the Roles of Product Manufacturers and Operators in the Service Chain," Boston, MA.

[37] Saxena, A., (2007), “Knowledge-Based Architecture for Integrated Condition Based Maintenance of Engineering Systems,” Georgia Institute of Technology.

[38] Rausand, M., (1998), “Reliability centered maintenance,” *Reliability Engineering & System Safety*, 60(2), pp. 121–132.

[39] Malik, M. A. K., (1979), “Reliable Preventive Maintenance Scheduling,” *AIIE Transactions*, 11(3), pp. 221–228.

[40] Sikorska, J. Z., Hodkiewicz, M., and Ma, L., (2011), “Prognostic modelling options for remaining useful life estimation by industry,” *Mechanical Systems and Signal Processing*, 25(5), pp. 1803–1836.

[41] Smith, A. M., (1992), “Reliability-Centered Maintenance,” McGraw-Hill, New York.

[42] Chen, D., and Trivedi, K. S., (2002), “Closed-form analytical results for condition-based maintenance,” *Reliability Engineering and System Safety*, 76(1), pp. 43–51.

[43] Marseguerra, M., Zio, E., and Podofillini, L., (2002), “Condition-based maintenance optimization by means of genetic algorithms and Monte Carlo simulation,” *Reliability Engineering & System Safety*, 77(2), pp. 151–165.

[44] Vachtsevanos, G., Lewis, F. L., Roemer, M., Hess, A., and Wu, B., (2006), “Intelligent Fault Diagnosis and Prognosis for Engineering Systems,” John Wiley & Sons, Inc., Hoboken, New Jersey.

[45] Jemielniak, K., O’Donnell, G., Teti, R., and Dornfeld, D., (2010), “Advanced monitoring of machining operations,” *CIRP Annals - Manufacturing Technology*, 59(2), pp. 717–739.

[46] Hu, J., Zhu, Y., Huang, H., and Lu, J., (2012), “Recent advances in shape–memory polymers: Structure, mechanism, functionality, modeling and applications,” *Progress in Polymer Science*, 37(12), pp. 1720–1763.

[47] Kang, I., Heung, Y. Y., Kim, J. H., Lee, J. W., Gollapudi, R., Subramaniam, S., Narasimhadevara, S., Hurd, D., Kirikera, G. R., Shanov, V., Schulz, M. J., Shi, D., Boerio, J., Mall, S., and Ruggles-Wren, M., (2006), “Introduction to carbon nanotube and nanofiber smart materials,” *Composites Part B: Engineering*, 37(6), pp. 382–394.

[48] Yu, M.-F., Files, B. S., Arepalli, S., and Ruoff, R. S., (2000), “Tensile Loading of Ropes of Single Wall Carbon Nanotubes and their Mechanical Properties,” *Physical Review Letters*, 84(24), pp. 5552–5555.

[49] Krishnan, A., Dujardin, E., Ebbesen, T. W., Yianilos, P. N., and Treacy, M. M. J., (1998), “Young’s modulus of single-walled nanotubes,” *Physical Review B*, 58(20), pp. 14013–14019.

[50] Benning, P. J., Poirier, D. M., Ohno, T. R., Chen, Y., Jost, M. B., Stepniak, F., Kroll, G. H., Weaver, J. H., Fure, J., and Smalley, R. E., (1992), “C-60 and C-70 fullerenes and potassium fullerides,” *Physical Review B*, 45(12), pp. 6899–6913.

[51] Iijima, S., (1991), “Helical microtubules of graphitic carbon,” *Nature*, 354(6348), pp. 56–58.

[52] Kong, J., (2000), “Nanotube Molecular Wires as Chemical Sensors,” *Science*, 287(5453), pp. 622–625.

[53] Baughman, R. H., Zakhidov, A. A., and Heer, W. A. de, (2002), “Carbon Nanotubes--the Route Toward Applications,” *Science*, 297(5582), pp. 787–792.

[54] Kreupl, F., Graham, A. P., Liebau, M., Duesberg, G. S., Seidel, R., and Unger, E., (2006), “Carbon nanotubes for interconnect applications,” IEDM Technical Digest. IEEE International Electron Devices Meeting, 2004., IEEE, pp. 683–686.

[55] Allen, M. J., Tung, V. C., and Kaner, R. B., (2010), “Honeycomb carbon: A review of graphene,” *Chemical Reviews*, 110(1), pp. 132–145.

[56] Stankovich, S., Dikin, D. A., Dommett, G. H. B., Kohlhaas, K. M., Zimney, E. J., Stach, E. A., Piner, R.

D., Nguyen, S. T., and Ruoff, R. S., (2006), "Graphene-based composite materials," *Nature*, 442(7100), pp. 282–286.

[57] Boland, C. S., Khan, U., Backes, C., Neill, A. O., Mccauley, J., Duane, S., Shanker, R., Liu, Y., Jurewicz, I., Dalton, A. B., and Coleman, J. N., (2014), "Terms of Use Bodily Motion Sensors Based on Graphene À Rubber Composites," (Xx), pp. 8819–8830.

[58] Sun, L., Huang, W. M., Ding, Z., Zhao, Y., Wang, C. C., Purnawali, H., and Tang, C., (2012), "Stimulus-responsive shape memory materials: A review," *Materials & Design*, 33, pp. 577–640.

[59] Leng, J., Lan, X., Liu, Y., and Du, S., (2011), "Shape-memory polymers and their composites: Stimulus methods and applications," *Progress in Materials Science*, 56(7), pp. 1077–1135.

[60] Ratna, D., and Karger-Kocsis, J., (2008), "Recent advances in shape memory polymers and composites: a review," *Journal of Materials Science*, 43(1), pp. 254–269.

[61] Murphy, E. B., and Wudl, F., (2010), "The world of smart healable materials," *Progress in Polymer Science*, 35(1–2), pp. 223–251.

[62] White, S. R., Sottos, N. R., Geubelle, P. H., Moore, J. S., Kessler, M. R., Sriram, S. R., Brown, E. N., and Viswanathan, S., (2001), "Autonomic healing of polymer composites," *Nature*, 409(6822), pp. 794–797.

[63] Naebe, M., Abolhasani, M. M., Khayyam, H., Amini, A., and Fox, B., (2016), "Crack Damage in Polymers and Composites: A Review," *Polymer Reviews*, 56(1), pp. 31–69.

[64] Ismail, H., Pasbakhsh, P., Fauzi, M. N. A., and Abu Bakar, a., (2008), "Morphological, thermal and tensile properties of halloysite nanotubes filled ethylene propylene diene monomer (EPDM) nanocomposites," *Polymer Testing*, 27(7), pp. 841–850.

[65] Su, J., Chen, S., and Zhang, J., (2011), "Effect of hot-air aging on properties of EPDM/SmBO3/EAA and EPDM/ATO/EAA composites," *Journal of Composite Materials*, 46(5), pp. 589–602.

[66] Sutanto, P., (2006), "Development of a Continuous Process for EPDM Devulcanization in an Extruder," University of Groningen.

[67] Salamone, J. C., Demby, A., and Alley, M., eds., (1996), "Ethylene-Propylene Elastomers," Polymeric Materials Encyclopedia: Volume 3 D-E, CRC Press Inc., Baton-Rouge, Florida, p. 9600.

[68] Kim, J.-H., and Kim, G.-H., (2014), "Effect of orientation and content of carbon based fillers on thermal conductivity of ethylene-propylene-diene/filler composites," *Journal of Applied Polymer Science*, 131(21).

[69] Seo, G.-B., and Kim, G.-H., (2014), "Effect of processing parameters on the surface resistivity of ethylene propylene diene terpolymer/multiwalled carbon nanotube nanocomposites," *Journal of Applied Polymer Science*, 131(8), p. n/a-n/a.

[70] Valentini, L., Biagiotti, J., Kenny, J. M., and Lopez Manchado, M. A., (2003), "Physical and mechanical behavior of single-walled carbon nanotube/polypropylene/ethylene-propylene-diene rubber nanocomposites," *Journal of Applied Polymer Science*, 89(10), pp. 2657–2663.

[71] van Duin, M., Orza, R., Peters, R., and Chechik, V., (2010), "Mechanism of Peroxide Cross-Linking of EPDM Rubber," *Macromolecular Symposia*, 291–292(1), pp. 66–74.

[72] Orza, R. a., Magusin, P. C. M. M., Litvinov, V. M., Van Duin, M., and Michel, M. a J., (2009), "Mechanism for peroxide cross-linking of EPDM rubber from MAS13C NMR spectroscopy," *Macromolecules*, 42, pp. 8914–8924.

[73] Deepalaxmi, R., and Rajini, V., (2014), "Performance evaluation of gamma irradiated SiR-EPDM blends," *Nuclear Engineering and Design*, 273, pp. 602–614.

[74] ITT Corporation, (2011), "High Purity Diaphragm Valves," p. 108.

[75] Nah, C., Oh, J., Mensah, B., Jeong, K.-U., Ahn, D. U., Kim, S.-J., Lee, Y., and Nam, S.-H., (2015), "Effects of thermal aging on degradation mechanism of flame retardant-filled ethylene-propylene-diene termonomer compounds," *Journal of Applied Polymer Science*, 132(4), pp. 1–9.

[76] Blackmore, P. D., Birtwhistle, D., Cash, G., and George, G. A., (1998), "Condition assessment of EPDM composite insulators using FTIR spectroscopy," *IEEE Transactions on Dielectrics and Electrical Insulation*, 5(1), pp. 132–141.

[77] Birtwhistle, D., Cash, G., George, G. A., and Hinde, D., (2006), "New Techniques for Estimating the Condition of High Voltage Polymeric Insulators," Engineering Asset Management, J. Mathew, J. Kennedy, L. Ma, A. Tan, and D. Anderson, eds., Springer London, London, pp. 949–956.

[78] Amin, M., Akbar, M., and Khan, M., (2007), "Aging Investigations of Polymeric Insulators: Overview and Bibliography," *IEEE Electrical Insulation Magazine*, 23(4), pp. 44–50.

[79] Santos, R. P., Oliveira Junior, M. S. De, Mattos, E. D. C., Diniz, M. F., and Dutra, R. D. C. L., (2013), "Study by FT-IR Technique and Adhesive Properties of Vulcanized EPDM Modified with Plasma," *Journal of Aerospace Technology and Management*, 5(1), pp. 65–74.

[80] Abdel-Aziz, M. M., and Basfar, A. A., (2000), "Aging of ethylene-propylene diene rubber (EPDM) vulcanized by γ-radiation," *Polymer Testing*, 19(5), pp. 591–602.

[81] Deepalaxmi, R., and Rajini, V., (2014), "Gamma and electron beam irradiation effects on SiR-EPDM blends," *Journal of Radiation Research and Applied Sciences*, pp. 1–8.

[82] Nair, T. M., Kumaran, M. G., and Unnikrishnan, G., (2004), "Mechanical and aging properties of cross-linked ethylene propylene diene rubber / styrene butadiene rubber blends," *Journal of Applied Polymer Science*, 93(6), pp. 2606–2621.

[83] Nair, T. M., Kumaran, M. G., Unnikrishnan, G., and Kunchandy, S., (2008), "Ageing studies of ethylene propylene diene monomer rubber/styrene butadiene rubber blends: Effects of heat, ozone, gamma radiation, and water," *Journal of Applied Polymer Science*, 107(5), pp. 2923–2929.

[84] Seo, Y.-D., Lee, H.-S., Kim, Y.-S., and Song, C.-S., (2011), "A Study on the Aging Degradation of Ethylene-Propylene-Diene Monomer (EPDM) Under Loca Condition," *Nuclear Engineering and Technology*, 43(3), pp. 279–286.

[85] Zhao, Q., Li, X., and Gao, J., (2007), "Aging of ethylene–propylene–diene monomer (EPDM) in artificial weathering environment," *Polymer Degradation and Stability*, 92(10), pp. 1841–1846.

[86] Nabil, H., Ismail, H., and Azura, a. R., (2013), "Comparison of thermo-oxidative ageing and thermal analysis of carbon black-filled NR/Virgin EPDM and NR/Recycled EPDM blends," *Polymer Testing*, 32(4), pp. 631–639.

[87] Delor-jestin, F., Lacoste, J., Barrois-oudin, N., Cardinet, C., and Lemaire, J., (2000), "Photo , thermal and natural ageing of ethylene propylene diene monomer (EPDM) rubber used in automotive applications. Influence of carbon black , crosslinking and stabilizing agents," *Polymer Degradation and Stability*, 67(3), pp. 469–477.

[88] Kwak, S. B., and Choi, N. S., (2011), "Thermo-Oxidative Degradation of a Carbon Black Compounded EPDM Rubber Hose," *International Journal of Automotive Technology*, 12(3), p. 401−408.

[89] Delor, F., Teissedre, G., Baba, M., and Lacoste, J., (1998), "Ageing of EPDM—2. Role of hydroperoxides in photo- and thermo-oxidation," *Polymer Degradation and Stability*, 60(2–3), pp. 321–331.

[90] Rana, S., (2006), "Preparation and Performance Evaluation of EPDM Nanocomposites under Accelerated

Weathering," *Journal of Thermoplastic Composite Materials*, 19(5), pp. 461–474.

[91] McGrath, P. B.; Crudele, F. D.; Burns, C., (2002), "Accelerated aging of polymer insulators," 2002 Annual Report Conference on Electrical Insulation and Dielectric Phenomena, pp. 379–382.

[92] Mitra, S., Ghanbari-Siahkali, A., Kingshott, P., Hvilsted, S., and Almdal, K., (2006), "An investigation on changes in chemical properties of pure ethylene-propylene-diene rubber in aqueous acidic environments," *Materials Chemistry and Physics*, 98(2–3), pp. 248–255.

[93] Mitra, S., Ghanbari-Siahkali, A., and Almdal, K., (2006), "A novel method for monitoring chemical degradation of crosslinked rubber by stress relaxation under tension," *Polymer Degradation and Stability*, 91, pp. 2520–2526.

[94] Mitra, S., Ghanbari-Siahkali, A., Kingshott, P., Rehmeier, H. K., Abildgaard, H., and Almdal, K., (2006), "Chemical degradation of crosslinked ethylene-propylene-diene rubber in an acidic environment. Part II. Effect of peroxide crosslinking in the presence of a coagent," *Polymer Degradation and Stability*, 91(1), pp. 81–93.

[95] Nandakumar, N., and Kurian, P., (2013), "Effect of chemical degradation on the mechanical properties of ethylene-propylene-diene (5-ethylidene-2-norbornene) terpolymer-BaSO4 nano composites," *Materials and Design*, 43, pp. 118–124.

[96] Harper, C. A., (2000), "Modern Plastics Handbook," McGraw-Hill, New York, NY.

[97] Redline, E. M., Celina, M. C., Harris, C. E., Giron, N. H., Sugama, T., and Pyatina, T., (2017), "Anomalous aging of EPDM and FEPM under combined thermo-oxidative and hydrolytic conditions," *Polymer Degradation and Stability*, 146, pp. 317–326.

[98] Pourmand, P., Hedenqvist, M. S., Furó, I., and Gedde, U. W., (2017), "Deterioration of highly filled EPDM rubber by thermal ageing in air: Kinetics and non-destructive monitoring," *Polymer Testing*, 64(October), pp. 267–276.

[99] Dijkhuis, K. a J., Noordermeer, J. W. M., and Dierkes, W. K., (2009), "The relationship between crosslink system, network structure and material properties of carbon black reinforced EPDM," *European Polymer Journal*, 45(11), pp. 3302–3312.

[100] Krevelen, D. W. van, (2009), "Properties of Polymers," Elsevier, Boston, MA.

[101] George, J., Bhagawan, S. S., and Thomas, S., (1996), "Thermogravimetric and Dynamic Mechanical Thermal Analysis of Pineapple Fibre Reinforced Polyethylene Composites," *Journal of Thermal Analysis*, 47, pp. 1121–1140.

[102] Beyler, C. L., and Hirschler, M. M., (2001), "Thermal Decomposition of Polymers," SFPE Handbook of Fire Protection Engineering, P.J. DiNenno, ed., National Fire Protection Association; Society of Fire Protection Engineers, Quincy, MA, pp. 110–131.

[103] Muraleedharan Nair, T., Kumaran, M. G., Unnikrishnan, G., and Pillai, V. B., (2009), "Dynamic Mechanical Analysis of Ethylene – Propylene – Diene Monomer Rubber and Styrene – Butadiene Rubber Blends," *Journal of Applied Polymer Science*, 112, pp. 72–81.

[104] Kok, C. M., and Yee, V. H., (1986), "The effects of crosslink density and crosslink type on the tensile and tear strengths of NR, SBR and EPDM gum vulcanizates," *European Polymer Journal*, 22(4), pp. 341–345.

[105] Pourmand, P., Linde, E., Hedenqvist, M. S., Furó, I., Dvinskikh, S. V., and Gedde, U. W., (2016), "Profiling of thermally aged EPDM seals using portable NMR, indenter measurements and IR spectroscopy facilitating separation of different deterioration mechanisms," *Polymer Testing*, 53, pp. 77–84.

[106] Planes, E., Chazeau, L., Vigier, G., and Fournier, J., (2009), "Evolution of EPDM networks aged by gamma irradiation – Consequences on the mechanical properties," *Polymer*, 50(16), pp. 4028–4038.

[107] Sanches, N. B., Cassu, S. N., Diniz, M. F., and Dutra, R. de C. L., (2014), "Characterization of Additives Typically Employed in EPDM Formulations by using FT-IR of Gaseous Pyrolyzates," *Polímeros Ciência e Tecnologia*, 24(3), pp. 269–275.

[108] ISO 7619-1, (2010), "Rubber, vulcanized or thermoplastic - Determination of indentation hardness - Part 1: Durometer method (Shore hardness)."

[109] Nasir, M., and Teh, G. K., (1988), "The effects of various types of crosslinks on the physical properties of natural rubber," *European Polymer Journal*, 24(8), pp. 733–736.

[110] ISO 178, (2001), "Plastics - Determination of flexural properties."

[111] ISO 815-1, (2008), "Rubber, vulcanized or thermoplastic - Determination of compression set - Part 1: At ambient or elevated temperatures."

[112] Stelescu, D. M., Airinei, A., Homocianu, M., Fifere, N., Timpu, D., and Aflori, M., (2013), "Structural characteristics of some high density polyethylene/EPDM blends," *Polymer Testing*, 32(2), pp. 187–196.

[113] Caruso, M. M., Davis, D. A., Shen, Q., Odom, S. A., Sottos, N. R., White, S. R., and Moore, J. S., (2009), "Mechanically-Induced Chemical Changes in Polymeric Materials," *Chemical Reviews*, 109(11), pp. 5755–5798.

[114] He, C., Wang, Y., Luo, Y., Kong, L., and Peng, Z., (2013), "Thermal degradation kinetics and mechanism of epoxidized natural rubber," *Journal of Polymer Engineering*, 33(4), pp. 331–335.

[115] Muraleedharan Nair, T., (2007), "Development and characterization of Ethylene propylene diene monomer rubber/Styrene butadiene rubber blends," Mahatma Gandhi University, Kottayam Karala, India.

[116] Setaram Instrumentation, "AN132 – Compositional analysis of rubber by TGA" [Online]. Available: http://www.setaram.com/application-notes/an132-compositional-analysis-of-rubber-by-tga/. [Accessed: 21-Sep-2016].

[117] Suenaga, T., Noguchi, K., Okamoto, Y., Sekii, Y., and Miyake, K., (2007), "Effect of antioxidants on thermal degradation of EPDM and XLPE," Proceedings of 2008 International Conference on Condition Monitoring and Diagnosis, CMD 2008, pp. 294–298.

[118] Baba, M., Gardette, J.-L., and Lacoste, J., (1999), "Crosslinking on ageing of elastomers: I. Photoageing of EPDM monitored by gel, swelling and DSC measurements," *Polymer Degradation and Stability*, 63, pp. 121–126.

[119] Luque de Castro, M. D., and Priego-Capote, F., (2010), "Soxhlet extraction: Past and present panacea," *Journal of Chromatography A*, 1217(16), pp. 2383–2389.

[120] Yun, J., and Isayev, A. I., (2007), "The effect of high power ultrasound on EPDM gum in extrusion process," *Journal of Applied Polymer Science*, 105(6), pp. 3698–3707.

[121] Flory, P. J., and Rehner, J., (1943), "Statistical Mechanics of Cross-Linked Polymer Networks I. Rubberlike Elasticity," *The Journal of Chemical Physics*, 11(11), pp. 512–520.

[122] Valentín, J. L., Carretero-González, J., Mora-Barrantes, I., Chassé, W., and Saalwächter, K., (2008), "Uncertainties in the determination of cross-link density by equilibrium swelling experiments in natural rubber," *Macromolecules*, 41(13), pp. 4717–4729.

[123] Carey, M. B., and Koenig, R. H., (1991), "Reliability assessment based on accelerated degradation: a case study," *IEEE Transactions on Reliability*, 40(5), pp. 499–506.

[124] Elsayed, E. A., and Chen, A. C.-K., "Recent research and current issues in accelerated testing," SMC'98

Conference Proceedings. 1998 IEEE International Conference on Systems, Man, and Cybernetics (Cat. No.98CH36218), IEEE, pp. 4704–4709.

[125] Loon Ching Tang, and Dong Shang Chang, (1995), "Reliability prediction using nondestructive accelerated-degradation data: case study on power supplies," *IEEE Transactions on Reliability*, 44(4), pp. 562–566.

[126] Park, C., and Padgett, W. J., (2006), "Stochastic Degradation Models With Several Accelerating Variables," *IEEE Transactions on Reliability*, 55(2), pp. 379–390.

[127] Jefferson, A., and Kinsella, B., (2008), "'Corrodere' of non-metallic materials in the mining, oil & gas industries (MOGI)," EUROCORR 2008 - European Corrosion Congress: Managing Corrosion for Sustainability, Edinburgh, United Kingdom, p. 135.

[128] Dixon, D., and Boyd, A., (2011), "Degradation and accelerated ageing of poly(ether block amide) thermoplastic elastomers," *Polymer Engineering & Science*, 51(11), pp. 2203–2209.

[129] Hamid, S. H., and Amin, M. B., (1995), "Lifetime prediction of polymers," *Journal of Applied Polymer Science*, 55(10), pp. 1385–1394.

[130] Miyano, Y., Nakada, M., and Cai, H., (2008), "Formulation of Long-term Creep and Fatigue Strengths of Polymer Composites Based on Accelerated Testing Methodology," *Journal of Composite Materials*, 42(18), pp. 1897–1919.

[131] Le Gac, P. Y., Choqueuse, D., Paris, M., Recher, G., Zimmer, C., and Melot, D., (2013), "Durability of polydicyclopentadiene under high temperature, high pressure and seawater (offshore oil production conditions)," *Polymer Degradation and Stability*, 98(3), pp. 809–817.

[132] Lee, S. H., Yoo, S. S., Kim, D. E., Kang, B. S., and Kim, H. E., (2012), "Accelerated wear test of FKM elastomer for life prediction of seals," *Polymer Testing*, 31(8), pp. 993–1000.

[133] Zio, E., (2009), "Reliability engineering: Old problems and new challenges," *Reliability Engineering & System Safety*, 94(2), pp. 125–141.

[134] Crumer, A. M., (2008), "Comparison Between Weibull and Cox Proportional Hazards Models," Southeast Missouri State University.

[135] Nelson, W., (1982), "Applied Life Data Analysis," John Wiley & Sons, Inc., Hoboken, NJ, USA.

[136] Varde, P. V., (2009), "Role of Statistical Vis-A-Vis Physics-Of- Failure Methods in Reliability Engineering," *Journal of Reliability and Statistical Studies*, 2(1), pp. 41–51.

[137] Venkatasubramanian, V., Rengaswamy, R., and Ka, S. N., (2003), "A review of process fault detection and diagnosis Part III : Process history based methods," *Computers & Chemical Engineering*, 27(3), pp. 327–346.

[138] Sim, S. H., and Endrenyi, J., (1988), "Optimal preventive maintenance with repair," *IEEE Transactions on Reliability*, 37(1), pp. 92–96.

[139] Compare, M., Martini, F., Mattafirri, S., Carlevaro, F., and Zio, E., (2015), "Semi-Markov model for the oxidation degradation mechanism in gas turbine nozzles," *IEEE Transactions on Reliability*, (Manuscript submitted for Publication).

[140] Baraldi, P., Balestrero, A., Compare, M., Benetrix, L., Despujols, A., and Zio, E., (2013), "A Modeling Framework for Maintenance Optimization of Electrical Components Based on Fuzzy Logic and Effective Age," *Quality and Reliability Engineering International*, 29(3), pp. 385–405.

[141] Moghaddass, R., and Zuo, M. J., (2014), "An integrated framework for online diagnostic and prognostic health monitoring using a multistate deterioration process," *Reliability Engineering & System Safety*, 124,

pp. 92–104.

[142] Liu, Y., Lin, P., Li, Y.-F., and Huang, H.-Z., (2015), "Bayesian Reliability and Performance Assessment for Multi-State Systems," *IEEE Transactions on Reliability*, 64(1), pp. 394–409.

[143] Levitin, G., Lisnianski, A., and Ushakov, I., (2003), "Reliability of Multi-state Systems: A Historical Overview," Mathematical and Statistical Methods in Reliability. Series On Quality, Reliability and Engineering Statistics, B. Lindqvist, and K. Doksum, eds., World Scientific, New Jersey, pp. 123–138.

[144] Bousquet, N., (2010), "Elicitation of Weibull priors," p. 21.

[145] Baraldi, P., Compare, M., and Zio, E., (2013), "Maintenance policy performance assessment in presence of imprecision based on Dempster–Shafer Theory of Evidence," *Information Sciences*, 245, pp. 112–131.

[146] Compare, M., Baraldi, P., Bani, I., Zio, E., and McDonnell, D., (2016), "A Bayesian Proportional Hazards Model for Multi-State Degradation Processes," *IEEE Transactions on Reliability*, (Manuscript submitted for Publication).

[147] Bousquet, N., (2010), "Eliciting vague but proper maximal entropy priors in Bayesian experiments," *Statistical Papers*, 51(3), pp. 613–628.

[148] Cox, D. R., and Oakes, D., (1987), "Analysis of Survival Data," Chapman and Hall, London.

[149] Kiassat, C., Safaei, N., and Banjevic, D., (2014), "Choosing the optimal intervention method to reduce human-related machine failures," *European Journal of Operational Research*, 233(3), pp. 604–612.

[150] Cox, D. R., (1972), "Regression Models and Life-Tables," *Journal of the Royal Statistical Society*, 34(2), pp. 187–220.

[151] Ansell, J., and Philipps, M., (1997), "Practical aspects of modelling of repairable systems data using proportional hazards models," *Reliability Engineering & System Safety*, 58, pp. 165–171.

[152] Kumar, D., and Klefsjo, B., (1994), "Proportional hazards model: a review," *Reliability Engineering and System Safety*, 44, pp. 177–188.

[153] Marton, I., Sanchez, A. I., and Martorell, S., (2015), "Ageing PSA incorporating effectiveness of maintenance and testing," *Reliability Engineering and System Safety*, 139, pp. 131–140.

[154] Kiassat, C., Safaei, N., and Banjevic, D., (2013), "Effects of operator learning on production output: a Markov chain approach," *Journal of the Operational Research Society*, 65(12), pp. 1814–1823.

[155] Ahmad, R., and Kamaruddin, S., (2012), "An overview of time-based and condition-based maintenance in industrial application," *Computers & Industrial Engineering*, 63(1), pp. 135–149.

[156] Schwabacher, M., and Goebel, K., (2007), "A Survey of Artificial Intelligence for Prognostics," AAAI Fall Symposium, NASA Ames Research Center, Moffett Field, California, pp. 107–114.

[157] Si, X.-S. S., Wang, W., Hu, C.-H. H., and Zhou, D.-H. H., (2011), "Remaining useful life estimation – A review on the statistical data driven approaches," *European Journal of Operational Research*, 213(1), pp. 1–14.

[158] Le Son, K., Fouladirad, M., Barros, A., Levrat, E., and Iung, B., (2013), "Remaining useful life estimation based on stochastic deterioration models: A comparative study," *Reliability Engineering & System Safety*, 112, pp. 165–175.

[159] Yan, J., Koç, M., and Lee, J., (2004), "A prognostic algorithm for machine performance assessment and its application," *Production Planning & Control*, 15(8), pp. 796–801.

[160] Wang, W., (2000), "A model to determine the optimal critical level and the monitoring intervals in condition-based maintenance," *International Journal of Production Research*, 38(6), pp. 1425–1436.

[161] Liao, H., Zhao, W., and Guo, H., (2006), "Predicting remaining useful life of an individual unit using

proportional hazards model and logistic regression model," *RAMS '06. Annual Reliability and Maintainability Symposium, 2006.*, 0(C), pp. 127–132.

[162] Zumel, N., (2011), "The Simpler Derivation of Logistic Regression," *Win-Vector LLC Data Science Blog* [Online]. Available: http://www.win-vector.com/blog/2011/09/the-simpler-derivation-of-logistic-regression/. [Accessed: 24-Jun-2015].

[163] Hosmer, D. W., Lemeshow, S., and Sturdivant, R. X., (2013), "Applied Logistic Regression," John Wiley & Sons, Inc., Hoboken, New Jersey.

[164] Giorgio, M., Guida, M., and Pulcini, G., (2011), "An age- and state-dependent Markov model for degradation processes," *IIE Transactions*, 43(9), pp. 621–632.

[165] Jenkinson, D., (2005), "The Elicitation of Probabilities – A Review of the Statistical Literature," BEEP Working Paper, Department of Probability and Statistics, University of Sheffield.

[166] Garthwaite, P. H., Kadane, J. B., and O'Hagan, A., (2005), "Statistical methods for eliciting probability distributions."

[167] Baraldi, P., Compare, M., and Zio, E., (2014), "Uncertainty treatment in expert information systems for maintenance policy assessment," *Applied Soft Computing Journal*, 22, pp. 297–310.

[168] Baraldi, P., Compare, M., and Zio, E., (2013), "Uncertainty analysis in degradation modeling for maintenance policy assessment," *Proceedings of the Institution of Mechanical Engineers, Part O: Journal of Risk and Reliability*, 227(3), pp. 267–278.

[169] Ge, H., and Asgarpoor, S., (2010), "Reliability evaluation of equipment and substations with fuzzy markov processes," *IEEE Transactions on Power Systems*, 25(3), pp. 1319–1328.

[170] Genschel, U., and Meeker, W. Q., (2010), "A Comparison of Maximum Likelihood and Median-Rank Regression for Weibull Estimation," *Quality Engineering*, 22(4), pp. 236–255.

[171] Czepiel, S. A., (2012), "Maximum Likelihood Estimation of Logistic Regression Models: Theory and Implementation," p. 23.

[172] Akaike, H., (1973), "Information theory as an extension of the maximum likelihood principle," Second International Symposium on Information Theory, B.N. Petrov, and F. Csaki, eds., Akademiai Kiado, Budapest, pp. 267–281.

[173] Pourhoseingholi, M. A., Hajizadeh, E., Moghimi Dehkordi, B., Safaee, A., Abadi, A., and Zali, M. R., (2007), "Comparing Cox regression and parametric models for survival of patients with gastric carcinoma.," *Asian Pacific journal of cancer prevention : APJCP*, 8(3), pp. 412–416.

[174] Williams, R., (2015), "Scalar Measures of Fit: Pseudo R2 and Information Measures (AIC & BIC)," Indiana.

[175] Cragg, J. G., and Uhler, R. S., (1970), "The Demand for Automobiles," *The Canadian Journal of Economics*, 3, pp. 386–406.

[176] Nagelkerke, N. J. D., (1991), "A note on a general definition of the coefficient of determination," *Biometrika*, 78(3), pp. 691–692.

[177] Kohavi, R., and Kohavi, R., (1997), "Wrappers for feature subset selection," *Artificial Intelligence*, 97(1–2), pp. 273–324.

[178] Zio, E., Baraldi, P., and Pedroni, N., (2006), "Selecting features for nuclear transients classification by means of genetic algorithms," *IEEE Transactions on Nuclear Science*, 53(3), pp. 1479–1493.

[179] Huda, S., Abdollahian, M., Mammadov, M., Yearwood, J., Ahmed, S., and Sultan, I., (2014), "A hybrid wrapper-filter approach to detect the source(s) of out-of-control signals in multivariate manufacturing

process," *European Journal of Operational Research*, 237(3), pp. 857–870.

[180] Uncu, Ö., and Türkşen, I. B., (2007), "A novel feature selection approach: Combining feature wrappers and filters," *Information Sciences*, 177(2), pp. 449–466.

[181] Kano, M., and Nakagawa, Y., (2008), "Data-based process monitoring, process control, and quality improvement: Recent developments and applications in steel industry," *Computers and Chemical Engineering*, 32(1–2), pp. 12–24.

[182] Yan, W., Shao, H., and Wang, X., (2004), "Soft sensing modeling based on support vector machine and Bayesian model selection," *Computers and Chemical Engineering*, 28(8), pp. 1489–1498.

[183] Kourti, T., (2005), "Application of latent variable methods to process control and multivariate statistical process control in industry," *International Journal of Adaptive Control and Signal Processing*, 19(4), pp. 213–246.

[184] Kresta, J. V., Marlin, T. E., and MacGregor, J. F., (1994), "Development of inferential process models using PLS," *Computers & Chemical Engineering*, 18(7), pp. 597–611.

[185] Mejdell, T., and Skogestad, S., (1991), "Composition Estimator in a Pilot-Plant Distillation Column Using Multiple Temperatures," *Society*, (1989), pp. 2555–2564.

[186] Mejdell, T., and Skogestad, S., (1991), "Estimation of distillation compositions from multiple temperature measurements using partial-least-squares regression," *Industrial & Engineering Chemistry Research*, 30(12), pp. 2543–2555.

[187] Lin, B., Recke, B., Knudsen, J. K. H., and Jørgensen, S. B., (2007), "A systematic approach for soft sensor development," *Computers and Chemical Engineering*, 31(5–6), pp. 419–425.

[188] Kourti, T., (2002), "Process analysis and abnormal situation detection: From theory to practice," *IEEE Control Systems Magazine*, 22(5), pp. 10–25.

[189] Kadlec, P., Grbić, R., and Gabrys, B., (2011), "Review of adaptation mechanisms for data-driven soft sensors," *Computers and Chemical Engineering*, 35(1), pp. 1–24.

[190] Dong, D., and McAvoy, T. J., (1996), "Nonlinear principal component analysis—Based on principal curves and neural networks," *Computers & Chemical Engineering*, 20(1), pp. 65–78.

[191] Abonyi, J., Farsang, B., and Kulcsar, T., (2014), "Data-driven development and maintenance of soft-sensors," 12th International Symposium on Applied Machine Intelligence and Informatics (SAMI), IEEE, pp. 239–244.

[192] Compare, M., Baraldi, P., Bani, I., Zio, E., and Mc Donnell, D., (2017), "Development of a Bayesian multi-state degradation model for up-to-date reliability estimations of working industrial components," *Reliability Engineering & System Safety*, 166, pp. 25–40.

[193] Jørgensen, K., Segtnan, V., Thyholt, K., and Næs, T., (2004), "A comparison of methods for analysing regression models with both spectral and designed variables," *Journal of Chemometrics*, 18(10), pp. 451–464.

[194] Wolpert, D. H., and Macready, W. G., (1997), "No free lunch theorems for optimization," *IEEE Transactions on Evolutionary Computation*, 1(1), pp. 67–82.

[195] Kano, M., Miyazaki, K., Hasebe, S., and Hashimoto, I., (1998), "Inferential Control of Distillation Composition Using Partial Least Squares Regression.," *Kagaku Kogaku Ronbunshu*, 24, pp. 425–430.

[196] Ruilan, L., Zhou, R., and Lingke, Z., (2016), "Soft Sensor of Melt Index Based on Sparse Least Square Support Vector Machine," pp. 9061–9064.

[197] Shimizu, K., (1996), "A tutorial review on bioprocess systems engineering," *Computers & chemical*

engineering, 20(6), pp. 915–941.

[198] Chéruy, A., (1997), "Software sensors in bioprocess engineering," *Journal of Biotechnology*, 52(3), pp. 193–199.

[199] Guenard, R., and Thurau, G., (2010), "Implementation of Process Analytical Technologies," Process Analytical Technology, John Wiley & Sons, Ltd, Chichester, UK, pp. 17–36.

[200] Helmdach, L., Feth, M. P., Minnich, C., and Ulrich, J., (2013), "Application of ATR-MIR spectroscopy in the pilot plant-Scope and limitations using the example of Paracetamol crystallizations," *Chemical Engineering and Processing: Process Intensification*, 70, pp. 184–197.

[201] Simon, L. L., Pataki, H., Marosi, G., Meemken, F., Hungerbühler, K., Baiker, A., Tummala, S., Glennon, B., Kuentz, M., Steele, G., Kramer, H. J. M., Rydzak, J. W., Chen, Z., Morris, J., Kjell, F., Singh, R., Gani, R., Gernaey, K. V, Louhi-Kultanen, M., O'Reilly, J., Sandler, N., Antikainen, O., Yliruusi, J., Frohberg, P., Ulrich, J., Braatz, R. D., Leyssens, T., von Stosch, M., Oliveira, R., Tan, R. B. H., Wu, H., Khan, M., O'Grady, D., Pandey, A., Westra, R., Delle-Case, E., Pape, D., Angelosante, D., Maret, Y., Steiger, O., Lenner, M., Abbou-Oucherif, K., Nagy, Z. K., Litster, J. D., Kamaraju, V. K., and Chiu, M.-S., (2015), "Assessment of Recent Process Analytical Technology (PAT) Trends: A Multiauthor Review," *Organic Process Research & Development*, 19(1), pp. 3–62.

[202] De Assis, A. J., and Filho, R. M., (2000), "Soft sensors development for on-line bioreactor state estimation," *Computers and Chemical Engineering*, 24(2–7), pp. 1099–1103.

[203] Desai, K., Badhe, Y., Tambe, S. S., and Kulkarni, B. D., (2006), "Soft-sensor development for fed-batch bioreactors using support vector regression," *Biochemical Engineering Journal*, 27(3), pp. 225–239.

[204] Coble, J. B., Ramuhalli, P., Bond, L. J., Hines, J. W., and Upadhyaya, B. R., (2012), "Prognostics and Health Management in Nuclear Power Plants: A Review of Technologies and Applications," VA.

[205] Casali, A., Gonzalez, G., Torres, F., Vallebuona, G., Castelli, L., and Gimenez, P., (1998), "Particle size distribution soft-sensor for a grinding circuit," *Powder Technology*, 99(1), pp. 15–21.

[206] Evans, P. C., and Annunziata, M., (2012), "Industrial Internet : Pushing the Boundaries of Minds and Machines."

[207] Engel, S. J., Gilmartin, B. J., Bongort, K., and Hess, A., (2000), "Prognostics, the Real Issues Involved with Predicting Life Remaining," Proceedings of IEEE Aerospace Conference, pp. 457–469.

[208] Sandborn, P., (2005), "A decision support model for determining the applicability of prognostic health management (PHM) approaches to electronic systems," Annual Reliability and Maintainability Symposium, 2005. Proceedings., IEEE, Arlington, VA, pp. 422–427.

[209] Zhao, W., Zio, E., and Baraldi, P., (2011), "Confidence in signal reconstruction by the Evolving Clustering Method," 2011 Prognostics and System Health Managment Confernece, IEEE, pp. 1–7.

[210] Saxena, A., Roychoudhury, I., and Celaya, J. R., (2010), "Requirements Specifications for Prognostics: An Overview," AIAA Infotech @ Aerospace, Atlanta, Georgia, pp. 1–16.

[211] Noroozi, A., Khakzad, N., Khan, F., Mackinnon, S., and Abbassi, R., (2013), "The role of human error in risk analysis: Application to pre- and post-maintenance procedures of process facilities," *Reliability Engineering and System Safety*, 119, pp. 251–258.

[212] Brune, R. L., Weinstein, M., and Fitzwater, M. E., (1983), "Peer-review study of the draft handbook for human-reliability analysis with emphasis on nuclear-power-plant applications, NUREG/CR-1278," Human Performance Technologies Inc., Thousand Oaks, California.

[213] Reason, J., (1990), "Human Error," Cambridge University Press, Cambridge.

[214] Dhillon, B. S., and Liu, Y., (2006), "Human error in maintenance: a review," *Journal of Quality in Maintenance Engineering*, 12(1), pp. 21–36.

[215] BioPhorum Operations Group, (2015), "Human Performance" [Online]. Available: http://www.biophorum.com/article/90/human-performance. [Accessed: 11-Mar-2015].

[216] Marx, D. A., and Graeber, R. C., (1994), "Human error in aircraft maintenance," Aviation psychology in practice, N. Johnston, N. McDonald, and R. Fuller, eds., Avebury, Aldershot, UK, pp. 87–104.

[217] Nakagawa, T., and Yasui, K., (1987), "Optimum Policies for a System with Imperfect Maintenance," *IEEE Transactions on Reliability*, R-36(5), pp. 631–633.

[218] Palaniappan, C., (2016), "Perspectives on human factors in a shifting operational environment," *Journal of Loss Prevention in the Process Industries*, 44, pp. 112–118.

[219] Okoh, P., and Haugen, S., (2014), "A study of maintenance-related major accident cases in the 21st century," *Process Safety and Environmental Protection*, 92(4), pp. 346–356.

[220] Tsang, A. H. C., (2002), "Strategic dimensions of maintenance management," *Journal of Quality in Maintenance Engineering*, 8(1), pp. 7–39.

[221] Saleh, J. H., and Marais, K., (2006), "Reliability: How much is it worth? Beyond its estimation or prediction, the (net) present value of reliability," *Reliability Engineering & System Safety*, 91(6), pp. 665–673.

[222] Lee, J., Ghaffari, M., and Elmeligy, S., (2011), "Self-maintenance and engineering immune systems: Towards smarter machines and manufacturing systems," *Annual Reviews in Control*, 35(1), pp. 111–122.

[223] Rasmussen, N. C., (1975), "Reactor safety study. An assessment of accident risks in U. S. commercial nuclear power plants. Executive Summary. WASH-1400 (NUREG-75/014)," Rockville, MD, USA.

[224] Khalaquzzaman, M., Kang, H. G., Kim, M. C., and Seong, P. H., (2011), "Optimization of periodic testing frequency of a reactor protection system based on a risk-cost model and public risk perception," *Nuclear Engineering and Design*, 241(5), pp. 1538–1547.

[225] Kvickström, K., (2010), "Maintenance optimization in nuclear power plants - modelling , analysis , and experimentation," University of Gothenburg.

[226] International Ergonomics Association, (2000), "What is ergonomics?" [Online]. Available: http://www.iea.cc/whats/index.html. [Accessed: 22-Jan-2015].

[227] The Nuclear Installations Inspectorate of the Health and Safety Executive, (2010), "Safety Assessment Principles for Nuclear Facilities Technical Assessment Guide T/AST/058 - Human Factors Integration," pp. 1–14.

[228] Kirwan, B., (1994), "A Guide to Practical Human Reliability Assessment," Taylor & Francis, London.

[229] Swain, A. D., and Guttmann, H. E., (1983), "Handbook of Human Reliability Analysis with Emphasis on Nuclear Power Plant Applications," Sandia National Laboratories, Albuquerque, New Mexico.

[230] Williams, J. C., (1986), "A proposed method for assessing and reducing human error," 9th Advances in Reliability Technology Symposium, University of Bradford.

[231] Gertman, D., Blackman, H., Marble, J., Byers, J., and Smith, C., (2005), "The SPAR-H human reliability analysis method," U.S. Nuclear Regulatory Commission: Division of Risk Analysis and Applications, Washington, DC, USA.

[232] Shorrock, S. T., and Kirwan, B., (1998), "TRACEr – a technique for the retrospective analysis of cognitive errors in Air Traffic Management," Engineering Psychology and Cognitive Ergonomics, D. Harris, ed., Ashgate Publishing, Aldershot, UK, UK, pp. 163–171.

[233] Carr, M. J., and Christer, A. H., (2003), "Incorporating the potential for human error in maintenance models," *Journal of the Operational Research Society*, 54(12), pp. 1249–1253.

[234] International Civil Aviation Organization (ICAO), (2003), "Human Factors Guidelines for Aircraft Maintenance Manual," p. 147.

[235] Australian Government Civil Aviation Authority, (2013), "Safety Behaviours: Human Factors for Engineers Resource Guide," p. 204.

[236] Ben-Daya, M., Duffuaa, S. O., Raouf, A., Knezevic, J., and Ait-Kadi, D., (2009), "Handbook of Maintenance Management and Engineering," Springer, London.

[237] Latorella, K. A., and Prabhu, P. V, (2000), "A review of human error in aviation maintenance and inspection," *International Journal of Industrial Ergonomics*, 26(2), pp. 133–161.

[238] Rankin, W., Hibit, R., Allen, J., and Sargent, R., (2000), "Development and evaluation of the Maintenance Error Decision Aid (MEDA) process," *International Journal of Industrial Ergonomics*, 26(2), pp. 261–276.

[239] Leão, B. P., Fitzgibbon, K. T., Puttini, L. C., and de Melo, G. P. B., (2008), "Cost-benefit analysis methodology for PHM applied to legacy commercial aircraft," IEEE Aerospace Conference, p. 12.

[240] Zhao, F., Tian, Z., and Zeng, Y., (2013), "Uncertainty Quantification in Gear Remaining Useful Life Prediction Through an Integrated Prognostics Method," *IEEE Transactions on Reliability*, 62(1), p. 14.

[241] Yu, B. Y., Syed Zubair, M. H. S., and Yang, M. C., (2013), "A Framework for System Design Optimization Based On Maintenance Scheduling With Prognostics and Health Management," Proceedings of ASME 2013 International Design Engineering Technical Conferences and Computers and Information in Engineering Conference, Portland, Oregan, p. 12.

[242] Farcasiu, M., and Prisecaru, I., (2014), "MMOSA - A new approach of the human and organizational factor analysis in PSA," *Reliability Engineering and System Safety*, 123, pp. 91–98.

[243] Chateauneuf, A., Cocheteux, F., Deffarges, F., and Sourget, F., (2011), "Reliability analysis of screwed connections in high-speed trains, considering fatigue, corrosion, and imperfect maintenance operations," *Proceedings of the Institution of Mechanical Engineers, Part O: Journal of Risk and Reliability*, 225(3), pp. 293–306.

[244] Aju Kumar, V. N., and Gandhi, O. P., (2011), "Quantification of human error in maintenance using graph theory and matrix approach," *Quality and Reliability Engineering International*, 27(8), pp. 1145–1172.

[245] Asadzadeh, S. M., and Azadeh, a., (2014), "An integrated systemic model for optimization of condition-based maintenance with human error," *Reliability Engineering and System Safety*, 124, pp. 117–131.

[246] Kiassat, C., and Konstandinidou, M., (2009), "Recognizing Significant Human-Related Factors Affecting System Reliability," Production & Operation Management Society (POMS) conference, Vancouver, BC, pp. 1–9.

[247] Kiassat, A. C., and Safaei, N., (2009), "Integrating human reliability analysis into a comprehensive maintenance optimization strategy," 4th World Congress on Engineering Asset Management: Engineering Asset Lifecycle Management, WCEAM 2009, Athens, Greece, pp. 561–566.

[248] Kiassat, A. C., (2013), "System Performance Analysis Considering Human-related Factors," University of Toronto.

[249] Chiu, C., Chiu, N.-H., and Hsu, C.-I., (2004), "Intelligent aircraft maintenance support system using genetic algorithms and case-based reasoning," *The International Journal of Advanced Manufacturing Technology*, 24(5–6), pp. 440–446.

[250] Devaney, M., and Cheetham, B., (2005), “Case-Based Reasoning for Gas Turbine Diagnostics,” 18th International FLAIRS Conference (FLAIRS-05).

[251] Varma, A., and Roddy, N., (1999), “ICARUS: design and deployment of a case-based reasoning system for locomotive diagnostics,” *Engineering Applications of Artificial Intelligence*, 12(6), pp. 681–690.

[252] Wiener, E. L., and Curry, R. E., (1980), “Flight-deck automation: Promises and problems,” *Ergonomics*, 23(10), pp. 995–1011.

[253] Crocoll, W. M., and Coury, B. G., (1990), “Status or Recommendation: Selecting the Type of Information for Decision Aiding,” Proceedings of the 34th Annual Meeting of the Human Factors & Ergonomic Society, Human Factors and Ergonomics Society, Santa Monica, CA, pp. 1524–1528.

[254] Sarter, N. B., and Schroeder, B., (2001), “Supporting Decision Making and Action Selection under Time Pressure and Uncertainty: The Case of In-Flight Icing,” *Human Factors*, 43(4), pp. 573–583.

[255] Salvendy, G., ed., (2012), “Handbook of Human Factors and Ergonomics,” John Wiley & Sons, Inc., Hoboken, NJ, USA.

[256] Jain, A. ., Duin, R. P. W., and Mao, J., (2000), “Statistical Pattern Recognition: A Review,” *IEEE Transactions on Pattern Analysis and Machine Intelligence*, 22(1), pp. 4–37.

[257] Yam, R. C. M., Tse, P. W., Li, L., and Tu, P., (2001), “Intelligent Predictive Decision Support System for Condition-Based Maintenance,” *The International Journal of Advanced Manufacturing Technology*, 17(5), pp. 383–391.

[258] Martignon, L., and Krauss, S., (2003), “Can l’homme eclaire be fast and frugal? Reconciling Bayesianism and bounded rationality,” Emerging perspectives on judgment and decision research, S. Schneider, and J. Shanteau, eds., Cambridge University Press, Cambridge, pp. 108–122.

[259] Lee, J., Kladwang, W., Lee, M., Cantu, D., Azizyan, M., Kim, H., Limpaecher, A., Yoon, S., Treuille, A., and Das, R., (2014), “RNA design rules from a massive open laboratory,” Proceedings of the National Academy of Sciences, pp. 2–7.

[260] Venkatasubramanian, V., Rengaswamy, R., and Kavuri, S. N., (2003), “A review of process fault detection and diagnosis Part II : Qualitative models and search strategies,” *Computers & Chemical Engineering*, 27(3), pp. 313–326.

[261] Billings, C. E., (1991), “Human-Centered Aircraft Automation : A Concept and Guidelines,” p. 122.

[262] Wickens, C. D., and Dixon, S. R., (2007), “The benefits of imperfect diagnostic automation: a synthesis of the literature,” *Theoretical Issues in Ergonomics Science*, 8(3), pp. 201–212.

[263] Madhavan, P., and Wiegmann, D. A., (2007), “Effects of information source, pedigree, and reliability on operator interaction with decision support systems.,” *Human Factors*, 49(5), pp. 5773–5785.

[264] Balfe, N., Wilson, J. R., Sharples, S., and Clarke, T., (2012), “Development of design principles for automated systems in transport control,” *Ergonomics*, 55(1), pp. 37–54.

[265] Bechhoefer, E., and Morton, B., (2012), “Condition monitoring architecture: To reduce total cost of ownership,” 2012 IEEE Conference on Prognostics and Health Management, IEEE, Denver, CO, pp. 1–9.

[266] Mathur, A., Cavanaugh, K. F., Pattipati, K. R., Willett, P. K., and Galie, T. R., (2001), “Reasoning and modeling systems in diagnosis and prognosis,” Proceedings of SPIE—The International Society for Optical Engineering: Component and Systems Diagnostics, Prognosis, and Health Management, P.K. Willett, and T. Kirubarajan, eds., Orlando, Florida, pp. 194–203.

[267] Goddard, K., Roudsari, A., and Wyatt, J. C., (2012), “Automation bias: a systematic review of frequency, effect mediators, and mitigators.,” *Journal of the American Medical Informatics Association : JAMIA*,

19(1), pp. 121–7.

[268] Guerlain, S. A., Smith, P. J., Obradovich, J. H., Rudmann, S., Strohm, P., Smith, J. W., Svirbely, J., and Sachs, L., (1999), "Interactive Critiquing as a Form of Decision Support: An Empirical Evaluation," *Human Factors: The Journal of the Human Factors and Ergonomics Society*, 41(1), pp. 72–89.

[269] ISO 9241, (2010), "Ergonomics of human-system interaction - Part 210: Human-centred design for interactive systems."

[270] Balfe, N., (2010), "Appropriate Automation of Rail Signalling Systems: A Human Factors Study," University of Nottingham.

[271] Muir, B. M., and Moray, N., (1989), "Operators' trust in and use of automatic controllers," Proceedings of the 22nd Annual Conference of the Human Factors Association of Canada, Human Factors Association of Canada, Ontario, pp. 163–166.

[272] De-Vries, P., Midden, C., and Bouwhuis, D., (2003), "The effects of errors on system trust, self-confidence, and the allocation of control in route planning," *International Journal of Human-Computer Studies*, 58(6), pp. 719–735.

[273] Wiegmann, D. A., Rich, A. M., and Zhang, H., (2001), "Automated diagnostic aids: The effects of aid reliability on users' trust and reliance," *Theoretical Issues in Ergonomics Science*, 2(4), pp. 352–367.

[274] Lee, J. D., and Moray, N., (1992), "Trust, control strategies and allocation of function in human-machine systems," *Ergonomics*, 35(10), pp. 1243–1270.

[275] Lee, J. D., and Moray, N., (1994), "Trust, self-confidence, and operators' adaptation to automation," *International Journal of Human-Computer Studies*, 40(1), pp. 153–184.

[276] Sarter, N. B., Woods, D. D., and Billings, C. E., (1997), "Automation surprises," Handbook of Human Factors and Ergonomics, G. Salvendy, ed., John Wiley & Sons, Inc., New York, pp. 1926–1943.

[277] Sheridan, T. B., (1999), "Human supervisory control," Handbook of Systems Engineering and Management, A.P. Sage, and W.B. Rouse, eds., John Wiley & Sons, Inc., New York, pp. 645–690.

[278] Dzindolet, M. T., Peterson, S. A., Pomranky, R. A., Pierce, L. G., and Beck, H. P., (2003), "The role of trust in automation reliance," *International Journal of Human-Computer Studies*, 58(6), pp. 697–718.

[279] Lee, J. D., and See, K. A., (2004), "Trust in automation: Designing for appropriate reliance," *Human Factors*, 46(1), pp. 50–80.

[280] Madhavan, P., and Wiegmann, D. A., (2007), "Similarities and differences between human-human and human-automation trust: An integrative review," *Theoretical Issues in Ergonomics Science*, 8(4), pp. 277–301.

[281] Sheridan, T. B., and Parasuraman, R., (2006), "Human-automation interaction," Reviews of human factors and ergonomics, R.S. Nickerson, ed., Human Factors and Ergonomics Society, Santa Monica, CA, pp. 89–129.

[282] Merritt, S. M., and Ilgen, D. R., (2008), "Not all trust is created equal: Dispositional and history based trust in human-automation interactions," *Human Factors*, 50(2), pp. 194–210.

[283] Sackett, D. L., Rosenberg, W. M. C., Gray, J. A. M., Haynes, R. B., and Richardson, W. S., (1996), "Evidence based medicine: what it is and what it isn't," *BMJ*, 312(7023), pp. 71–72.

[284] Berner, E. S., ed., (2007), "Clinical Decision Support Systems: Theory and Practice," Springer New York, New York, NY.

[285] Uckun, S., Goebel, K., and Lucas, P. J. F., (2008), "Standardizing research methods for prognostics," 2008 International Conference on Prognostics and Health Management, Ieee, pp. 1–10.

[286] Popov, A., Fink, W., and Hess, A., (2013), "PHM for Astronauts – A New Application," Annual Conference of the Prognostics and Health Management Society 2013, S. Sankararaman, and I. Roychoudhury, eds., PHM Society, New Orleans LA, pp. 566–572.

[287] Shibl, R., Lawley, M., and Debuse, J., (2013), "Factors influencing decision support system acceptance," *Decision Support Systems*, 54(2), pp. 953–961.

[288] Alexander, G. L., (2006), "Issues of trust and ethics in computerized clinical decision support systems.," *Nursing administration quarterly*, 30(1), pp. 21–9.

[289] Dreiseitl, S., and Binder, M., (2005), "Do physicians value decision support? A look at the effect of decision support systems on physician opinion," *Artificial Intelligence in Medicine*, 33(1), pp. 25–30.

[290] ProcessIT Europe, (2013), "European Roadmap for Industrial Process Automation."

[291] Chen, T., and Tsai, H.-R., (2016), "Ubiquitous manufacturing: Current practices, challenges, and opportunities," *Robotics and Computer-Integrated Manufacturing*, 45, pp. 126–132.

[292] (2013), "Grade E1 Diaphragm," *ITT Corporation* [Online]. Available: http://www.engvalves.com/Products/Pure-Flo-Grade-E1-Diaphragm/. [Accessed: 27-Jan-2015].

[293] Agresti, A., (2013), "Categorical Data Analysis," John Wiley & Sons, Inc., Hoboken, New Jersey.

[294] Harrell, F. E., Lee, K. L., Matchar, D. B., and Reichert, T. A., (1985), "Regression models for prognostic prediction: advantages, problems, and suggested solutions.," *Cancer treatment reports*, 69(10), pp. 1071–77.

[295] Lund, A., and Lund, M., (2015), "Laerd Statistics," *Lund Research Ltd* [Online]. Available: https://statistics.laerd.com. [Accessed: 24-Nov-2015].

[296] O'Brien, R. M., (2007), "A Caution Regarding Rules of Thumb for Variance Inflation Factors," *Quality & Quantity*, 41(5), pp. 673–690.

[297] Kutner, M., Nachtsheim, C., and Neter, J., (2004), "Applied Linear Regression Models," McGraw-Hill, New York, NY.

[298] Menard, S., (2001), "Applied Logistic Regression Analysis," Sage Publications, Inc., Thousand Oaks, California.

[299] Hair, J. F., Black, W. C., Babin, B. J., and Anderson, R. E., (2010), "Multivariate Data Analysis," Prentice Hall, New Jersey.

[300] Whittingham, M. J., Stephens, P. A., Bradbury, R. B., and Freckleton, R. P., (2006), "Why do we still use stepwise modelling in ecology and behaviour?," *Journal of Animal Ecology*, 75(5), pp. 1182–1189.

[301] Steyerberg, E. W., Eijkemans, M. J. C., and Habbema, J. D. F., (1999), "Stepwise selection in small data sets: A simulation study of bias in logistic regression analysis," *Journal of Clinical Epidemiology*, 52(10), pp. 935–942.

[302] Ohlsson, P.-A., (2013), "Diaphragm Valve Development – Challenging Traditional Thinking," *Pharmaceutical Engineering*, 33(6), pp. 2–5.

[303] Jones, T. A., (2003), "Book Review: Experiments: Planning, Analysis, and Parameter Design Optimization," *Mathematical Geology*, 35(2), pp. 227–229.

[304] Collins, L. M., Dziak, J. J., and Li, R., (2009), "Design of experiments with multiple independent variables: A resource management perspective on complete and reduced factorial designs.," *Psychological Methods*, 14(3), pp. 202–224.

[305] ISO 22088-3, (2006), "Plastics - Determination of resistance to environmental stress cracking (ESC) - Part 3: Bent strip method."

[306] Andena, L., Castellani, L., Castiglioni, A., Mendogni, A., Rink, M., and Sacchetti, F., (2013), "Determination of environmental stress cracking resistance of polymers: Effects of loading history and testing configuration," *Engineering Fracture Mechanics*, 101, pp. 33–46.

[307] Cheng, J. J., Polak, M. A., and Penlidis, A., (2011), "Influence of micromolecular structure on environmental stress cracking resistance of high density polyethylene," *Tunnelling and Underground Space Technology*, 26(4), pp. 582–593.

[308] Chugh, A., (2011), "Diaphragm Valves Types, Construction, Applications and Advantages," *Piping Guide* [Online]. Available: http://www.pipingguide.net/2013/11/diaphragm-valves-types-construction.html. [Accessed: 15-Oct-2016].

[309] ISO 3506-1, (2015), "Mechanical properties of corrosion-resistant stainless steel fasteners - Part 1: Bolts, screws and studs."

[310] Budynas, R. G., and Nisbett, J. K., (2011), "Shigley's Mechanical Engineering Design," McGraw-Hill, New York, NY.

[311] Mullins, L., and Tobin, N. R., (1965), "Stress softening in rubber vulcanizates. Part I. Use of a strain amplification factor to describe the elastic behavior of filler-reinforced vulcanized rubber," *Journal of Applied Polymer Science*, 9(9), pp. 2993–3009.

[312] Molazemhosseini, A., Tourani, H., Naimi-Jamal, M. R., and Khavandi, A., (2013), "Nanoindentation and nanoscratching responses of PEEK based hybrid composites reinforced with short carbon fibers and nano-silica," *Polymer Testing*, 32(3), pp. 525–534.

[313] Mullins, L., (1948), "Effect of Stretching on the Properties of Rubber," *Rubber Chemistry and Technology*, 21(2), pp. 281–300.

[314] Planes, E., Chazeau, L., Vigier, G., Fournier, J., and Stevenson-Royaud, I., (2010), "Influence of fillers on mechanical properties of ATH filled EPDM during ageing by gamma irradiation," *Polymer Degradation and Stability*, 95, pp. 1029–1038.

[315] Di Lorenzo, F., and Seiffert, S., (2015), "Nanostructural heterogeneity in polymer networks and gels," *Polym. Chem.*, 6(31), pp. 5515–5528.

[316] Wang, S., Yeh, P., Nien, Y., and Shih, Y., (2009), "Preparation and Properties of Modified EPDM / Silica Composites," Chaoyang University of Science and Technology, Taichung City, Taiwan.

[317] McGrosky, D. T., (2014), "Compound Identification in Quality Control," *Satori Seal Corporation* [Online]. Available: http://www.satoriseal.com/technical/technical_articles/compound_identification_in_quality_control.html.

[318] Yesiltas, M., and Glotch, T. D., (2016), "Chemical Composition of Queen Alexandra Range 97008: An Organic-Rich Unequlibrated Ordinary Chondrite," 47th Lunar and Planetary Science Conference, Texas.

[319] Khan, M. S., and Heinrich, G., (2011), "PTFE-Based Rubber Composites for Tribological Applications," Advanced Rubber Composites, G. Heinrich, ed., Springer-Verlag, Heidelberg, pp. 249–311.

[320] Pervez, T., Qamar, S. Z., and Velden, M. V. D., (2012), "Comparison between fresh and exposed swelling elastomer," *Journal of Elastomers and Plastics*, 44(3), pp. 237–250.

[321] Litvinov, V. M., (2001), "Strain-induced phenomena in amorphous and semicrystalline elastomers. Solid state 1H NMR T2 relaxation under uniaxial compression," *Macromolecules*, 34(24), pp. 8468–8474.

[322] Teissedre, G., Pilichowski, J. F., Chmela, S., and Lacoste, J., (1996), "Ageing of EPDM—I: Photo and thermal stability of EPDM hydroperoxides," *Polymer Degradation and Stability*, 53(2), pp. 207–215.

[323] ALS Environmental, (2014), "Petroleum Hydrocarbon Ranges" [Online]. Available: http://www.caslab.com/Petroleum-Hydrocarbon-Ranges/. [Accessed: 29-Oct-2016].

[324] Baraldi, P., Sogaro, A., Konstandinidou, M., and Nivolianitou, Z., (2013), "An interface for enhancing repeatability in Human Reliability Analysis," *International Journal of Performability Engineering*, 9(2), pp. 149–161.

[325] Hammersley, M., and Atkinson, P., (1995), "Ethnography: Principles in Practice," Routledge, London.

[326] Zio, E., Baraldi, P., Librizzi, M., Podofillini, L., and Dang, V. N., (2009), "A fuzzy set-based approach for modeling dependence among human errors," *Fuzzy Sets and Systems*, 160(13), pp. 1947–1964.

[327] Sheskin, D. J., (2011), "Handbook of parametric and nonparametric statistical procedures," CRC Press Inc., Boca Raton, FL.

[328] Myers, J. L., Well, A. D., and Lorch, R. F. J., (2010), "Research design and statistical analysis," Routledge, New York, NY.

[329] Cohen, J., (1988), "Statistical power analysis for the behavioral sciences," Psychology Press, New York, NY.

[330] Anderson, T. W., and Darling, D. A., (1952), "Asymptotic Theory of Certain 'Goodness of Fit' Criteria Based on Stochastic Processes," *The Annals of Mathematical Statistics*, 23(2), pp. 193–212.

[331] ElMaraghy, H. a., Kuzgunkaya, O., and Urbanic, R. J., (2005), "Manufacturing Systems Configuration Complexity," *CIRP Annals - Manufacturing Technology*, 54(1), pp. 445–450.

[332] Richard J Charnigo, E. L. A., (2013), "Markov Chains and Semi-Markov Models in Time-to-Event Analysis," *Journal of Biometrics & Biostatistics*.

[333] Grall, a., Bérenguer, C., and Dieulle, L., (2002), "A condition-based maintenance policy for stochastically deteriorating systems," *Reliability Engineering & System Safety*, 76(2), pp. 167–180.

[334] Lee, S. G., and Ng, Y. C., (2005), "Hybrid case-based reasoning for on-line product fault diagnosis," *The International Journal of Advanced Manufacturing Technology*, 27(7–8), pp. 833–840.

[335] Lehane, M., Halasz, M., Orchard, R., and Wylie, R., (1998), "Integrated Diagnostic System (IDS) for Aircraft Fleet Maintenance," Proceedings of the Fifteenth National Conference on Artificial Intelligence (AAAI 98), J. Mostow, and C. Rich, eds., AAAI Press, Menlo Park, CA, pp. 26–30.

[336] Walker, M., and Kapadia, R., (2009), "Integrated Design of On-line Health and Prognostics Management," Annual Conference of the Prognostics and Health Management Society, San Diego, CA, pp. 1–15.

[337] Baraldi, P., Di Maio, F., Pappaglione, L., Zio, E., and Seraoui, R., (2012), "Condition monitoring of electrical power plant components during operational transients," *Proceedings of the Institution of Mechanical Engineers, Part O: Journal of Risk and Reliability*, 226(6), pp. 568–583.

[338] Hines, J. W., and Garvey, D. R., (2006), "Development and Application of Fault Detectability Performance Metrics for Instrument Calibration Verification and Anomaly Detection," *Journal of Pattern Recognition Research*, 1, pp. 2–15.

[339] Garcıa-Alvarez, D., (2009), "Fault detection using principal component analysis (PCA) in a wastewater treatment plant (WWTP)," In Proceedings of the International Student's Scientific Conference.

[340] Ding, J., Hines, J. W., and Rasmussen, R., (2003), "Independent component analysis for redundant sensor validation," Proceedings of the 2003 Maintenance and Reliability Conference (MARCON 2003), Knoxville, TN.

[341] Laouti, N., Sheibat-Othman, N., and Othman, S., (2011), "Support vector machines for fault detection in wind turbines," Proceedings of IFAC World Congress, pp. 7067–7072.

[342] Baraldi, P., Di Maio, F., Genini, D., and Zio, E., (2013), "A Fuzzy Similarity Based Method for Signal Reconstruction during Plant Transients," Prognostics and System Health Management Conference PHM-2013, pp. 889–894.

[343] Puig, V., Quevedo, J., Escobet, T., Nejjari, F., and de las Heras, S., (2008), "Passive robust fault detection of dynamic processes using interval models," *IEEE Transactions on Control Systems Technology*, 16, pp. 1083–1089.

[344] Montes de Oca, S., Puig, V., and Blesa, J., (2012), "Robust fault detection based on adaptive threshold generation using interval LPV observers," *International Journal of Adaptive Control and Signal Processing*, 26(3), pp. 258–283.

[345] Baraldi, P., Di Maio, F., Rigamonti, M., and Zio, E., (2013), "Transients Analysis of a Nuclear Power Plant Component for Fault Diagnosis," *Chemical Engineering Transactions*, 33, pp. 895–900.

[346] Venkatasubramanian, V., Rengaswamy, R., Yin, K., and Kavuri, S. N., (2003), "A review of process fault detection and diagnosis Part I : Quantitative model-based methods," *Computers & Chemical Engineering*, 27(3), pp. 293–311.

[347] Hashemian, H. M., (2011), "State-of-the-Art Predictive Maintenance Techniques," *IEEE Transactions on Instrumentation and Measurement*, 60(1), pp. 226–236.

[348] Watanabe, S., (1972), "Frontiers of pattern recognition: The Proceedings. IEEE Computer Society. Pattern Recognition Committee," Academic Press.

[349] ISO 13381-1, (2015), "Condition monitoring and diagnostics of machines - Prognostics - Part 1: General guidelines."

[350] Mintzberg, H., and Simon, H. a., (1977), "The New Science of Management Decision, Revised Edition.," *Administrative Science Quarterly*, 22(2), p. 342.

[351] Ketteler, G., (1999), "Analysis of Requirements for Monitoring Systems," Proceedings of the Second International Workshop on Intelligent Manufacturing Systems, H. Van Brussel, and P. Valckenaers, eds., Katholieke Universiteit Leuven - Departement Werktuigkunde, Leuven, Belgium, pp. 721–725.

[352] Butler, M., (2013), "Predictive Analytics in Business: Strategy, Methods, Technology."

[353] German Federal Ministry of Education and Research, (2013), "Zukunftsbild „Industrie 4.0" Hightech-Strategie."

[354] Bohn, H., Bobek, A., and Golatowski, F., (2006), "SIRENA - Service Infrastructure for Real-time Embedded Networked Devices : A service oriented framework for different domains," Proceedings of the International Conference on Networking, International Conference on Systems and International Conference on Mobile Communications and Learning Technologies (ICNICONSMCL'06), Washington, DC, USA, p. 43.

[355] Deugd, S. De, Carroll, R., Kelly, K. E., Millett, B., and Ricker, J., (2006), "SODA : Service-Oriented Device Architecture," *Pervasive Computing, IEEE*, 5(3), pp. 94–96.

[356] Souza, L. M. S. de, Spiess, P., Guinard, D., Moritz, K., and Karnouskos, S., (2008), "SOCRADES : A Web Service Based Shop Floor Integration Infrastructure," Internet of Things 2008 Conference, C. Floerkemeier, M. Langheinrich, E. Fleisch, F. Mattern, and S.E. Sarma, eds., Zurich, Switzerland, pp. 50–67.

[357] Karnouskos, S., Colombo, A. W., Jammes, F., Delsing, J., and Bangemann, T., (2010), "Towards an architecture for service-oriented process monitoring and control," IECON 2010 - 36th Annual Conference on IEEE Industrial Electronics Society, Ieee, Glendale, AZ, pp. 1385–1391.

[358] Lee, J., and Lapira, E., (2014), “Recent Advances and Trends in Predictive Manufacturing in Industry 4.0 Environment,” *Uptime Magazine*, pp. 16–21.

[359] Han, J., Kamber, M., and Pei, J., (2012), “Data Mining: Concepts and Techniques,” Morgan Kaufmann Publishers for Elsevier.

[360] Venkatasubramanian, V., (2005), “Prognostic and diagnostic monitoring of complex systems for product lifecycle management: Challenges and opportunities,” *Computers & Chemical Engineering*, 29(6), pp. 1253–1263.

[361] Fox, A., (2009), “Biosimilar Medicines—New Challenges for a New Class of Medicine,” *Journal of Biopharmaceutical Statistics*, 20(1), pp. 3–9.

[362] Schellekens, H., (2009), “Biosimilar therapeutics--what do we need to consider?,” *NDT Plus*, 2(Supplement 1), pp. i27–i36.

[363] Shire, S. J., (2009), “Formulation and manufacturability of biologics,” *Current Opinion in Biotechnology*, 20(6), pp. 708–714.

[364] Newcombe, C., and Newcombe, A. R., (2007), “Antibody production: Polyclonal-derived biotherapeutics,” *Journal of Chromatography B-Analytical Technologies in the Biomedical and Life Sciences*, 848(1), pp. 2–7.

[365] Demain, A. L., (2009), “Antibiotics: Natural products essential to human health,” *Medicinal Research Reviews*, 29(6), pp. 821–842.

[366] Kresse, G.-B., (2009), “Biosimilars – Science, status, and strategic perspective,” *European Journal of Pharmaceutics and Biopharmaceutics*, 72(3), pp. 479–486.

[367] Talele, T. T., Gillespie, M., and Korlipara, V. L., (2012), “Pharmaceutical Biotechnology,” Foyes Principles of Medicinal Chemistry, D.A. Williams, ed., Lippincott Williams & Wilkins, Philadelphia, PA, pp. 210–263.

[368] Kozlowski, S., Woodcock, J., Midthun, K., and Behrman Sherman, R., (2011), “Developing the Nation’s Biosimilars Program,” *New England Journal of Medicine*, 365(5), pp. 385–388.

[369] Chen, F., (2009), “Magnetically Enhanced Centrifugation for Continuous Biopharmaceutical Processing,” Massachusetts Institute of Technology.

[370] Rader, R. A., (2013), “FDA Biopharmaceutical Product Approvals and Trends in 2012,” *BioProcess International*, 19(1), pp. 18–27.

[371] Walsh, G., (2010), “Biopharmaceutical benchmarks 2010.,” *Nature biotechnology*, 28(9), pp. 917–24.

[372] Baeshen, M. N., Al-Hejin, A. M., Bora, R. S., Ahmed, M. M. M., Ramadan, H. a I., Saini, K. S., Baeshen, N. a, and Redwan, E. M., (2015), “Production of Biopharmaceuticals in E. coli: Current Scenario and Future Perspectives,” *Journal of Microbiology and Biotechnology*, 25(7), pp. 953–962.

[373] Zhu, J., (2012), “Mammalian cell protein expression for biopharmaceutical production,” *Biotechnology Advances*, 30(5), pp. 1158–1170.

[374] (2015), “IMS Health Market Prognosis: Total Unaudited and Audited Global Pharmaceutical Market by Region 2014 – 2019.”

[375] Otto, R., Santagostino, A., and Schrader, U., eds., (2014), “From Science to Operations: Questions, Choices and Strategies for Success in Biopharma,” p. 21.

[376] (2013), “2013 Biopharmaceutical Research Industry Profile,” p. 78.

[377] Anderson, R., (2014), “Pharmaceutical industry gets high on fat profits,” *BBC Business News* [Online]. Available: http://www.bbc.co.uk/news/business-28212223.

[378] (2014), “Information for Consumers (Biosimilars),” *U.S. Food and Drug Administration* [Online]. Available: http://www.fda.gov/Drugs/DevelopmentApprovalProcess/HowDrugsareDevelopedandApproved/ApprovalApplications/TherapeuticBiologicApplications/Biosimilars/ucm241718.htm.

[379] Vincent Ryan, (2013), “Pharma jobs shed over patent cliff,” *Irish Examiner*.

[380] (2013), “Pfizer to invest $130m in Cork and Dublin at Ringaskiddy and Grange Castle,” *RTE Business News* [Online]. Available: http://www.rte.ie/news/business/2013/0711/461797-pfizer-to-invest-130m-in-cork-and-dublin-plants/. [Accessed: 15-Jan-2015].

[381] (2011), “Guidelines for Process Safety in Bioprocess Manufacturing Facilities,” Center for Chemical Process Safety of the American Institute of Chemical Engineers and John Wiley & Sons, Inc., Hoboken, New Jersey.

[382] Gammell, P., (2010), “The Art, Science and Beauty of Mammalian Cell Culture,” *Biotech Course - Cell Culture*.

[383] Tegge, G., (1987), “Biotechnology. A Comprehensive Treatise in 8 Volumes. Vol. 4: Microbial Products II,” Wiley-VCH Verlag GmbH & Co. KGaA, Weinheim, Germany.

[384] Biwer, A., Griffith, S., and Cooney, C., (2005), “Uncertainty analysis of penicillin V production using Monte Carlo simulation.,” *Biotechnology and bioengineering*, 90(2), pp. 167–79.

[385] Stanbury, P. F., Whitaker, A., and Hall, S. J., (1995), “Principles of Fermentation Technology,” Elsevier Ltd, Oxford, U.K.

[386] Shukla, A. a., and Gottschalk, U., (2013), “Single-use disposable technologies for biopharmaceutical manufacturing,” *Trends in Biotechnology*, 31(3), pp. 147–154.

[387] Percy, J., (2010), “Purification,” *Biotech Course - Purification*.

[388] Othmer, K., (2007), “Concise Encyclopedia of Chemical Technology,” John Wiley & Sons, Inc., Hoboken, New Jersey.

[389] Subramanian, G., ed., (2012), “Biopharmaceutical Production Technology, Volume 1,” Wiley-VCH Verlag GmbH & Co. KGaA, Weinheim, Germany.

[390] (2014), “Business Operations Grange Castle Biotech Plant, Dublin,” *Pfizer Healthcare Ireland* [Online]. Available: https://www.pfizer.ie/operations.cfm#biotech. [Accessed: 07-Jul-2014].

[391] International Standards Organisation, “Aseptic processing of health care products — Part 4: Clean-in-place technologies.”

[392] ISO 13408-5, (2006), “Aseptic processing of health care products - Part 5: Sterilization in place.”

[393] Flickinger, M. C., ed., (2013), “Downstream Industrial Biotechnology: Recovery and Purification,” John Wiley & Sons, Inc., Hoboken, New Jersey, New Jersey.

[394] Sheridan, G., (2012), “Validation and Control of SIP,” IMB GMP Information Seminar, Irish Medicines Board, Dublin, p. 32.

[395] Hamill, L., (2011), “Understanding Hydraulics,” Palgrave Macmillan, Basingstoke.

Appendix A – From CBM to PHM

8.1 Condition based maintenance overview

Many manufacturing processes suffer increasing wear with usage and age and are subject to failures resulting from this deterioration. For many types of equipment this deterioration can be observed with effective sensorisation technology, such as cumulative wear, crack growth in metal, erosion, corrosion, fatigue, consumption etc. [333]. Some typical sensors used to measure such variables are strain gauges, ultrasonic sensors, accelerometers, acoustic emissions sensors, microelectromechanical systems etc. Once such sensor data has been collected and unwanted noisy artefacts removed, the most significant step in the CBM architecture is the feature extraction of normal and/or faulty conditions. This critical step sets the stage for the accurate and timely diagnosis of equipment faults. The extracted feature-vector is an essential input into prognostic algorithms which then may be later developed [44]. The problem of establishing an efficient condition based maintenance strategy then lies in developing an adequate predictive model describing the future evolution of the system degradation while balancing profit and system availability. The optimisation of a condition based maintenance strategy basically amounts to determining the threshold level of the monitored degradation condition beyond which maintenance has to be performed [43].

A recent major shift in the CBM philosophy was observed with the introduction of expert systems within the CBM framework. Artificial-intelligence based systems such as case based reasoning, model based reasoning, and probabilistic belief networks have been used to include the attributes of system learning and adaptation. This significantly improved the state of the art over previous systems [37]. However, these maintenance systems use only quantitative information available from the sensors to automate the diagnosis task, and almost no use of qualitative information is made [249–251]. On the other hand, as discussed previously, some maintenance systems only consider qualitative information and ignore sensor measurements [334,335]. Little evidence can be found in the literature were both quantitative and qualitative information is utilised at the same time. The difficulty in building a common platform to process both quantitative and qualitative data has hindered the use of such a hybrid system. The integration of these information sources would lead to improved system availability and reliability by increasing interaction via information sharing and coordination for timely maintenance [37].

8.2 Prognostics and health management overview

In many industrial settings today the output from PHM systems constitutes a decision support system used to aid decision makers, as entirely autonomous systems have not seen widespread industrial integration. Recent developments in measurement devices, data storage capacities, data processing, and computational capabilities have occurred concurrently with advancements in industrial internet technologies. These developments are in part encouraging high risk industries such as the military, nuclear, petrochemical, automotive, pharmaceutical, and aerospace to adopt PHM systems for increasing system availability, minimising unscheduled shutdowns, reducing maintenance costs, and increasing safety [336]. In these high risk industries in particular, detecting and isolating faults and subsequently predicting the RUL of critical components is a crucial task. If logistical support services, particularly maintenance activities and associated spare parts inventory management are to operate as efficiently as possible to achieve this goal, active contributions from multiple disciplines are required. These are typically cited as being from the engineering sciences, computer science, reliability engineering, communications, management sectors etc. Performance assessments of PHM systems currently evaluate the technical and economic feasibility of diagnostic and prognostic technologies, with little to no consideration given to end-user requirements. Even though many successful R&D activities in the PHM domain are conducted by large international organisation such as General Electric, Boeing, Lockheed, and Honeywell, PHM still lacks widespread acceptance as a technology standard in industry [44].

Fault detection and diagnosis

Within fault detection, several empirical signal reconstruction models have been explored to estimate the expected values of measured variables under both changing and steady state process conditions. Some of the most commonly researched techniques today include auto-associative kernel regression [337], artificial neural networks [338], evolving clustering methods [209], principle component analysis [256,339], independent principle component analysis for redundant sensor validation [340], support vector machines [341], and fuzzy similarity [342]. For robust determination of anomaly detection certainty several methods can be found in the literature. For example, in threshold-based methods, very common in industrial CBM schemes, the process of an anomaly is concluded when the residual measured values exceed a predefined threshold [343,344]. Another example is using statistical methods such as the sequential probability ratio test in which anomaly detection is concluded if the probability distribution function of the measured residual differs from the probability distribution function calculated during normal conditions [338]. However, these methods have some practical difficulties in industrial applications such as the setting of the threshold value in threshold-based methods and certain parameters within statistical methods. The industrial integration difficulty is exacerbated when no information about the confidence of the fault detection outcome is provided, potentially leading to distrust in the system state predictions.

System diagnostics lead to increased overall equipment effectiveness in a number of ways. This is because when an alarm is triggered due to an identified system event, a decision must be taken to [18]:

1. Ignore the alarm
    - This increases the chances for potential accidents and catastrophic equipment failure in the case of a true alarm event.
2. Stop the equipment
    - This will lead to additional utilised manpower resources, lost production time, and extra costs in the case of a false alarm.
3. Further manual investigations without stopping the system
    - In the case of false alarms, this again leads to extra costs and manpower.

Advanced event diagnosis, subsequent to some data processing or information handling step, is integral within the scope of system and sensor control. The goal is to handle and analyse data or signals collected via data acquisition modules for better understanding and interpretation of the information contained within that data. Two facets of diagnostics are event isolation and identification. Event isolation locates the anomaly source, and event identification determines the nature of the anomaly when it is detected. As such it is considered posterior event analysis [7]. An automated event diagnosis system is therefore used after an event detection module concludes that there are sufficient abnormal conditions in a system at a time t, in order to identify the root cause(s) of the occurred abnormality, on the basis of the observed signals which are representative of the system behaviour. This can be considered as a classification problem in which specific classes of event are associated to specific values of observed measured variables, where the classification schemes are either supervised or unsupervised [256,345,346]. Signals detected by sensors are subjected to analogue and digital signal conditioning and processing with the aim of generating functional signal features which can be correlated with system state and / or process conditions. Sensor signal features are then fed to and evaluated by cognitive decision making support systems for diagnosis [45].

As part of an integrated process control event determination framework, diagnostic system elements use signals from process sensors, such as resistance temperature detectors, thermocouples, differential pressure transmitters, flow transmitters etc., to both help verify the performance of the sensors and process-to-sensor interfaces, and to identify problems in the process. When signals from test sensors whose parameters can be measured and correlated directly with equipment condition are included, the diagnostic capabilities of the system can increase exponentially [347]. The design of a diagnostic system requires careful attention to the following issues: definition of pattern classes, sensing environment, pattern representation, feature extraction and selection, cluster analysis, classifier design and learning, selection of training and test samples, and performance evaluation [256]. A critical part of developing and implementing effective diagnostic routines and technologies is based on the ability to detect events early enough in order to do something useful with the information. Fault isolation and diagnosis uses the detection event(s) as the start of the process for classifying the fault within the system being monitored. Specific requirements in terms of confidence bounds must be identified and defined for robust diagnosis of all event modes. As a minimum, the following probabilities should be used to specify event detection and diagnosis accuracy [44]:

- The probability of anomaly detection, including false alarm-rate and real fault probability statistics
- The probability of specific fault diagnosis classifications using specific confidence bounds and severity predictions

The literature on diagnostics is both vast and diverse primarily due to the wide variety of systems, components and parts under consideration. Hundreds of papers in this area, including theories and practical applications, appear every year in academic journals, conference proceedings and technical reports [7]. Vast repositories of diagnostics research, over 1.2 million written articles in the Scopus database, appear in fields as diverse as medicine, engineering, neuroscience, astronomy, molecular biology, psychology, computer science, chemical engineering, the arts, humanities, and economics. However, in spite of almost 50 years of research and development in this field, the general problem of recognizing complex patterns with arbitrary orientation, location, and scale remains unsolved. New and emerging applications such as enhanced data management schemes require ever more robust and efficient diagnostic techniques to identify, isolate, and classify complex process states as they occur in real time. Watanabe [348] opines that "pattern recognition is a fast-moving and proliferating discipline. It is not easy to form a well-balanced and well-informed summary view of the newest developments in this field. It is still harder to have a vision of its future progress".

Fault prognosis

ISO13381-1 [349] presents a full definition of remaining useful life estimation within fault prognosis methodologies. It defines prognostics as 'an estimation of time to failure and risk for one or more existing and future failure modes'. Specifically, the standard suggests that prognostics requires consideration of:

- existing failure modes and deterioration rates
- initiation criteria for future failure modes
- interrelationship between failure modes and their deterioration rates
- sensitivity of monitoring and analysis techniques to deterioration rates of failure modes
- the effect of maintenance on failure degradations
- the conditions and assumptions underlying the prognoses

Zio [18] and Sikorska et al [40] defined the distinction to be made among first-principle model-based, reliability model-based and process sensor data-driven prognostic approaches, referred to as white box, black box and grey box models, respectively. First-principle approaches are mathematical models derived from first principles to describe the degradation process leading to failure. While the most accurate prognostics approach, it is often not a realistic developmental option in complex industrial environments given multiple, complicated, stochastic processes of degradation. Reliability model-based approaches estimate the RUL of equipment under industrial usage conditions. The parameters of the reliability models can be estimated on the basis of historical data related to the equipment failure behaviour, i.e., time to failure data is used to tune the parameters of the failure time distribution. The most common method of which is by Weibull analysis. It is also possible to include the effects of environmental stressors under which the equipment operates to estimate the RUL of equipment under given usage conditions. This can be done for example via proportional hazard models. Unfortunately, in practice the availability of sufficiently representative data is rare, especially for very reliable equipment and for new equipment for which feedback data is scarce or non-existent. Knowledge based approaches assess the similarity between an observed situation and a databank of previously defined failures, and deduce the life expectancy from previous events. Sub-categories include expert systems and fuzzy systems. Finally, there are approaches which do not use any explicit model and rely exclusively on process data measured by sensors related to the degradation and failure states of the equipment. Empirical techniques like artificial neural networks, support vector machines, local Gaussian regression, and pattern similarity are typical examples. The advantage of these methods lies in the direct use of the measured process data for equipment failure [18,40].

8.2.1 PHM as a decision support system

Sandborn [29] states that methods used to obtain and store large amounts of information has largely been perfected, and as a result, a sort of information overload is prevalent, where it is not uncommon that a lot more information exists than organisations know how to use. Sandborn opines that the key now is to develop methods to make decisions based on that information. The goal of applied PHM technology is to provide decision support. Therefore, the final form of the output from a PHM system, driven by the context of the user, is actionable information that supports improved decision making, as decision support systems are designed only to support the intelligence, design, or choice phases of human decision makers [17,350]. A comprehensive study was conducted by Ketteler [45] on the requirements for equipment monitoring and decision support systems in the machining/manufacturing domain regarding their reliability, flexibility, and user friendliness, using the input of industries from Japan, the USA, Canada, and Europe. Data from machine builders, end-users, and monitoring system suppliers was collected and analysed. The main conclusions are applicable across multiple industries, dealing with the theme of industrial integration, and lack thereof, of online decision support capabilities aiding maximum throughput. Ketteler concludes that less than 38% of end-users were at the time satisfied with available monitoring systems, the main reasons for this being the lack of system reliability, too many false alarms, and the complicated nature of the monitoring systems. Reliability was defined as high detection rates with low false alarms. The most important expectations for end-users when using decision support systems were less downtime of the production equipment, less scrap production, higher productivity, easier decision support system operability, and less false alarms. Given the need for greater operability, decision support systems and associated technologies need to move out of the realm of esoterica, enabling full practical implementation within organisations. Many analytics technologies still focus on the technical aspects with insufficient regard for the monitoring of model performance and the sharing of information in a collaborative environment. Although this is one of the less glamorous aspects of predictive technologies, in many ways it is one of the most important, as without the establishment of the industrial context or the confidence levels in predictive models the technology will always be underexploited and untrusted [352].

8.2.2 Future challenges and state-of-the-art in PHM:

Integrated process control technologies must meet the challenge facing industry in the first half of the 21st century. This challenge, commonly labelled 'Industry 4.0' [353], is what has been termed as the fourth industrial revolution, where future industrial process production will be characterised by industrial internet driven smart factories centred around adaptability and resource efficiency designed to minimise operational and maintenance costs through increased operational equipment effectiveness. In 2010 Teti et al [45] identified and proposed a roadmap of recommended research to solve the needs and provide the key enabling technologies for intelligent sensor technology by 2017. Among these are:

- New sensors and sensor systems
- Transformation of stand-alone sensors used primarily in open and closed loop control to sensors that are a part of an intelligent system for process system diagnosis and characterisation
- Advanced sensor signal and data processing
- Innovative signal and data processing techniques, assisted by cognitive tools and methods
- Intelligent sensor monitoring
- Intelligent sensor monitoring systems including, as part of their packaging, abilities for self-calibration and self-diagnostics, signal conditioning, and decision making

ProcessIT Europe [290], an innovation centre focusing on manufacturing automation solutions for EU process industries, outline the elements expected to be key in the expansion of large-scale integrated process control technologies and sensor systems required to drive Industry 4.0. Among these are improvements in automation system functionality to enable the integration of traditionally separated sensors and systems, along with greater internet compatibility and open standards, such as those developed under recent EU funded projects SIRENA, SODA, SOCRADES, and AESOP [354–357]. Machine to machine communications using Internet of Things principles will form the Cyber-Physical Systems predicted to enable the new adaptive control archetypes used to improve plant operations. Part of the description of the 'ideal concept' for tomorrow's process industries includes the use of soft-sensors using model-based state-of-the-art estimation techniques. New inline sensors will enable new measurement possibilities and directly support improved process monitoring and control, as measurements from previously inaccessible highly uncertain production processes become available in real time. These advancements are critically needed to continually improve the possibilities for efficient plant operations through the visualisation, virtualisation, and simulations of a plant and its automation systems [290]. General Electric outlined their own similar initiative titled 'The Industrial Internet' [206]. Central to this initiative is an integration of three fundamental elements which embody the essence of the Industrial Internet, 'Intelligent Machines', 'Advanced Analytics', and 'People at Work'. To meet this challenge Evans and Annunziata [206] stress the need to deploy advanced sensors, instrumentation, and interface systems. The authors argue in particular that human-machine interaction will be a critical step in blending the hardware and software components required to support the minimal input and undesired output of future industrial automation systems. Lee and Lapira [358] opine that adoption of the internet of things ideology within Industry 4.0 presents a unique opportunity for organisations to create tools and technologies that can identify and quantify organisational uncertainties. This would allow an organisation to determine an objective estimation of the assets and processes and the resultant manufacturing readiness of the organisation. The authors argue that interactive PHM systems are the next phase in the evolution of modern industries, providing insights which give decision makers the opportunity to proactively implement solutions to prevent production losses.

Some of the key state-of-the-art challenges which must be met by system and sensor diagnostic technologies include adaptive control for complex process applications. Adaptive control principles apply particularly to systems with inherent high uncertainty which are highly sensitive and require a paradigm shift in terms of sensor driven data control, and therefore require solutions that are more advanced than the simple process control loops currently in use. Adaptive control essentially refers to the ability of a system to carry out regular quality and safety checking via the use of the novel sensing technologies and methodologies proposed, to detect an anomaly, and to make immediate changes to system inputs when needed to avoid potential catastrophic loss. For example, a test signal can be 'injected' into a system or sensor suite to measure the response and thereby diagnose performance [347]. A self-maintaining machine/process can monitor and diagnose itself, and if any kinds of failure or degradation are detected, it can still continue with its critical functions for a period of time until maintenance or other pertinent actions become feasible. Intelligent diagnostic schemes will act as a key enabler of the adaptive control technologies of the future. It is envisaged that adaptive control capabilities will be achieved by either the addition of intelligence to existing legacy process systems, or building the required intelligence into future systems. The ability to append an additional embedded reasoning system to legacy equipment will form part of the technological advancements required to meet the challenges of the 'Fourth Industrial Revolution' [222,353].

Cyber-physical systems typically consist of a large number of interacting physical and information components which may be interconnected so as to form large heterogeneous cyber-physical networks. Cyber-physical systems and networks will be ubiquitous and form a critical component of modern and future information infrastructure. Data generated in cyber-physical systems are dynamic, volatile, noisy, inconsistent, and interdependent, containing rich spatiotemporal information, and they are critically important for real-time decision making. In comparison with typical spatiotemporal data mining, mining cyber-physical data for process control and diagnostic purposes requires linking the current process state with a large information base, performing real-time calculations, and returning prompt responses. Research in the area includes rare-event detection and anomaly analysis, reliability and trustworthiness in data analysis, effective spatiotemporal data analysis, and the integration of stream data mining with real-time automated control processes [359]. Two of the key concepts defining the future of EU process industries are ubiquitous self-diagnostics to avoid the use of low quality data, and technologies which avoid overly large big data streams[290]. Automated event diagnosis systems are essential to enable further investigations while avoiding system shutdown [18].

Modern technological advances have resulted in a myriad of complex systems, processes and products whose increasingly complicated processes, systems and products pose considerable challenges in their analysis and control for successful operation and use over their lifecycles. Modern process interactions thrive in complex systems where the combined effects of uncertainty and operational adversity are not properly addressed either in design or in operation. Given the size, scope and complexity of the systems and interactions, it is becoming increasingly difficult for plant personnel to anticipate, diagnose and control fault events in a timely manner. There exist therefore considerable incentives, but also challenges, in developing appropriate prognostic and diagnostic methodologies for monitoring, analysing, interpreting and controlling fault events in the process industries [360].

Appendix B – Biopharmaceutical operations

9.1 Introduction

Biopharmaceutical products are clinical reagents, vaccines, and drugs produced using modern biotechnology methods for in vivo diagnostic, preventive, and therapeutic uses. Essentially, biologics are medicines in which the clinically active ingredient is made in or isolated from a living system [20,21].

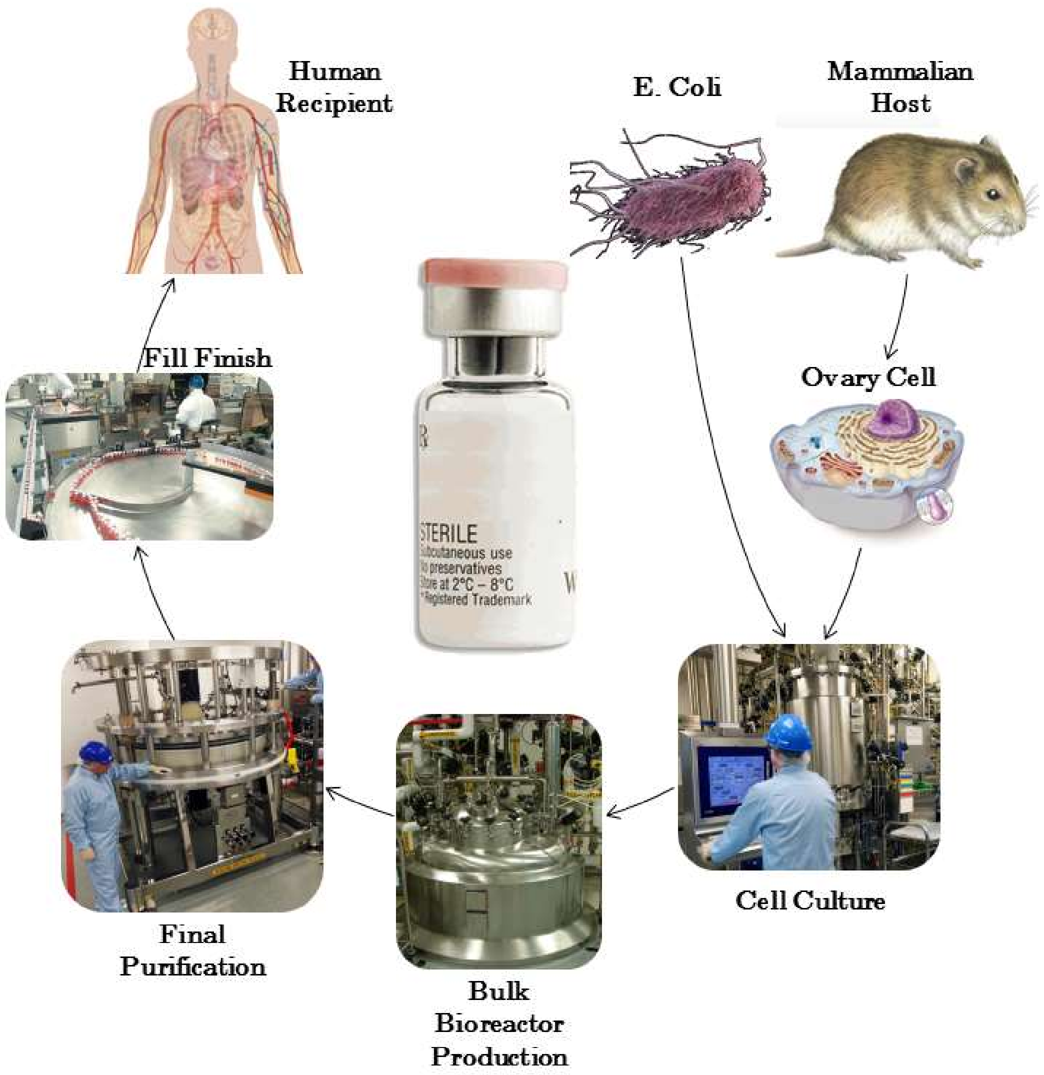

Figure 9.1: Typical biologic drug processing stream

Biologics therefore are pharmaceuticals derived from living organisms or cells and biological processes, rather than chemical synthesis, historically the most common means for drug production [361]. Most clinically useful biological products are extracted from living systems and then purified for human use, consisting of large and complex protein molecules produced using recombinant DNA, hybridoma, or other modern biopharmaceutical technologies [20,362]. All extracts from living systems, including certain vaccines and gene therapy drugs, may be considered biologic drugs [20,363–365]. Biological drug molecules and derived proteins are much larger than chemically-synthesised drugs, and this large molecular size is associated with a more complex structure, as illustrated in figure 9.2. This makes biologics less stable than their chemically-synthesised small-molecule counterparts. As such large proteins are susceptible to structural damage due to heat, temperature, prolonged storage, denaturants, organic solvents, oxygen, pH changes, and other factors such as excess shaking that can affect their relative biological activity [366]. To avoid this type of damage, extreme diligence must be exercised throughout the entire manufacturing process and the final product must be carefully shipped, stored, and handled when it leaves the manufacturing site [366]. Supply-chain issues are critical for biologic drugs since appropriate conditions also need to be maintained during transport and storage [367]. The final product must be periodically monitored to detect potential structural damage [366].

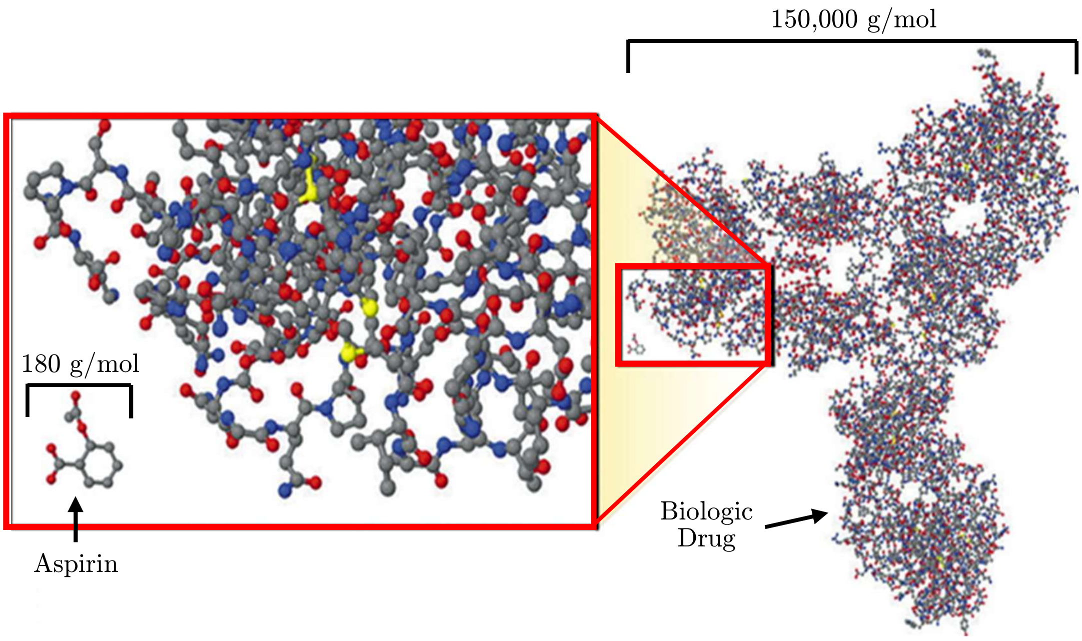

Figure 9.2: Comparison between small molecule drug 'Aspirin' and a typical large molecule monoclonal antibody biologic drug. Adapted from [368]

The relative complexity of the manufacturing process is another area of difference between conventional small molecule pharmaceuticals and biologic products. While manufacturing of small molecule drugs requires a high level of sophistication and quality control, it is less complex and exacting than the production of biologics [361]. One important difference is that it is easier to maintain sterility within a chemical manufacturing process where the conditions are generally unfavourable to biological growth and the product can be subjected to sterilisation technologies. Manufacturing of biologics on the other hand is a complex and demanding process [21]. Strict adherence to well-defined manufacturing conditions is necessary to guarantee batch uniformity and reproducibility. The biological manufacturing process is, by definition, an environment that is favourable to biologic growth. Elimination of potential contaminants requires sophisticated technologies since the fragile protein products cannot be subjected to the kinds of sterilisation techniques that can be employed for non-biologic products [363].

The first approved recombinant protein, insulin, was produced in the early 1980s [369]. Since then the biopharmaceutical industry has evolved significantly, and up to 2012, there were a total of 494 new FDA biopharmaceutical medicine approvals, as shown in figure 9.3 [370].

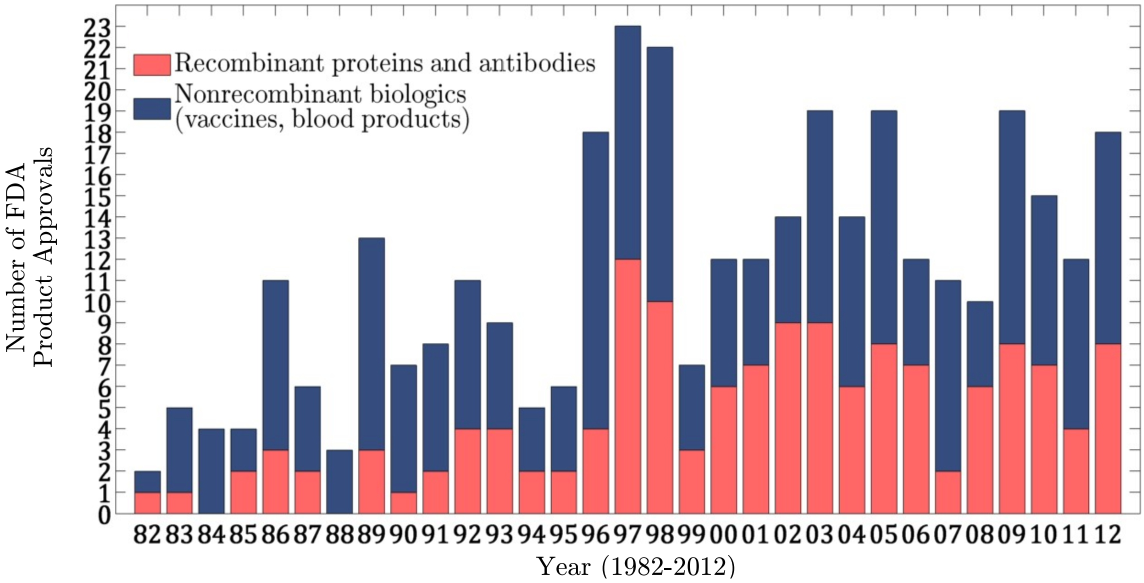

Figure 9.3: FDA new biopharmaceutical approvals, 1982–2012. Adapted from [370]

Analysis of products approved from 2006 to 2010 show that medicines based on mammalian cells, in particular Chinese hamster ovaries, and Escherichia coli (E. Coli) remain the workhorses of biopharmaceutical production. Of the 58 products approved in those years, 32 are produced in mammalian cell lines, whereas 17 are produced using E. Coli [371].

Table 9.1: Examples of biopharmaceuticals produced via E. coli [372]

Biopharmaceutical products	Therapeutic indication	Year of approval
Humulin (rh insulin)	Diabetes	1982
IntronA (interferon α2b)	Cancer, hepatitis, genital warts	1986
Roferon (interferon α2a)	Leukemia	1986
Humatrope (somatropin rh growth hormone)	Childhood hGH deficiency	1987
Betaferon (interferon β-1b)	Multiple sclerosis	1993
Rapilysin (reteplase)	Acute myocardial infraction	1996
Ontak (denileukin diftitox)	Cutaneous T-cell lymphoma	1999
Kineret (anakinra)	Rheumatoid arthritis	2001
Natrecor (nesiritide)	Congestive heart failure	2001
Somavert (pegvisomant)	Acromegaly	2003
Preotact (human parathyroid hormone)	Osteoporosis	2006

Table 9.2: : Examples of biopharmaceuticals produced in Mammalian cell lines [373]

Biopharmaceutical products	Therapeutic indication	Year of approval
EPOs	Anemia	1989
Cerezyme	Gaucher Disease	1994
Clotting Factors	Hemophilia episodes	1997
Enbrel	Rheumatoid arthritis	1998
Herceptin	Breast cancer	1998
Synagis	Respiratory syncytial virus infection	1998
Avastin	Cancer	2004
Stelama (Ustekinumab)	Plaque Psoriasis	2009
Arzerra (Ofatumumab)	Chronic Lymphocytic Leukemia	2009
Prolia (Denosumab)	Osteoporosis	2010
Belatacept (CTL4-Ig Fusion)	Prevention of acute rejection in adult kidney transplant patients	2011
Yervoy (Ipilimumab)	Metastatic melanoma	2011

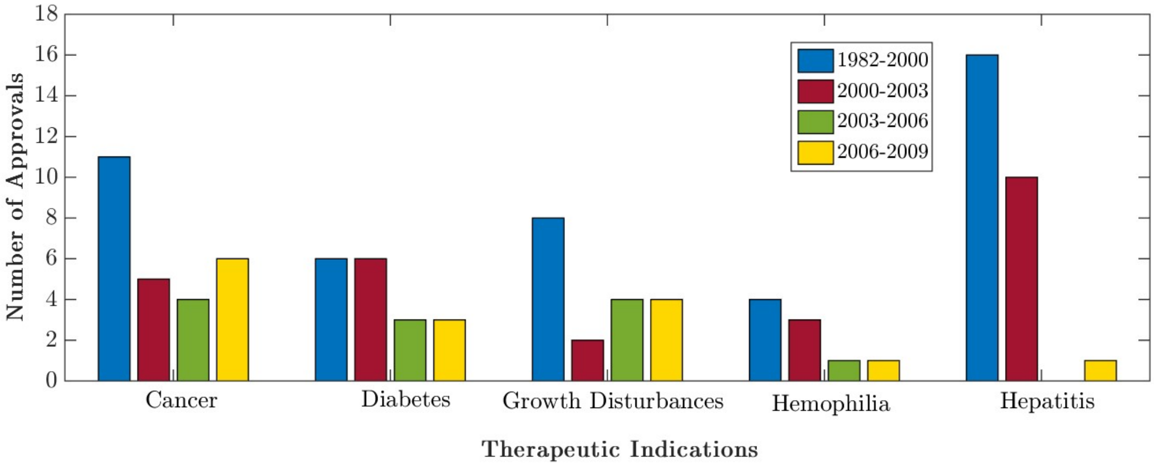

Figure 9.4: Most common therapeutic indications of biologic drugs 1982-2009. Adapted from [371]

In terms of revenues generated, biopharmaceuticals remain a sizeable but distinct subset of pharmaceutical operations worldwide, today accounting for approximately 30% of the entire pharmaceutical industry. In 2014 global pharmaceutical revenues were approximately \$1057 billion with a projected growth of between 5% and 8% per annum until 2019, while biopharmaceutical revenues using a broad biotechnology definition accounted globally for approximately \$305 billion [374–376]. Between 2008 and 2014 the biopharmaceutical industry grew at twice the rate of the conventional pharmaceutical industry. In 2008 biotechnology accounted for 15% of the pharmaceutical industry with revenues of approximately \$100 billion, compared with \$650 billion for all pharmaceuticals [19,375].

Appendix B – Biopharmaceutical operations

The current and projected industry growth rates of pharmaceuticals and biopharmaceuticals is illustrated in figure 9.5.

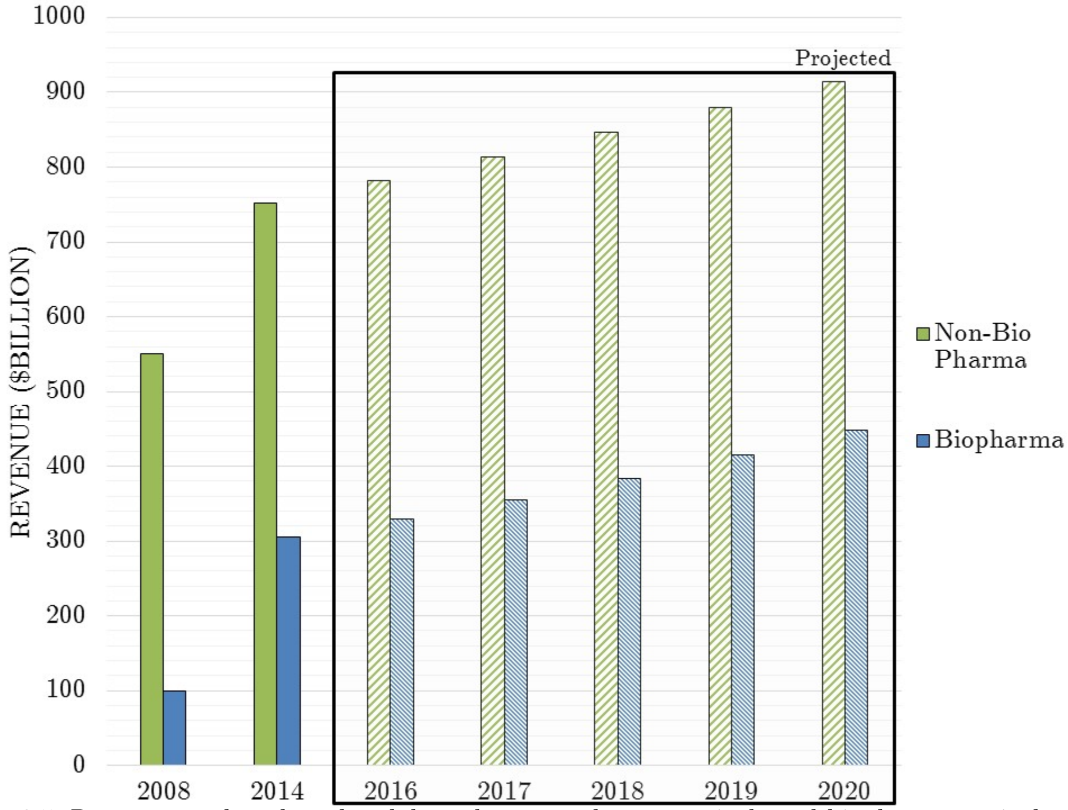

Figure 9.5: Revenue market share breakdown between pharmaceuticals and biopharmaceuticals: 2008 to 2020

Although some of this revenue is offset by marketing and R&D costs, profit margins remain high for the industry as a whole, with pharmaceuticals having the largest profit margins of the five main industrial sectors, including banking, automotive, petrochemical, and media [377].

Table 9.3: World's ten largest pharmaceutical firms - revenue and profit margins 2013 [377]

Company	Total Revenue ($bn)	R&D Spend ($bn)	Sales and marketing spend ($bn)	Profit ($bn)	Profit margin (%)
Johnson & Johnson (US)	71.3	8.2	17.5	13.8	19
Novartis (Swiss)	58.8	9.9	14.6	9.2	16
Pfizer (US)	51.6	6.6	11.4	22.0	43
Hoffmann-La Roche (Swiss)	50.3	9.3	9.0	12.0	24
Sanofi (France)	44.4	6.3	9.1	8.5	11
Merck (US)	44.0	7.5	9.5	4.4	10
GSK (UK)	41.4	5.3	9.9	8.5	21
Astra Zeneca (UK)	25.7	4.3	7.3	2.6	10
Eli Lilly (US)	23.1	5.5	5.7	4.7	20
AbbVie (US)	18.8	2.9	4.3	4.1	22

One of the most drastic changes in the biopharmaceutical landscape in recent years is the rise of biosimilars, a drug product that is highly similar to a licensed biological product, and for which there are no clinically meaningful differences between the original biological product and the biosimiliar in terms of the safety, purity, and potency of the product [371,378]. The rise of biosimilars can be seen as a direct consequence of the growing risk of drastic revenue reductions due to a phenomenon known as the patent cliff [377]. The patent cliff refers to an abrupt drop in sales of a product following the loss of exclusive manufacturing rights as medicines come to the end of their patent life, with sales often falling by as much as 85% [379]. There are three distinct phases to the life cycle of a new medicine:

1. R&D phase up to market launch
2. the period between launch and loss of exclusivity (i.e. the patent cliff)
3. the period following the loss of exclusivity, when generic companies can enter the market offering biosimiliars

During the first phase, companies identify potential new medicines and take them through intensive pre-clinical and clinical trials. During the second phase, companies market the developed medicines in order to recover the upfront investments with a view to making a profit. Following loss of exclusivity, generic medicines can enter the market. Typically, ten or more biosimilars can be expected to enter the market as soon as patents and market exclusivities expire [370]. The onset of the patent cliff is significant as it is a driver for companies to drastically reduce their manufacturing costs and overheads. For example, in Ireland between 2008 and 2013 an estimate from the Irish Pharmaceutical Healthcare Association put the level of job losses as high as 20% of the total workforce employed in the pharmaceutical sector as a direct impact of the patent cliff [379]. Upgrading complex biopharmaceutical processing operations to counteract the effect of the patent cliff often requires significant investment of plant and equipment. For example Pfizer invested $300 million in the Grange Castle site between 2011 and 2013 in order to expand an existing manufacturing suite and build a new multi-product processing area, as a result of biologic drugs coming off patent [380].

Minimising financial losses post patent loss creates a strong driver for flexibility in the biopharmaceutical manufacturing strategies employed today. New and innovative manufacturing approaches are required to meet increased output demands, lower operating costs, high turn-over portfolio rates, and ever stricter quality demands. A key part of this is adaptability in the maintenance of key equipment, in order to maximise equipment reliability and availability. As staffing levels are reduced and equipment and processes become more complex, intelligent maintenance schemes enabled by TES and PHM must replace obsolete and labour intensive preventive maintenance systems to ensure equipment up-time is maximised. The increased demand on machinery in the sector places a growing importance on keeping all the equipment operational to ensure output-critical usage [44]. As part of that effort, this work aims to address the need for increasing maintenance adaptability and reliability of critical valve components.

9.2 Biopharmaceutical process operations

Biopharmaceutical processes can be divided into two distinct phases: fermentation, known as upstream processing, and product recovery, known as downstream processing. Upstream processing involves the preparation of media and the growth of bacterial or mammalian organisms, typically E. Coli or Chinese hamster ovaries, followed by the separation of the cell mass from the bioreactor growth media [381,382]. Downstream processing involves product recovery and final purification of the product, with the product being the cells, or extracellular products in solution, or components remaining in the cells [381]. The upstream and downstream processes are shown in figure 9.6.

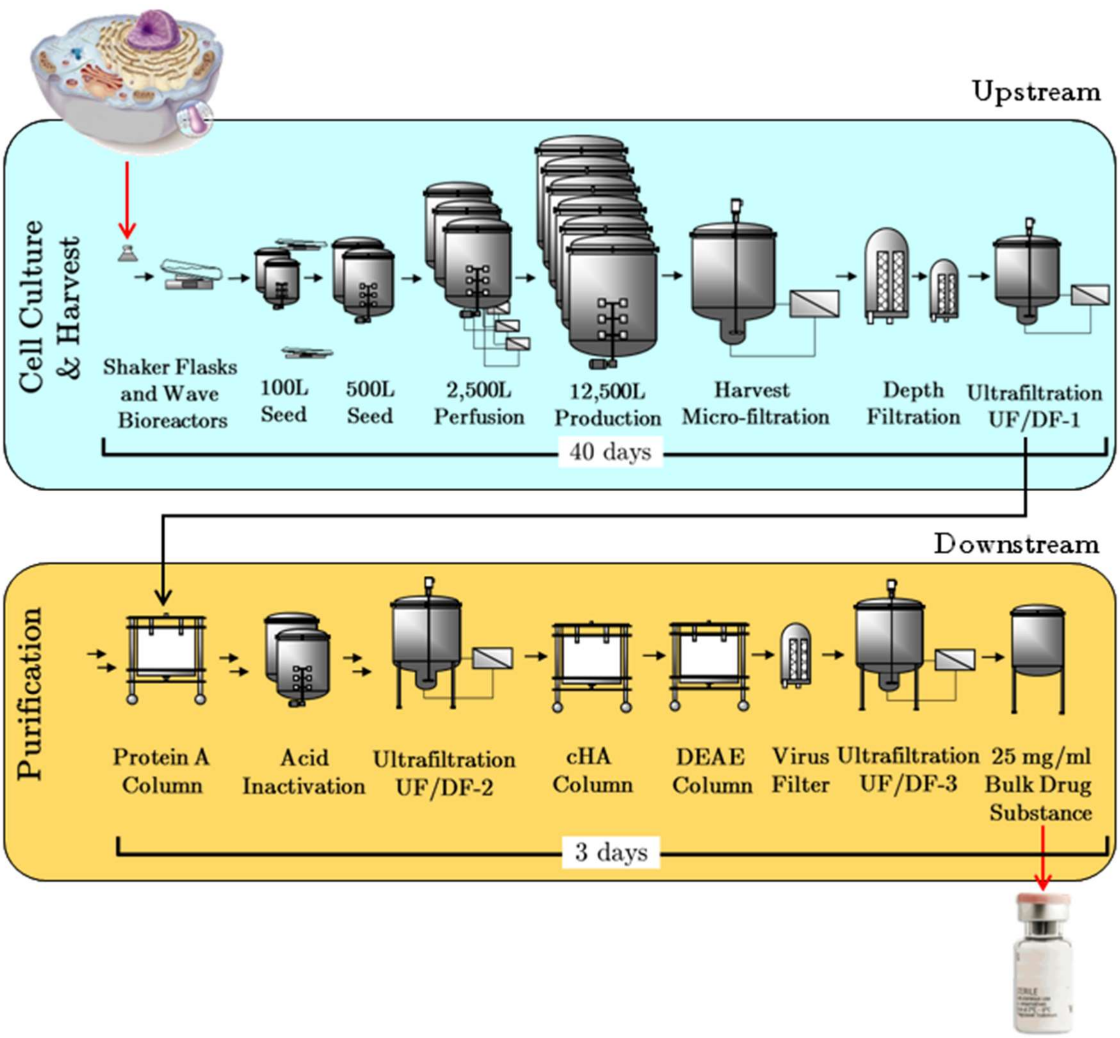

Figure 9.6: Typical biopharmaceutical batch manufacturing process

9.2.1 Upstream processing

Upstream bioprocessing focuses on cell growth in order to achieve appropriate quantities of biomass, a growth catalyst, and to achieve target product concentrations. Important considerations are the growth rate of the organisms, culture stability, and organism quantity. In essence, upstream processing is a scale up process from shaker flasks containing only a few millilitres of the active product, to large seed bioreactors ranging in size from 1,000 – 25,000 litres [381,382]. The structure and layout of a typical bioreactor is shown below in figure 9.7. Safeguarding the correct operation of the highlighted services are hundreds of ancillary components, particularly valves, both automated and manual, controlling flow directionality and ensuring that the correct ingredients are applied at the correct time. The failure of any component within the ancillary equipment portfolio therefore can have major impacts on production.

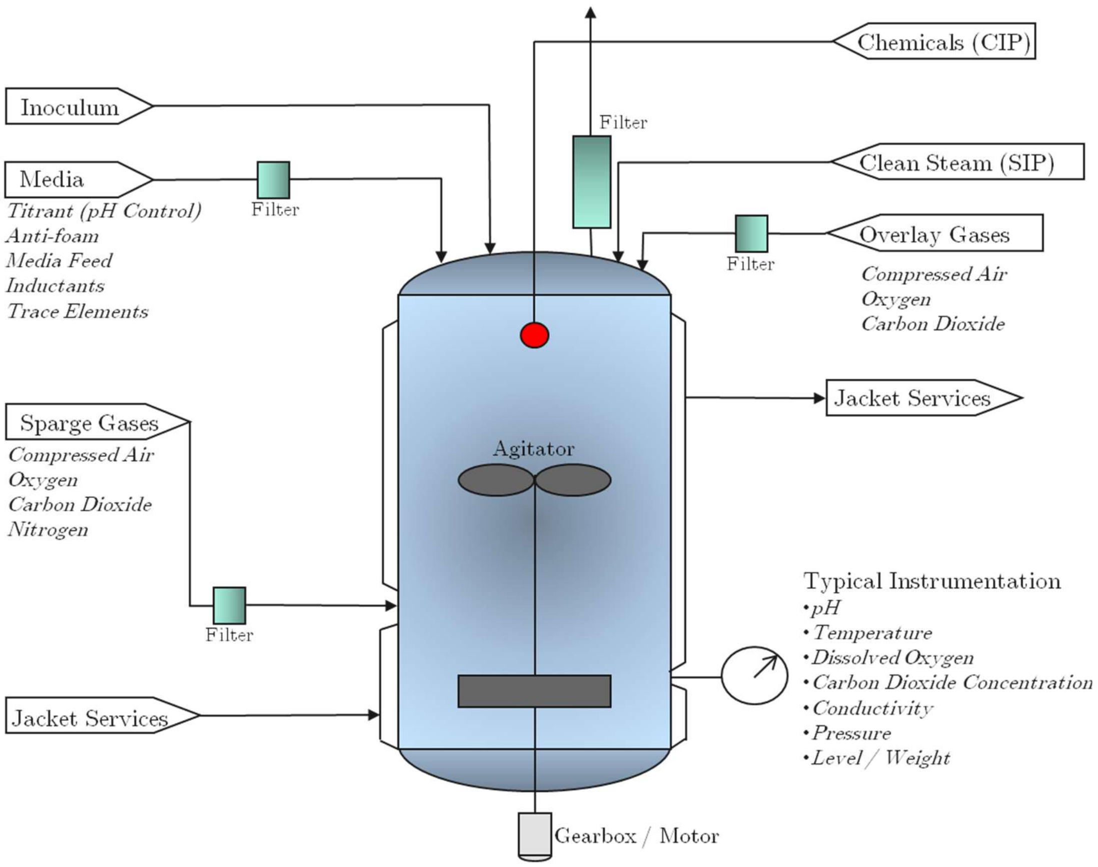

Figure 9.7: Basic bioreactor layout and associated inputs and outputs

To demonstrate the complexity of a full bioreactor system, a mock-up of a typical bioreactor piping and instrumentation diagram (P&ID) is shown in figure 9.8. The bioreactor is highlighted in bold. Several valve banks are highlighted in blue to demonstrate their numbers on a typical bioreactor.

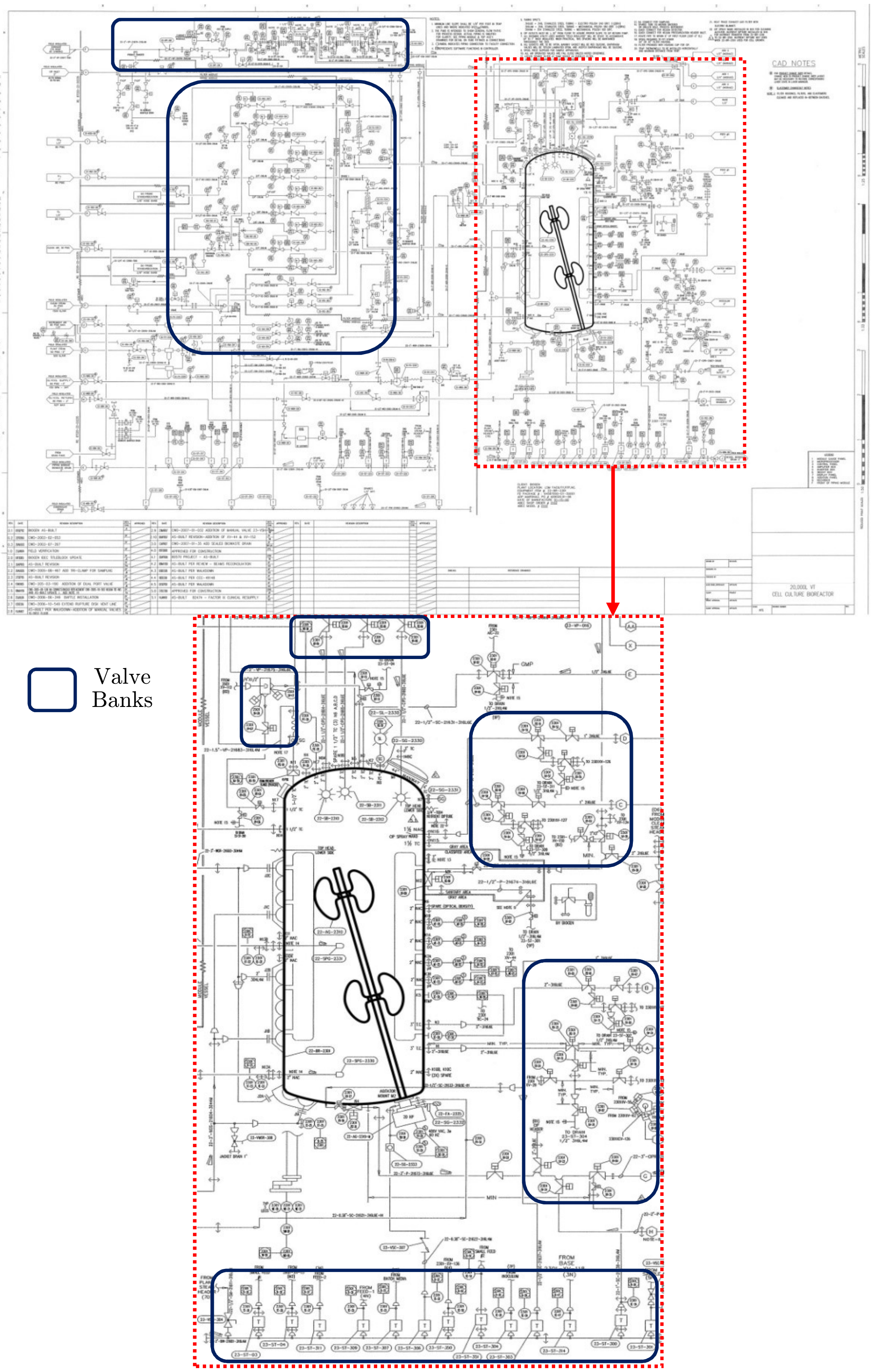

Figure 9.8: P&ID of a typical seed bioreactor

A typical fermentation process begins with the cells which produce the product grown in a shake flask for approximately four days before they are introduced to a seed tank, where they inoculate a cell expansion medium and propagate [383]. The cell expansion media is a highly nutritious suspension that provides the environment needed for the cells to survive [381]. The main nutrients needed for most media for living cells are glucose and glutamine [383]. Mammalian cells have a much slower growth rate than invasive foreign cells, therefore cleanliness and asepsis are critical for successful cell culture as viral and microbial contamination readily destroy cell cultures. Mammalian cells have sophisticated nutritional requirements for growth in culture, such as amino acids, vitamins, lipids, as well as complex physicochemical requirements, such as pH and osmolality [382].

Table 9.4: Typical growth media ingredients in biopharmaceutical processes [381]

Microbial	Mammalian
Glucose solution	Amino acids and vitamins
Ammonium sulphate	Soy protein hydrolysate solution
Protein hydrolysate	Methotrexate
Growth factors	Trace elements, including iron and zinc
Water	Salts
pH control	Glucose
Selective agent – typically antibiotic	Potassium phosphate
-	Water

Growth in the seed reactor lasts about three days. The media containing production bioreactor is then inoculated with these cells. Acid and alkali addition maintain a pH of between 6.8 and 7.4. Temperature is kept at 25°C. Dissolved oxygen addition and agitation are very important and both processes are tightly controlled. Maximum levels of product are produced within eight to ten days in the production bioreactor. A fed-batch mode with periodic feeding or perfusion batch mode with continual feeding is typically operated with glucose and fresh nutrients added throughout the fermentation process [383]. Biomass, viscosity and oxygen demand all increase with continued time in the bioreactor [384,385]. An overview of the upstream cell culture process flow is shown in Figure 9.9.

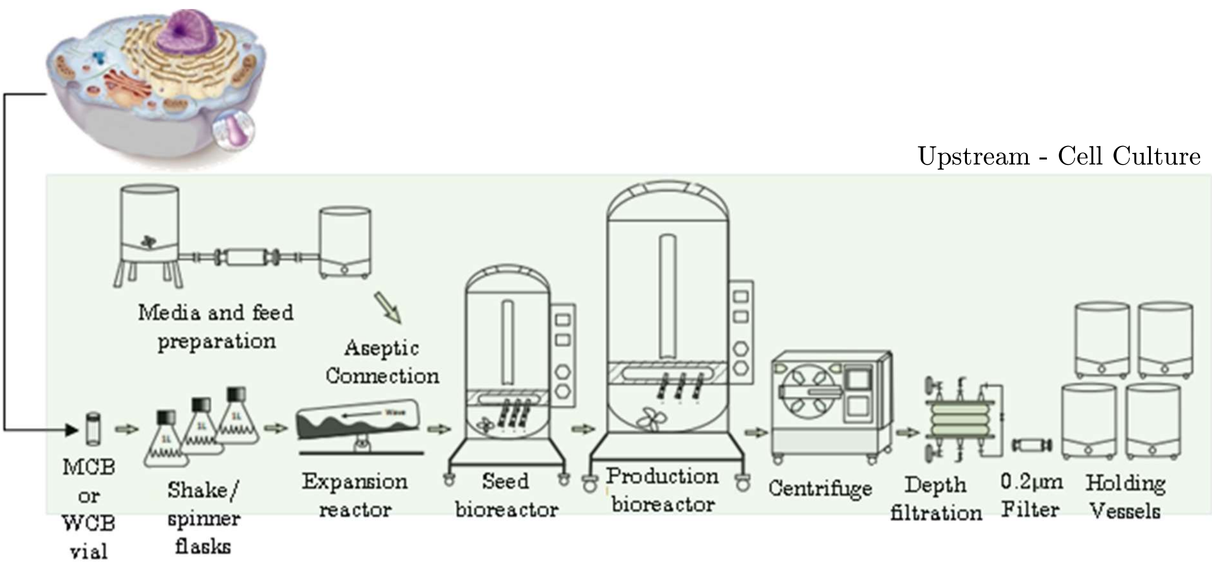

Figure 9.9: Biopharmaceutical upstream cell culture process flow. Adapted from [386]

Different modes of cell culture are used depending on the product type, cell stability, specific cell line productivity and other factors. The three main modes of cell culture, shown in figure 9.10, are [382]:

- Serial batch
    - Periodic cell feeding, every 3-4 days, followed by a partial-volume harvest, and then re-feed of the remaining cells
        - Simplest culture mode. Highly viable due to reduced product exposure, but low volume harvest
- Fed-batch
    - Cells fed periodically, and the entire culture is harvested typically after 1-3 weeks
        - Commonly employed in the production of antibodies. Lower viability than serial batch, but higher volume harvest
- Perfusion
    - Continually feed and harvest the media while retaining cells
        - High volumetric productivity, but presents significant facilities and process robustness challenges as it is a very difficult processes to control

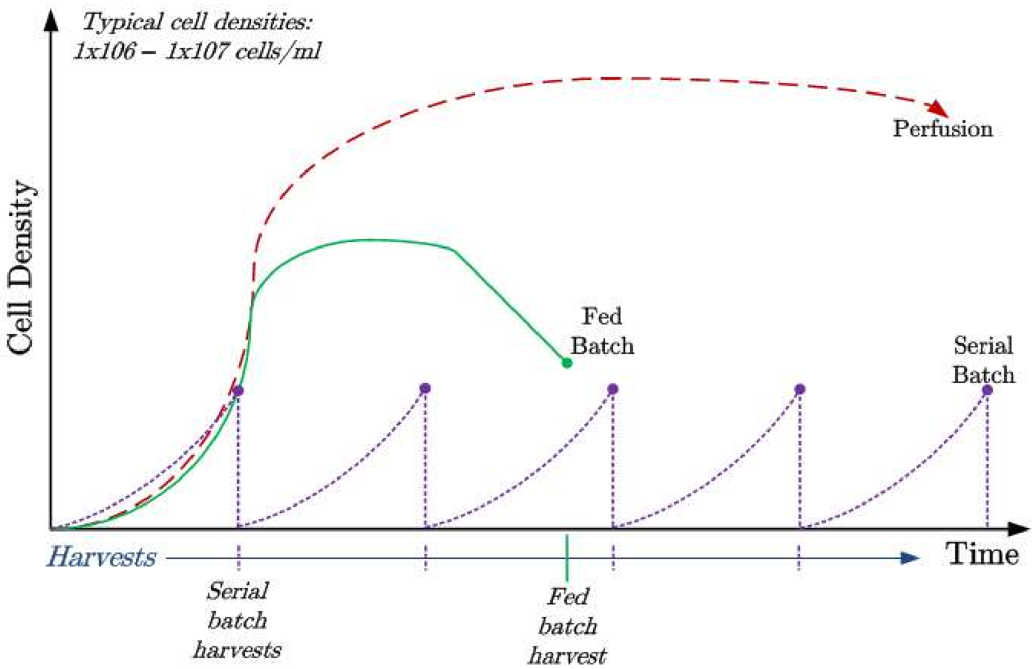

Figure 9.10: Cell density as a function of culture mode. Adapted from [382]

9.2.2 Downstream processing

Downstream processing focuses on product purification, which involves cell removal and clarification, impurity removal, and final product concentration [387]. It is necessary to isolate the product from the fermentation broth, and so the product is recovered from the waste cell mass in order to be further purified before vial filling operations [381,388]. Downstream processes consist of multiple ultrafiltration and microfiltration steps [387]. Typical downstream process steps are described below, and shown in figure 9.11 [389]:

1. Recovery:
    a. Non mechanical means including freezing and the use of detergents and enzymes
    b. High pressure means including centrifugation and homogenisation
    c. Mechanical grinding
2. Separation
    a. Extraction and precipitation
    b. Filtration including microfiltration and ultra-filtration
3. Purification
    a. Chromatography operations, e.g. size-exclusion filtration
    b. Ion exchange
    c. Hydrophobic interaction
    d. Affinity chromatography
    e. Normal and reverse high performance liquid chromatography
4. Filling
    a. Bulk - larger quantities in the region of 5 - 100L
    b. End-product - placement of product into final container or closure system e.g. syringe vials for vaccines
5. Bioanalysis
    a. The proof that the product is safe, pure and the method is efficient

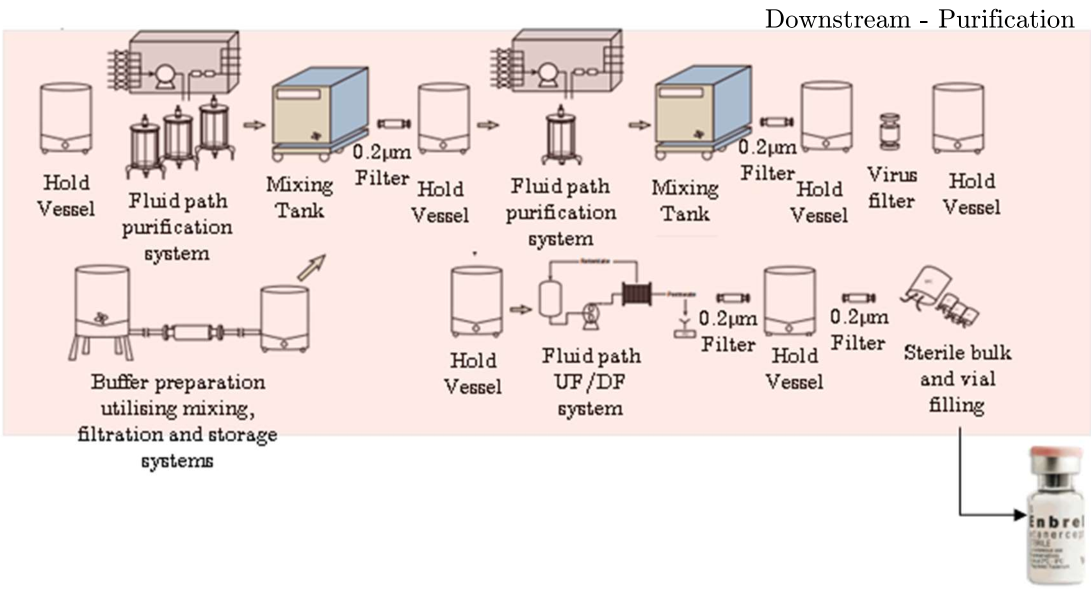

Figure 9.11: Biopharmaceutical downstream purification process flow. Adapted from [386]

Anti-viral filtration is conducted along with continuous contamination monitoring throughout the process, with strict regulatory requirements in place to test and evaluate the viral safety of the product. Potential sources of contamination include [387]:

- Endogenous viruses that occur in the cell line, passed on between generations
    - e.g. Chinese hamster ovaries cells contain a non-infectious retrovirus like particle
- Adventitious viruses introduced during production
    - Use of a contaminated animal derived raw material
    - Contamination during the handling of cells/ growth medium during production
    - Discontinuity of the sterile boundary resulting in loss of the hermetically sealed environment, e.g. valve diaphragm rupture

9.3 Pfizer Ireland Pharmaceuticals

Pfizer Ireland Pharmaceuticals Grange Castle site is a €1.8 billion biotechnology facility and is one of the largest integrated biotechnology plants in the world. Principal manufacturing technologies include large-scale mammalian cell culture, protein purification, vaccines conjugation, and aseptic syringe filling. The site manufactures biological active ingredients for the treatment of rheumatoid arthritis, psoriasis, ankylosing spondylitis, and vaccines for the prevention of pneumococcal disease, particularly meningitis. These drugs serve most major markets and geographical areas, including the United States, Canada, the European Union, Central and South America, the Middle East, and Asia Pacific including Australia, New Zealand, Japan, China, and Korea. The site also manufactures investigational medicinal products for use in clinical trials. Grange Castle houses Pfizer's biotherapeutics research organisation working on drug discovery and optimisation projects in collaboration with other Pfizer research and development sites [390]. As biopharmaceutical manufacturing operations are so highly regulated, and because the manufactured products are intended for direct injection into adults and infants with often compromised immune systems, there is a strong emphasis on high quality products and employee and environmental safety, all within cost effective manufacturing structures. This can only be achieved through high equipment availability, maximising batch yield rates, and a zero defects policy which emphasises no deviations, and no reworks. Defects in manufacturing would lead to significant lost output, large additional costs, adverse regulatory attention, and if undetected, potential patient harm. It is therefore imperative that strict controls are in place, from both manufacturing and maintenance perspectives.

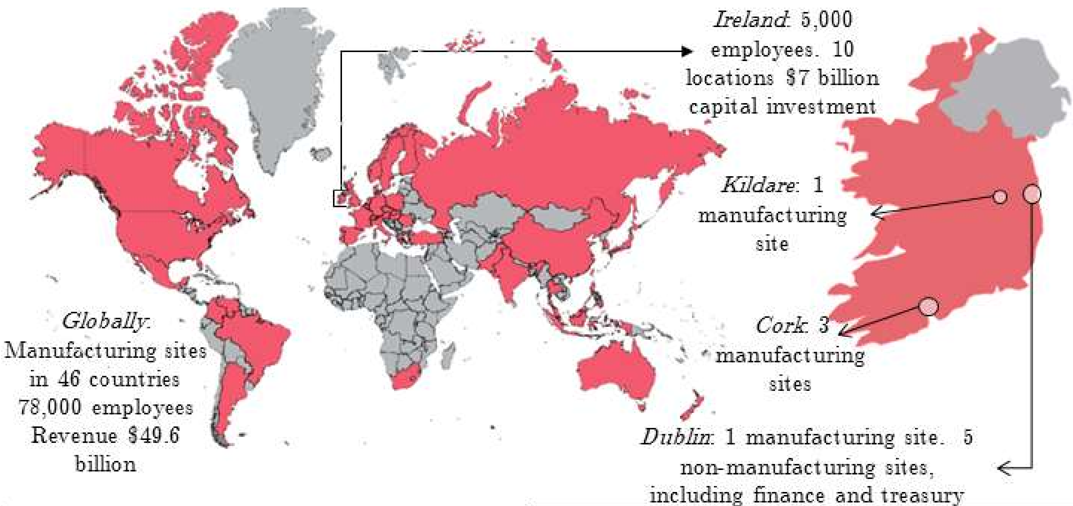

Pfizer Ireland Grange Castle	
No. of Employees	1,450
Biologics Manufactured: Therapeutic Indication	**Prevnar 13**: Pneumococcal pneumonia **Enbrel**: Autoimmune diseases **Somavert**: Acromegaly **Trumenba**: Meningitis Group B
Site Size	360,000m^2

Figure 9.12: Pfizer manufacturing presence globally and locally

9.3.1 Case study facility description

The case study investigated in this work pertains to the perfusion skids, 2,500 litre and 12,500 litre production bioreactors, and 20,000 litre media hold vessels within upstream processing in the Drug Substance Proteins manufacturing facility at the Grange Castle site, as illustrated in figure 9.13. The Drug Substance facility can cater for multiple products on a campaign basis, with the blockbuster drug Enbrel being the primary drug manufactured, an immunological agent used to treat numerous autoimmune diseases. Enbrel is a mammalian cell culture biologic, derived from Chinese hamster ovary cells. Product intermediates are considered non-toxic, non-hazardous, and do not include any allergenic or potent ingredients such as additive hormones. Drug Substance Proteins is the largest manufacturing area in the Grange Castle site.

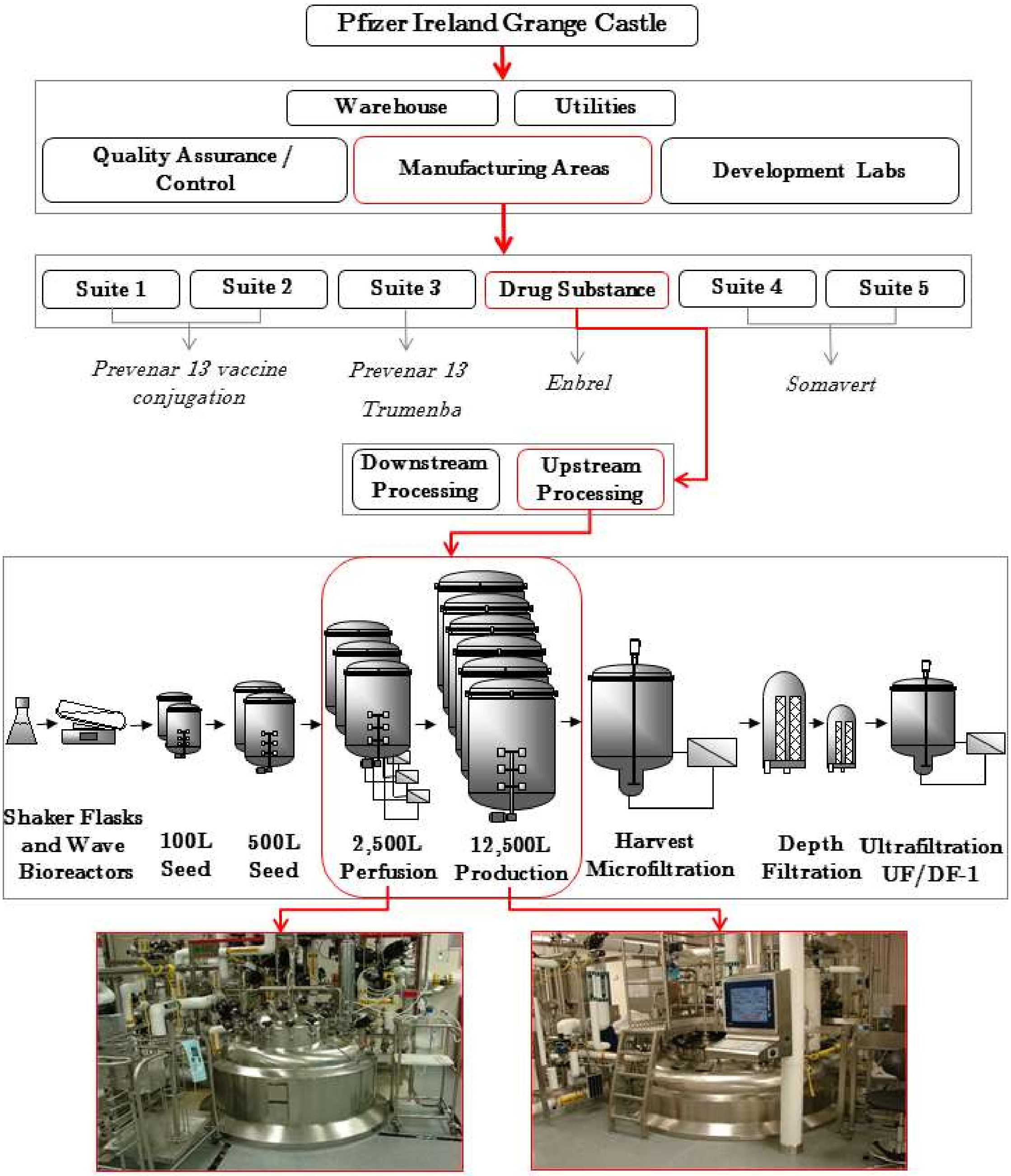

Figure 9.13: Organisational manufacturing structure of Pfizer Ireland Grange Castle Site

Case study facility upstream process description

Upstream processing is the beginning of mammalian cell protein expression. The cells are grown in a range of bioreactors in the cell culture suite. The suite consists of bioreactors, media hold vessels, and perfusion skids, ranging in size from 100 litres to 20,000 litres. The media preparation suite consists of media vessels which are used to prepare media for the culture of the cells and/or induce protein expression in the bioreactors. Firstly, vessels in cell culture and media are either cleaned via chemical means using clean-in-place (CIP) methods, or steamed using steam-in-place (SIP) cycles. They are then pressure tested prior to use. Appropriate media is transferred from the media vessels to the bioreactors in cell culture, passing through sterilising filters. Inoculation of the cells takes place through a line which has undergone a validated SIP cycle. The vessel is kept under positive pressure by introducing filtered air into the reactor head space. All process parameters, such as temperature, agitation, pH and dissolved oxygen levels, are manipulated to optimise cell growth. CO_2 and titrant are filtered into the vessel to control pH while O_2 and air sparge are filtered to maintain correct dissolved oxygen levels. Autoclaved antifoam is aseptically added to control foaming in the bioreactors. Cell culture duration is approximately 3 days, and is 0.1μm filtered prior to use.

The culture is then transferred from a 500L bioreactor to a perfusion system which consists of a 2,500L bioreactor, perfusion skids, and a 20,000L media hold vessel. In order to increase cell density fresh media is added to the bioreactor by perfusion, while at the same time waste by-products are removed. A microfiltration system of 0.65μm aseptically recirculates the cells while the level in the bioreactor is held constant via fresh media from the media hold vessel. After several days of perfusion the culture is transferred to 12,500L bioreactors where it continues to propagate and grow for approximately two weeks. A nutrient feed medium is introduced into the culture at specific intervals.

When the production bioreactor completes after two weeks, the cell culture transferred to a harvest vessel where the cells are removed from the culture as it passes through a microfiltration skid. As the culture recirculates the filter membranes retain the cells. The cell-less culture containing the protein fluid, called the permeate, is filtered again as it passes into a permeate vessel, and is concentrated seven-fold. The permeate is then further filtered down to 0.22μm in order to reduce particle load, and is collected in a permeate hold tank until it reaches eight-fold concentration levels. At this point it is filtered to 0.1μm and passed to a downstream purification vessel.

Clean-in-Place cycle description

CIP cycles, defined in ISO 13408-4 [391], are designed to offer a high level of assurance that potential cross-product contamination from one batch cycle to the next does not occur, by assuring that product soils have been removed from all product contact surfaces prior to further processing. The majority of systems, including auxiliary components such as valves and valve elastomers, are CIP'd as part of a standard cleaning circuit. Other components such as some gaskets and O-rings are cleaned within loads in separate equipment washers. The CIP regime cycles for the bioreactors and perfusion skids in this case study are described in

figure 9.14 below. The critical process steps deemed most likely to contribute to system and component degradation are highlighted in red.

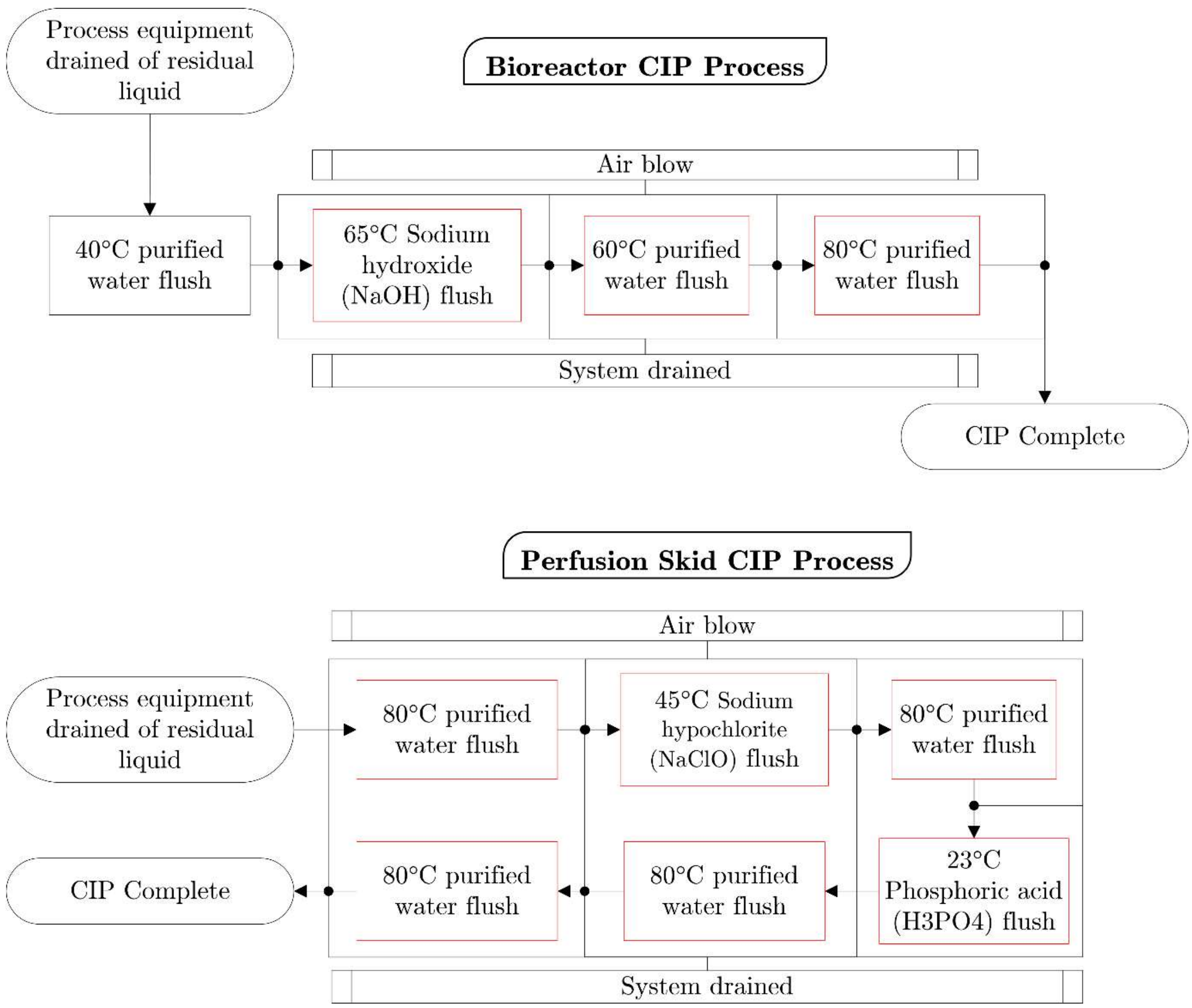

Figure 9.14: CIP Process flow for Bioreactors and Perfusion Skids

Each target chosen for cleaning is designated by a CIP circuit number, which is composed of a number of CIP loops. A CIP loop is an individual section of line or vessel to be cleaned. The loops are cleaned and rinsed in a predetermined sequence to ensure effective cleaning. Each CIP loop in the circuit must complete the same CIP step before the next CIP loop or step can start for that CIP circuit. To supply the loops, CIP routes are used, which are paths through which fluid is supplied and returned between a CIP makeup unit and a CIP user. Within these routes are supply and return valve rings, which are used to segregate CIP circuits ensuring against leakage and product cross-contamination. The flow rate selected for the loops is designed to provide turbulent flow within all process lines, full coverage of vessel internals when using spray balls, and flooding of the piping. The turbulent flow criteria means CIP lines operate at a minimum flow rate of 1.5 m/s to achieve the additional cleaning effect by turbulent flow. The flow tolerances used in the CIP phase ensures that turbulent flow coverage is always achieved prior to commencing the loop timer. All wash timers for each loop are detailed in the associated functional design specification (FDS), a master document detailing the process steps. Cleaning parameters, such as exposure time, temperature, conductivity, and flow rate, are monitored throughout the sequence via in-line control measurements and FDS timers and alarm limits. This ensures the conformity of the cleaning cycles to the FDS requirements. The cleaning agents employed during CIP were developed to provide optimal conditions for protein degradation and removal. CIP supply flow path cleans through all process contact valve diaphragms, with the cleaning cycle designed such that process soils are readily removed from equipment surfaces of different materials of construction. The chemicals used in the CIP streams are described in table 9.5.

Table 9.5: CIP chemical used in case study vessels

System	Chemical	Concentration	Temperature	Flow Rate
Bioreactors/Media Hold Vessels	Sodium hydroxide (NaOH)	20,000 ppm	65°C	>1.5 m/s
Perfusion skids	Sodium hypochlorite (NaClO)	600 ppm	45°C	>1.5 m/s
	Phosphoric acid (H3PO4)	10,000 ppm	23°C	>1.5 m/s

The main advantage of CIP processes is that they allow parts of equipment or an entire process system to be cleaned without being dismantled, reducing the need for disassembling connections under clean conditions. For example, tanks, vessels, freeze-dryers, piping and other processing equipment used for manufacture may be cleaned in place. CIP processes are followed by a SIP process, as described in ISO 13408-5 [392].

Steam-in-Place cycle description

SIP cycles following CIP cycles are the final system sterilisation step before production takes place [392]. The most important issue to consider in establishing SIP technology is the design of the system to ensure that it is able to successfully sterilise manufacturing equipment to the desired level of sterility assurance. SIP processes follow the basic cycle described in figure 9.15 [393]:

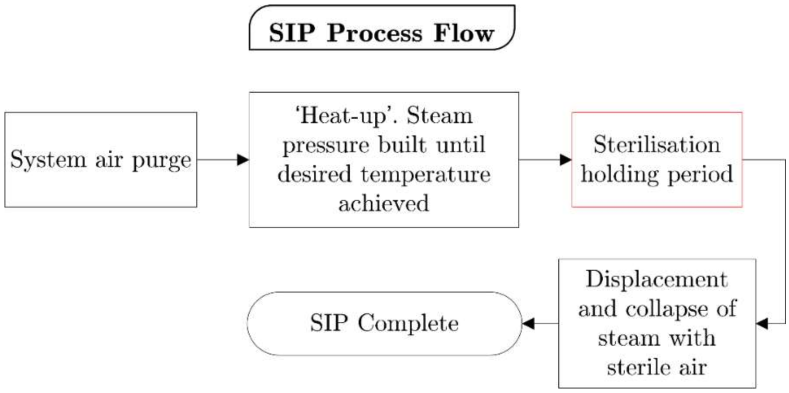

Figure 9.15: SIP process flow for bioreactors and perfusion skids

The initial air purge is critical to the efficacy of steam sterilisation, as any air left in the system introduces a poorly controllable heat transfer resistance, directly affecting sterilisation kinetics. For example, in comparison to the pipe volume, a 1°C temperature drop can be predicted from just 0.1% residual air [393]. Air is purged by displacing it with steam as drain vents are left open, which are equipped with steam traps. The critical requirements associated with SIP include proper steam distribution, non-condensable gases removal, and continuous condensate elimination [394]. Critical process parameters for steam sterilisation are time, temperature, and steam pressure. The saturated steam parameters for the SIP cycles for the bioreactors and perfusion skids investigated in this case study are given in table 9.6 below.

Table 9.6: Bioreactor and perfusion skid SIP process parameters

Temperature (°C)	Pressure (barG)
>121.1	>1.04

In order to validate the efficacy of the SIP cycle, those locations within the system deemed most difficult to sterilise are established. It is then demonstrated that at these locations sterilisation is effective to the predetermined acceptable level of biological indicators [394]. To aid biological sterilisation, high flow rates are again used to generate turbulence. During the heat up phase, the system pressure is increased up to the steam supply pressure by closing all vents and drains. Once the system has been brought to the appropriate pressure, slightly greater than 1.04 barG, the pressure is held for a minimum amount of time to ensure there is no leakage in the system. This pressure hold test will determine a leak by triggering an alarm if the pressure drops below the predetermined limit over several minutes. Once pressure has been established, saturated steam is introduced and held in the system for a predetermined amount of time calculated to ensure a specific level of bioburden will be eradicated during that time. For this reason, the minimum saturated steam temperature of 121.1°C is often referred to as the kill temperature. Once the system has been above 121.1°C for the appropriate amount of time, the system pressure is reduced by the gradual introduction of sterile air. Steam temperature is maintained at a minimal amount greater than 121.1°C. While higher temperatures may increase the rate of biological eradication, it also increases demands on all process systems, including SIP supply and user systems and ancillary equipment. The complete process flow map from batch production, to CIP cleaning, to SIP sterilisation, is shown in figure 9.16 below. The average CIP and SIP durations per batch for the vessels in this case study over a 24-month period are shown below in table 9.7.

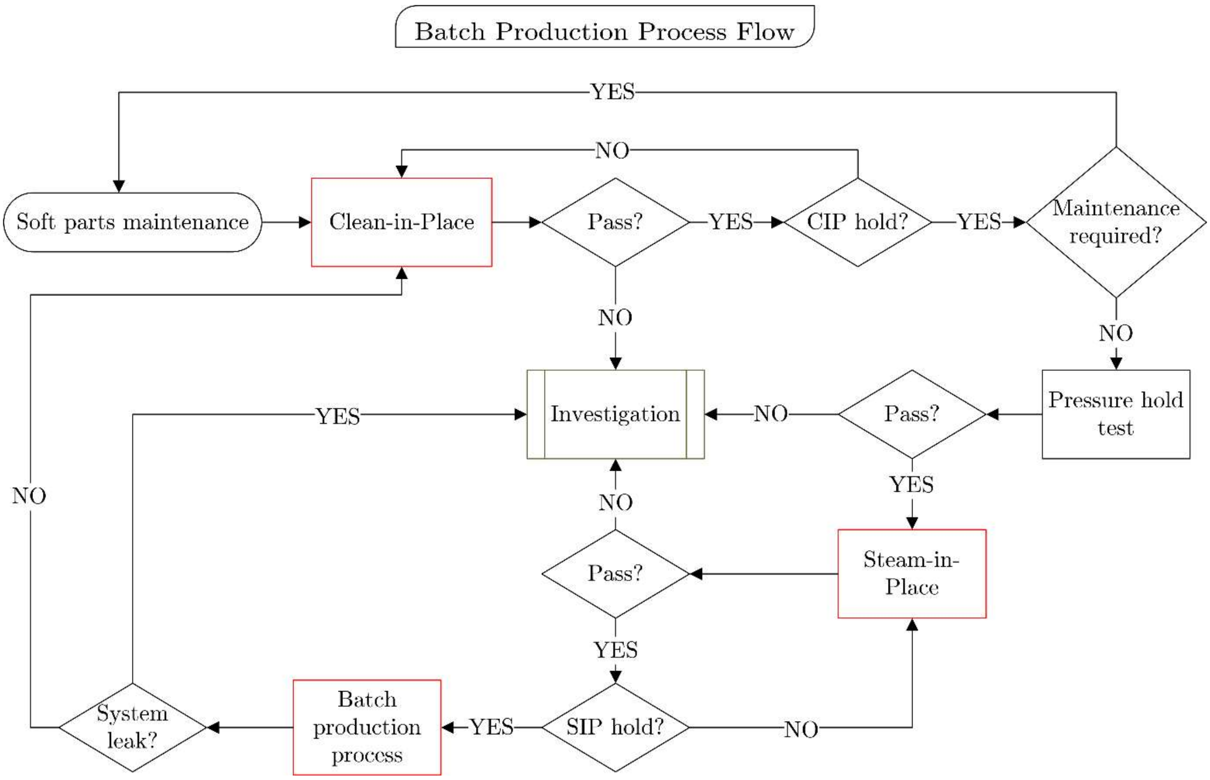

Figure 9.16: Full batch production process flow

Table 9.7: 24-month SIP and CIP durations per batch 2013 - 2015

System	SIP Sterilisation Period per Batch (Hrs:Min)			CIP Cleaning Period per Batch (Hrs:Min)		
	24 Month Average	*24 Month Maximum*	*24 Month Minimum*	*24 Month Average*	*24 Month Maximum*	*24 Month Minimum*
2,500L Bioreactors	5:52	9:49	2:23	6:48	10:34	5:56
12,500L bioreactors	7:06	11:03	3:54	6:17	11:31	5:32
20,000 Media Hold Vessels	9:15	17:29	7:20	4:27	11:40	2:12
Perfusion Skids	11:37	18:16	5:25	7:41	14:32	3:18

9.3.2 Diaphragm failure impact

Elastomer failures pose a major risk in the biopharmaceutical industry as a whole. Next to calibrations, valve diaphragm maintenance is the most cost intensive part of maintenance in biopharmaceutical operations. A survey of BioPhorum member companies in 2012 demonstrated that for a typical biotech plant, soft parts [30]:

- maintenance programs account for over 50% of all planned maintenance activities
- drive 20% of all equipment related deviations
- account for approximately 10% of all corrective maintenance actions
- present the number one contamination risk

If a diaphragm cracks in service, before batch production can begin again, the cause of the crack must be investigated and concluded. Depending on the source and the age of the crack, this can result in long periods of production downtime. To compound this effect, all completed production batches in storage, produced since the last diaphragm maintenance procedure, will not be cleared for release until it can be guaranteed that they too were not affected by the diaphragm failure. To elucidate the financial risk of seal integrity loss, a single batch of Enbrel, the biologic in scope of this work, produces approximately 4kg of active drug substance and costs between $3-4 million to manufacture. This risk is recognised industry wide. Jones [30] quotes Divakar Amin, then engineering manager of final product manufacturing at Bayer HealthCare; "*two recent incidents involving valve failure during the fill-finish process caused leakage into a final processing operation. The cost of the lost batch each time was measured in millions of dollars*". To illustrate this point, figure 9.17 details the breakdown in costs sitewide in the Grange Castle facility during 2013. As shown, the Drug Substance facility accounts for 50% of the total spare parts consumed on an annual basis. Of that 50%, 46% relates to 'soft' parts, 50% relates to 'hard' parts, and 4% is counted as miscellaneous. The 46% soft parts figure breaks down primarily into O-rings, seals, gaskets, and valve diaphragms. Valve diaphragms, both EPDM and PTFE types, account for 50% of the total soft parts budget, with a share of 25% each. This equates to valve diaphragms accounting for 11.5% of the total spare parts budget for the site, by far the largest single contributor to the overall site costs.

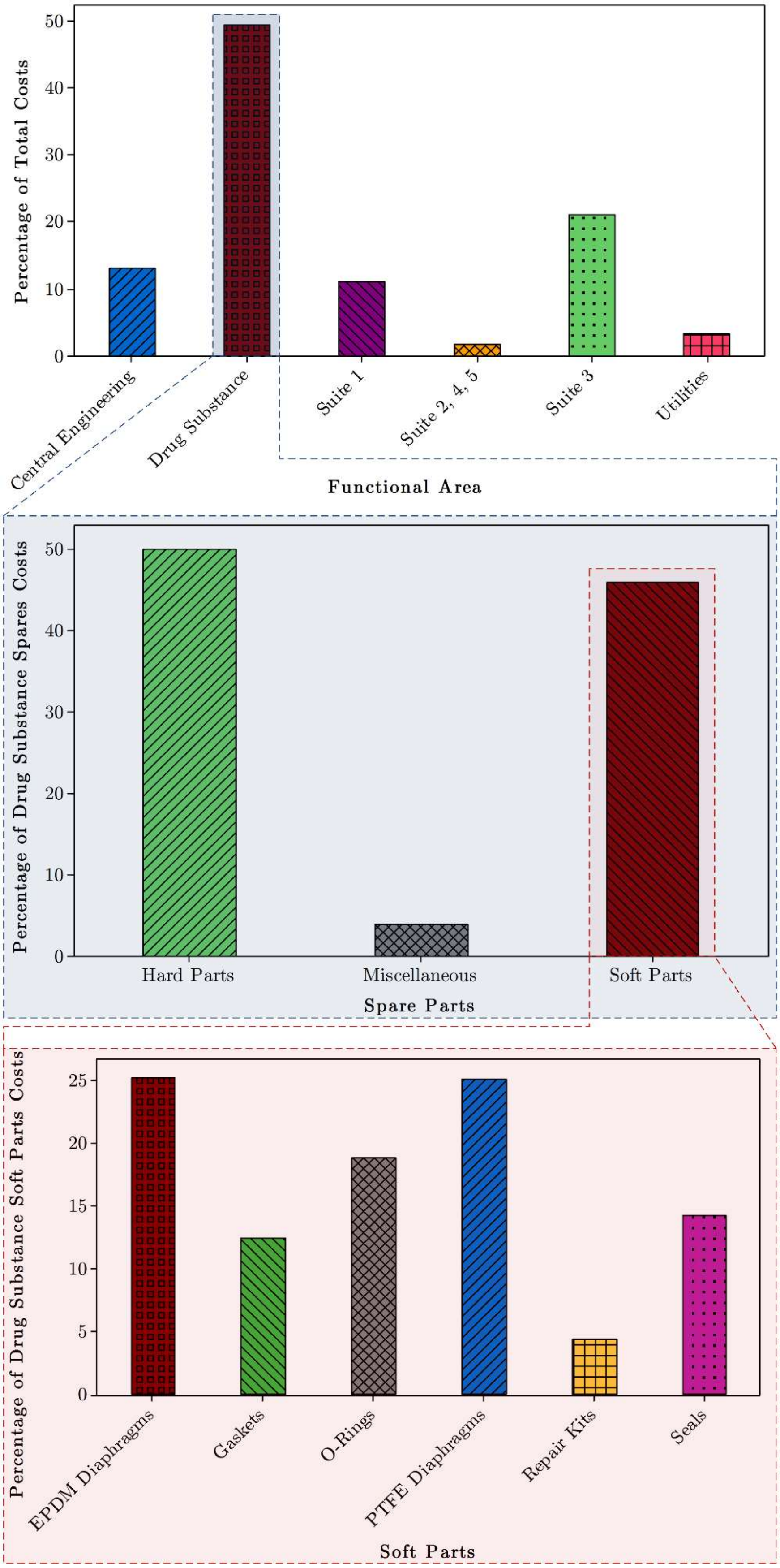

Figure 9.17: Pfizer Grange Castle spare parts costs breakdown 2013

Some of the common difficulties associated with seals usage encountered in the biopharmaceutical industry includes [29]:

- loss of pressure and hermetic boundary inside process vessels due to seal failure
- loss of cleaning and sterilisation effectiveness due to excessive elastomer surface roughness
- excessive adhesion to stainless steel process equipment often resulting in equipment damage, operator injury, or tedious maintenance practices
- marginal performance in common process streams including clean steam
- industrial manufacturing processes of seals often lack robust systems, inspections, or change control procedures, contributing to:
    - inconsistent service life
    - lack of process and ingredient traceability
    - potential contamination of drug product or process utilities

The consequences of an EPDM diaphragm failure in service, due to either gradual degradation or sudden catastrophic failure, are classified as microbiological/endotoxin, chemical, and/or physical. Microscopic microbial contamination is detected by in-process testing which is performed at each process stage from media preparation onwards. Endotoxin testing is performed at each process stage from harvest onwards. The release of endotoxins is associated with certain types of Gram negative bacteria. They occur when the bacterial cell is disrupted or destroyed. Endotoxins are difficult to remove by filtration as they tend to aggregate and could be retained by downstream systems and concentrated by ultrafiltration/diafiltration steps. A failed diaphragm can result in:

- Microbial and/or endotoxin contamination due to external ingress as the sterile system boundary is compromised. Microbial and/or endotoxin contamination is considered to be any amount present over a specified limit for a given process stage
- Microbial and/or endotoxin contamination due to internal ingress as insufficiently cleaned diaphragm surfaces come into contact with the process stream. This can occur due to severe material degradation, such that CIP and SIP cannot sufficiently penetrate the surface creases/blisters leading to microbial and/or endotoxin proliferation
- Chemical contamination due to internal ingress, leading to batch contamination or impacting process conditions such as pH, due to the sterile system boundary being compromised via:
    - process fluids retained in the diaphragm itself or the valve bonnet which subsequently leak into the product stream
    - process fluids leaked into mating process lines because of passing valves due to cracked diaphragms
    - valve bonnet constituents leaking into the process stream, such as lubricants used in the mechanical sections of the actuator
- Physical contamination due to foreign matter deposited in the product stream as the EPDM degrades and disintegrates

If a diaphragm fails before or during an SIP cycle external air can pass through a cracked diaphragm and leak into the system voiding the saturated steam conditions. Internal air could also leak from the system during and cause the formation of a slight vacuum during cool down which can allow organisms to proliferate post sterilisation. Saturated steam passing uncontrolled through a cracked diaphragm internally would destroy any biologic downstream of the valve, and externally would pose a significant safety hazard to personnel.

Table 9.8 details the maximum volume of chemical that could be retained in the bonnet of a valve due to diaphragm failure. For example, the valve bonnet hold-up of a 4-inch diaphragm could be up to 0.930L, and if this volume were to leak back into the process stream during batch harvest it could have a devastating impact on the biologic.

Table 9.8: Valve bonnet volume for multiple valve sizes

Diaphragm Size (Inch)	Bonnet Volume [Liter]
0.5	0.011
0.75	0.02
1	0.038
1.5	0.088
2	0.155
3	0.524
4	0.930

The chemicals that could be potentially introduced into the manufacturing process as a result of a damaged diaphragm include:

- 60°C reverse osmosis water
- 80°C water for injection
- 65°C Sodium hydroxide (NaOH)
- 25°C Nitrilotriacetic acid $N(CH_2CO_2H_3)$
- 45°C Sodium hypochlorite (NaClO)
- 23°C Phosphoric acid (H_3PO_4)

To calculate the potential consequence of a diaphragm crack occurring in service, such that the sealing ability of the diaphragm were to be compromised, the unintended flow of chemicals passing through different sized failed diaphragms was calculated via equation (9.1) for discharge through a small orifice [395]:

$$Q = C_D A (2gH)^{\frac{1}{2}} \tag{9.1}$$

Where:

Q = Volumetric Flow Rate (m^3/s)

C_D = Orifice Opening Shape Coefficient

A = Area of the Crack

g = $9.81 m/s^2$

H = Pressure Head (m)

A value of 0.62 was used for C_D, corresponding to a sharp edged orifice, the assumed shape for a crack [395].

The pressure differential was converted to pressure head H via Equation (9.2):

$$P = 0.0981H \tag{9.2}$$

The standard pressure of a closed system during production is 3 bar gauge; assuming one side of a valve is fully pressurised to 3 bar gauge whilst the other remains at ambient air pressure, a pressure differential of 3 bar represents the worst case scenario on two sides of a closed valve. This pressure differential was used to calculate the potential litres per hour flow rate through a failed valve due to a crack. The area A of the crack was calculated as a percentage of the total product contact area of the diaphragm, from 0.5% to 5%.

Table 9.9: Unwanted volumetric flow through a 1% crack in various diaphragm sizes

Diaphragm Size (Inch)	Product Contact Area (mm^2)	Crack Size (% of product contact area)	Upstream Pressure (BarG)	Downstream Pressure (BarG)	Flow Rate (m^3/hr)	Flow Rate (Litres/Hour)
0.5	1134	1%	3	0	0.6193	619.27
0.75	1809	1%	3	0	0.9881	988.09
1	2463	1%	3	0	1.3449	1344.91
1.5	4536	1%	3	0	2.4771	2477.10
2	6647	1%	3	0	3.6299	3629.87
3	14526	1%	3	0	7.9322	7932.20

As figure 9.18 demonstrates, the worst case scenario of a 3 inch diaphragm with a 5% crack would mean that over 39,660 litres per hour could pass through the diaphragm unwanted, which would be catastrophic for the process. Even the 'best case' scenario, a 0.5% crack in a 0.5inch diaphragm, would mean approximately 309 l/hr of chemical could pass through a failed diaphragm, again with potentially disastrous consequences for the batch in production.

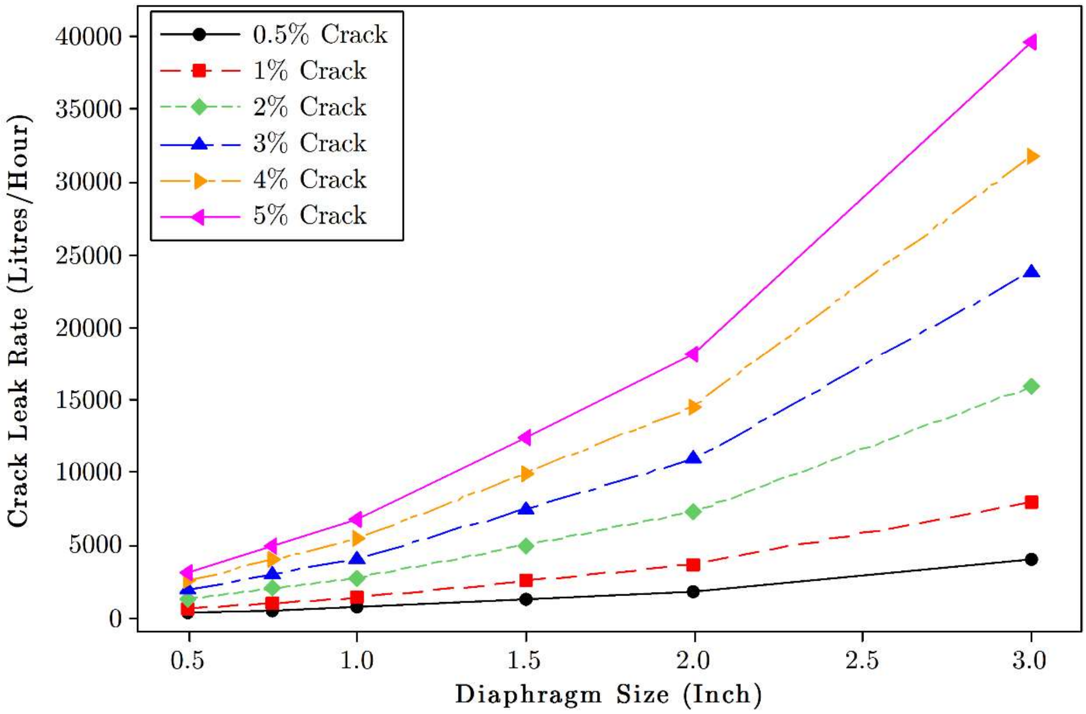

Figure 9.18: Leakage flow through a cracked diaphragm for varying diaphragm and crack sizes

Appendix C - Process variables statistical analysis results

10.1 Filter approach results – cracking failure mode

10.1.1 Full dataset model 1

A logistic regression was performed to ascertain the effects of maintenance window interval, diaphragm age, steam exposure, 60°C RO exposure, 23°C H3PO4, 45°C NaClO, diaphragm size, and 65°C NaOH exposure on the likelihood that diaphragms have developed cracking in service.

Table 10.1: Binary logistic regression model for diaphragm cracking in the full dataset including 65°C NaOH exposure

	β	S.E.	Wald	df	Sig.	Exp(β)	95% C.I. for Exp(β)	
							Lower	Upper
ECO Interval (Hrs)	.000	.000	2.924	1	.087	1.000	1.000	1.000
Age of Diaphragm at Installation (Hrs)	.000	.000	.153	1	.695	1.000	1.000	1.000
Cumulated Steam Exposure (Hrs)	.006	.005	1.066	1	.302	1.006	.995	1.016
60°C Return Osmosis Exposure (Hrs)	.090	.094	.906	1	.341	1.094	.909	1.317
23°C Phosphoric Acid Exposure (Hrs)	.023	.128	.032	1	.857	1.023	.797	1.314
45°C Sodium Hypochlorite Exposure (Hrs)	.030	.022	1.876	1	.171	1.030	.987	1.075
Diaphragm size 0.5 Inch	2.019	1.225	2.717	1	.099	7.533	.683	83.110
Diaphragm size 1 Inch	.711	1.041	.467	1	.495	2.037	.265	15.684
Diaphragm size 1.5 Inch	21.740	12432.172	.000	1	.999	$2.8x10^9$	.000	*
Diaphragm size 2 Inch	.888	1.481	.360	1	.549	2.431	.133	44.282
65°C Sodium Hydroxide Exposure (Hrs)	-.025	.034	.565	1	.452	.975	.913	1.042
Constant	-27.9	12432.172	.000	1	.998	.000	*	*

The logistic regression model was statistically significant with a Chi-Square, $\chi^2(11)$, = 25.740, P = 0.007. The model explained 32.6% of the variance in crack events based on the psuedo R^2 metric of Cragg & Uhler and Nagelkerke. The model correctly classified 87.6% of cases, however the true positive value of crack events was only 16.7%. The true negative value was 99.1%. None of the predictor variables were shown to be statistically significant at the 5% significance level. It would appear that a lack of data for the 1.5 inch diaphragms contributed to that variable becoming unstable in the analysis. At the 10% significance level however, the maintenance window interval time and the 0.5-inch diaphragm size are significant.

10.1.2 Full dataset model 2

A logistic regression was performed to ascertain the effects of maintenance window interval, diaphragm age, steam exposure, 60°C return osmosis (RO) exposure, 23°C H3PO4, 45°C NaClO, diaphragm size, and 80°C water for injection (WFI) exposure on the likelihood that diaphragms have developed cracking in service. The results were identical to model 1 from the full dataset. The regression model was statistically significant with a Chi-Square, $\chi^2(11)$, = 25.693, P = 0.007. The model explained 32.6% of the variance in crack events based on the psuedo R^2 metric of Cragg & Uhler and Nagelkerke. The predictive ability of the model was identical. None of the predictor variables were shown to be statistically significant at the 5% significance level. At the 10% significance level the maintenance window interval time is significant.

Table 10.2: Binary logistic regression model for diaphragm cracking in the full dataset including 80°C WFI exposure

	β	S.E.	Wald	df	Sig.	Exp(β)	95% C.I. for EXP(β)	
							Lower	Upper
ECO Interval (Hrs)	.000	.000	2.868	1	.090	1.000	1.000	1.000
Age of Diaphragm at Installation (Hrs)	.000	.000	.108	1	.742	1.000	1.000	1.000
Cumulated Steam Exposure (Hrs)	.006	.005	1.087	1	.297	1.006	.995	1.016
60°C Return Osmosis Exposure (Hrs)	.040	.056	.505	1	.477	1.040	.933	1.161
23°C Phosphoric Acid Exposure (Hrs)	.073	.158	.212	1	.645	1.076	.789	1.466
45°C Sodium Hypochlorite Exposure (Hrs)	.031	.021	2.264	1	.132	1.032	.991	1.075
Diaphragm size 0.5 Inch	1.899	1.217	2.433	1	.119	6.677	.615	72.558
Diaphragm size 1 Inch	.613	1.044	.345	1	.557	1.846	.239	14.268
Diaphragm size 1.5 Inch	21.687	12337.228	.000	1	.999	2.6x109	.000	*.
Diaphragm size 2 Inch	.818	1.473	.309	1	.579	2.267	.126	40.682
80°C Water for Injection Exposure (Hrs)	-.010	.017	.316	1	.574	.990	.957	1.025
Constant	-27.78	1.2x104	.000	1	.998	.000	*	*

10.1.3 Full dataset model 3

A logistic regression was performed to ascertain the effects of maintenance window interval, diaphragm age, steam exposure, 60°C RO exposure, 23°C H3PO4, 45°C NaClO, diaphragm size, and total actuations on the likelihood that diaphragms have developed cracking in service. The logistic regression model was statistically significant with a Chi-Square, $\chi^2(11)$, = 26.954, P = 0.005. The model explained 34% of the variance in crack events, based on the psuedo R^2 metric of Cragg & Uhler and Nagelkerke. The model performed slightly better than models 1 and 2, correctly classifying 88.4% of cases. Again, the true positive value of crack events was low at 22.2%, rendering the model useless in a practical sense. The true negative value was 99.1%. None of the predictor variables were shown to be statistically significant at the 5% significance level. At the 10% significance level the maintenance window interval time is again significant along with NaClO exposure.

Table 10.3: Binary logistic regression model for diaphragm cracking in the full dataset including total actuations

	β	S.E.	Wald	df	Sig.	Exp(β)	95% C.I. for EXP(β)	
							Lower	Upper
ECO Interval (Hrs)	.000	.000	3.532	1	.060	1.000	1.000	1.000
Age of Diaphragm at Installation (Hrs)	.000	.000	.030	1	.863	1.000	1.000	1.000
Cumulated Steam Exposure (Hrs)	.005	.006	.855	1	.355	1.005	.994	1.017
60°C Return Osmosis Exposure (Hrs)	.047	.060	.618	1	.432	1.049	.932	1.180
23°C Phosphoric Acid Exposure (Hrs)	.033	.128	.067	1	.796	1.034	.805	1.327
45°C Sodium Hypochlorite Exposure (Hrs)	.038	.022	2.925	1	.087	1.039	.994	1.085
Diaphragm size 0.5 Inch	1.688	1.223	1.906	1	.167	5.410	.492	59.470
Diaphragm size 1 Inch	.506	1.048	.233	1	.630	1.658	.213	12.934
Diaphragm size 1.5 Inch	21.701	12374.5	.000	1	.999	$2.7\text{x}10^9$	.000	*.
Diaphragm size 2 Inch	.717	1.492	.231	1	.631	2.048	.110	38.145
Total Actuations	.000	.000	1.053	1	.305	1.000	.999	1.000
Constant	-27.5	12374.499	.000	1	.998	.000	*	*

10.1.4 Bioreactor dataset model 1

A logistic regression was performed to ascertain the effects of maintenance window interval, diaphragm age, steam exposure, sodium hydroxide exposure, 80°C WFI exposure, and diaphragm size on the likelihood that diaphragms have developed cracking in service. The logistic regression model was statistically significant with a Chi-Square, $\chi^2(9)$, = 20.353, P = 0.016. The model explained 39.4% of the variance in crack events, based on the psuedo R^2 metric of Cragg & Uhler and Nagelkerke. The model correctly classified 91.9% of cases, however the sensitivity, or true positive value, of crack events was only 36.4%. The specificity, or true negative value, was 100%. Of the ten predictor variables, only the 1.0-inch size of diaphragms were shown to be statistically significant. The 1.0 inch diaphragm size had the lowest significance of 0.035 with an odds ratio of 16.096. This suggests that this size of diaphragm may represent a greater risk of cracking in service. The ECO interval and the 0.5-inch diaphragms were significant at the 10% significance level.

Table 10.4: Binary logistic regression model for diaphragm cracking in bioreactors including 80°C WFI

	β	S.E.	Wald	df	Sig.	Exp(β)	95% C.I. for EXP(β)	
							Lower	Upper
ECO Interval (Hours)	.000	.000	2.932	1	.087	1.000	1.000	1.000
Age of Diaphragm at Installation (Hours)	.000	.000	.447	1	.504	1.000	1.000	1.000
Cumulated Steam Exposure (Hrs)	.007	.006	1.422	1	.233	1.007	.996	1.018
Cumulated NaOH Exposure (Hrs)	.006	.024	.060	1	.806	1.006	.960	1.054
80°C Water for Injection Exposure (Hrs)	-.012	.021	.304	1	.581	.988	.948	1.030
Diaphragm Size	*	*	5.690	4	.224	*	*	*
Diaphragm Size 0.5 Inch	3.110	1.793	3.007	1	.083	22.413	.667	753.438
Diaphragm Size 1.0 Inch	2.779	1.318	4.445	1	.035	16.096	1.216	213.075
Diaphragm Size 1.5 Inch	-98.694	3.475^{21}	.000	1	1.000	.000	.000	*.
Diaphragm Size 2.0 Inch	1.475	1.247	1.398	1	.237	4.370	.379	50.390
Constant	-6.225	1.980	9.886	1	.002	.002	*	*

10.1.5 Bioreactor dataset model 2

A logistic regression was performed to ascertain the effects of maintenance window interval, diaphragm age, steam exposure, sodium hydroxide exposure, diaphragm size, and 60°C RO water exposure on the likelihood that diaphragms have developed cracking in service. The logistic regression model was statistically significant with a Chi-Square, $\chi^2(9)$, = 20.496, P = 0.015. The model explained 39.7% of the variance in crack events, based on the psuedo R^2 metric of Cragg & Uhler and Nagelkerke. Identical to the results of model 1 the model correctly classified 91.9% of cases, with a sensitivity of 36.4% and a specificity of 100%. Of the ten predictor variables, none were shown to be statistically significant at the 5% significance level. The 1.0 inch diaphragm size had the lowest significance of 0.064 with an odds ratio of 15.206. The ECO interval was the only other variable to have a P value less than 0.1.

Table 10.5: Binary logistic regression model for diaphragm cracking in bioreactors including 60°C RO water exposure

	β	S.E.	Wald	df	Sig.	Exp(β)	95% C.I. for EXP(β)	
							Lower	Upper
ECO Interval (Hours)	.000	.000	2.857	1	.091	1.000	1.000	1.000
Age of Diaphragm at Installation (Hours)	.000	.000	.199	1	.656	1.000	1.000	1.000
Cumulated Steam Exposure (Hrs)	.006	.006	1.015	1	.314	1.006	.995	1.017
Cumulated NaOH Exposure (Hrs)	-.028	.037	.575	1	.448	.972	.904	1.045
60°C Return Osmosis Water Exposure (Hrs)	.078	.103	.583	1	.445	1.082	.884	1.323
Diaphragm Size	*	*	5.746	4	.219	*	*	*
Diaphragm Size 0.5 Inch	-1.797	1.818	.977	1	.323	.166	.005	5.849
Diaphragm Size 1.0 Inch	-3.204	1.733	3.419	1	.064	.041	.001	1.212
Diaphragm Size 1.5 Inch	-21.969	14904.062	.000	1	.999	.000	.000	*
Diaphragm Size 2.0 Inch	-.456	1.754	.068	1	.795	.634	.020	19.741
Constant	-2.707	1.595	2.879	1	.090	.067	*	*

10.1.6 Bioreactor dataset model 3

A logistic regression was performed to ascertain the effects of maintenance window interval, diaphragm age, steam exposure, sodium hydroxide exposure, diaphragm size, and total actuations on the likelihood that diaphragms have developed cracking in service. The logistic regression model was statistically significant with a Chi-Square, $\chi^2(9)$, = 21.464, P = 0.011. The model explained 41.3% of the variance in crack events, based on the psuedo R^2 metric of Cragg & Uhler and Nagelkerke. Identical to the results of models 1 and 2 the model correctly classified 91.9% of cases, with a sensitivity of 36.4% and a specificity of 100%. Of the ten predictor variables, again the 1.0 inch diaphragms were shown to be statistically significant, with the lowest significance of 0.044 with an odds ratio of 15.206. In line with expert opinion from both industrial domain experts and the diaphragm OEM, total actuations appears to have no effect on cracking probability, with an odds ratio of exactly 1.0 and a p value of 0.308. The ECO interval was again the only other variable to have a significance value lower than 0.1.

Table 10.6: Binary logistic regression model for diaphragm cracking in bioreactors including total actuations

	β	S.E.	Wald	df	Sig.	Exp(β)	95% C.I. for EXP(β)	
							Lower	Upper
ECO Interval (Days)	.000	.000	3.422	1	.064	1.000	1.000	1.000
Age of Diaphragm at Installation (Days)	.000	.000	.527	1	.468	1.000	1.000	1.000
Cumulated Steam Exposure (Hrs)	.006	.006	.991	1	.320	1.006	.994	1.018
Cumulated NaOH Exposure (Hrs)	.010	.023	.177	1	.674	1.010	.966	1.055
Total Actuations	.000	.000	1.039	1	.308	1.000	.999	1.000
Diaphragm Size	*	*	4.788	4	.310	*	*	*
Diaphragm Size 0.5 Inch	2.724	1.829	2.218	1	.136	15.244	.423	549.731
Diaphragm Size 1.0 Inch	2.722	1.354	4.040	1	.044	15.206	1.070	216.070
Diaphragm Size 1.5 Inch	-98.922	3.493^{21}	.000	1	1.000	.000	.000	*
Diaphragm Size 2.0 Inch	1.307	1.294	1.021	1	.312	3.695	.293	46.645
Constant	-6.132	2.018	9.237	1	.002	.002	*	*

10.1.7 Perfusion skid dataset model 1

A logistic regression was performed to ascertain the effects of maintenance window interval, diaphragm age, total number of actuations, diaphragm size, steam exposure, and 80°C WFI exposure, on the likelihood that diaphragms have developed cracking in service. From the output shown in Table 10.7 we can reject the logistic regression model as it is not statistically significant with a Chi-Square, $\chi^2(8)$, = 11.630, P = 0.168. The model explained 40.3% of the variance in crack events, based on the psuedo R^2 metric of Cragg & Uhler and Nagelkerke. The model correctly classified 83.7% of cases. The sensitivity was only 14.3% while the specificity was 97.2%. Of the nine predictor variables, none were statistically significant, even at the 10% significance level.

Table 10.7: Binary logistic regression model for diaphragm cracking in perfusion skids including steam exposure and 80°C WFI exposure

	β	S.E.	Wald	df	Sig.	Exp(β)	95% C.I. for EXP(β)	
							Lower	Upper
ECO Interval (Hours)	.000	.000	.105	1	.746	1.000	.999	1.001
Age of Diaphragm at Installation (Hours)	-.001	.001	.891	1	.345	.999	.998	1.001
Total Actuations	-.003	.005	.313	1	.576	.997	.988	1.007
Diaphragm Size 0.5 Inch	1.706	2.347	.528	1	.467	5.509	.055	548.564
Diaphragm Size 1.0 Inch	1.216	1.932	.396	1	.529	3.372	.077	148.655
80°C Water for Injection Exposure (Hrs)	.088	.082	1.160	1	.281	1.092	.930	1.283
Cumulated Steam Exposure (Hrs)	.018	.038	.235	1	.628	1.019	.946	1.097
Constant	-1.951	2.661	.538	1	.463	.142	*	*

10.1.8 Perfusion skid dataset model 2

A logistic regression was performed to ascertain the effects of maintenance window interval, diaphragm age, total number of actuations, diaphragm size, steam exposure, and 23°C phosphoric acid exposure, on the likelihood that diaphragms have developed cracking in service. From the output shown in Table 10.8 we can reject the logistic regression model as it is not statistically significant with a Chi-Square, $\chi^2(8)$, = 13.873, P = 0.085. The model explained 46.8% of the variance in crack events, based on the psuedo R^2 metric of Cragg & Uhler and Nagelkerke. The model correctly classified 86% of cases. The sensitivity was only 28.6% while the specificity was 97.2%. Of the nine predictor variables, none were found to be statistically significant.

Table 10.8: Binary logistic regression model for diaphragm cracking in perfusion skids including steam exposure and 80°C WFI exposure

	β	S.E.	Wald	df	Sig.	Exp(β)	95% C.I. for EXP(β)	
							Lower	Upper
ECO Interval (Hours)	.000	.001	.111	1	.740	1.000	.999	1.002
Age of Diaphragm at Installation (Hours)	-.001	.001	.784	1	.376	.999	.996	1.002
Total Actuations	-.007	.008	.926	1	.336	.993	.978	1.008
Diaphragm Size 0.5 Inch	3.448	4.243	.660	1	.417	31.423	.008	128547.271
Diaphragm Size 1.0 Inch	2.789	3.976	.492	1	.483	16.260	.007	39378.350
23°C Phosphoric Acid Exposure (Hrs)	1.334	1.030	1.679	1	.195	3.797	.505	28.577
Cumulated Steam Exposure (Hrs)	.038	.050	.559	1	.455	1.038	.941	1.146
Constant	-2.6	4.111	.400	1	.527	.074	*	*

10.1.9 Perfusion skid dataset model 3

A logistic regression was performed to ascertain the effects of maintenance window interval, diaphragm age, total number of actuations, diaphragm size, 45°C sodium hypochlorite exposure, and 80°C WFI exposure, on the likelihood that diaphragms have developed cracking in service. From the output shown in Table 10.9 we can reject the logistic regression model as it is not statistically significant with a Chi-Square, $\chi^2(8)$, = 11.475, P = 0.176. The model explained 39.8% of the variance in crack events, based on the psuedo R^2 metric of Cragg & Uhler and Nagelkerke. The model correctly classified 83.7% of cases. The sensitivity was 14.3% while the specificity was again 97.2%. Of the nine predictor variables, again none were found to be statistically significant.

Table 10.9: Binary logistic regression model for diaphragm cracking in perfusion skids including steam exposure and 80°C WFI exposure

	β	S.E.	Wald	df	Sig.	Exp(β)	95% C.I. for EXP(β)	
							Lower	Upper
ECO Interval (Hours)	.000	.000	.065	1	.799	1.000	.999	1.001
Age of Diaphragm at Installation (Hours)	-.001	.001	.859	1	.354	.999	.998	1.001
Total Actuations	-.002	.004	.205	1	.651	.998	.990	1.006
Diaphragm Size 0.5 Inch	1.645	2.353	.489	1	.485	5.182	.051	522.01
Diaphragm Size 1.0 Inch	1.106	1.899	.339	1	.560	3.021	.073	124.96
45°C Sodium Hypochlorite Exposure (Hrs)	.018	.058	.097	1	.756	1.018	.909	1.141
80°C Water for Injection Exposure (Hrs)	.076	.069	1.221	1	.269	1.079	.943	1.235
Constant	-1.593	2.562	.387	1	.534	.203	*	*

10.1.10 Perfusion skid dataset model 4

A logistic regression was performed to ascertain the effects of maintenance window interval, diaphragm age, total number of actuations, diaphragm size, 45°C sodium hypochlorite exposure, and 23°C H3PO4 exposure, on the likelihood that diaphragms have developed cracking in service. We can reject the logistic regression model as it is not statistically significant with a Chi-Square, $\chi^2(8)$, = 12.068, P = 0.098. The model explained 41.6% of the variance in crack events, based on the psuedo R^2 metric of Cragg & Uhler and Nagelkerke. The model correctly classified 83.4% of cases. The sensitivity was 28.6% with a specificity of 100%. Of the nine predictor variables, again none were found to be statistically significant. As the sodium hypochlorite exposure variable is not significant in comparison to the 80°C WFI exposure variable and 23°C H3PO4 exposure variable, which are themselves not significant in comparison to the other variables, we can conclude that sodium hypochlorite exposure is also not significant in comparison to the other modelled variables.

Table 10.10: Binary logistic regression model for diaphragm cracking in perfusion skids including steam exposure and 23°C H3PO4 exposure

	β	S.E.	Wald	df	Sig.	Exp(β)	95% C.I. for EXP(β)	
							Lower	Upper
ECO Interval (Hours)	.000	.001	.110	1	.740	1.00	.999	1.002
Age of Diaphragm at Installation (Hours)	-.002	.001	1.116	1	.291	.998	.996	1.001
Total Actuations	-.006	.008	.685	1	.408	.994	.979	1.009
Diaphragm Size 0.5 Inch	3.913	4.447	.775	1	.379	50.1	.008	305170.771
Diaphragm Size 1.0 Inch	.479	1.367	.123	1	.726	1.61	.111	23.505
45°C Sodium Hypochlorite Exposure (Hrs)	.024	.084	.082	1	.775	1.02	.868	1.209
23°C Phosphoric Acid Exposure (Hrs)	1.362	1.025	1.766	1	.184	3.91	.524	29.126
Constant	-2.05	4.280	.229	1	.632	.129	*	*

10.2 Filter approach results – gradual degradation failure mode

10.2.1 Full dataset model 1

A logistic regression was performed to ascertain the effects of maintenance window interval, diaphragm age, steam exposure, 60°C RO exposure, 23°C H3PO4, 45°C NaClO, diaphragm size, and 65°C NaOH exposure on the likelihood that diaphragms have transitioned from degradation state 1 to state 2 in service.

Table 10.11: Binary logistic regression model for degradation state transition in the full dataset including 65°C NaOH exposure

	β	S.E.	Wald	df	Sig.	Exp(β)	95% C.I. for EXP(β)	
							Lower	Upper
ECO Interval (Hrs)	.000	.000	3.028	1	.082	1.000	1.000	1.000
Age of Diaphragm at Installation (Hrs)	.000	.000	.015	1	.904	1.000	1.000	1.000
Cumulated Steam Exposure (Hrs)	.031	.010	8.904	1	.003	1.031	1.011	1.052
60°C Return Osmosis Exposure (Hrs)	.120	.134	.792	1	.373	1.127	.866	1.466
23°C Phosphoric Acid Exposure (Hrs)	.072	.113	.402	1	.526	1.075	.860	1.342
45°C Sodium Hypochlorite Exposure (Hrs)	.009	.022	.191	1	.662	1.009	.968	1.053
Diaphragm size 0.5 Inch	-1.57	1.642	.923	1	.337	.207	.008	5.162
Diaphragm size 1 Inch	-1.50	1.528	.971	1	.324	.222	.011	4.432
Diaphragm size 1.5 Inch	1.99	1.783	1.246	1	.264	7.320	.222	241.220
Diaphragm size 2 Inch	-2.28	1.920	1.421	1	.233	.101	.002	4.368
65°C Sodium Hydroxide Exposure (Hrs)	-.078	.045	2.992	1	.084	.925	.847	1.010
Constant	-2.69	4.649	.334	1	.564	.068	*	*

The logistic regression model was statistically significant with a Chi-Square, $\chi^2(11)$, = 42.412, P = <0.0005. The model explained 43.7% of the variance in state transition events, based on the psuedo R^2 metric of Cragg & Uhler and Nagelkerke. The model correctly classified 83.1% of cases, with a true positive value of state transition events of 41.4%. The true negative value was 95.8%. Steam exposure was significant at the 5% significance level, while NaOH exposure and the ECO interval were significant at the 10% significance level. No interaction variable between the three significant variables was found to be significant.

10.2.2 Full dataset model 2

A logistic regression was performed to ascertain the effects of maintenance window interval, diaphragm age, steam exposure, 60°C RO exposure, 23°C H3PO4, 45°C NaClO, diaphragm size, and 80°C WFI exposure on the likelihood that diaphragms have transitioned from degradation state 1 to state 2 in service. The regression model was statistically significant with a Chi-Square, $\chi^2(11)$, = 41.625, P = <0.0005. The model explained 43% of the variance in state transition events, based on the psuedo R^2 metric of Cragg & Uhler and Nagelkerke. The model correctly classified 81.5% of cases, with a true positive value of state transition events of 37.9%. The true negative value was 94.7%. Steam exposure was significant at the 5% significance level, while the ECO interval was significant at the 10% significance level. The interaction variable between the two significant variables was not found to be significant.

Table 10.12: Binary logistic regression model for degradation state transition in the full dataset including 80°C WFI exposure

	β	S.E.	Wald	df	Sig.	Exp(β)	95% C.I. for EXP(β)	
							Lower	Upper
ECO Interval (Hrs)	.000	.000	2.904	1	.088	1.000	1.000	1.000
Age of Diaphragm at Installation (Hrs)	.000	.000	.128	1	.721	1.000	1.000	1.000
Cumulated Steam Exposure (Hrs)	.029	.010	8.128	1	.004	1.029	1.009	1.050
60°C Return Osmosis Exposure (Hrs)	-.001	.106	.000	1	.989	.999	.812	1.228
23°C Phosphoric Acid Exposure (Hrs)	.368	.257	2.050	1	.152	1.445	.873	2.394
45°C Sodium Hypochlorite Exposure (Hrs)	.015	.022	.439	1	.508	1.015	.972	1.059
Diaphragm size 0.5 Inch	-1.73	1.608	1.170	1	.279	.176	.008	4.105
Diaphragm size 1 Inch	-1.57	1.506	1.096	1	.295	.207	.011	3.955
Diaphragm size 1.5 Inch	1.737	1.741	.996	1	.318	5.681	.187	172.190
Diaphragm size 2 Inch	-2.36	1.901	1.544	1	.214	.094	.002	3.912
80°C Water for Injection Exposure (Hrs)	-.057	.045	1.577	1	.209	.944	.864	1.033
Constant	-2.39	4.560	.275	1	.600	.091	*	*

10.2.3 Full dataset model 3

A logistic regression was performed to ascertain the effects of maintenance window interval, diaphragm age, steam exposure, 60°C RO exposure, 23°C H3PO4, 45°C NaClO, diaphragm size, and total actuations on the likelihood that diaphragms have transitioned from degradation state 1 to state 2 in service. The regression model was statistically significant with a Chi-Square, $\chi^2(11)$, = 36.062, P =

<0.0005. The model explained 38.1% of the variance in state transition events, based on the psuedo R^2 metric of Cragg & Uhler and Nagelkerke. The model correctly classified 80.6% of cases, with a true positive value of state transition events of 34.5%. The true negative value was 94.7%. Steam exposure and ECO interval were significant at the 5% significance level, while NaClO exposure was significant at the 10% significance level.

Table 10.13: Binary logistic regression model for degradation state transition in the full dataset including total actuations

	β	S.E.	Wald	df	Sig.	Exp(β)	95% C.I. for EXP(β)	
							Lower	Upper
ECO Interval (Hrs)	.000	.000	6.860	1	.009	1.000	1.000	1.000
Age of Diaphragm at Installation (Hrs)	.000	.000	.249	1	.618	1.000	1.000	1.000
Cumulated Steam Exposure (Hrs)	.022	.008	6.781	1	.009	1.022	1.005	1.039
60°C Return Osmosis Exposure (Hrs)	-.032	.073	.192	1	.661	.969	.840	1.117
23°C Phosphoric Acid Exposure (Hrs)	.059	.113	.269	1	.604	1.060	.849	1.324
45°C Sodium Hypochlorite Exposure (Hrs)	.033	.019	2.933	1	.087	1.033	.995	1.073
Diaphragm size 0.5 Inch	-1.76	1.628	1.180	1	.277	.171	.007	4.149
Diaphragm size 1 Inch	-1.53	1.534	1.002	1	.317	.215	.011	4.354
Diaphragm size 1.5 Inch	1.567	1.738	.812	1	.368	4.790	.159	144.577
Diaphragm size 2 Inch	-2.33	1.891	1.518	1	.218	.097	.002	3.959
Total Actuations	.000	.000	.558	1	.455	1.000	1.000	1.000
Constant	-2.65	4.610	.332	1	.565	.070	*	*

The logistic regression table including the interaction term between steam and NaClO exposure is shown in table 10.14 below.

Table 10.14: Binary logistic regression model for degradation state transition in the full dataset including total actuations and steam/NaClO interaction variable

	β	S.E.	Wald	df	Sig.	Exp(β)	95% C.I. for EXP(β)	
							Lower	Upper
ECO Interval (Hrs)	.000	.000	5.226	1	.022	1.000	1.000	1.000
Cumulated Steam Exposure (Hrs)	.023	.009	6.029	1	.014	1.023	1.005	1.042
45°C Sodium Hypochlorite Exposure (Hrs)	.105	.046	5.100	1	.024	1.110	1.014	1.216
Steam Exposure * 45°C Sodium Hypochlorite Exposure	-.001	.000	5.296	1	.021	.999	.999	1.000
Constant	-5.18	1.092	22.471	1	.000	.006	*	*

10.2.4 Bioreactor dataset model 1

A logistic regression was performed to ascertain the effects of maintenance window interval, diaphragm age, steam exposure, sodium hydroxide exposure, 80°C WFI exposure, and diaphragm size on the likelihood that diaphragms have transitioned from degradation state 1 to state 2 in service. The regression model was statistically significant with a Chi-Square, $\chi^2(11)$, = 29.779, P = <0.0005. The model explained 44.8% of the variance in state transition events, based on the psuedo R^2 metric of Cragg & Uhler and Nagelkerke. The model correctly classified 81.7% of cases, with a true positive value of state transition events of 47.6%. The true negative value was 93.4%. Steam exposure and ECO interval were significant at the 5% significance level. The interaction term was not found to be significant.

Table 10.15:Binary logistic regression model degradation state transition in bioreactors including 80°C WFI

	β	S.E.	Wald	df	Sig.	Exp(β)	95% C.I. for EXP(β)	
							Lower	Upper
ECO Interval (Hours)	.000	.000	4.552	1	.033	1.000	1.000	1.000
Age of Diaphragm at Installation (Hours)	.000	.000	.000	1	.986	1.000	1.000	1.000
Cumulated Steam Exposure (Hrs)	.020	.008	5.534	1	.019	1.020	1.003	1.037
Cumulated NaOH Exposure (Hrs)	-.018	.032	.307	1	.580	.983	.923	1.046
80°C Water for Injection Exposure (Hrs)	-.013	.033	.153	1	.695	.987	.925	1.054
Diaphragm Size 0.5 Inch	-15.34	35487.73	.000	1	1.000	2.58×10^{9}	.000	*
Diaphragm Size 1.0 Inch	-20.23	35487.73	.000	1	1.000	1.627×10^{9}	.000	*
Diaphragm Size 1.5 Inch	-18.67	35487.73	.000	1	1.000	7.737×10^{9}	.000	*
Diaphragm Size 2.0 Inch	-21.57	35487.73	.000	1	1.000	4.269×10^{10}	.000	*
Constant	-4.476	1.347	11.05	1	.001	.011	*	*

10.2.5 Bioreactor dataset model 2

A logistic regression was performed to ascertain the effects of maintenance window interval, diaphragm age, steam exposure, sodium hydroxide exposure, diaphragm size, and 60°C RO water exposure on the likelihood that diaphragms have transitioned from degradation state 1 to state 2 in service. The regression model was statistically significant with a Chi-Square, $\chi^2(6)$, = 30.516, P = <0.0005. The model explained 45.7% of the variance in degradation state transition events, based on the psuedo R^2 metric of Cragg & Uhler and Nagelkerke. The model correctly classified 80.5% of cases, with a true positive value of state transition events of 42.9%. The true negative value was 93.4%. Steam exposure and ECO interval were significant at the 5% significance level. The interaction term was not found to be significant.

Table 10.16: Binary logistic regression model degradation state transition in bioreactors including 60°C RO water exposure

	β	S.E.	Wald	df	Sig.	Exp(β)	95% C.I. for EXP(β)	
							Lower	Upper
ECO Interval (Hours)	.000	.000	4.982	1	.026	1.000	1.000	1.000
Age of Diaphragm at Installation (Hours)	.000	.000	.017	1	.896	1.000	1.000	1.000
Cumulated Steam Exposure (Hrs)	.018	.008	4.919	1	.027	1.019	1.002	1.035
Cumulated NaOH Exposure (Hrs)	-.057	.041	1.946	1	.163	.945	.872	1.023
60°C Return Osmosis Water Exposure (Hrs)	.117	.122	.917	1	.338	1.124	.885	1.429
Diaphragm Size 0.5 Inch	-20.72	35174.92	.000	1	1.000	2.26 x10^9	.000	*
Diaphragm Size 1.0 Inch	-20.04	35174.92	.000	1	1.000	1.966 x10^9	.000	*
Diaphragm Size 1.5 Inch	-18.47	35174.92	.000	1	1.000	9.449 x10^9	.000	*
Diaphragm Size 2.0 Inch	-21.36	35174.92	.000	1	1.000	5.25 x10^{10}	.000	*
Constant	-4.39	1.341	10.766	1	.001	.012	*	*

10.2.6 Bioreactor dataset model 3

A logistic regression was performed to ascertain the effects of maintenance window interval, diaphragm age, steam exposure, sodium hydroxide exposure, diaphragm size, and total actuations on the likelihood that diaphragms have transitioned from degradation state 1 to state 2 in service. The regression model was statistically significant with a Chi-Square, $\chi^2(6)$, = 31.819, P = <0.0005. The model explained 47.3% of the variance in degradation state transition events, based on the psuedo R^2 metric of Cragg & Uhler and Nagelkerke. The model correctly classified 85.4% of cases, with a true positive value of state transition events of 66.7%. The true negative value was 91.8%. Steam exposure, NaOH exposure, and ECO interval were significant at the 5% significance level. No interaction term was found to be significant among the three significant variables.

Table 10.17: Binary logistic regression model for degradation state transition in bioreactors including total actuations

	β	S.E.	Wald	df	Sig.	Exp(β)	95% C.I. for EXP(β)	
							Lower	Upper
ECO Interval (Days)	.000	.000	6.306	1	.012	1.000	1.000	1.000
Age of Diaphragm at Installation (Days)	.000	.000	.001	1	.981	1.000	1.000	1.000
Cumulated Steam Exposure (Hrs)	.018	.009	4.069	1	.044	1.018	1.001	1.036
Cumulated NaOH Exposure (Hrs)	-.056	.028	4.043	1	.044	.946	.896	.999
Total Actuations	.000	.000	2.420	1	.120	1.000	1.000	1.001
Diaphragm Size 0.5 Inch	-19.21	37789.878	.000	1	1.000	4.563x10^{9}	.000	*
Diaphragm Size 1.0 Inch	-18.21	37789.878	.000	1	1.000	1.231x10^{9}	.000	*
Diaphragm Size 1.5 Inch	16.982	37789.878	.000	1	1.000	4.213x10^{9}	.000	*
Diaphragm Size 2.0 Inch	-20.54	37789.878	.000	1	1.000	1.202x10^{10}	.000	*
Constant	-4.834	1.442	11.244	1	.001	.008	*	*

10.2.7 Perfusion skid dataset model 1

A logistic regression was performed to ascertain the effects of maintenance window interval, diaphragm age, total number of actuations, diaphragm size, steam exposure, and 80°C WFI exposure, on the likelihood on the likelihood that diaphragms have transitioned from degradation state 1 to state 2 in service. The regression model was not statistically significant with a Chi-Square, $\chi^2(8)$, = 13.278, P = 0.103. The model explained 43.6% of the variance in degradation state transition events, based on the psuedo R^2 metric of Cragg & Uhler and Nagelkerke. The model correctly classified 76.2% of cases, with a true positive value of state transition events of only 12.5%. The true negative value was 91.2%. Steam exposure was the only the only significant variable at the 5% or 10% significance levels.

Table 10.18: Binary logistic regression model for degradation state transition in perfusion skids including steam exposure and 80°C Water for Injection exposure

	β	S.E.	Wald	df	Sig.	Exp(β)	95% C.I. for EXP(β)	
							Lower	Upper
ECO Interval (Hours)	.000	.0004	1.476	1	.224	1.000	1.000	1.001
Age of Diaphragm at Installation (Hours)	-4.845	.0002	.062	1	.803	1.000	1.000	1.000
Total Actuations	-.005	.0040	1.396	1	.237	.995	.988	1.003
Diaphragm Size 0.5 Inch	24.97	45877.4	.000	1	1.00	7.04x10^{9}	.000	*
Diaphragm Size 1.0 Inch	26.10	45877.4	.000	1	1.00	2.17x10^{9}	.000	*
80°C Water for Injection Exposure (Hrs)	.080	.0784	1.040	1	.308	1.083	.929	1.263
Cumulated Steam Exposure (Hrs)	.084	.0390	4.645	1	.031	1.088	1.008	1.174
Constant	-7.217	3.684	3.838	1	.050	.001	*	*

10.2.8 Perfusion skid dataset model 2

A logistic regression was performed to ascertain the effects of maintenance window interval, diaphragm age, total number of actuations, diaphragm size, steam exposure, and 23°C phosphoric acid exposure, on the likelihood on the likelihood that diaphragms have transitioned from degradation state 1 to state 2 in service. The regression model was not statistically significant with a Chi-Square, $\chi^2(8)$, = 13.720, P = 0.056. The model explained 44.8% of the variance in degradation state transition events, based on the psuedo R^2 metric of Cragg & Uhler and Nagelkerke. The model correctly classified 81% of cases, with a true positive value of state transition events of only 12.5%. The true negative value was 97.1%. Steam exposure was significant at the 10% significance level.

Table 10.19: Binary logistic regression model for degradation state transition in perfusion skids including steam exposure and 23°C phosphoric acid exposure

	β	S.E.	Wald	df	Sig.	Exp(β)	95% C.I. for EXP(β)	
							Lower	Upper
ECO Interval (Hours)	.000	.0006	.682	1	.409	1.000	.999	1.002
Age of Diaphragm at Installation (Hours)	.000	.0004	.542	1	.461	1.000	.999	1.001
Total Actuations	-.017	.0147	1.400	1	.237	.983	.955	1.012
Diaphragm Size 0.5 Inch	23.09	45877.4	.000	1	1.000	$1.07x10^{10}$	.001	*
Diaphragm Size 1.0 Inch	25.34	45877.4	.000	1	1.000	$1.02x10^{11}$	.175	*
23°C Phosphoric Acid Exposure (Hrs)	1.855	1.5399	1.451	1	.228	6.393	.313	130.764
Cumulated Steam Exposure (Hrs)	.151	.0903	2.785	1	.095	1.163	.974	1.388
Constant	-6.825	5.019	1.850	1	.174	.001	*	*

The following backwards stepwise elimination logistic regression results reveal H3P04 and steam exposure to be significant at the 5% level. The new regression model is statistically significant with a Chi-Square, $\chi^2(4)$, = 9.037, P = 0.029. The models predictive ability was slightly improved, whereby it again correctly classified 81% of cases, but with a true positive value of state transition events of 25%. The true negative value was 94.1%. No interaction term was found to be significant.

Table 10.20: Backwards stepwise elimination binary logistic regression model for degradation state transition in perfusion skids including steam exposure and 23°C phosphoric acid exposure

	β	S.E.	Wald	df	Sig.	Exp(β)	95% C.I. for EXP(β)	
							Lower	Upper
Cumulated Steam Exposure (Hrs)	.061	.031	3.925	1	.048	1.063	1.001	1.130
23°C Phosphoric Acid Exposure (Hrs)	.960	.490	3.840	1	.050	2.612	1.000	6.823
Total Actuations	-.008	.004	3.396	1	.065	.992	.984	1.000
Constant	-3.045	1.376	4.898	1	.027	.048	*	*

10.2.9 Perfusion skid dataset model 3

A logistic regression was performed to ascertain the effects of maintenance window interval, diaphragm age, total number of actuations, diaphragm size, 45°C sodium hypochlorite exposure, and 80°C Water for Injection exposure, on the likelihood that diaphragms have transitioned from degradation state 1 to state 2 in service. From the output shown in Table 10.9 we can reject the logistic regression model as it is not statistically significant with a Chi-Square, $\chi^2(8)$, = 10.851, P = 0.210. The model explained 36.6% of the variance in state transition events, based on the psuedo R^2 metric of Cragg & Uhler and Nagelkerke. The model correctly classified 76.2% of cases. However the sensitivity was <1% while the specificity was 94.1%. 45°C sodium hypochlorite exposure was significant at the 5% level. No interaction terms were found to be significant.

Table 10.21: Binary logistic regression model for degradation state transition in perfusion skids including 45°C sodium hypochlorite exposure and 80°C Water for Injection exposure

	β	S.E.	Wald	df	Sig.	Exp(β)	95% C.I. for EXP(β)	
							Lower	Upper
ECO Interval (Hours)	.000	.0003	2.341	1	.126	1.000	1.000	1.001
Age of Diaphragm at Installation (Hours)	.000	.0002	1.370	1	.242	1.000	1.000	1.001
Total Actuations	-.004	.0034	1.201	1	.273	.996	.990	1.003
Diaphragm Size 0.5 Inch	27.25	4.58 x10^4	.000	1	1.000	6.83 x10^{11}	.000	*
Diaphragm Size 1.0 Inch	26.6	4.58 x10^4	.000	1	1.000	3.58 x10^{11}	.000	*
45°C Sodium Hypochlorite Exposure (Hrs)	.143	.0683	4.375	1	.036	1.153	1.009	1.319
80°C Water for Injection Exposure (Hrs)	.019	.0609	.101	1	.750	1.020	.905	1.149
Constant	-1.593	2.562	.387	1	.534	.203	*	*

10.2.10 Perfusion skid dataset model 4

A logistic regression was performed to ascertain the effects of maintenance window interval, diaphragm age, total number of actuations, diaphragm size, 45°C sodium hypochlorite exposure, and 23°C H3PO4 exposure, on the likelihood that diaphragms have transitioned from degradation state 1 to state 2 in service. We can reject the logistic regression model as it is not statistically significant with a Chi-Square, $\chi^2(8)$, = 12.487, P = 0.131. The model explained 41.3% of the variance in crack events, based on the psuedo R^2 metric of Cragg & Uhler and Nagelkerke. The model correctly classified 83.4% of cases. The sensitivity was 28.6% with a specificity of 100%. Of the nine predictor variables, again only 45°C sodium hypochlorite exposure was significant at the 5% level.

Table 10.22: Binary logistic regression model for degradation state transition in perfusion skids including steam exposure and 23°C H3PO4 exposure

	β	S.E.	Wald	df	Sig.	Exp(β)	95% C.I. for EXP(β)	
							Lower	Upper
ECO Interval (Hours)	.000	.0003	2.306	1	.129	1.000	1.000	1.001
Age of Diaphragm at Installation (Hours)	.000	.0002	1.347	1	.246	1.000	1.000	1.001
Total Actuations	-.010	.0072	1.867	1	.172	.990	.976	1.004
Diaphragm Size 0.5 Inch	26.603	4.5×10^{4}	.000	1	1.000	3.57×10^{11}	.000	*
Diaphragm Size 1.0 Inch	26.291	4.5×10^{4}	.000	1	1.000	2.61×10^{11}	.000	*
45°C Sodium Hypochlorite Exposure (Hrs)	.199	.0998	3.976	1	.046	1.220	1.003	1.484
23°C Phosphoric Acid Exposure (Hrs)	.717	.6442	1.239	1	.266	2.048	.579	7.240
Constant	-2.05	4.280	.229	1	.632	.129	*	*

10.3 Wrapper approach results – gradual degradation failure mode

10.3.1 Bioreactor systems

The covariates chosen to represent the bioreactor systems for the wrapper approach investigations are the following:

- Steam Exposure (Hrs)
- NaOH Exposure (Hrs)
- Maintenance Interval (Hrs)

Using this combination of variables, the full list of potential nested models is written as:

$$\sum \frac{n!}{(n-r)!\,(r!)}_{r=(1,\ldots,n)} \tag{10.3.1}$$

where n = number of covariates in the model. This results in a total of 7 nested models. Using the number of variables in each model and computing the log likelihood for each model allows the computation of the AIC value for that model. Details of all nested models and their respective log likelihood and AIC values are as shown in table 10.23.

Table 10.23: Bioreactor nested models AIC and Pseudo R^2 values

Model Number	Number of Model Variables	Variables Included			Pseudo R^2	Akaike Information Criterion
1	3	Cumulated Steam Exposure (Hrs)	Cumulated NaOH Exposure (Hrs)	ECO Interval (Hrs)	0.443	59.013
2	1	Cumulated Steam Exposure (Hrs)	-	-	0.112	65.082
3	1	-	Cumulated NaOH Exposure (Hrs)	-	0.041	75.237
4	1	-	-	ECO Interval	0.347	25.846
5	2	Cumulated Steam Exposure (Hrs)	Cumulated NaOH Exposure (Hrs)	-	0.353	63.86
6	2	Cumulated Steam Exposure (Hrs)	-	ECO Interval	0.414	49.092
7	2	-	Cumulated NaOH Exposure (Hrs)	ECO Interval	0.352	59.959

10.3.2 Perfusion systems

The covariates chosen to represent the perfusion systems for the wrapper approach investigations are the following, resulting in 31 nested models, the results of which are shown in table 10.24.

- Steam Exposure (Hrs)
- NaClO Exposure (Hrs)
- Maintenance Interval (Hrs)
- H3PO4 Exposure (Hrs)
- Steam / NaClO Exposure Interaction (Hrs)

Table 10.24: Perfusion nested models AIC and Pseudo R2 values

Model Number	Number of Model Variables	Variables Included					Pseudo R^2	Akaike Information Criterion
1	5	Cumulated Steam Exposure (Hrs)	Cumulated NaClO Exposure (Hrs)	Cumulated H3PO4 Exposure (Hrs)	Eco Interval (Hrs)	Steam - NaClO Interaction	0.552	20.694
2	1	Cumulated Steam Exposure (Hrs)	-	-	-	-	0.074	28.372
3	1	-	Cumulated NaClO Exposure (Hrs)	-	-	-	0.055	28.88
4	1	-	-	Cumulated H3PO4 Exposure (Hrs)	-	-	0.021	29.805
5	1	-	-	-	Eco Interval (Hrs)	-	0.022	29.78

6	1	-	-	-	-	Steam - NaClO Interaction	0.011	30.061
7	2	-	-	-	Eco Interval (Hrs)	Steam - NaClO Interaction	0.022	32.41
8	2	-	-	Cumulated H3PO4 Exposure (Hrs)	-	Steam - NaClO Interaction	0.043	31.207
9	2	-	-	Cumulated H3PO4 Exposure (Hrs)	Eco Interval (Hrs)	-	0.076	30.33
10	2	-	Cumulated NaClO Exposure (Hrs)	-	-	Steam - NaClO Interaction	0.19	27.071
11	2	-	Cumulated NaClO Exposure (Hrs)	-	Eco Interval (Hrs)	-	0.058	30.819
12	2	-	Cumulated NaClO Exposure (Hrs)	Cumulated H3PO4 Exposure (Hrs)	-	-	0.086	30.049
13	2	Cumulated Steam Exposure (Hrs)	-	-	-	Steam - NaClO Interaction	0.294	23.867
14	2	Cumulated Steam Exposure (Hrs)	-	-	Eco Interval (Hrs)	-	0.081	30.176
15	2	Cumulated Steam Exposure (Hrs)	-	Cumulated H3PO4 Exposure (Hrs)	-	-	0.121	29.065
16	2	Cumulated Steam Exposure (Hrs)	Cumulated NaClO Exposure (Hrs)	-	-	-	0.079	30.236
17	3	-	-	Cumulated H3PO4 Exposure (Hrs)	Eco Interval (Hrs)	Steam - NaClO Interaction	0.076	32.33
18	3	-	Cumulated NaClO Exposure (Hrs)	-	Eco Interval (Hrs)	Steam - NaClO Interaction	0.202	28.726
19	3	-	Cumulated NaClO Exposure (Hrs)	Cumulated H3PO4 Exposure (Hrs)	-	Steam - NaClO Interaction	0.19	29.071
20	3	-	Cumulated NaClO Exposure (Hrs)	Cumulated H3PO4 Exposure (Hrs)	Eco Interval (Hrs)	-	0.089	31.958
21	3	Cumulated Steam Exposure (Hrs)	-	-	Eco Interval (Hrs)	Steam - NaClO Interaction	0.299	25.712
22	3	Cumulated Steam Exposure (Hrs)	-	Cumulated H3PO4 Exposure (Hrs)	-	Steam - NaClO Interaction	0.517	18.045
23	3	Cumulated Steam	-	Cumulated H3PO4	Eco Interval (Hrs)	-	0.121	31.059

		Exposure (Hrs)		Exposure (Hrs)				
24	3	Cumulated Steam Exposure (Hrs)	Cumulated NaClO Exposure (Hrs)	-	-	Steam - NaClO Interaction	0.362	23.622
25	3	Cumulated Steam Exposure (Hrs)	Cumulated NaClO Exposure (Hrs)	-	Eco Interval (Hrs)	-	0.084	32.11
26	3	Cumulated Steam Exposure (Hrs)	Cumulated NaClO Exposure (Hrs)	Cumulated H3PO4 Exposure (Hrs)	-	-	0.146	30.356
27	4	Cumulated Steam Exposure (Hrs)	Cumulated NaClO Exposure (Hrs)	Cumulated H3PO4 Exposure (Hrs)	Eco Interval (Hrs)	-	0.263	28.862
28	4	Cumulated Steam Exposure (Hrs)	Cumulated NaClO Exposure (Hrs)	Cumulated H3PO4 Exposure (Hrs)	-	Steam - NaClO Interaction	0.519	19.963
29	4	Cumulated Steam Exposure (Hrs)	Cumulated NaClO Exposure (Hrs)	-	Eco Interval (Hrs)	Steam - NaClO Interaction	0.545	20.622
30	4	Cumulated Steam Exposure (Hrs)	-	Cumulated H3PO4 Exposure (Hrs)	Eco Interval (Hrs)	Steam - NaClO Interaction	0.518	20.016
31	4	-	Cumulated NaClO Exposure (Hrs)	Cumulated H3PO4 Exposure (Hrs)	Eco Interval (Hrs)	Steam - NaClO Interaction	0.223	30.093

Appendix D – FTIR Analysis of Surface Oxidation

Shown below are the FTIR analysis results from six category 1 diaphragm samples who showed no other signs of degradation apart from surface discoloration. As shown, there is oxidation present on the material surface which is responsible for the change in material colour. This damage is not believed to impact the mechanical strength of the material significantly.

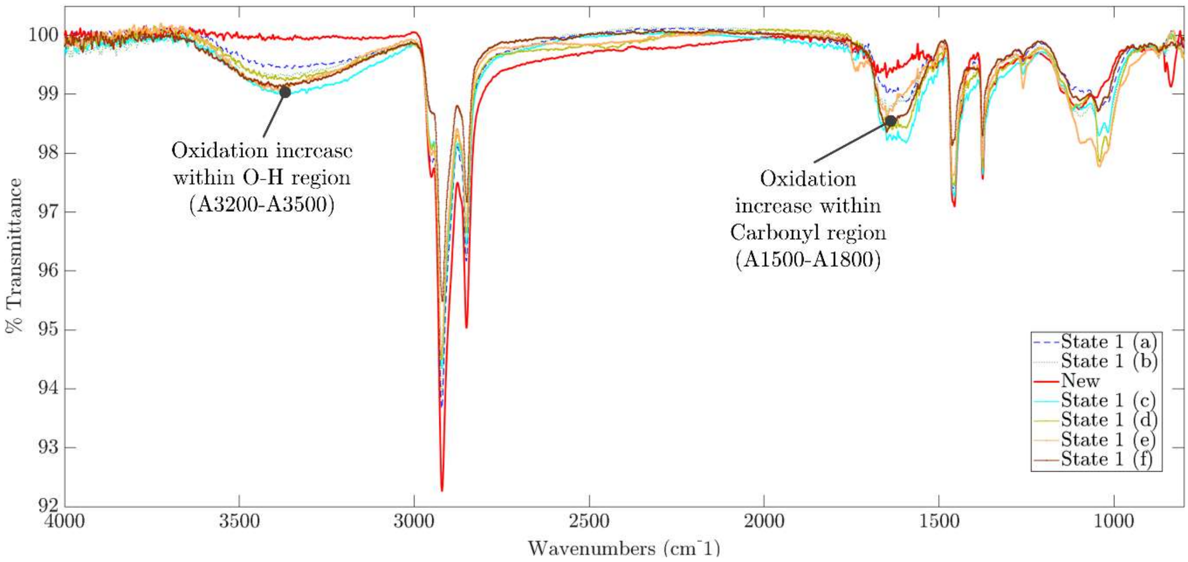

Figure 11.1: FTIR results of six degradation category 1 diaphragm samples

Appendix E – Human Factors Questionnaire

12.1 Overview

The basic structure of the interviews centred on the following questions, however the interviews were structured in a semi-formal manner to help elicit a more natural response from the interviewees:

- What makes maintenance process more difficult from a technician's perspective?
- Could any of the valve components become damaged during installation or maintenance?
- In what ways can a valve be installed incorrectly?
- How much does each of the following factors increase the risk of incorrect installation, if at all?
    - Valve complexity
    - Valve size
    - Procedure information for the valve
    - Accessibility of the installation location
    - Lighting in the installation location
    - Noise in the installation location
    - Distractions in the installation location
    - Technician experience level
    - Time available to perform the task
    - Time of day or night

2.

The SHELL (software, hardware, environment, liveware) model was also used as it and places emphasis on the human being and human interfaces with other components. Based on the SHELL model the technicians were asked if any of the following points contributed to maintenance difficulty:

Software

- Procedures
- Time available (time pressure)

Hardware

- Tools and equipment
- Valve

Environment

- Lighting
- Access
- Noise
- Distractions
- Time of day
- Fatigue
- Attention
- Training
- Experience

Liveware

- Supervision

- Other maintainers

The transcript covering the main points of the discussions between the author and maintenance technicians is given below:

- Access to the valve identified as potentially making the ECO process more difficult from a maintainer's perspective – main issue encountered
- Access to bolts can be particularly difficult behind banks of pipe-work, at height, or in small crawl spaces – getting tools into awkward to reach locations is problematic – in particular it can be hard to get torque wrenches into some locations during final torque pass
- Interstitial area in particular contains fibreglass / old caustic spills – makes access more difficult and can increase ECO difficulty
- More than one maintainer working on a difficult to reach valve can help alleviate the problem – often done on an ad-hoc basis when help is needed
- Time-constraints not an issue during standard ECO's – only during extreme circumstances but a rare occurrence – maintainers focus on doing the job right rather than quickly
- Over tightening or uneven tightening of bolts is potential source of diaphragm / valve damage during ECO's – exacerbated by poor access to the valves – more likely when tool access is more difficult
- Misalignment not an issue – maintainers well aware of need for correct alignment due to sealing issues
- Training has had a positive impact on diaphragm lifetime – 70% to 80% of maintainers time is valve maintenance – training helps keep certain issues fresh – helps alleviate complacency – is currently adequate
- Torque wrenches probably don't need calibrating
- ECO procedures robust – no need to change – do not increase risk of installation errors
- Valve size can have an impact on installation difficulty – smaller sizes more difficult due to small size of bolts / washers, particularly when gowned up
- Environmental issues (temperature, noise, lighting) have little impact on ECO difficulty
- Experience of techs, contractors or staff, has little effect on probability of incorrect ECO
- Refresher training – perhaps once every 12 months - identified as potential way to keep training fresh in the minds of the maintainers